

THE UNIVERSITY OF HULL

**Non-standard methodology in organic
synthesis: mechanochemistry with macrocycles
and sporopollenin**

being a Thesis submitted for the Degree of Doctor of
Philosophy in the University of Hull

by

Bassim Habeeb Abdulwahaab, MSc

August 2016

ACKNOWLEDGEMENTS

Firstly, I would like to thank God for His mercies and blessing and His prophet Mohammad, who has kept me on the right path. I would also like to thank my family for providing me with the financial support without which taking up this opportunity would not have been possible.

I would like to wholeheartedly thank my supervisor, Professor Steve Archibald, for his continued support, advice, encouragement and optimism throughout the last four years. I would also like to thank Dr Benjamin Burke and Dr Juozas Domarkas for their advice, discussions and encouragement throughout my PhD studies. I wish to thank Dr Grahame Mackenzie, who has helped me solve problems and given me inspiration and ideas for my sporopollenin project. I also would to thank everyone in lab C222 for their support.

I wish to thank Rob Lewis and Bob Knight for sorting out the NMR problems so quickly and Carol Kennedy for performing the CHN analyses. I also wish to thank Dr Kevin Welham for mass spectrometry analyses.

Special thanks go to my dear wife, Fada for her support and patience with me throughout my PhD studies. You have been there through the difficult times and the good and so my successes are your successes. You have been my endless source of support and I am forever thankful. My dear children Al-Hassen, Mostafa and Fatima, I thank you very much for your patience with me throughout my PhD.

ABSTRACT

Glyoxal-bridged bisaminal tetraazamacrocyclic derivatives of 1,4,7,10-tetraazacyclododecane (cyclen) and 1,4,8,11-tetraazacyclotetradecane (cyclam) can be *N*-functionalized to incorporate coordinating groups or for conjugation to biomolecules. Herein, an improved *N*-functionalisation methodology is presented using mechanochemistry which reduces reaction times in comparison with conventional synthetic routes. A range of six alkyl halides were reacted with cyclen and cyclam bisaminal derivatives in various ratios to form mono- and bis-functionalized quaternary ammonium salts. CB-TE2A, a commonly used chelator in positron emission tomography medical imaging, has been synthesized using non-conventional synthetic methodologies (grinding and microwave heating) with intermediates characterized by 2D NMR and single crystal XRD. The overall synthesis time of CB-TE2A from cyclam could be shortened to 5 days from the 35 days required for the conventional synthesis.

Sporopollenin exines are made from a natural biopolymer with unusually resistant materials. Spores extracted from the Date Palm (*Phoenix dactylifera* L.), were treated with ammonia to produce amide groups on the surface with a loading of ($0.642 \text{ mmol. gm}^{-1} \pm 0.04$), which can be converted a primary amine by reduction with lithium aluminum hydride ($0.6 \text{ mmol. gm}^{-1} \pm 0.05$). The attendance of the primary amine and precursor amide groups were determined by elemental combustion analysis (CHN), ICP-OES, Fourier transform infrared spectroscopy and solid-state NMR. The primary amine group methyl iodide for salt formation, and phenyl isothiocyanate and benzene sulfonyl chloride for nucleophilic addition and substitution respectively

Lycopodium clavatum (L C) was extracted from fresh pollen and spores, and then mechanochemistry was used to make a basic form by attachment of 1,6-hexane diamine with a loading of ($1.7 \text{ mmol. gm}^{-1} \pm 0.04$) this was followed by attachment of a macrocyclic chelator DOTA (which has a high affinity for gallium(III)). The sporopollenin derivatives were radiolabeled with ^{68}Ga isotope at room temperature (yield 55%) and 90°C (92% RCY). The stability was tested in competition with transferrin, PBS (95%) and simulated gastric fluid (94%).

ABBREVIATIONS

ATSM	diacetyl-bis(4-methylsemicarbazone)
BFC	bifunctional chelator
BP	bisphosphonate
Bq	becquerel's
Br	broad
CB	cross bridged
CB-TE2A	2,2'-(1,4,8,11-Tetraazabicyclo[6.6.2]hexadecane-4,11-diyl)diacetic acid
CHN	carbon, hydrogen, nitrogen analysis
COSHH	control of substances hazardous to health
cyclam	1,4,8,11-tetraazacyclotetradecane
cyclen	1,4,7,10-tetraazacyclododecane
3D	three dimensional
2D	two dimension nuclear magnetic resonance
DCM	dichloromethane
DMA	dimethylacetamide
DMF	dimethylformamide
DMSO	dimethyl sulfoxide
DOTA	1,4,7,10-tetraazacyclododecane-1,4,7,10-tetraacetic acid
d	doublet
FTIR	fourier transform infra-red
g	gram
HRMS	high resolution mass spectrometry
ICP-OES	Inductively coupled plasma optical emission spectroscopy
MS	mass spectrometry
mg	milligram
MHz	megahertz
min	minute
ml	millilitre
mmol	milimole

MeCN	acetonitrile
MeOH	methanol
NMR	nuclear magnetic resonance
PET	positron emission tomography
r.t.	room temperature
SM	starting material
SPION	super-paramagnetic iron oxide nanoparticle VII
SB	side bridged
SP	sporopollenin
SEM	scanning electron microscope
$t_{1/2}$	half-life
THF	tetrahydrofuran
TMS	tetramethylsilane
THF	tetrahydrofuran
TLC	thin layer chromatography
t	triplet
UV	ultra-violet
US	ultrasound
δ	chemical shift

Contents

1. Introduction	2
1.1 Non-standard organic synthesis techniques	2
1.2 Non-standard methods to drive chemical reactions	2
1.2.1 Sonochemistry	2
1.2.2 Microwave chemistry	4
1.2.2.1 Principles of microwave heating in chemistry.....	6
1.2.2.2 Microwave assisted synthesis techniques.....	7
1.2.2.3 Microwave accelerated reduction and hydrogenation.....	8
1.2.3 Mechanochemistry	11
1.2.3.1 Ball milling in inorganic synthesis.....	12
1.2.3.2 Ball milling in organic synthesis.....	14
2.2 Azamacrocyclic compounds	16
2.2.1 Tetraazamacrocycles	16
2.2.1.1 The chelate effect.....	18
2.2.1.2 The macrocycle effect.....	19
2.2.1.3 Restricted cyclam/cyclen.....	20
2.2.1.4 Application of azamacrocycles.....	21
2.2.1.4.1 Catalyst development	21
2.2.1.4.2 Radiopharmaceutical development	23
2.2.1.4.3 Metal complexes with affinity to proteins	24
2.1 Aims	28
2.2 Development of bifunctional chelators (BFCs)	30
2.3 Positron Emission Tomography (PET).....	32
2.3.1 ⁶⁴Cu as a radiometal for PET	33
2.4 Preparation of BFCs via mechanochemistry.....	35
2.4.1 Glyoxal-bridged tetraazamacrocycles as BFCs	35

2.4.2	Glyoxal bridged cyclam/cyclen	36
2.4.3	Alkylation of bridged macrocycles	37
2.4.3.1	Alkylation of bridged cyclam with various alkyl halides via conventional methods	38
2.4.3.2	Alkylation of bridged cyclam with 4-cyanobenzylbromide via mechanochemistry.....	40
2.4.3.3	Alkylation of bridged cyclam with various alkyl halides <i>via</i> mechanochemistry.....	41
2.4.3.3.1	Analysis of a key intermediate, 17.....	45
2.4.3.3.1.1	2D NMR analysis of compound 17	45
2.4.3.3.1.2	X-ray crystallographic structure determination compound 17	48
2.4.3.4	Comparison between conventional method and mechanochemistry.....	49
2.4.3.5	Alkylation of bridged cyclen with various alkyl halides.....	50
2.4.3.6	Comparison between glyoxal bridged cyclam and cyclen.....	54
2.4.4	Reduction method of quaternary ammonium salts via microwave.....	55
2.4.5	Reduction of nitro to amine.....	58
2.4.6	Efficient synthesis of CB-TE2A.....	59
2.5	Conclusion	63
3.	Surface activation of date spore exines	65
3.1	Aims	65
3.2	Sporopollenin biopolymer characteristics	67
3.2.1	Exine.....	68
3.2.2	Method of extraction	70
3.2.3	Uses of Sporopollenin	71
3.2.4	Application of sporopollenin exine.....	71
3.2.4.1	Solid phase peptide synthesis.....	71
3.2.4.2	Use as an ion exchange medium.....	73
3.2.4.3	Encapsulation.....	74

3.2.4.4	Drug delivery.....	75
3.2.3	Availability of different types of sporopollenin	75
3.2.1	Date palm (<i>Phoenix dactylifera</i> L.)	76
3.3	Characterisation and functionalisation of date spore exines	78
3.3.1	Extraction of date spore exines.....	81
3.3.2	Reaction with ammonia	83
3.3.3	Treatment of aminated sporopollenin with 2M HCl _(aq)	84
3.3.4	Ion exchange properties of ammonia - treated date sporopollenin	85
3.3.5	Reduction of date spore exine	86
3.3.6	Further derivatisation of sporopollenin.....	88
3.3.8	Solid state NMR characterisation.....	89
3.4	Conclusion	91
4.	Chapter 4: Radiolabeling of sporopollenin	93
4.1	Aims	93
4.2	Introduction	94
4.2.1	Radiolabelling for monitoring of medical plant extracts' behaviour <i>in vivo</i>	95
4.2.2	Molecular Imaging	96
4.2.3	Why image sporopollenin exines.....	98
4.2.4	Chemistry of gallium	99
4.3	Functionalisation of sporopollenin exines	101
4.3.1	Isolation of exines	101
4.3.2	Amination of sporopollenin by mechanochemistry	101
4.3.2	Functionalisation of sporopollenin with the azamacrocyclic DOTA	105
4.3.3	Radiolabelling of sporopollenin with gallium-68.....	108
4.3.3.1	Phosphate-buffered saline and transferrin stability measurements.....	112
4.4	Conclusion	118

5.	Concluding Remarks and Future Directions	120
6.	Experimental	129
6.1	General notes.....	129
6.2	Method used for ⁶⁸ Ga preparation	129
6.3	Materials.....	130
6.4	Instrumentation	130
6.4.1	Grinding equipment	130
6.4.2	Microwave apparatus	130
6.4.3	NMR spectroscopy	130
6.4.4	MS.....	131
6.4.5	Single crystal X-ray diffraction	131
6.4.6	CHN	131
6.4.7	ICP-OES.....	131
6.4.8	Scanning electron microscope (SEM)	131
6.4.9	Fourier transform infrared (FTIR)	131
6.4.10	Radio-Thin layer chromatography (Radio-TLC)	132
6.4.11	Method for calculation of nitration in mmol/g	132
6.5	Experimental procedures.....	133
6.5.1	Synthesis of dodecahydro-3a,5a,8a,10a-tetraazapyrene (1) and decahydro-2a,4a,6a,8a-tetraazacyclopenta [fg] acenaphthylene (2)	133
6.5.2	Synthesis of Mono- and Bis-N-Alkylation of Glyoxal-Bridged Cyclam via Grinding.....	134
6.5.2.1	Synthesis of 10 a-(4-Cyanobenzyl)dodecahydro-1H-3a,5a,8a,10a-tetraazapyren-10a-ium Bromide (3).....	135
6.5.2.2	Synthesis of 10a-(4-Nitrobenzyl)dodecahydro-1H-3a,5a,8a,10a-tetraazapyren-10a-ium Bromide (4).....	136
6.5.2.3	Synthesis of 10a-(4-Methylbenzyl)dodecahydro-1H-3a,5a,8a,10a-tetraazapyren-10a-ium Bromide (5).....	137

6.5.2.4 Synthesis of 10a-Benzyldecacyhydro-1H-3a,5a,8a,10a-tetraazapyren-10a-ium bromide (6).....	138
6.5.2.5 Synthesis of 10a-(3,5-Dibromobenzyl)decacyhydro-1H-3a,5a,8a,10a-tetraazapyren-10a-ium bromide (7).....	139
6.5.2.6 Synthesis of 10a-(2-(tert-Butoxy)-2-oxoethyl)decacyhydro-1H-3a,5a,8a,10a-tetraazapyren-10a-ium Bromide (8).....	140
6.5.2.7 Synthesis of mono and Bis-N-Alkylation substituted bridged cyclen via grinding	140
General Procedure.....	140
6.5.2.8 Synthesis of 8a-(4-Cyanobenzyl)decacyhydro-1H-2a,4a,6a,8a-tetraazacyclopenta[fg] acenaphthylen 8a ium bromide (9).....	141
6.5.2.9 Synthesis of 8a-(4-Nitrobenzyl)decacyhydro-1H-2a,4a,6a,8a-tetraazacyclopenta[fg] acenaphthylen-8a-ium Bromide (10).....	142
6.5.2.10 Attempted preparation of 4,11-8a-(4-Methylbenzyl)decacyhydro-1H-2a,4a,6a,8a-tetraazacyclopenta[fg] acenaphthylen-8a-ium Bromide (11). Actual preparation of a mixture of (11) and (23).....	143
6.5.2.13 Attempted preparation of 8a-(2-(tert-Butoxy)-2-oxoethyl) decacyhydro-2a, 4a,6a,8a-tetraazacyclopenta [fg]acenaphthylene-8a-ium Bromide (14). Actual preparation of a mixture of (14) and (26).....	146
6.5.3.16 Attempted preparation of 4a,8a-Bis(4-cyanobenzyl)decacyhydro-2a,4a,6a,8a-tetraazacyclopenta [fg]acenaphthylene-4a,8a-diium bromide (21) . Actual preparation of a mixture of (21) and (9).....	148
6.5.2.17 Attempted preparation of 4a,8a-Bis(4-nitrobenzyl)decacyhydro-2a,4a,6a,8a-tetraazacyclopenta[fg] acenaphthylene-4a,8a-diium bromide (22). Actual preparation of a mixture of (22) and (10).....	149
6.5.2.18 Synthesis of 4a,8a-Bis(4-methylbenzyl)decacyhydro-2a,4a,6a,8a-tetraazacyclopenta[fg] acenaphthylene-4a,8a-diium bromide (23).....	149
6.5.2.19 Attempted preparation of 4a,8a-Bis-benzyldecacyhydro-2a,4a,6a,8a-tetraazacyclopenta[fg] acenaphthylene-4a,8a-diium bromide (24). Actual preparation of a mixture of (24) and (12).....	150

6.5.2.20	Attempted preparation of 4a,8a-Bis(3,5-dibromobenzyl) dodecahydro 2a,4a,6a,8a-tetraazacyclopenta [fg]acenaphthylene-4a,8a-dium bromide (25). Actual preparation of a mixture of (25) and (13).....	150
6.5.2.21	Synthesis of 4a,8a-Bis(2-(tert-butoxy)-2-oxoethyl)dodecahydro 2a,4a,6a,8a-tetraaza- cyclopenta[fg]acenaphthylene-4a,8a-dium bromide (26).	151
6.5.3	Synthesis of 4,11-Bis(4-methylbenzyl)-1,4,8,11-tetraaza bicycle[6.6.2]hexa decane(29).....	152
6.5.4	Synthesis of 1,4,8,11-Tetra-azabicyclo [6.6.2]hexadecane (38).....	153
6.5.5	Synthesis of 3a-[4-cyanobenzyl]-8a[methyl]-decahydro-3a,5a,8a,10a,tetra aza- pyrenium diiodide (13).....	154
6.5.6	Synthesis of 1-[4-cyanobenzyl]-8-[methyl]- 1,4,8,11-tetraazabicyclo [6.6.2] hexadecane (14).	155
6.5.7	Synthesis of 1-[4-aminomethylbenzyl]-8-[methyl]-1,4,8,11-tetraazabicyclo [6.6.2] hexadecane (15). ²⁹²	157
6.5.8	Synthesis of 5-(4-methylbenzyl)-1,5,8,12tetraazabicyclo[10.2.2] hexa decane (30).....	158
6.5.9	Synthesis of 10a-(4-((decahydro-1H-3a,5a,8a,10a-tetraazapyren-5a-ium-5a(6H)-yl)methyl) benzyl)-7-(4-nitrobenzyl)dodecahydro-6H-3a,5a,8a,10a- tetraazapyren-10a-ium (31).....	159
6.5.10	Synthesis of 8-(4-(1,5,8,12-tetraazabicyclo[10.2.2]hexadecan-5-ylmethyl) benzyl)-3-(4-nitrobenzyl)-1,5,8,12-tetraazabicyclo[10.2.2]hexadecane (32).	159
6.5.10	Synthesis of 8a-((1H-benzo[d]imidazol-2-yl)methyl)-4a- methyldecahydro-2a,4a, 6a, 8a-tetraaza cyclopenta[fg] acenaphthylene-4a,8a- diium(34).....	160
6.5.11	Synthesis of 4-((1H-benzo[d]imidazol-2-yl)methyl)-10-methyl-1,4,7,10-tetra azabicyclo[5.5.2]tetradecane (35).....	161
6.5.12	5a,5a''-(1,4-phenylenebis(methylene))bis(dodecahydro-1H-3a,5a,8a,10a- tetra azapyren-5a-ium) (27)	162
6.5.13	Synthesis of 1,4-bis((1,5,8,12-tetraazabicyclo[10.2.2]hexadecan-5-yl) methyl) benzene (28)	162

6.5.14	Synthesis of 5-(4-nitrobenzyl)-1,5,8,12-tetraazabicyclo[10.2.2]hexadecane (36).	163
6.5.15	Synthesis of 4-((1,5,8,12-tetraazabicyclo[10.2.2]hexadecan-5-yl)methyl)aniline (37).....	164
6.6	Extraction of date spore exine microcapsules (<i>Phoenix dactylifera</i>) with HCl (39)	165
6.6.1	Synthesis of 41 by reaction with ammonia (39)	166
6.6.2	Synthesis of 40 by treatment of 39 with hydrochloric acid	166
6.6.3	Synthesis of 43 by treatment of 39 with sodium hydroxide.....	166
6.6.4	Synthesis of 44 by treatment of 41 with sodium hydroxide.....	167
6.6.5	Synthesis of 45 by reduction of 42 with lithium aluminium hydride	167
6.6.6	Synthesis of 46 by treatment of 45 with hydrochloric acid	168
3.6.7	Synthesis of 47 by Hoffman quaternisation of 45.....	168
6.6.8	Synthesis of 48	169
6.6.9	Synthesis of 49	169
6.7	Amination of sporopollenin (50) by mechanochemistry	170
6.7.1	Synthesis of 51	170
6.7.2	Synthesis of 53	171
6.7.3	Synthesis of 54	171
6.7.4	Synthesis of 2-(4-chlorophenyl)-N-(4-((11-methyl-1,4,8,11-tetraazabicyclo[6.6.2] hexa decan-4-yl)methyl)benzyl)acetamide (58)	172
6.7.5	Synthesis of N-(6-acetamidohexyl)-2-(4-chlorophenyl)acetamide carboxylate of sporopollenin 59	173
6.7.6	Synthesis of 2,2',2''-(10-(2-((6-acetamidohexyl)amino)-2-oxoethyl)-1,4,7,10-tetraazacyclododecane-1,4,7-triyl)triacetic acid sporopollenin 60	174
6.8	Radiolabeling of sporopollenin	174
6.8.1	Synthesis of Ga-68 complex of sporopollenin (<i>Lycopodium clavatum</i>) ([⁶⁸ Ga]49).....	174

6.8.2	Synthesis of ^{68}Ga complex of <i>N</i> -(6-aminohexyl)acetamide sporopollenin ([^{68}Ga]51).....	175
6.8.3	Synthesis of ^{68}Ga complex for 2,2',2''-(10-(2-((6-acetamidohexyl)amino)-2-oxoethyl)-1,4,7,10-tetraazacyclododecane-1,4,7-triyl)triacetic acid ([^{68}Ga]60)	175
6.8.4	Radiochemical stability	175
6.8.4.1	Apo-transferrin (apo-TF) stability of Ga-68 complex of aminated sporopollenin.....	176
6.8.4.2	Phosphate buffer solution stability of ^{68}Ga complex of aminated sporopollenin.....	176
6.8.4.3	Simulated gastric fluid (SGF).....	177
References.....		178
Appendices		188

Table of Tables

Table 1. Conventional method for alkylation of bridged cyclam with various alkyl halides..	39
Table 2. Grinding method for alkylation of bridged cyclam with 4-cyanobenzylbromide.....	41
Table 3. 30 minutes grinding of bridged cyclam with various alkyl bromides.....	43
Table 4. 3 h grinding of bridged cyclam with various alkyl bromide	44
Table 5. 2D ^1H NMR for compound 17.....	47
Table 6. 2D ^{13}C NMR for compound 17.....	47
Table 7. 30 minutes grinding of bridged cyclen with various alkyl bromide	51
Table 8. 3 h grinding of bridged cyclen with various alkyl bromide.	52
Table 9. Conventional method for alkylation of bridged cyclen with various alkyl halides. ^a	53
Table 10. Preparation of SB/CB via microwave	56
Table 11- Empirical formulae of different sporopollenins	69
Table 12- Sodium and nitrogen content of compound 4 and 5	86
Table 13- Elemental result for derivatisation of sporopollenin	89
Table 14- Grinding sporopollenin with hexane-1,6-diamine	102
Table 15- Result for chloride analysis to compound 50.1 and 50.2.....	102
Table 16- Grinding sporopollenin with different chain length diamine.....	105
Table 17- Multiple attempts to optimise grinding for the peptide coupling reaction	107

Table of Figures

Figure 1- Commercial device for ultrasonic irradiation ¹⁰	2
Figure 2 - Device for microwave irradiation.	4
Figure 3- The electromagnetic spectrum diagram	5
Figure 4- Electric field and magnetic field components of microwaves	6
Figure 5 - Planetary ball milling equipment.....	11
Figure 7- Structures of cyclam and cyclen	18
Figure 8- Linear and cyclic ligands used by Cabbiness and Margerum. ⁶⁵	19
Figure 9- First donor dissociation in linear chelate vs macrocycle. ⁷⁴	19
Figure 10- Ethylene bridged between adjacent nitrogens (SB) or opposite nitrogens (CB) forming side or cross bridged macrocycles respectively.	20
Figure 11- Structure of side bridged SB L ³ and cross bridged CB L ⁴ cyclen	21
Figure 12- Macrocyclic ligand cross bridged cyclams.....	22
Figure 13- Structure of tetraacetic acid derivatives of cyclen DOTA L ⁸ and cyclam TETA L ⁹ ...	23
Figure 14- Chemical structure for DO2A L ¹⁰ and CB-TE2A L ¹¹	24
Figure 15- Gadolinium(III) complex	24
Figure 16- Chemical structure of the bicyclam AMD3100 and Bis CB cyclam.	25
Figure 6- Chemical structure of CB-TE2A.....	29
Figure 17- Cyclam/cyclen based chelators undergoing trials for PET imaging and radiotherapy ¹²⁰⁻¹²²	31
Figure 18- Schematic representation of the principle behind PET. ¹¹⁷	33
Figure 19- Representative chelators for ⁶⁴ Cu labelling	34
Figure 20- SB Monocyclam ligands bearing functional pendant arms.....	35
Figure 21- Structure of CB monomacrocycles bearing functional pendant arms.....	36
Figure 22- Molecular structure of bridged cyclam on left (cis configuration). Ball and stick representation on right, indicating the presence of two exo and two endo lone pairs. Grey = carbon atoms, blue = nitrogen atoms.	37
Figure 23- Schematic configuration for compound 17 as shown by 2D NMR	45
Figure 24- ORTEP plot with atoms drawn as 50% probability ellipsoids. The full macrocycle is represented. Symmetry equivalent atoms are generated by the operator $i = -x, y, 1.5-z$	48
Figure 25- Simplified structure of the exine (red) and intine (blue) ¹⁷⁰	68
Figure 26- The schematic diagram showing the nexine and the sexine within the exine. ¹⁷⁰ ..	69
Figure 27- A Morphological diagram of a date tree and B Date palm. ^{17,224}	77
Figure 28- SEM images of date spores (a) before extraction (b) after extraction.	82

Figure 29 -FTIR spectra for date sporopollenin before/after treatment with ammonia and after reduction by lithium aluminium hydride	87
Figure 30 - ¹³ C solid state NMR for sporopollenins 39 , 41 and 45	90
Figure 31 -Radiolabelling of sporopollenin and functionalised sporopollenin	93
Figure 32 -Lycopodium clavatum SEM.....	98
Figure 33 -Primary amine nitrogen and schematic showing crosslinking via formation of two amide bonds for the diamine with sporopollenin.	103
Figure 34 -SEM image for sporopollenin before and after grinding for 1h.	104
Figure 35 -The position of free gallium and sporopollenin complex on radio-TLC	110
Figure 36 -Radio-TLC for gallium-68 reactions with 50 , 51 and 60 at room temperature ...	110
Figure 37 - Radio-TLC for gallium-68 reactions with 50 , 51 and 60 at 90°C.....	111
Figure 38 - Radio-TLC stability of [⁶⁸ Ga] 50 in PBS at 37 °C for 1h, 2h and 3h.....	113
Figure 39 -Potential method for attachment of gallium-68 with aminated sporopollenin ..	114
Figure 40 -Radio-TLC stability of [⁶⁸ Ga] 51 against transferrin at 37°C for 1h, 2h and 3h	115
Figure 41 -Radio-TLC stability of [⁶⁸ Ga] 51 complex in SGF at 37°C	117
Figure 43 -Aminated date sporopollenin	121
Figure 44 -Primary amine date sporopollenin	122
Figure 45 -Aminated sporopollenin with 1,6-diaminohexane	123
Figure 46 -Aminated sporopollenin with DOTA	124

Table of schemes

Scheme 1- Synthesis of Michael adducts using ultrasound irradiation	3
Scheme 2- Three different examples of solvent free reactions. ^{29, 30,31}	8
Scheme 3- Reduction of nitro groups via microwave (sealed-vessel and open vessel)	9
Scheme 4- Reduction of nitro compounds with Mo(CO) ₆ and DBU	9
Scheme 5- Reduction of nitro groups using cyclohexadiene.....	10
Scheme 6- Hydrogenation of pyridines.....	10
Scheme 7- Polymethylhydrosiloxane (PMHS) reduction of ketone.....	10
Scheme 8 - General ball milling routes to alloys.....	13
Scheme 9- Ball milling routes to metal oxides.	13
Scheme 10- Knoevenagel condensation.	14
Scheme 11- Solvent-free N-allylation of hydrazones.	14
Scheme 12- Direct oxidative amidation.....	15
Scheme 13- Solvent-free peptide synthesis.	15
Scheme 14- The chelate effect.....	18
Scheme 15- Synthetic pathway to mono and bis substituted cyclam/cyclen azamacrocycle derivatives.....	28
Scheme 16- Synthetic pathway to SB and CB cyclam/cyclen.....	29
Scheme 17- Synthetic pathway to bridged cyclam/cyclen.	36
Scheme 18- Synthetic pathway for alkylation of bridged cyclam with 4-cyanobenzylbromide.	40
Scheme 19- General schematic for mono- and bis-N-alkylation of cyclam	42
Scheme 20- General schematic for mono- and bis-N-alkylation of cyclen	50
Scheme 21- Synthetic pathways to SB and CB cyclam.....	56
Scheme 22- Synthetic pathways to SB cyclam.....	57
Scheme 23- Reduction of quaternary ammonium salts via microwave to synthesis of SB cyclam and CB cyclen.	57
Scheme 24- Synthetic pathways to reduction of nitro to amine.....	58
Scheme 25- Synthetic pathways to SB and reduction of nitro to amine in one step.	59
Scheme 26- Alternative pathway to synthesis of CB-cyclam	60
Scheme 27- Synthesis of CB-TE2A via efficient synthesis.....	62
Scheme 28- A proposed synthetic pathway to amine functionalised date palm spores via amide formation.	65

Scheme 29-Synthetic strategies to modify the primary amino group on the surface of compound 45	66
Scheme 30-Sporopollenin in peptide synthesis³⁵	72
Scheme 31-Functionalised sporopollenin used as an ion exchange medium	73
Scheme 32-Extraction and functionalisation of date palm sporopollenin.....	81
Scheme 33 Preparation of date sporopollenin exines.¹⁸¹	81
Scheme 34-Treatment of date sporopollenin with ammonium hydroxide.....	83
Scheme 35-Treatment of aminated date sporopollenin with hydrochloric acid	84
Scheme 36-Reaction of date sporopollenin and aminated sporopollenin with sodium hydroxide.....	85
Scheme 37-Reduction of aminated date sporopollenin.....	86
Scheme 38-Three different reactions suitable for primary amine product 45.....	88
Scheme 39-Amination of sporopollenin with N,N-diethylethylenediamine.²⁸⁰	101
Scheme 40-Amination of sporopollenin with hexane diamine	103
Scheme 41-Protonated aminated sporopollenin with 2M hydrochloric acid at RT	104
Scheme 42-Grinding sporopollenin with different chain lengths of diamine	105
Scheme 43-Grinding a macrocycle with an amino with a carboxylic acid containing reagent.....	106
Scheme 44-Grinding of aminated sporopollenin with carboxylic acid.....	107
Scheme 45-Grinding aminated sporopollenin with DOTA	108
Scheme 46-The compounds which used in radiolabelling experiments.....	108
Scheme 47Gallium-68 radiolabelling of native and functionalised sporopollenin	109
Scheme 48- General schematic for mono- and bis-N-alkylation of cyclam/cyclen.....	120
Scheme 49-Reaction of hydrochloric acid with aminated date sporopollenin	122
Scheme 50-Amination of sporopollenin exine	124
Scheme 51- Proposed reaction of Lycopodium clavatum and date spore with cyclam/cyclen drevatives.....	126
Scheme 52- Proposed scheme for radiolabeling of Lycopodium clavatum and date spore derivatives.....	127

Chapter 1

Introduction

1. Introduction

1.1 Non-standard organic synthesis techniques

In the last decade, less conventional organic synthetic methodologies have become a very important part of organic synthesis development. The aim is for efficient, high yielding and more sustainable processes that can avoid the extensive use of toxic and/or hazardous reagents and solvents, harsh reaction conditions, and costly catalysts.¹⁻³ The use of green chemical methodologies (the design of chemical products and processes to reduce or eliminate the use and generation of hazardous substances) is a key driver in the development of alternatives to traditional synthetic processes extensively employed in the past.³⁻⁶ Making chemistry greener is not only limited to the replacement of reagents, catalyst or solvent, but also includes unconventional, more environmentally sound ways to promote a targeted chemical transformation. These include mechanochemistry, microwave irradiation, ultrasound, and other catalyst-free and/or solvent-free methods.⁷

1.2 Non-standard methods to drive chemical reactions

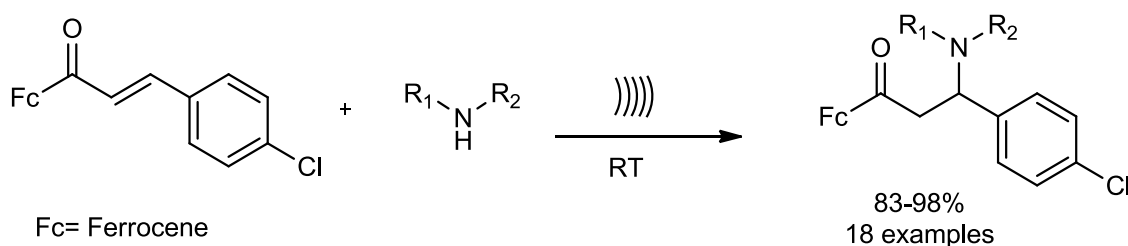
1.2.1 Sonochemistry

Ultrasonic irradiation technology (**Figure 1**) has been extensively investigated in chemical synthesis. Ultrasonic waves, passing through the liquid medium, form a large number of microbubbles which grow and collapse in an extremely short time (microseconds), and produces an effect called 'ultrasonic cavitation'.^{8,9}



Figure 1- Commercial device for ultrasonic irradiation.¹⁰

Theoretical calculations on sonochemical processes and the experimental data collected suggest that ultrasonic cavitations could generate local temperatures up to 5000 K and local pressures up to 500 atm., with heating and cooling rates greater than 10^9 K s^{-1} .¹¹ Sonication chemistry has been demonstrated to be applicable in various research fields such as nanomaterial synthesis, biodiesel production and even in food and drink pasteurization.¹² For example, Yang *et al.* successfully employed ultrasound irradiation to produce an efficient Michael addition of ferrocenylenones to aliphatic amines at room temperature and in the absence of solvents and catalysts with 0.5-2 h reaction time, see **Scheme 1**.¹³



Scheme 1- Synthesis of Michael adducts using ultrasound irradiation.

1.2.2 Microwave chemistry

In the past 25 years, the heating of chemical reactions using microwave energy, see Figure 2 has become an increasingly popular area of research in the scientific community.¹² These developments have moved microwave synthesis from a laboratory curiosity to an established method that is much more commonly used with a number of commercial devices on the market.¹³



Figure 2 - Device for microwave irradiation, see Section 6.4.2.

In 1986 an initial report on the use of microwave irradiation was published.¹⁴ Following this paper, the area blossomed with scientists publishing thousands of research articles over the next 25 years.¹³ Most of the reported examples were based on the use of microwave radiation to significantly reduce reaction times and increase purities by minimising undesirable side reactions in comparison with classical heating method.^{12,13} These enabling technological advantages have then also been exploited in the context of medicinal chemistry/drug discovery and in addition, varied fields including peptide synthesis, synthesis of polymers, material sciences, nanomaterial production and biochemical processes.¹⁵⁻²⁰ In the 21st century microwave synthesis could now be considered a well-established scientific technique with over 25 years of development.²¹ It is now much more common to use non-classical forms of heating which undoubtedly acted as driving force for the provision and availability of carefully designed commercial scientific microwave reactors optimised for chemical applications.²¹

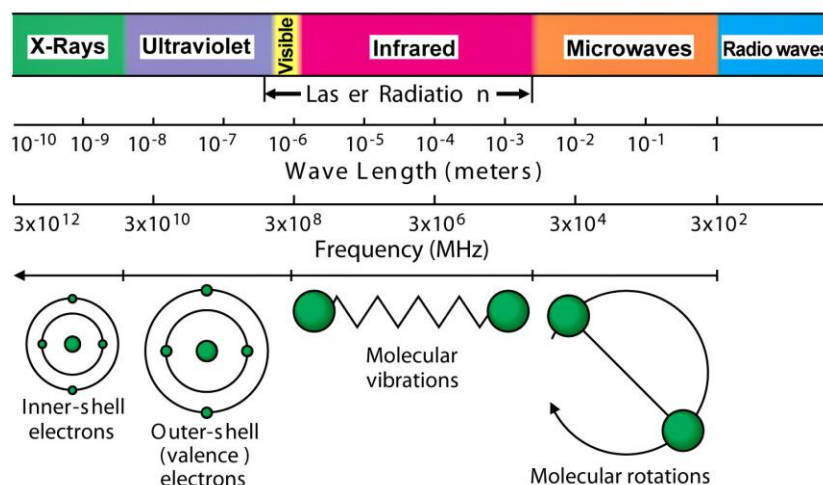


Figure 3-*The electromagnetic spectrum diagram.*

The microwave region of the electromagnetic spectrum is located between infrared radiation and radiowaves, wavelengths for microwaves are between 1 mm - 1 m, corresponding to frequencies between 0.3 and 300 GHz, see **(Figure 3)**. Molecular structure is not affected at this wavelength, the impact is a molecular rotation affect.²¹ Many of the band frequencies in the microwave region are occupied by communication and microwave radar equipment.²² Generally, in order to prevent interference, the wavelength for industrial and domestic microwave apparatus intended for heating is regulated to 12.2 cm with a frequency of (+/-0.050) GHz. Of course, the uses of microwaves for heating materials have been known for a long time, with more than a 60 year of history in development of microwave oven equipment to use in the kitchen.²³ Due to the increased interest in alternate reaction methodologies , coupled with the availability of commercial microwave equipment for organic chemistry there has been a significant recent rise in the number of publications.²²

1.2.2.1 Principles of microwave heating in chemistry

If a single-mode microwave was used to heat two samples containing water and dioxane in the same conditions (radiation power and time), the final temperature will be higher in the water sample. All electromagnetic radiation can be divided into two categories, electric field and magnetic field components. The electric field component is responsible for the dielectric heating, which is affected by two major mechanisms.²³

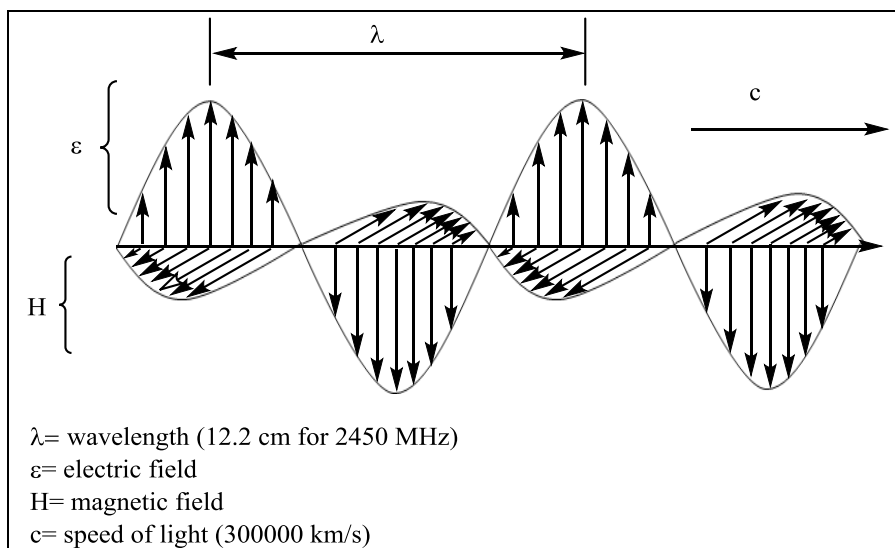


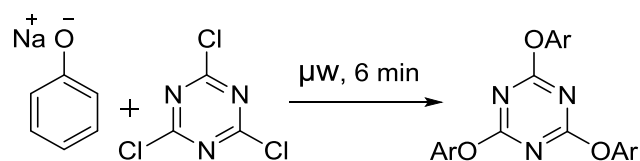
Figure 4-*Electric field and magnetic field components of microwaves*

The dipolar polarisation mechanism occurs via the interactions of the electric field component with the matrix. A dipole moment in a substance is important to generate heat by microwave (e.g. as observed in water molecules). Because of the sensitivity of a dipole to external electric fields the water molecule will attempt to align itself with the field by rotation, the energy for rotation is provided by the applied field. As a result of the low frequency in the microwave region, the dipoles can respond to the alternating electric fields and therefore rotate. The rotation frequency is not high enough to follow the field. Hence, the dipoles faces a different phase because the field is already changing. The phase difference between the orientation of the field and that of the dipole cause molecular friction and collisions to increase the dielectric heating.

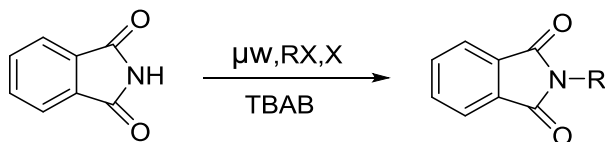
The conduction mechanism comes from the second major interaction between the electric field component and the sample. For example, if there are two samples containing distilled water and tap water heated by single-mode microwave at same condition (rotation power and time) the final temperature will be higher in the tap water sample. The reason for this phenomenon is due to the ions in the solution. The ions will move through the solution by the effect of the electric field, causing an increase in collision rates to produce heat. In comparison, the heat production for the conductivity mechanism is much greater in comparison to the dipolar mechanism. There are also other reasons influencing the heat increase when using microwave irradiation, such as interfacial polarisation, loss angle, superheating effect and modes.

1.2.2.2 Microwave assisted synthesis techniques

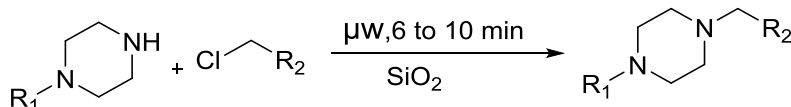
Due to the advantages associated with the process, the development of microwave assisted reactions in organic chemistry has reduced the time of reactions, decreased the cost and amount of energy required, hence it is a sustainable procedure and is commonly used as a green chemistry method.^{24,25} Microwave heating can be carried out under high pressure, to decrease reaction time and increase yield.²⁶ The reactants can also play the role of solvent if one of them is a liquid to allow reaction in a solvent free environment.²⁶ Many researchers have been working to try to improve solvent free conditions to give environmentally friendly processes.^{27,28} There are generally three different types of solvent free reactions including the use of neat reactants, solid liquid phase transfer and solid mineral support, see Scheme 2.²⁶



Formation of substituted aromatic triazines (neat reactants)



Synthesis of N-alkyl phthalimides using phthalimide, alkyl halides, potassium carbonate and TBAB (solid-liquid)

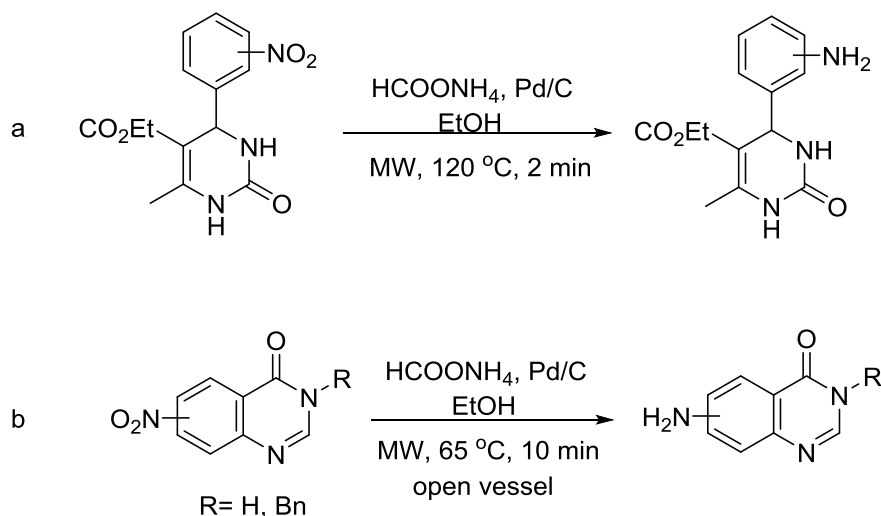


Piperidines and Chloroalkanes react in the presence of silica as the solid support

Scheme 2-Three different examples of solvent free reactions. ^{29, 30,31}

1.2.2.3 Microwave accelerated reduction and hydrogenation

Catalytic transfer hydrogenation using hydrogen donors (e.g. ammonium formate and a palladium catalyst (palladium-on-charcoal (Pd/C)) is one of the most popular reduction processes carried out under microwave conditions. There are two approaches possible for the reduction of the aromatic nitro groups to the corresponding amine when using microwave conditions; sealed-vessel conditions or open vessel. Kappe *et al.* have shown that the microwave accelerated reduction of aromatic nitro groups can be completed quickly with sealed-vessel conditions, but care must be taken not to generate too much pressure in the microwave reaction vessel due to formation of ammonia, CO₂ and hydrogen (**Scheme 3 (a)**).³² Alexandre and co-workers found that the reaction under open vessel conditions (atmospheric pressure/ reflux) are longer as the reaction temperature is limited by boiling point of solvent (**Scheme 3 (b)**).³³



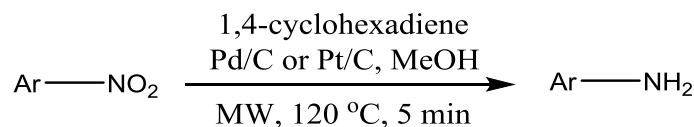
Scheme 3-*Reduction of nitro groups via microwave (sealed-vessel and open vessel)*

In 2007, Spencer and co-workers described a method for reduction of a nitro group to an amine, which was chemoselective and tolerates a broad range of functional groups, their microwave method for the reduction of nitroarenes to anilines is mediated by Mo(CO)_6 and DBU (**Scheme 4**). They found that the addition of DBU was important to increase the aniline yield.³⁴



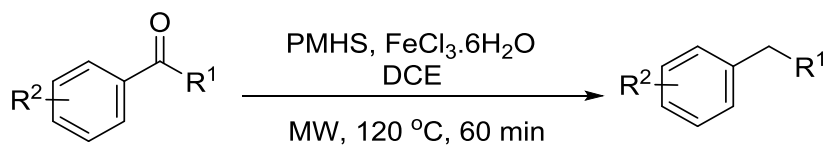
Scheme 4-*Reduction of nitro compounds with Mo(CO)_6 and DBU*

The group of Quinn used similar conditions to those described previously with a palladium catalyst to reduce the heteroaromatic nitro groups with 1,4-cyclohexadiene used as a hydrogen donor (**Scheme 5**). The resulting aryl amines are important synthetic targets and intermediates in the synthesis of biologically relevant molecules.³⁵



Scheme 5-Reduction of nitro groups using cyclohexadiene

Taddei and co-workers have reported on the synthesis of piperidines by hydrogenation of the corresponding pyridine derivative (**Scheme 6**).³⁶ They used a bespoke accessory to introduce the hydrogen gas into the microwave vial. In order to get reproducible hydrogenation, they pre-reduced PtO₂ to Pt in the presence of acetic acid with hydrogen combined with microwave heating 50 °C for 15 minutes, this was followed by addition of pyridine and refilling the vial with hydrogen.

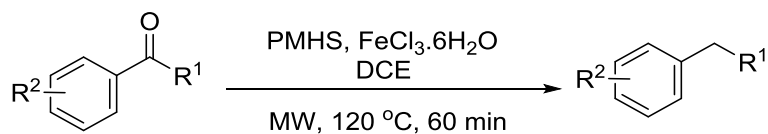


R¹= H, Me, Et, cyclic, Ph

DCE= 1,2-dichloroethane

Scheme 6-Hydrogenation of pyridines

Campagne et al. have described a suitable microwave method for the highly chemoselective reduction of ketones and aldehydes. They used polymethylhydrosiloxane (PMHS) as a reducing agent and iron(III) chloride hexahydrate as a Lewis acid (**Scheme 7**). They found, in general, that aromatic ketones gave higher yields than nonaromatic ketones.³⁷



R¹= H, Me, Et, cyclic, Ph

Scheme 7-Polymethylhydrosiloxane (PMHS) reduction of ketone

1.2.3 Mechanochemistry

Application of mechanical action such as grinding, milling, rubbing or shearing in order to induce a chemical transformation is called mechanochemistry.^{38,39} In recent years, the capacity of mechanochemistry to generate complex molecules has attracted the attention of a broad audience from different research areas such as organic chemistry and catalysis, inorganic chemistry, and has been applied to the screening of inorganic, metallo-organic pharmaceutical materials and/or nanoparticle preparations.^{40,41} For example the synthesis of peptides under solvent-free conditions by means of ball-milling activation,⁴² and quantitative synthesis of mono- and bis-(thio)ureas or mixed thiourea–ureas through a one-pot mechanochemical method.⁴³ Mechanochemistry is based on a principle that, once an intimate mixture of chemicals is subjected to a mechanical stress, frictional energy released at microscopic level is sufficient to overcome the energy barrier and produce the chemical transformation. Mechanochemical synthesis is carried out either manually using a mortar and a pestle or by employing a specialised machine such as a planetary ball mill (PBM), see **Figure 5**.⁴⁴

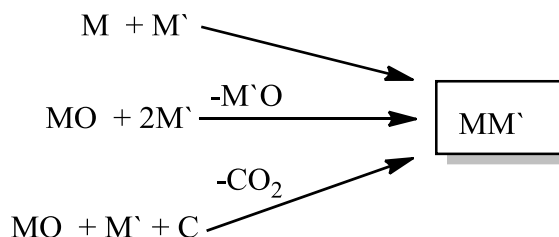


Figure 5 - Planetary ball milling equipment, see Section 6.4.1.

Manual grinding is the easiest to set up and thus the most cost-effective way to effect a mechanochemical reaction. However, it has been shown that the manual grinding method lacks the required robustness and reproducibility.⁴⁵ This is due to hard to control variations in applied force, especially for longer reaction times, which directly depend on the physical characteristics of the researcher carrying out the work. Thus, the outcome of the reaction is no longer defined by the chemistry, but by subjective factors. Use of automated ball milling apparatus overcomes this problem in giving the possibility to standardise reaction conditions by controlling different parameters including reaction time and transferred energy density.^{44,46} Two different types of ball mills are commercially available for the chemical synthesis laboratory: vibration or mixer ball mills (MBMs) and planetary ball mills (PBMs). There are reasons to prefer the use of PBM due to the potential for wet and dry reactions, fine and ultrafine grinding of particles down to the nanometre size range as well the simple set up, ease of cleaning and moderate cost of the device.^{47,48} The recent increased attention on mechanochemistry is due to its speed, high energy and solvent efficiency as compared to conventional in solution laboratory techniques.^{49,50} As a result, simple milling protocols have been improved further by developing new methods, such as liquid or/and ion assisted grinding (LAG or ILAG).^{49,51}

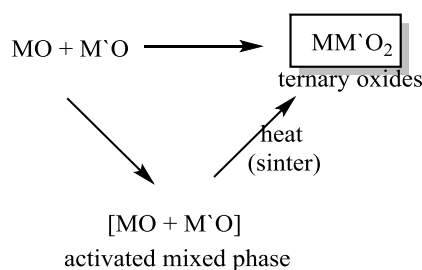
1.2.3.1 Ball milling in inorganic synthesis

Faraday (1820) reported the first example of an entirely solventless mechanochemical reaction, using a mortar and pestle to grind AgCl to produce Ag.⁵² The modern field of mechanochemistry began with mechanical alloying, using high velocity ball milling to combine elements or alloys to produce a single homogenous alloy. Nowadays the term mechanochemistry is widely used to describe this process along with chemical reactions to produce alloys and inorganic compounds using ball milling.³⁸ Through this processes there is an obvious reduction in particle size and crystallite, products are frequently in nanoparticle or amorphous phases.⁵³



Scheme 8 - General ball milling routes to alloys.

Scheme 8 shows the main routes to produce Cu-Co, Fe-Mo and Mn-Al alloys *via* a simple combination of alloys and elements in ball milling, with the boron also used to produce alloys containing boron in the Ni-Nb-B and Ti-Al-B systems. For these reactions it is typical to use argon to avoid the risk of atmospheric oxidation of the metals. These reactions generally require relatively long milling times (24 to 300 h).³⁸



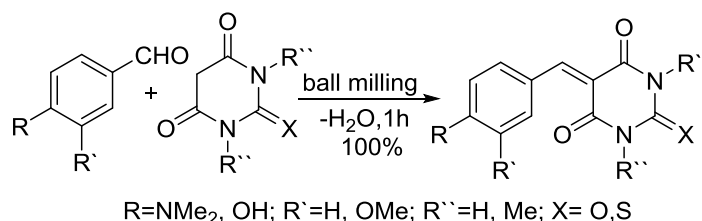
Scheme 9- Ball milling routes to metal oxides.

Inorganic oxide synthesis can be produced by mechanochemistry as well via a different route see Scheme 9. The most commonly used procedure is the mixture of different binary oxides (similar to high temperature ceramic synthesis) however this relies on the continuous fracture and mixing of the grains to create a homogenous product, as there will often be little thermodynamic driving force in the reaction itself. Numerous materials have been prepared via this method such as $CrVO_4$, $LaVO_4$ and preoveskites such as $MnFe_2O_4$ and $ZnFe_2O_4$, the mechanochemical synthesis of inorganic oxides can be carried out in the presence of air in cases where the materials are fully oxidized³⁸. They generally need short milling times between 2 and 24 hours.^{38,54,55}

Synthesis of sulphides *via* mechanochemical processes has focused principally on semi-conductor nanoparticles, through direct fusion of the metal and sulphur, this method was effective for CdS, $\text{Cd}_x\text{Zn}_{1-x}\text{S}$ and FeS.^{38,55} Metals nitrides such as TiN, ZrN, VN and CrN can also be prepared through the ball milling process with applied high pressure of nitrogen for more than 10 h. In a similar manner, ball milling metals in the presence of ammonia can produce Mo_2N , GaN, BN and Si_3N_4 .³⁸

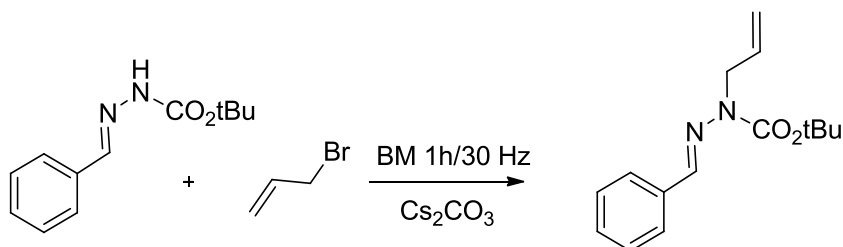
1.2.3.2 Ball milling in organic synthesis

Ball milling in organic synthesis has received more attention in recent years because it can promote reactions between solids quickly and quantitatively, and can be used in solvent free organic synthesis. Formation of C-C bonds from small building blocks to produce larger complex structures is a key area of interest. Solvent free ball milling was used by Kaupp in 2003 carried out a reaction to form C-C bonds, see Scheme 10.⁵⁶



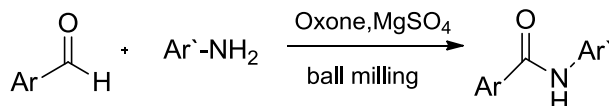
Scheme 10- Knoevenagel condensation.

Lamaty *et al* in 2011 successfully performed the *N*-alkylation of hydrazones under solvent-free conditions without the use of a metal catalyst, see Scheme 11.⁵⁷



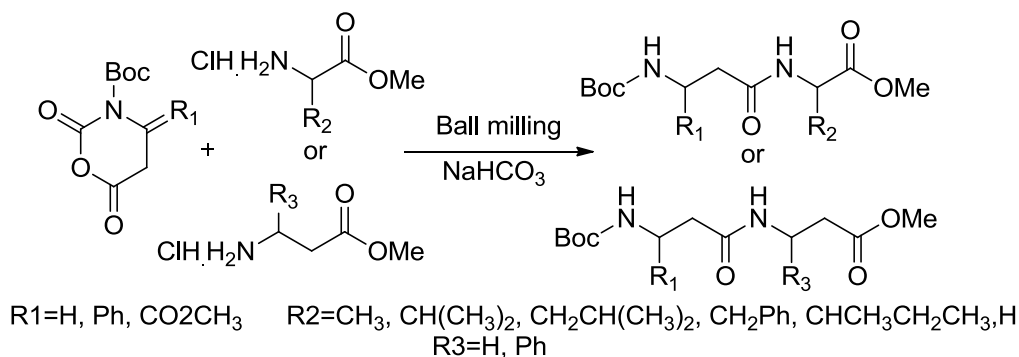
Scheme 11- Solvent-free *N*-allylation of hydrazones.

Amides play a very important role in synthetic and biological chemistry, where amide linkages constitute a defining molecular feature of proteins. The classical procedure to generate an amide functional group requires expensive transition metal catalysts and/or toxic reagents. Wang solved these problems via an improved solvent-free ball milling route for the directamidation of aryl aldehydes with anilines see **Scheme 12**.⁵⁸



Scheme 12-Direct oxidative amidation

Also, in the last few decades there has been significant progress in the area of peptide synthesis but many challenges remain. Reduction of the amount of solvent used for peptide synthesis is one of these challenges. Lamaty prepared a peptidic product under solvent free conditions with a ball milling procedure through opening of urethane-protected α -amino acid *N*-carboxyanhydrides with α -amino acid derivatives,⁵⁹ see **Scheme 13**, in the presence of NaHCO_3 as base. Different di and tripeptides were also synthesised in high yields.



Scheme 13-Solvent-free peptide synthesis.

2.2 Azamacrocyclic compounds

In the last few decades, macrocyclic compounds have been developed to play important roles in medical applications through the formation of metal complexes (chelates).⁶⁰ Azamacrocycles, such as cyclam and cyclen, form thermodynamically and kinetically stable metal ion complexes with a range of transition metals and lanthanide ions.⁶¹ These compounds can be used for magnetic resonance imaging (MRI) or as radiopharmaceuticals for cancer diagnosis and therapy.⁶²

Azamacrocycles provide multiple sites (carbon or nitrogen atoms) for functionalisation; this, coupled with the wide range of pendant arms available, has led to a large array of related, but structurally different, macrocyclic chelating ligands. The addition of a pendant arm to a macrocyclic skeleton offers a number of advantages; *(i)* it can increase the number of donor atoms for coordination to a metal centre. In this respect, pendant arms can facilitate complexation reactions, directing the metal ion into the macrocyclic cavity; *(ii)* additional functionality, useful for conjugation to other molecules of interest (bioconjugation); *(iii)* it may provide an important opportunity to modify the macrocycle properties improving biological activity; *(iv)* finally, it could be used to increase the overall stability of the chelate. These opportunities to tune the properties constitute an important part of macrocycle design.

2.2.1 Tetraazamacrocycles

Macrocycles, containing multiple electron donating nitrogen and/or oxygen atoms, either included in the cycle or attached to it via side chains, act as polydentate metal chelators.⁶³ Normally, a macrocyclic chelator contains at least three donor atoms within at least a nine membered ring. The ring size is a major factor influencing cavity size which, together with number of electron donating atoms, predetermines a macrocycle's affinity for a given metal ion. The other factors affecting stability of metal complexes are macrocycle backbone flexibility, hybridisation state and configuration of donating atoms. Due to increased electronegativity and electron orbital geometry

considerations, nitrogen containing polyazamacrocycles form stronger metal complexes with transition metal ions than oxygen containing polyoxomacrocycles.⁶⁴ Electron donating atoms can be bridged by saturated or unsaturated bonds producing more or less flexible/fixed conformations which can be further rigidified/ stabilised by additional bridging.⁶⁵ The introduction of unsaturated bonds reduces the flexibility which usually leads to a decreased propensity for metal chelation. However, pre-organisation of the macrocycle by bridging may result in more stable or preferred conformations of metal complexes.⁶⁵

Macrocyclic structures have been optimized for increased affinity towards certain type of metal, *e.g.* transition metals or lanthanide cations.⁶⁶ These complexes have been widely used as MRI contrast agents,^{62,67} luminescent probes,⁶⁸ DNA cleavage agents and radiolabelled drugs.⁶⁹

Due to the ability to form kinetically and thermodynamically stable complexes with various cations including transition metals, cyclam (1,4,8,11-tetraazacyclotetradecane) (**Figuer 6**) is one of the most used macrocyclic polyamines. Usually, metal selectivity is achieved by varying the nature of the pendant arms on the nitrogen atoms. The majority of studies have focused on synthesis and application of symmetric four-arm substituted derivatives.⁷⁰ However, there are more and more reports on targeted synthesis of mono-, di- or tri-substituted derivatives which are of interest by themselves or as intermediates in synthesis of cyclam functionalized with different arms.⁶¹ The 12 membered tetraazamacrocyclic derivatives based on cyclen with pendant arms on the nitrogen atoms, such as DOTA (1,4,7,10-tetraazacyclododecane-1,4,7,10-tetraacetic acid) are well-known azamacrocyclic compounds used in medical applications and are preorganised chelators.^{71,72}

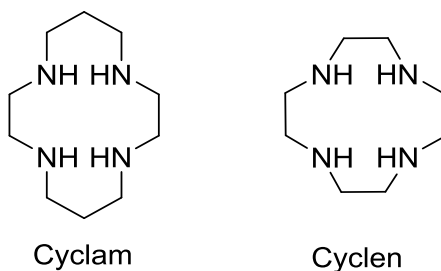
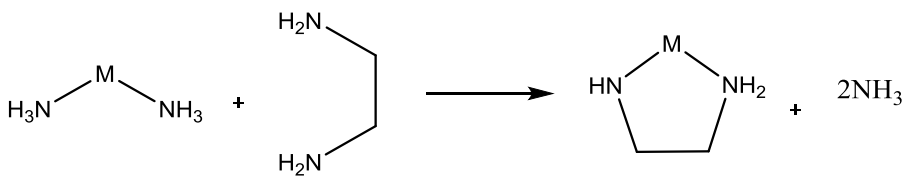


Figure 6-Structures of cyclam and cyclen

2.2.1.1 The chelate effect

In 1952 Schwarzenbach described the chelate effect. This concept explains the enhanced stability of a complex containing polydentate ligands over one having similar monodentate ligands.⁷³ The chelate effect can be explained by thermodynamic considerations: the binding entropy of the chelated complex is higher compared to the binding entropy of separate donor atoms and metal centre, enhancing the stability of the complex. 'Free' energy is gained when a bidentate or polydentate ligand binds to a metal ion in comparison to the corresponding number of monodentate ligands. **Scheme 14** illustrates the replacement of monodentate ligands with a bidentate ligand with demonstrating the increase in entropy (2 units to make 3 units).



Scheme 14-The chelate effect.

2.2.1.2 The macrocycle effect

The phenomenon that complexes containing macrocyclic ligand are more stable than complexes formed with open chain linear ligand, known as “macrocycle effect”, was first described by Cabbiness and Margerum in 1969 whilst studying copper(II) complexes with L^1 and L^2 (**Figure 7**).⁶⁵

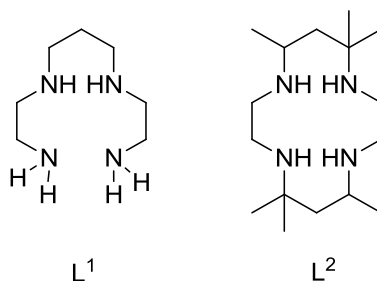


Figure 7-Linear and cyclic ligands used by Cabbiness and Margerum.⁶⁵

The decomposition of a complex formed with open chain ligands is facilitated by dissociation of the terminal donor atom from a metal centre. This is not possible in the case of closed ring systems due to the absence of terminal donor atom, thus, dissociation should follow a more complicated pathway. The macrocyclic ligand must change its conformation in order to weaken one of the metal - donor atom bonds and initiate the dissociation (**Figure 8**). The change of conformation is energy prohibitive which results in less probable dissociation/ more stable complex.

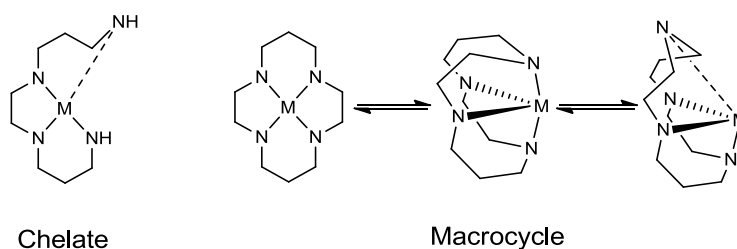


Figure 8-First donor dissociation in linear chelate vs macrocycle.⁷⁴

2.2.1.3 Restricted cyclam/cyclen

The first reports of the synthesis of the internally ethyl bridged macrocycles were from Wainwright and Hancock in the 1980s,^{75,76} followed by Weisman and Wong in the 1990s.⁷⁷ The addition of an ethylene bridge, either between opposite or adjacent nitrogens, results in structurally restricted macrocyclic skeletons. Cross bridge (CB) structures are formed when opposite nitrogens are connected. Connection of adjacent nitrogens results in side bridged (SB) structures, see **Figure 11**.

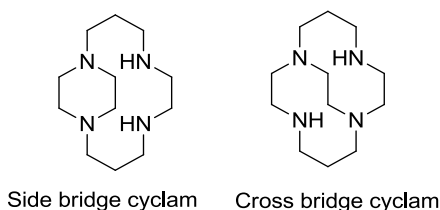


Figure 9- Ethylene bridge between adjacent nitrogens (SB) or opposite nitrogens (CB) forming side or cross bridged macrocycles respectively.

Strengthening the structural backbone reflects on many parameters including flexibility, basicity, ring size, steric strain and, most importantly, configuration. Reduction of internal glyoxal bridge on mono-N-alkylated derivative leads to side bridged cyclam, when reduction of bis-N-alkylated intermediate results in cross bridged derivative. Addition of either SB or CB ethylene bridges restricts cyclam macrocycle in one preferential configuration.

Similar side-bridged and cross-bridged macrocyclic species have been synthesised using cyclen.⁷⁸ The synthesis of the bridged species, first published by Wainwright and co-workers in 1982, was carried out using 1,2-dibromoethane.⁷⁸ CB cyclen was formed starting from bis-N-alkylated intermediate, while alkylation of mono-N-alkylated precursor, generated the side bridged cyclen see **Figure 10**.

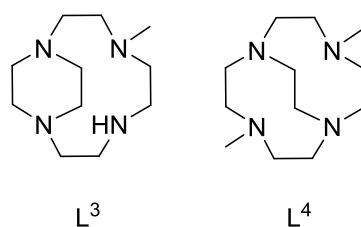


Figure 10-Structure of side bridged SB L³ and cross bridged CB L⁴ cyclen

2.2.1.4 Application of azamacrocycles

In the last decades, research in medicinal inorganic chemistry started to expand by exploiting a variety of chelating ligands to modify and control the properties in various systems.⁷⁹⁻⁸¹ Macrocyclic chelators form complexes with high thermodynamic and kinetic stability when complexed with transition metals.^{60,61} As already mentioned, the affinity of tetraaza macrocycles for a given metal depends on ring size, macrocycle backbone flexibility, and the nature and number of coordinating atoms. Thus, different macrocyclic polyamine derivatives have been produced exhibiting increased affinity and concurrent complex stability towards certain metal cations (transition metal or lanthanide).⁶⁶ Depending on the chelated metal, tetraazamacrocyclic complexes have found use in a range of applications. The majority of applications relate to medical imaging agents such as MRI contrast agents containing gadolinium(III),^{62,82} optical agents containing europium(III) and terbium(III),⁸³⁻⁸⁵ along with nuclear medicine probes with gallium-68,^{86,87} technetium-99m^{88,89} and copper-64^{90,91} amongst others. Tetraazamacrocyclic complexes with various metals have also been used as protein binding agents,^{92,93} anti-malarial drugs^{94,95} and as catalysts.^{41,96}

2.2.1.4.1 Catalyst development

The use of metal complexes with suitable ligands in catalysis plays a very important role in the understanding of reaction mechanisms and widening of the scope of synthetic chemistry.⁹⁷ Kinetic and thermodynamic stabilities of metal complexes, subjects of previously described chelator and macrocycle effects, are important in

determining their efficacy as catalysts.⁹⁸ Many-oxidising enzymes contain a metal centre, usually iron, fixed in macrocyclic porphyrin system,⁹⁹ which has been extensively mimicked using synthetic ligands yielding a variety of rationally designed oxidation catalysts. As an acyclic example, Salen, bis(salicylal-ethylenediimine), a prototype of tetra- and pentadentate Schiff-base ligands, which has been successfully applied in asymmetric oxidations, can be cited.^{97,100}

Rigid macrocyclic ligands (bridged cyclam derivatives) have been extensively used in catalyst design due to their ability to strongly bind transition metal ions via four coordination bonds, leaving two coordination sites on the metal free for interaction with substrate and/or oxidant.^{101,102} Weisman and collaborators were the first to report CB cyclam complexes with copper and zinc and to investigate their application, see **Figure 11**.^{77,103}

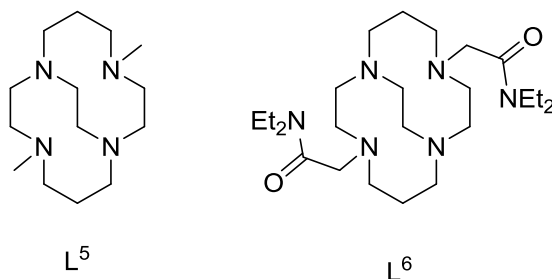


Figure 11-Macrocyclic ligand cross bridged cyclams

Transition metal complexes with the ethylene cross-bridged cyclam ligand, Me₂EBC (L⁵) (4,11-dimethyl-1,4,8,11-tetraazabicyclo[6.6.2]hexadecane), received more attention as their kinetic stabilities were expected to be exceptionally high,^{97,104} even with such labile metal ions as manganese(II).⁹⁴

2.2.1.4.2 Radiopharmaceutical development

In recent years, research in medicinal inorganic chemistry has expanded by taking advantage of a diversity of chelating ligands to modify and control the properties of metal ions in biological systems.¹⁰⁵ Macrocyclic complexes of Gd^{3+} have been widely used as MRI contrast agents.^{62,67} Currently, most chelators which are used as contrast agent in MRI are based on 12-membered cyclen (L^8) and 14-membered cyclam (L^9), see **Figure 12**.¹⁰⁶

Functionalisation of macrocyclic compounds through an NH group opens up wider biomedical application for this chelator as a multipurpose construct for use in many of imaging techniques via varying the metal centre (*e.g.* ^{111}In for SPECT imaging, ^{177}Lu or ^{90}Y for radioimmunotherapy, ^{86}Y for PET imaging).^{83,105,107}

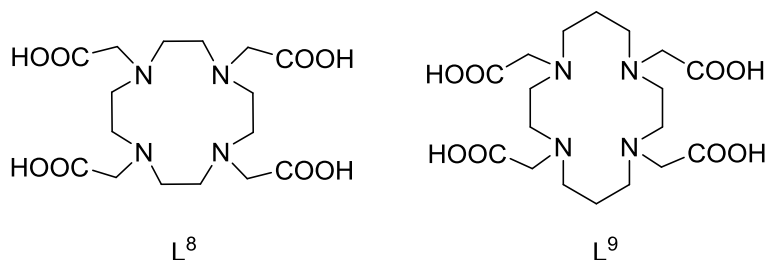


Figure 12-Structure of tetraacetic acid derivatives of cyclen DOTA L^8 and cyclam TETA L^9

Macrocycles are also used in positron emission tomography (PET), see **Figure 13**. The imaging technique relies on the radionuclide being delivered selectively to the target area (the tumour), the tight binding of the radionuclide is required to achieve high thermodynamic stability *in vivo* whilst also being kinetically inert.⁶¹ Most bifunctional chelators used for $^{64/67}Cu$ isotopes are based around the cyclam and cyclen macrocycles because in addition to the complexes meeting the previously stated requirements of kinetic and thermodynamic stability, such ligands can rapidly coordinate metal ions and require resistance to transmetallation *in vivo*.¹⁰⁸⁻¹¹⁰

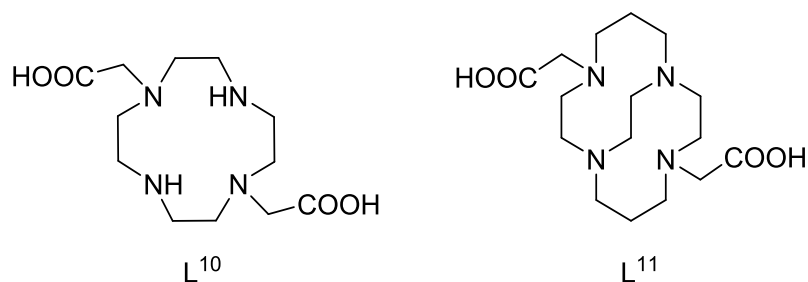


Figure 13-Chemical structure for DO2A L^{10} and CB-TE2A L^{11}

2.2.1.4.3 Metal complexes with affinity to proteins

In recent years, metal complexes able to bind directly to biological target proteins have received a great attention for their potential use as diagnostic probes or in therapy. For example, Caravan and co-workers have prepared gadolinium(III) complex, L^{12} (**Error! Reference source not found.**), which binds to human serum albumin and could be used as a contrast agent to visualise blood pool by MRI imaging.⁸²

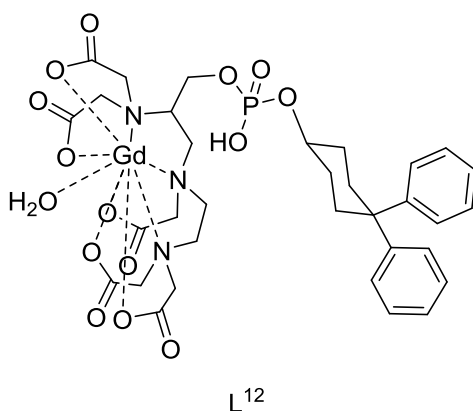


Figure 14-Gadolinium(III) complex

Protein binding can be accomplished either through coordination of the metal centre with amino acid side chains of the protein, or via weak ionic interactions between macrocyclic ligand and the protein.¹¹¹ Binding of macrocyclic complexes with proteins via coordination of metal centre requires suitable coordinating moieties to be available on the protein target and the macrocyclic chelator to have coordination sites displayed

correctly in space. This opens possibilities for the design of protein targeting pharmacophores which take into account not only secondary interactions, but also coordination interactions.⁶⁴

CXCR4, a chemokine receptor involved in the HIV infection process and in the metastatic spread of some cancers, is a prime example of a protein biological target targeted by metal complexes. De Clercq and co-workers in 1995 synthesised a series of bicyclams and tested their activity against HIV. They found AMD3100 (**Error! Reference source not found.**) can act as an HIV inhibitor by blocking the virus entry into cells.¹¹² These bicyclams were non-restricted, hence the formation of less stable metal complexes. Archibald and co-workers synthesised a xylyl linked SB bicyclam, which has high activity against HIV. This group went on to prepare a CB bicyclam derivative (**Error! Reference source not found.**), and confirmed that its copper(II) complex not only has high affinity for the CXCR4 receptor in cellular assays, in comparison to AMD3100, but also an increased residence time at the receptor.¹¹³ This results reflect the ability of the copper(II) complex to form coordination bonds with aspartate residues in the receptor binding pocket rather than the H-bonding interactions for AMD3100.

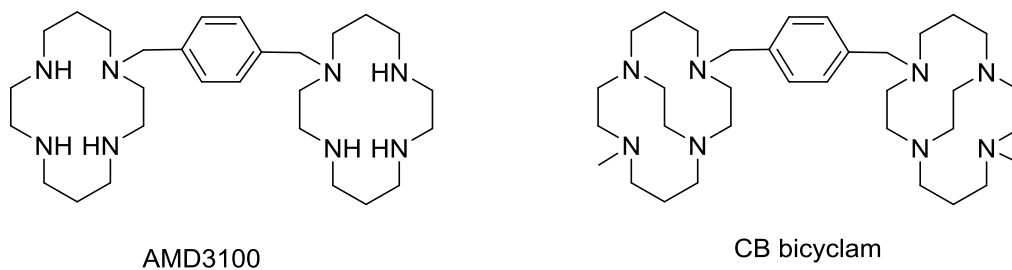


Figure 15-Chemical structure of the bicyclam AMD3100 and Bis CB cyclam.

2.3 Overall aim of this research

Non-standard organic methodologies offer several benefits over traditional methods, as described in Section 1.2.3. Mechanochemistry has not yet been exploited in the synthesis of macrocyclic compounds or the functionalisation of biopolymers. The aim of this work is to combine these aspects and to validate radiolabelling of the materials for potential future medical imaging studies.

The key aims were to:

- Generate new synthetic protocols for macrocyclic molecules with challenging syntheses to increase efficiency
- Investigate sporopollenin biomaterials and methods for surface functionalisation
- Determine protocols for stable radiolabelling of sporopollenins to allow study and tracking *in vivo* in future investigations of these materials in drug delivery applications.

Chapter two details the utilization of mechanochemistry on various glyoxal-bridged cyclen and cyclam derivatives to improve upon them by reducing reaction times and increasing the yields. In Chapter three the relatively unexplored natural polymer (date spore) is characterised *via* a series of modifications studies and surface functional groups available for reaction are generated. Chapter four, includes details of using mechanochemistry for surface modification of sporopollenin (extract from *Lycopodium clavatum* L.C) and subsequent gallium-68 radiolabelling to generate a tool that can potentially be used to understand the behaviour of sporopollenin *in vivo*.

Chapter 2

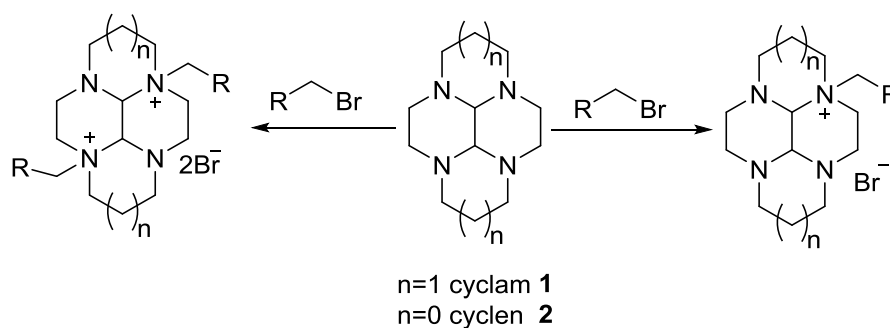
Efficient mono- and di-alkylation of
glyoxal-bridged tetraazamacrocycles
via mechanochemistry and
microwave irradiation

1. Efficient mono- and di-alkylation of glyoxal-bridged tetraaza macrocycles via mechanochemistry and microwave irradiation

2.1 Aims

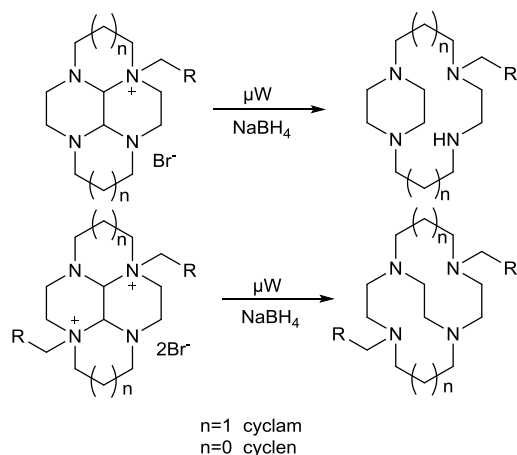
The overall aim of the work presented in this chapter is to describe the synthesis of various structurally reinforced cyclen and cyclam azamacrocyclic derivatives in a more efficient manner than the currently applied methods (see Section 2.3.3.1) by employing grinding and microwave methodologies. This can be sub-divided into the following goals:

(i) Application of mechanochemical activation to alkylation of bridged cyclam and cyclen derivatives with various alkyl halides (**Figure 15**) with an aim to reduce long reaction times (Section 2.3.2).



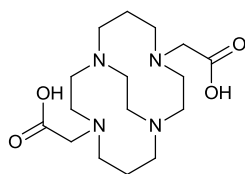
Scheme 15-Synthetic pathway to mono and bis substituted cyclam/cyclen azamacrocyclic derivatives

(ii) Application of microwave activation for reduction of macrocyclic precursors to side-bridged and cross-bridged derivatives (**Figure 16**) with an aim to shorten reaction times and to minimise the amount of reducing reagent required (Section 2.4.4).



Scheme 16-Synthetic pathway to SB and CB cyclam/cyclen

(iii) Combine ball milling and microwave activation techniques to reduce the reaction time required for the synthesis of precursor for CB-TE2A (**Figure 16**), an important copper(II) chelator used to form radiopharmaceuticals (Section 2.3.5).



CB-TE2A

Figure 16-Chemical structure of CB-TE2A

2.2 Development of bifunctional chelators (BFCs)

A bifunctional chelator (BFC) is a molecular reagent that contains three main parts: a ligand framework (A) linking a conjugation group (B), which could be used to attach a targeting moiety, to a binding unit (C), responsible for chelating the metal ion (**Figure 17**). BFCs play an important role in targeting of radiopharmaceuticals to different tissues or malignant growths. Bifunctional chelators (BFC) commonly used in radiopharmaceuticals in medical imaging often derive from N-functionalised azamacrocycles.^{108,114} An ideal BFC should fulfill a set of requirements.¹¹⁵ It should coordinate to the radionuclide in a high yield to form a stable complex. The chelator should prevent any accidental changes of redox potential and it must be suitable for the nature and oxidation state of the radionuclide. Moreover, additional attention should be given to the selection of the bifunctional chelator in order to assure its stability under particular conditions that may be required for the conjugation reaction with the targeting molecule, *i.e.* pH, temperature, reaction time. The stereochemistry of a BFC is important when synthesising radiopharmaceuticals targeting for specific receptors.¹¹⁶ The high thermodynamic stability and kinetic inertness of metal complexes with BFCs at neutral pH are important in order to keep the metal chelate intact under physiological conditions.^{105,117} The *in vivo* decomposition of metal chelates would release free metal ions which are often attracted to bones and may cause bone marrow toxicity.¹¹⁸ The biological stability of BFC complexes can be assured by respecting basic coordination chemistry principles, such as, using charged donor groups choosing a suitable ligand denticity, and creating a chelating cavity size appropriate to the ionic radius of the radionuclide.¹¹⁹

The bifunctional chelators used for $^{64/67}\text{Cu}$ are often based on cyclam macrocycle.¹⁰⁸ Whereas, cyclam ligands are well suited for copper(II) complexation, because the formed complexes are highly stable, kinetically inert and resist well to the copper(II) exchange *in vivo* (**Figure 17**).

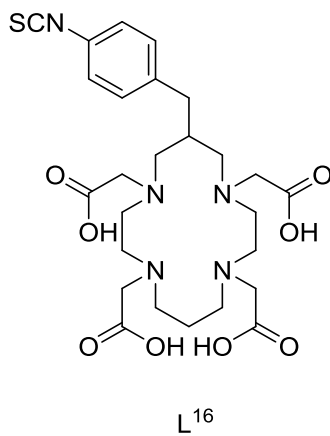
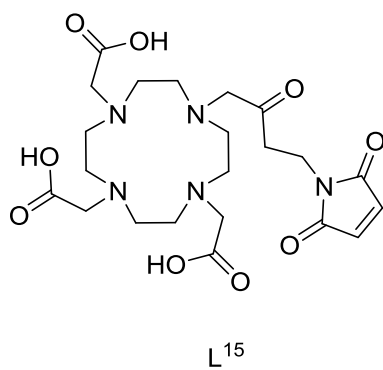
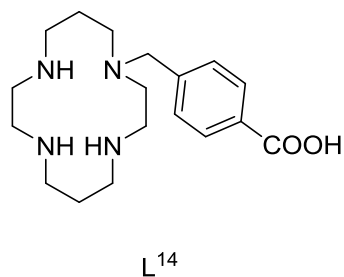
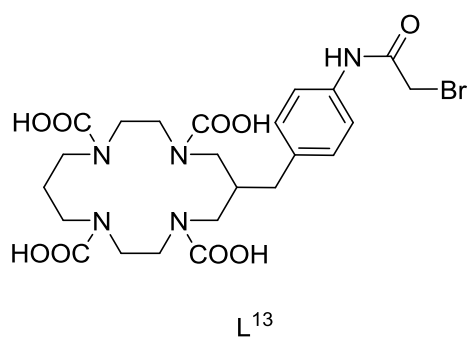
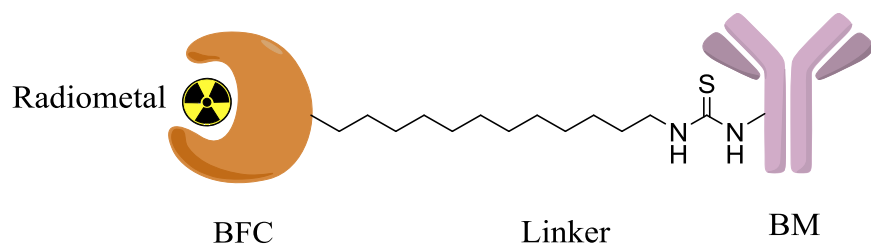


Figure 17-Cyclam/cyclen based chelators undergoing trials for PET imaging and radiotherapy¹²⁰⁻¹²²

2.3 Positron Emission Tomography (PET)

Positron Emission Tomography (PET) imaging has been accepted in a clinic as a reliable diagnostic method offering advantages such as good resolution, high sensitivity and accurate quantification of results.¹¹⁷ A very small amount of radiolabelled tracer is needed to image a biological process, therefore, it can be administered to the patient without any pharmacological effect.¹²³ The most common PET radioisotope – fluorine-18 – is quite short lived ($t_{1/2}=109.8$ min), thus, is not suitable for imaging longer biological processes. Moreover, it is cyclotron produced which increases the costs and as a consequence limits its availability.^{123,124} Positron emitting radiometals, such as gallium-68, are produced in generators which can increase availability.¹²⁵ However, metals are often toxic and need to be chelated in order to be biocompatible,¹¹⁸ thus, research in metal chelators are of increasing importance.¹²⁶ Apart from clinical diagnostic application, PET imaging plays an important role in the process of drug development and evaluation.^{127,128}

When the tracer is injected into the subject, its radionuclide decays by emitting a positron which travels a short distance before a collision and annihilation with an electron. Two, almost opposite, annihilation γ -rays (photons) of 511 keV are generated and can be detected by a circular array of the gamma cameras constituting a PET scanner. Once data are processed by computer, a 3D image of tracer accumulation in the body can be created, revealing, presence or absence of biological targets or phenomena (**Figure 18**).¹¹⁷

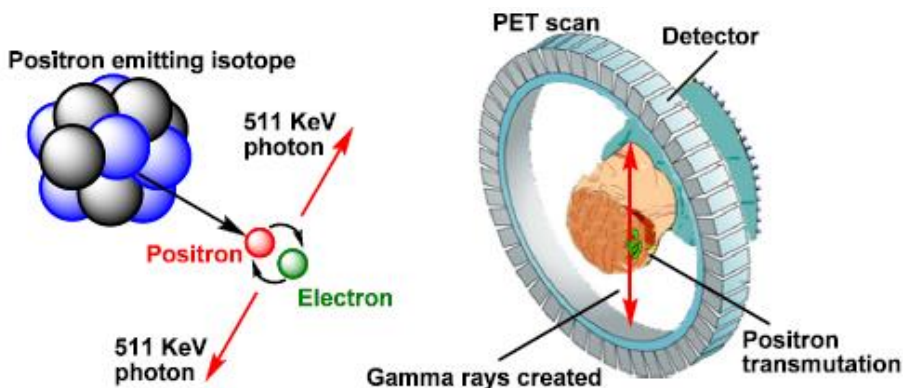


Figure 18-Schematic representation of the principle behind PET.¹¹⁷

The choice of the PET radionuclide depends on the biological process one wants to study.^{129,130} In particular, physical half-life plays an important role in radionuclide selection, because, on one hand, it should allow the chemical incorporation (radiolabeling reaction) of the radionuclide in the tracer, and on the other hand, match its biological half-life in order to avoid unnecessary radiation exposure and to obtain good target to background detection ratio.¹¹⁷

2.3.1 ⁶⁴Cu as a radiometal for PET

At present, much attention has been focused on copper-64, a longer-lived positron emitting radionuclide ($t_{1/2} = 12.7$ h), which has favourable properties for radiotherapeutic applications and diagnostic PET imaging of longer biological processes.¹³¹

Bifunctional chelators BFCs have been utilised to make stable complexes with ⁶⁴Cu *in vivo* to targeting biomolecules.¹³² Given the longer expected presence of ⁶⁴Cu complexes in the body in order to achieve a high uptake of the copper radionuclide in the tissue or organ of interest, the *in vivo* stability of the complex is paramount. Acyclic chelators, such as EDTA, DTPA and their derivatives, have been utilised for complexing ⁶⁴Cu, however, the stability of these chelates are low *in vitro* and *in vivo* (Figure 19).^{117,133,134} To enhance the *in vivo* stability, researchers have turned to chelators that

take advantage of both the macrocyclic and chelate effects, see Section 1.2.1.1 and section 1.2.1.2. TETA, DOTA and NOTA are the most important chelators studied (Figure 19).¹³⁵ It was found that DOTA, TETA and their derivatives offered limited *in vivo* stability resulting in dissociation of ^{64}Cu from these macrocycles and its high retention in liver. Recently, a great improvement in ^{64}Cu chelation chemistry came into sight when propyl CB-TE2A was synthesised. It can be metallated at room temperature and retains chelating properties of its parent ethyl bridged cyclam but further *in vivo* validation is required.¹³⁶ A kryptand based chelator, AmBaSar (Figure 19), is another example of azamacrocycle forming an extraordinary stable ^{64}Cu complexes *in vitro* and *in vivo* under physiological conditions.¹¹⁷

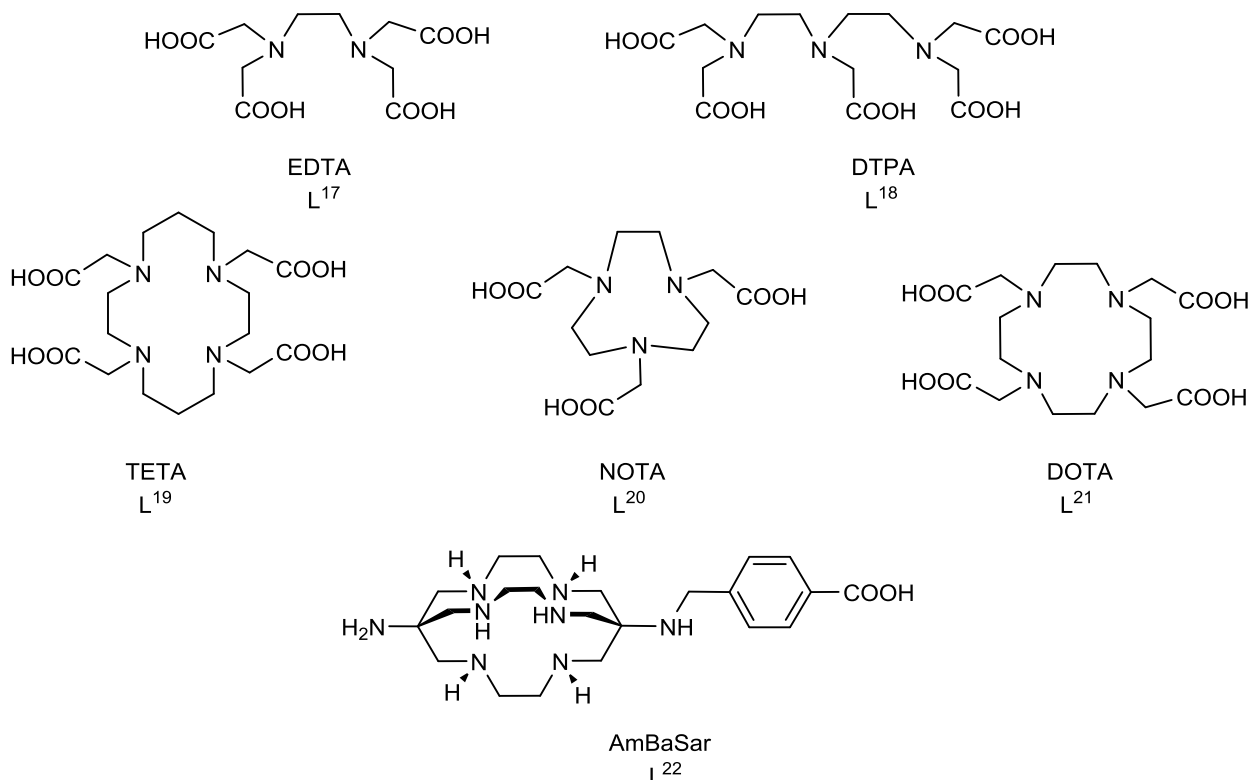


Figure 19-Representative chelators for ^{64}Cu labelling

2.4 Preparation of BFCs via mechanochemistry

2.4.1 Glyoxal-bridged tetraazamacrocycles as BFCs

BFCs are usually prepared by functionalisation of azamacrocyclic ligands through either the nitrogen or carbon atoms. Due to the wide diversity of potential pendant arms available, a large array of related but structurally different macrocyclic ligands have been generated. There are a number of advantages to incorporating pendant arms on the macrocycles. Foremost, the number of donor atoms for coordination to a metal centre can be increased which facilitates complexation reactions, guiding the metal ion into the macrocyclic cavity. Further, a pendant arm can function as an attachment point to attach the chelator to targeting molecules of interest. These advantages are significant and must be taken into account when designing macrocyclic ligands.

When an ethylene bridged is added to form a bisaminal, only one configuration (cis) is formed which can be selectively mono-*N*-alkylated and used to form the SB cyclam chelators, bis-*N*-alkylation presents the possibility to form CB compounds. Archibald *et al.* have synthesised SB ligands with functional pendant arms, such as nitrophenyl, aminophenyl and carboxylic acid derivatives (**Figure 20**).^{93,137}

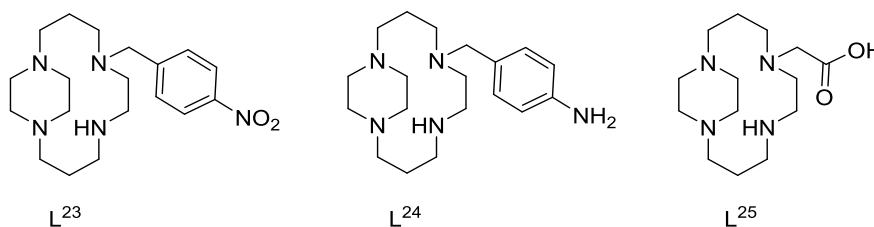


Figure 20-SB Monocyclam ligands bearing functional pendant arms

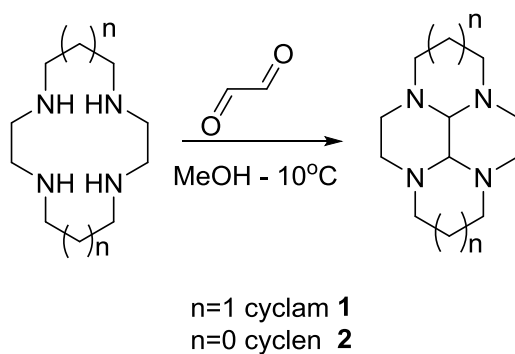
Weisman and Wong were the first researchers to report the synthesis of a CB cyclam compound and Bencini, a few years later, published the synthesis of the analogous CB cyclen compound.^{77,138} Wong and co-workers detailed the synthesis of CB-TE2A in 2000 and an analogous CB-cyclen derivative CB-DO2A was also synthesised by the same group (**Figure 21**).¹³⁹ Boswell *et al.* studied the *in vivo* stability of ⁶⁴Cu²⁺

Chemical structures of the ligands are shown below:

CB-TE2A

CB-DO2A

Configurationally restricted azamacrocycles are accessible from glyoxal bridged intermediates which are easily prepared as described by Handel and Le Baccon by reacting the azamacrocycle precursor (cyclam/cyclen) with glyoxal in methanol at -10°C (**Scheme 17**).¹⁴¹



36

The addition of glyoxal to rigidify the carbon skeleton allows for control of the reactivity of the amine groups as forces the resulting macrocycle into the *cis* configuration (**Figure 22**). This configuration gives two nitrogen lone pairs pointing out of the structural cavity (termed *exo*) and two lone pairs pointing into the structural cavity (termed *endo*), making only two of the four nitrogen positions (*exo* lone pairs) available for reaction.

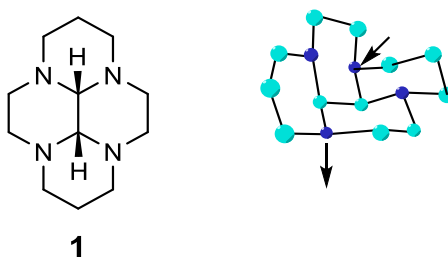


Figure 22-Molecular structure of bridged cyclam on left (*cis* configuration). Ball and stick representation on right, indicating the presence of two *exo* and two *endo* lone pairs. Grey = carbon atoms, blue = nitrogen atoms.

2.4.3 Alkylation of bridged macrocycles

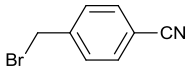
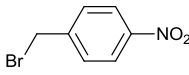
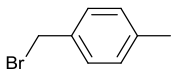
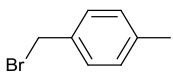
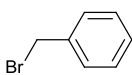
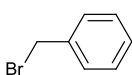
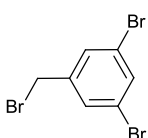
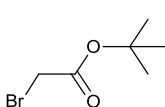
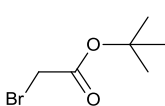
A large number of research groups have paid considerable attention to the production of pendant arm derivatives of macrocycles due to the realised and potential applications in radiopharmaceuticals, catalysis, and biomimetic chemistry.^{142,139} From the two dimensional structures of azamacrocycles, one would expect that all nitrogen atoms are in the same environment and should react in a similar fashion. However, this is not always the case, as explained in Section 2.4.2. For glyoxal bridged cyclam, the initial alkylation take place on one of the more sterically accessible *exo* nitrogens. The second alkylation, which is usually slower than the first alkylation, occurs on the second *exo* nitrogen, which is less sterically hindered than the remaining *endo* nitrogens.¹³⁹ Under conventional conditions, alkylation of glyoxal-bridged cyclam by different benzyl or alkyl bromides proceeds slowly (from 16 h to 21 days) and/or requires a large excess of

alkylating reagent as the second alkylation process is slow and the bridged species is sensitive to elevated temperatures.^{143,144}

2.4.3.1 Alkylation of bridged cyclam with various alkyl halides via conventional methods

Conventional “in solution” chemistry can provide access to mono *N*-alkylated glyoxal bridged macrocycles, however, this transformation requires a large excess of the alkyl bromide reagent and, dependent on reactivity of the alkyl bromide, may take several days, **Table 1** is a compilation of some examples from the literature for *N*-alkylation of bridged cyclam.^{139,145}

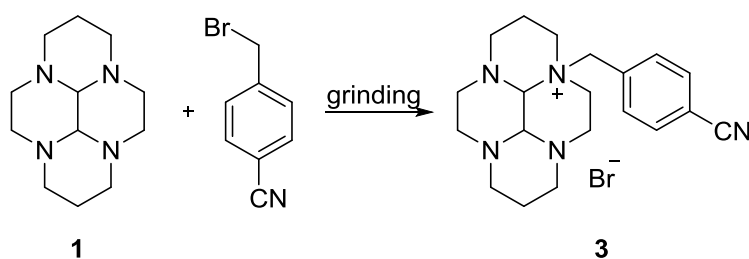
Table 1. Conventional method for alkylation of bridged cyclam with various alkyl halides

Br-R	Macrocycle / alkyl bromide ratio	Time	Alkylation yield, %	Product	Ref
	1 : 2.5	2 days	78	3	146
	1 : 4	24 hours	87	4	146
	1 : 1	16 hours	85	5	146
	1 : 3	24 hours	93	17	146
	1 : 4	16 hours	88	6	146
	1 : 16	16 days	85	18	146
	1 : 1	16 hours	82	7	146
	1 : 4	16 hours	93	8	146
	1 : 15	21 days	70	20	146

The reaction is usually stopped at the mono-alkylation stage by selection of a suitable solvent and reagent concentration/ ratio, to cause the precipitation of a mono-substituted product.¹⁴⁷ Di *N*-alkylation, under conventional conditions, is even more challenging due to the reduced reactivity of the second *exo*-nitrogen and may require up to three weeks reaction time to reach completion (see **Table 1**).^{143,147}

2.4.3.2 Alkylation of bridged cyclam with 4-cyanobenzylbromide via mechanochemistry

The alkylation methods for bridged cyclam reported in literature are time consuming and require a large amount of alkyl halide and organic solvent, hence are ripe for improvement. Therefore, in this work, and in an effort to address these issues, mechanochemistry has been used as novel methodology. The initial experiment in this investigation was grinding glyoxal bridged cyclam with 4-cyanobenzyl bromide in the presence of a small amount of acetonitrile (90 μ L) for a relatively short period of time (30 minutes), which gave a mono N-substituted macrocycle (**3**) in quantitative yield (Table 2 and Scheme 18).



Scheme 18-Synthetic pathway for alkylation of bridged cyclam with 4-cyanobenzylbromide.

Increasing the amount of alkyl bromide to 4 equivalents and grinding time up to 3 h did not improve the already impressive 98% yield for mono-4-cyanobenzyl substitution (**3**). This discovery encouraged investigation of this method for the preparation of compounds using various alkyl bromides, followed by application of this methodology to the analogous macrocycle cyclen and cyclam see Section 2.4.3.3 and 2.4.3.5.

Table 2. Grinding method for alkylation of bridged cyclam with 4-cyanobenzylbromide.

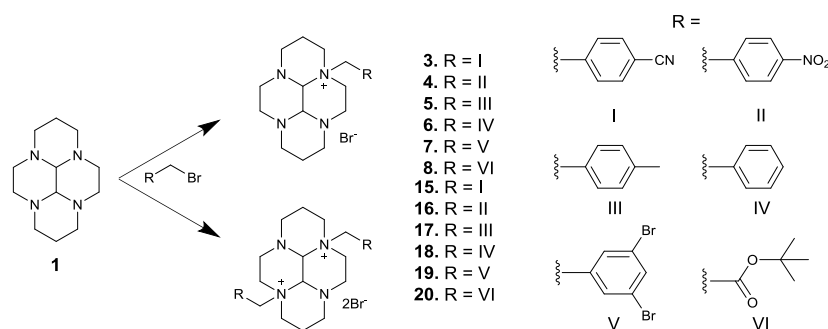
Product	Ratio	Br-R	Time	Alkylation yield ^a , %	Ref
3	1:1		30 minutes	97 ± 2 ^b	This work
3	1:4		3 hour	98	This work

^a Alkylation yield is based on the macrocycle and is calculated by dividing the mass of product(s) obtained by the theoretical mass. ^b An average of three independent experiments

2.4.3.3 Alkylation of bridged cyclam with various alkyl halides via mechanochemistry

Various alkyl bromides (4-methylbenzyl, benzyl, 4-nitrobenzyl and 3,5-dibromobenzyl bromides, and *t*-butyl bromoacetate) were used in the series of reactions. The choice of the alkyl bromides was guided by mechanistic and future application considerations: (i) 4-cyano and 4-nitrobenzyl substituents are of interest for a subsequent reduction to benzylamine or aniline derivatives and the use of the resultant amino group for a further bioconjugation purposes to generate bifunctional chelators.^{83,92,148} (ii) Di-*N*-substituted non-functionalised benzyl and tolyl derivatives are key intermediates in cross-bridged cyclen / cyclam synthesis.^{95,149} (iii) *N*-*t*-butyl acetate derivatives can be deprotected to reveal free carboxylates which can either act as supplementary metal chelating groups or, again, be used for bioconjugation.^{143,150} Reactivity of benzyl bromides is governed by the nature of the phenyl ring substituents which effect electron density and the distribution of partial charges on the different atoms of the molecule. Highly reactive bromides would be preferred for synthesis of di-alkylated products, whereas less reactive bromides might be of interest for preparation of exclusively mono substituted derivatives.

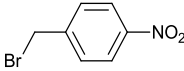
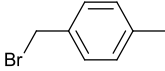
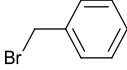
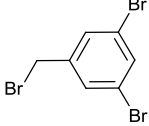
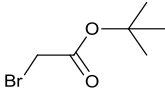
Mechanochemical alkylation of glyoxal-bridged cyclam and cyclen was carried out using a planetary ball mill (PBM) apparatus under LAG conditions (90 μ L acetonitrile) at a 100 mg of azamacrocycle scale. Grinding of the bridged cyclam with a stoichiometric amount of 4-nitrobenzyl, 4-tolyl, benzyl, 3,5-dibromobenzyl bromide or *t*-butyl bromoacetate for 30 mins produced only mono-*N*-substituted derivatives **3-8** with isolated yields of 98%, 85%, 90%, 81%, 64% and 34% respectively (**Scheme 19** and **Table 3**).



Scheme 19-General schematic for mono- and bis-N-alkylation of cyclam

Bis-substitution of bridged cyclam was attempted by employing a four-fold excess of the same series of alkyl bromides and using a 3 h grinding time (**Table 4**). These optimised conditions were determined after multiple trials while varying reaction time, the ratio of reagents and the number of grinding balls. The reaction of 4-tolyl benzyl bromide to form **7** was carried out using a 1:1 molar ratio for 3 hours showing no significant increase (< 5%) in yield.

Table 3. 30 minutes grinding of bridged cyclam with various alkyl bromides

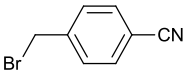
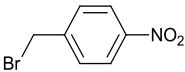
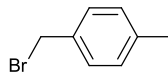
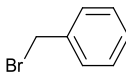
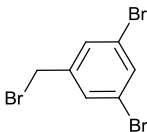
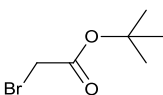
Product	Br-R	Alkylation yield ^a , %	Ref
4		85	This work
5		89 ± 1^b	This work
6		81	This work
7		64	This work
8		32	This work

^a Alkylation yield is based on a macrocycle and is calculated by dividing the mass of product(s) obtained by the theoretical mass for a given mixture of mono-armed and doubled-armed products. ^b An average of three independent experiments.

An attempt was made to optimise the conditions required to either (a) increase the yields of the mono-substituted products or (b) drive the reactions to form the bis-substituted compounds. As mentioned before, increasing the amount of alkyl bromide to 4 equivalents and grinding time up to 3 hours did not improve already impressive 98% yield for mono-4-cyanobenzyl substitution (**3**), but did increase the *t*-butyl bromoacetate mono-substituted product (**8**) yield to 50% and allowed to push the 4-nitrobenzyl and 3,5-dibromobenzyl bromide mono-substitution reactions almost to completion (98% (**4**) and 92% (**7**), respectively, **Table 4**). These alkyl halides did not react further to form bis-alkylated macrocycles upon increase of reaction time and/or molar ratio. The use of benzyl bromide under these conditions gives a 2 to 1 mixture of mono (**6**) and di (**18**) *N*-substituted compounds, but when 4-tolyl bromide was used, exclusively di-*N*-substituted derivative (**17**) was obtained in an almost quantitative 95% yield (**Table 4**). It is worth noting that the reactivity of the different benzyl/alkyl bromides observed in the mechanochemical syntheses mirrors that of the conventional in solution reactions, *i.e.*

even when used in excess, deactivated 4-nitro and 3,5-dibromobenzyl bromides gave exclusively mono-substituted products (**Table 4**) and only the use of an excess of the reactive 4-tolyl bromide yielded a pure di *N*-substituted product (**Table 4**).

Table 4. 3 h grinding of bridged cyclam with various alkyl bromide

Product	Br-R	Alkylation yield ^a , %	Ref
2		98 ± 1^b	This work
4		98	This work
17		95 ± 1^b	This work
6^c		99	This work
7		92	This work
8		50	This work

^a Alkylation yield is based on the macrocycle and is calculated by dividing the mass of product(s) obtained by the theoretical mass for a given mixture of mono-armed and doubled-armed products; ^b An average of three independent experiments; ^c In 2 to 1 mixture with **18**.

2.4.3.3.1 Analysis of a key intermediate, 17

Compound **17** is a novel key intermediate in the synthesis process to form CB-TE2A, therefore, further analysis was carried out in order to fully characterise its structure. Full assignment of the NMR was carried out using 2D-NMR techniques (FDQ-COSY and HMQC) and single crystal X-ray crystallography to investigate its structure.

2.4.3.3.1.1 2D NMR analysis of compound 17

Two-dimensional nuclear magnetic resonance spectroscopy (2D NMR) is a nuclear magnetic resonance spectroscopy (NMR) method which generates data represented in a space defined by two frequency axes rather than one. It was first proposed by Jean Jeener in 1971; since then, many scientists such as Richard Ernst have applied the idea to develop the many techniques used in 2D NMR.¹⁵¹

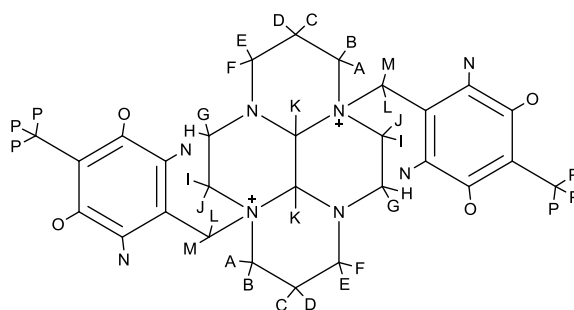


Figure 23-Schematic configuration for compound **17** as shown by 2D NMR

2D NMR spectra confirmed structure of **17** as shown in **Figure 23** and **Table 9**. The 2D NMR (^1H , ^{13}C) spectrum has peaks for 16 non-equivalent protons and 12 corresponding non-equivalent carbon atoms. The ^1H peaks at 1.88 ppm (C) and 2.31 ppm (D) map onto the carbon with a ^{13}C shift of $\delta = 18.53$ ppm and are assigned to the $\text{CH}_2\text{CH}_2\text{CH}_2$ protons. The signal at $\delta = 1.88$ ppm (C) gives a cross-peak in the 2D [^1H , ^1H] COSY NMR spectrum to the signals at $\delta = 2.31$ ppm (D) and ^{13}C $\delta = 18.53$ ppm, $\delta = 2.81$ ppm (E) and ^{13}C $\delta = 47.34$ ppm, and $\delta = 3.71$ ppm (A) and ^{13}C $\delta = 51.81$ ppm. The signal at 2.31 ppm (D) makes a cross-peak with $\delta = 3.59$ ppm (B) and ^{13}C $\delta = 51.81$ ppm, $\delta = 1.88$ ppm (C) and ^{13}C $\delta = 18.53$ ppm, and $\delta = 3.18$ ppm (F) and ^{13}C $\delta = 47.34$ ppm. The

peaks at 3.59 ppm (B) and 3.71 ppm (A) they have same ^{13}C shift $\delta = 51.81$ ppm and are assigned as the **CH₂CH₂CH₂** protons. The signal at $\delta = 3.71$ ppm (A) gives a cross-peak with signals at ($\delta = 3.59$ ppm (B) ^{13}C $\delta = 51.81$ ppm) and ($\delta = 1.88$ ppm (C) ^{13}C $\delta = 18.53$ ppm), whereas the signal at $\delta = 3.71$ ppm (A) gives a cross-peak with signals at ($\delta = 3.59$ ppm (B) ^{13}C $\delta = 51.81$ ppm) and ($\delta = 1.88$ ppm (C) ^{13}C $\delta = 18.53$ ppm). The protons corresponding to CH₂CH₂**CH₂** which gives signals at 2.81 ppm (E) and 3.18 ppm (F) they have same ^{13}C shift ($\delta = 47.34$ ppm) The signal at $\delta = 2.81$ ppm (E) gives a cross-peak with signals ($\delta = 1.88$ ppm (C) ^{13}C $\delta = 18.53$ ppm), ($\delta = 2.31$ ppm (D) ^{13}C $\delta = 18.53$ ppm) and ($\delta = 3.18$ ppm (F) ^{13}C $\delta = 47.34$ ppm). While proton (F) at 3.18 ppm makes a cross-peak with ($\delta = 2.81$ ppm (E) ^{13}C $\delta = 47.34$ ppm) and ($\delta = 2.31$ ppm (D) ^{13}C $\delta = 18.53$ ppm).

The peaks at 3.56 ppm (J) and 4.35 ppm (I) related to the same ^{13}C shift ($\delta = 46.53$ ppm) and are appropriated as the **CH₂CH₂** protons. The signals at 3.59 ppm (J) makes a cross-peak with proton G ($\delta = 3.18$ ppm, ^{13}C $\delta = 60.91$ ppm), H ($\delta = 3.59$ ppm, ^{13}C $\delta = 60.91$ ppm) and I ($\delta = 4.35$ ppm, ^{13}C $\delta = 46.53$ ppm), whereas the signal $\delta = 4.35$ ppm (I) gives a cross-peak with signals at ($\delta = 3.18$ ppm (G) ^{13}C $\delta = 60.91$ ppm), ($\delta = 3.59$ ppm (H) ^{13}C $\delta = 60.91$ ppm) and ($\delta = 3.59$ ppm (J) ^{13}C $\delta = 46.53$ ppm). The peaks at 3.59 ppm (H) and 3.18 ppm (G) belong to the same ^{13}C shift ($\delta = 60.91$ ppm) and are assigned as the **CH₂CH₂** protons. The signals at 3.59 ppm (H) gives a cross-peak with proton G ($\delta = 3.18$ ppm, ^{13}C $\delta = 60.91$ ppm), H ($\delta = 3.59$ ppm, ^{13}C $\delta = 60.91$ ppm) and I ($\delta = 4.35$ ppm, ^{13}C $\delta = 46.53$ ppm), whereas the signal $\delta = 4.35$ ppm (I) gives a cross-peak with signals at ($\delta = 3.18$ ppm (G) ^{13}C $\delta = 60.91$ ppm), ($\delta = 4.35$ ppm (I) ^{13}C $\delta = 46.53$ ppm) and ($\delta = 3.59$ ppm (J) ^{13}C $\delta = 46.53$ ppm). The peaks at 4.71 ppm (L) and 5.21 ppm (M) both related to same ^{13}C shift ($\delta = 62.88$ ppm) and are corresponding for Ph**CH₂**, data illustrates both of them make cross-peak for each other. The peaks at 7.45 ppm (N) and 7.37 ppm (O) which have ^{13}C shift ($\delta = 142.88$ ppm) and ($\delta = 130.60$ ppm) respectively and are assigned as phenyl protons. Found N proton makes cross-peak with another N proton corresponding for different aromatic carbon, whereas proton O gives cross-peak with N at 7.45 ppm ^{13}C δ

= 142.88 ppm and P at 2.37 ppm ^{13}C δ = 20.98 ppm. All these 2D NMR data confirm the structure of compound **17**.

Table 5. 2D ^1H NMR for compound 17

Atom, ^1H	δ , ppm	Mult	J, Hz	FDQ-COSY
C	1.88	d	15.2	A,D,E
D	2.31-2.17	m		B,C,F
P	2.37	s		O
E	2.81	d	12.5	C,D,F
F	3.18	d	12.5	E,D
G	3.18	d	12.5	H,I
J	3.59-3.33	m		G,H,I
B	3.59-3.33	m		A,D
H	3.59-3.33	m		G,I,J
A	3.71	t	12.3	B,C
I	4.35	t	11.5	G,H,J
L	4.71	d	13.0	M
K	5.08	d	8.1	
M	5.21	d	13.0	L
O	7.37	d	7.9	N,P
N	7.45	d	7.9	N

Table 6. 2D ^{13}C NMR for compound 17

δ , ppm	Atom, ^{13}C , HMQC
18.53	C _{CD}
20.98	C _p
46.53	C _{IJ}
47.34	C _{EF}
51.81	C _{AB}
60.91	C _{HG}
62.88	C _{LM}
77.22	C _K
122.08	C-C _p
130.60	C _O
133.67	C-C _{LM}
142.88	C _N

2.4.3.3.1.2 X-ray crystallographic structure determination compound 17

In order to determine the structure of **17** in the solid state, single crystals of **17** and **23**, suitable for single-crystal X-ray structure determination, were obtained within 2-7 days from vapour diffusion of diethyl ether into a methanolic solution at room temperature. The X-ray crystal structures confirm the identity of **17** and **23** (**Figure 24**) and show that the cis geometry has been adopted around the bisaminal bridged, as expected from the synthetic method used. The two 'exo' nitrogen atoms, where the lone pairs points out of the central cavity, have been alkylated to form quaternized derivatives. A useful comparison of the relative strains on the alkylated bisaminal macrocycles can be obtained by examining the bond angles around the benzyl substituted nitrogens. The 14-membered cyclam ring **17** has bond angles in the range 107.5-112.6° around the quaternized ring nitrogen and the equivalent positions in the 12-membered cyclen derivative (form II of **23**) show more flexibility with a wider range of angles from 101.5- 113.3°. This matches with the reactivity observed in the formation of these products.

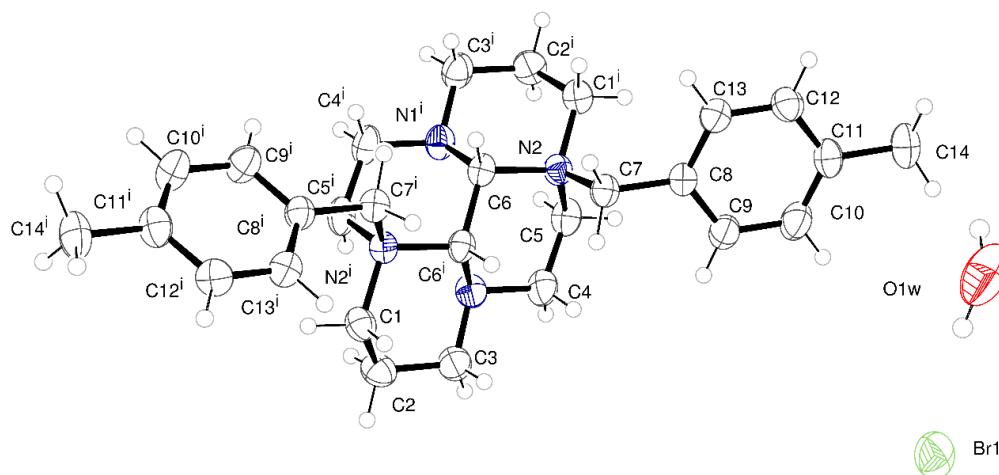


Figure 24-ORTEP plot with atoms drawn as 50% probability ellipsoids. The full macrocycle is represented. Symmetry equivalent atoms are generated by the operator $i = -x, y, 1.5-z$.

The macrocycle resides on a twofold screw axis within the crystal and the second half is generated from the first by application of this symmetry operation. There is limited hydrogen bonding within the structure between the water and the bromide anions.

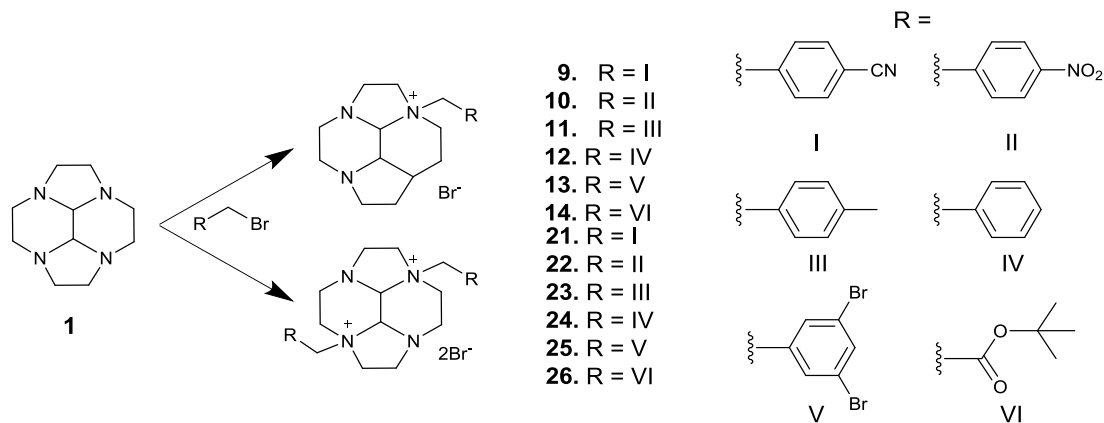
2.4.3.4 Comparison between conventional method and mechanochemistry

In the conventional method, pure mono-substituted products with cyclam or cyclen can be synthesised in various yields and in different product ratios, depending on the reactivity of alkyl bromide and reaction time (up to several days). The process of di-alkylation is more challenging because of the decreased reactivity of the second *exo* nitrogen, requiring up to three weeks (**Table 1** and **Table 9**).^{143,147} The conventional method requires a large amount of the solvent making it less green.

In case of mechanochemistry, the mono- and di substitution synthesised from grinding bridged cyclam/cyclen in the ratio 1:1 for mono-substitution and 1:4 for di-substitution. The yield for both was almost close to quantitative (**Table 3, Table 4, Table 7** and **Table 8**). This method requires 30 minutes for mono- substitution and 3 hours for di-substitution. The reactions run in the presence of solvent (90 μ l), known as liquid assistant grinding (LAG). On the other hand, the reactions could run without solvent, called net grinding (NG), making it a more green method.

2.4.3.5 Alkylation of bridged cyclen with various alkyl halides

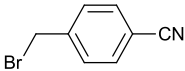
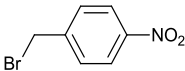
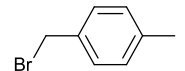
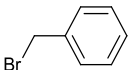
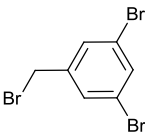
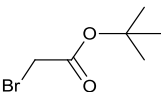
The same methodology was subsequently applied to synthesis of cyclen derivatives, however, a clean production of either mono or bis substituted products was more an exception than the rule, confirming increased glyoxal-bridged cyclen reactivity to alkylation (**Scheme 20** and **Table 5**).¹⁵²



Scheme 20-General schematic for mono- and bis-N-alkylation of cyclen

A clean mono substituted product (**9** and **13**, respectively) was obtained only using a short grinding time (30 minutes) and stoichiometric amounts of deactivated 4-cyanobenzyl and 3,5-dibromo benzyl bromides in a quite high 87% yield for the former and an average 60% yield for the latter (**Table 7**).

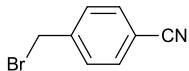
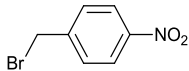
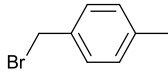
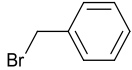
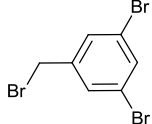
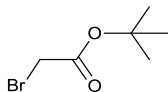
Table 7. 30 minutes grinding of bridged cyclen with various alkyl bromide

Product	Br-R	Alkylation yield ^a , %	Ref
9		87 ± 2^b	This work
10^c		65	This work
11^d		75 ± 3^b	This work
12^e		79	This work
13		60	This work
14^f		68	This work

^a Alkylation yield is based on a macrocycle and is calculated by dividing the mass of product(s) obtained by the theoretical mass for a given mixture of mono-armed and doubled-armed products. ^b An average of three independent experiments. ^c In 10 to 1 mixture with **22**. ^d In 5 to 1 mixture with **23**. ^e In 17 to 1 mixture with **24**. ^f In 2 to 1 mixture with **26**.

A pure di-substituted product (23 and 26 in 94% and 86% respective yields) was available only for reactive 4-tolyl and *t*-butyl acetyl bromides use 4-fold excess of alkyl bromide and 3 h grinding, see **Table 8** . For that reason, apart from shortening reaction times, advantages of mechanochemical syntheses over conventional approach were less obvious.

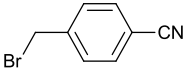
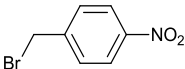
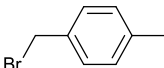
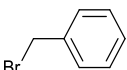
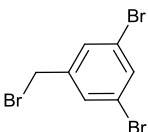
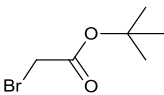
Table 8. 3 h grinding of bridged cyclen with various alkyl bromide.

Product	Br-R	Alkylation yield ^a , %	Ref
21^g		86 ± 1^b	This work
22^h		96	This work
23		94 ± 1^b	This work
24ⁱ		98	This work
25^j		92	This work
26		86	This work

^a Alkylation yield is based on a macrocycle and is calculated by dividing the mass of product(s) obtained by the theoretical mass for a given mixture of mono-armed and doubled-armed products. ^b An average of three independent experiments. ^g In 1 to 8 mixture with **7**. ^h In 3 to 1 mixture with **10**, ⁱ In 1 to 1 mixture with **12**. ^j In 1 to 4 mixture with **13**.

We should note, however, that conventional solution syntheses suffer from the similar problem and pure compounds (**9** and **13**, respectively) could be obtained only using deactivated 4-nitro and 3,5-dibromo benzyl bromides (**Table 9**).

Table 9. Conventional method for alkylation of bridged cyclen with various alkyl halides.^a

Product	Br-R	Alkylation yield ^b , %	Ref
9^d		72	This work
10		88 ± 1^c	This work
11^e		77	This work
12^f		72	This work
13		84 ± 1^c	This work
14^g		60	This work

^a All reactions carried out for 24 hours. ^b Alkylation yield is based on a macrocycle and is calculated by dividing the mass of product(s) obtained by the theoretical mass for a given mixture of mono-armed and doubled-armed products. ^c An average of two independent experiments. ^d In 5 to 1 mixture with **21**. ^e In 6 to 1 mixture with **23**. ^f In 8 to 1 mixture with **24**. ^g In 4 to 1 mixture with **26**.

2.4.3.6 Comparison between glyoxal bridged cyclam and cyclen

In the case of cyclam, pure mono-substituted products were obtained in yields ranging from 64% to 97% in reactions with all attempted benzyl bromides, in a 1:1 ratio and 30 minutes' reaction time. Increase in 4-nitrobenzyl and 3,5-dibromobenzyl bromide amounts and reaction time improved preparation yields from 85% to 98% and from 64% to 92%, respectively. The most reactive benzyl and tolyl bromides in 1:4 ratio and 3 h reaction time gave either a mixture of mono- and bis-substituted products or a pure bis-substituted product, respectively (**Table 4**).

In the case of cyclen, only reactions with deactivated 4-cyanobenzyl and 3,5-dibromobenzyl bromides, 1:1 ratio, 30 minutes reaction time, allowed exclusive preparation of mono-substituted products, with 89% and 60% yield, respectively. Under identical conditions, the alkylation with tolyl, benzyl and even deactivated 4-nitrobenzyl bromide gave mixtures of mono and bis-substituted products. In case of tolyl bromide, the alkylation can be driven to completion by using a four-fold excess and by increasing the time of grinding to 3 hours. However, other benzyl bromides, even under these improved conditions, gave mixtures of mono and bis-substituted products (**Table 8**). A pure di-substituted product (**23** and **26** in 94% and 86% respective yields) was available only for reactive 4-tolyl and *t*-butyl acetyl bromides use 4-fold excess of alkyl bromide and 3 h grinding (**Table 8**). For that reason, apart from shortening reaction times, advantages of mechanochemical syntheses over conventional approach (**Table 9**) were less obvious.

As a result of the above, the comparison between reactivity of cyclam and cyclen under LAG conditions reveals that, as expected, cyclen is more reactive towards alkylation than cyclam, due to the rigidified nature of the macrocycle exposing exo nitrogen atoms, pure mono-substituted product of the former can be obtained only when using deactivated 4-cyanobenzyl bromide. However, this increased reactivity

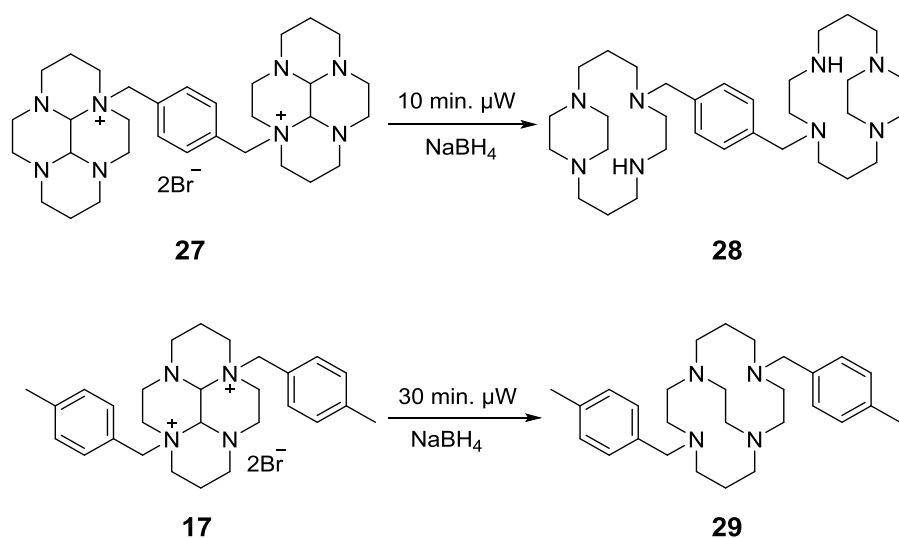
allows preparation of pure bis-substituted cyclen (**26**) using electronically neutral *t*-butyl bromoacetate, which was not possible in the case of cyclam.

2.4.4 Reduction method of quaternary ammonium salts via microwave

The synthesis of bridged tetraazamacrocycles are interesting nowadays due to the remarkable basicity, redox behaviour and coordination chemistry.¹⁵³ The modifications of macrocyclic structure based on the ethylene or propylene bridging of the adjacent (side- bridged SB) or opposite (cross-bridged CB) nitrogen atoms have been reported according to different methods. These two kinds of rigid (or constrained) macrocycles exhibit interesting and different behaviours in coordination chemistry.¹⁵⁴

In the last century, Wainwright and collaborators reported the first case of bridging by a simple cis-alkylation of the macrocycle.⁷⁶ Cross-bridging of tetraazamacrocycles via the use of bisaminal chemistry was reported for the first time by Weisman, Wong and co-workers.⁷⁷ This method was later adopted by Kolinski to synthesise adjacent-bridged cyclam.¹⁵⁵ The common route proceeds slowly (from hours for SB and 14 days for CB).

Here, new methodology is presented for the preparation of side or cross bridging of tetraazamacrocycles using bisaminal chemistry with microwave radiation for reduction of the quaternary ammonium salts. Application of microwave irradiation permits a very fast (from 10 minutes to 30 minutes) access to side-bridged or cross-bridged products. in comparable yields with conventional methods requiring a relatively low amount of reducing reagent (NaBH_4) and solvent. The optimised conditions were chosen after multiple trials while varying ratio of reagents (**Scheme 21** and **Table 10**).



Scheme 21-Synthetic pathways to SB and CB cyclam

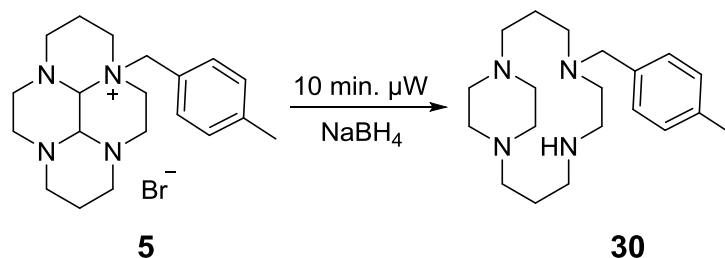
Finally, the best results were obtained when reduced the amount of sodium borohydride (5 eq. for SB and 10 eq. for CB) was slowly added to a solution of quaternary ammonium substituted cyclam/cyclen ethanol/water (9:1) and the mixture was irradiated for 10 minutes (SB) or 30 minutes (CB), see **Table 10**.

Table 10. Preparation of SB/CB via microwave

Product	NaBH ₄ , eq.	SB or CB	Time, minutes	Yield	Ref
28	1	SB	10	51%	This work
28	2	SB	10	69%	This work
28	4	SB	10	70%	This work
28	5	SB	10	98%	This work
29	5	CB	30	77%	This work
29	10	CB	30	87%	This work

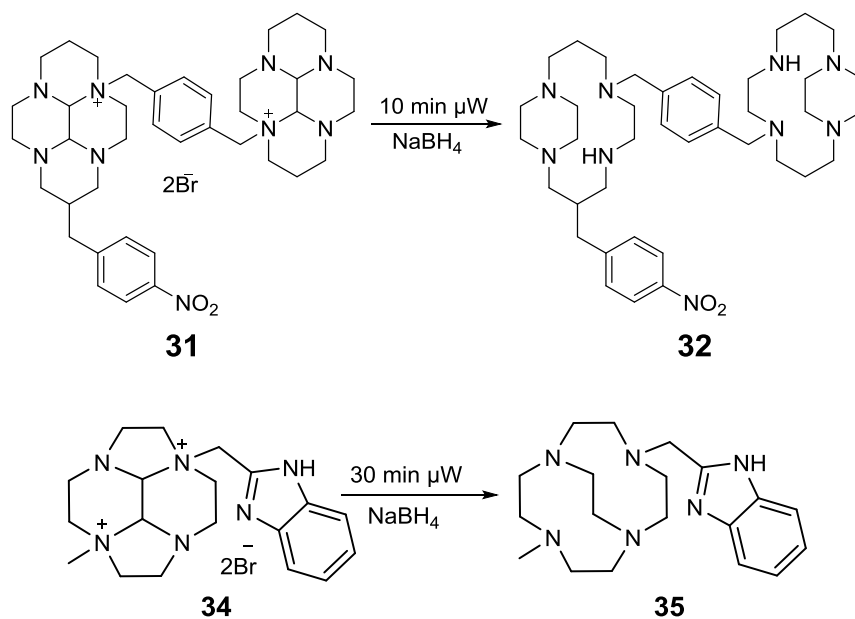
The incorporation of an ethylene bridged between two adjacent or opposite nitrogens in the tetraazamacrocycles has been successfully achieved by several groups using a variety of synthetic routes. The reductive ring cleavage step for the cross bridged analogue takes 14 days compared to hours for the side bridged derivative. Whereas

applying a microwave technique has successfully prepared side bridged cyclam derivatives **30** in 10 minutes 98% yield (**Scheme 22**) and cross bridged cyclam **29** in 30 minutes 87% yield, see **Table 10**.



Scheme 22-Synthetic pathways to SB cyclam.

After the success of the methodology to synthesise simple (side bridged and cross bridged) tetraazamacrocycles for bifunctional chelator synthesis, the method was applied to other more complex novel chelators for various other applications, see **Scheme 23**.

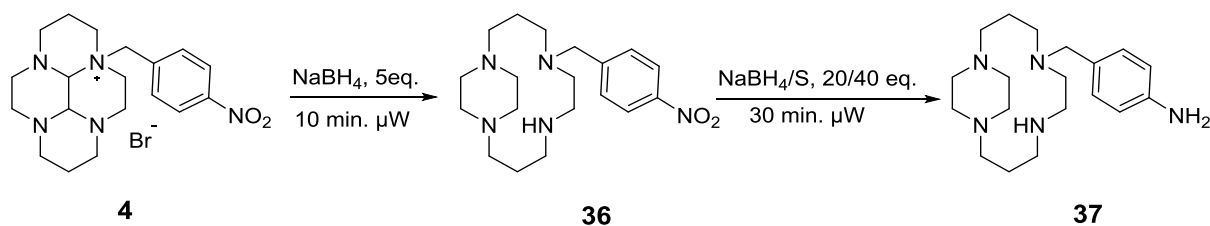


Scheme 23-Reduction of quaternary ammonium salts via microwave to synthesis of SB cyclam and CB cyclen.

2.4.5 Reduction of nitro to amine

Synthesis of amines by reduction of nitro compounds are important as they allow the formation of bioconjugatable compounds, this method is traditionally carried out using high pressure hydrogenation.¹⁵⁶ In modern organic synthesis using NaBH_4 as a moderate reducing agent has brought about fundamental changes in the reduction of functional groups.¹⁵⁷ Under normal conditions, sodium borohydride alone does not reduce nitro compounds.¹⁵⁶ However, combination of this reagent with transition metal halides or salts such as $\text{NaBH}_4/\text{CoCl}_2$ and $\text{NaBH}_4/\text{FeCl}_2$ increase the reducing power.¹⁵⁶ Lalancette *et al.* have reported sulfurated borohydride as a selective reducing reagent, that is able to convert nitro to the corresponding amine without disturbing other groups.¹⁵⁸

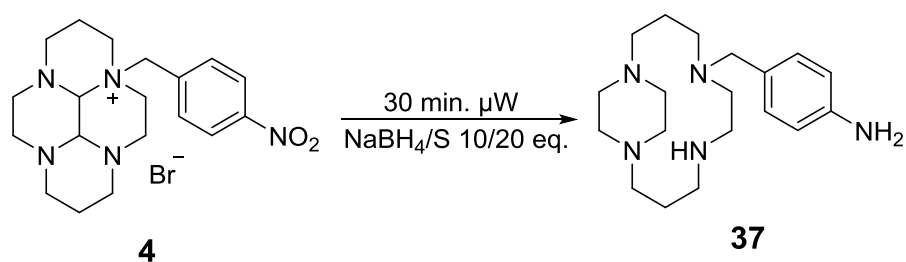
Here, a new methodology for the conversion of a nitro group to the corresponding amine by using microwave radiation is presented. After preparing **36** from **4** via microwave method as described in section 2.3.3. *In situ*, the sulfurated borohydride is prepared from stirring of sodium borohydride and sulphur (20:40 eq.) in dry THF under nitrogen for one hour. During this time, a release of hydrogen gas occurs as the sulfurated product forms (NaBH_2S_3). The addition of **36** was add as a solution in dry THF and reaction mixture heated by microwave for 30 minutes the product was extracted with dichloromethane to form a yellow oil in 80% yield (**Scheme 24**).



Scheme 24-Synthetic pathway to reduction of nitro to amine.

After the success of efficient two-step reduction using NaBH_4 based agents it was thought that it may be possible to complete both in one-pot. *In situ* the sulfurated

borohydride (NaBH_2S_3) was prepared as mentioned before. The addition of **4** was added as a solution in dry THF and reaction mixture heated by microwave for 30 minutes to give the desired product **37** (**Scheme 25**). This method would allow the formation of an amine terminating macrocyclic bifunctional chelator in a two-step fashion from glyoxal cyclam in 30 minutes, with an overall yield of 78.4%.

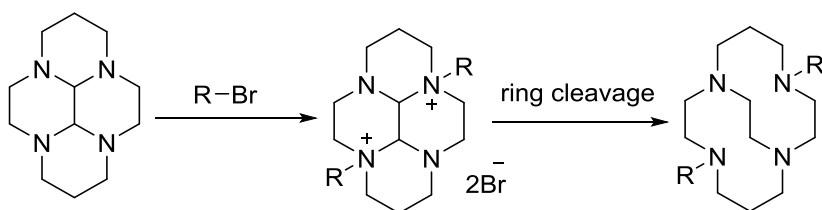


Scheme 25-Synthetic pathways to SB and reduction of nitro to amine in one step.

2.4.6 Efficient synthesis of CB-TE2A

Due to the increased kinetic stability of their metal complexes, CB cyclam derivatives are preferred candidates for radiometal chelation in biomedical applications, especially in the use of copper(II) radioisotopes.¹⁵⁹

Two general methods are used to N-functionalise CB cyclam system. The first procedure consists of addition of the selected pendent arms onto the tetracyclic bisaminal directly at the start of the synthesis. Then, reductive ring cleavage yields the cross bridged species already substituted with the desired arms, see **Scheme 26**. This strategy, however, is limited to the specific cases when a highly reactive side arm precursor is available due to the extremely low reactivity of the second animal nitrogen atom.^{139,76}



R= desired arm

Scheme 26-Alternative pathway to synthesis of CB-cyclam

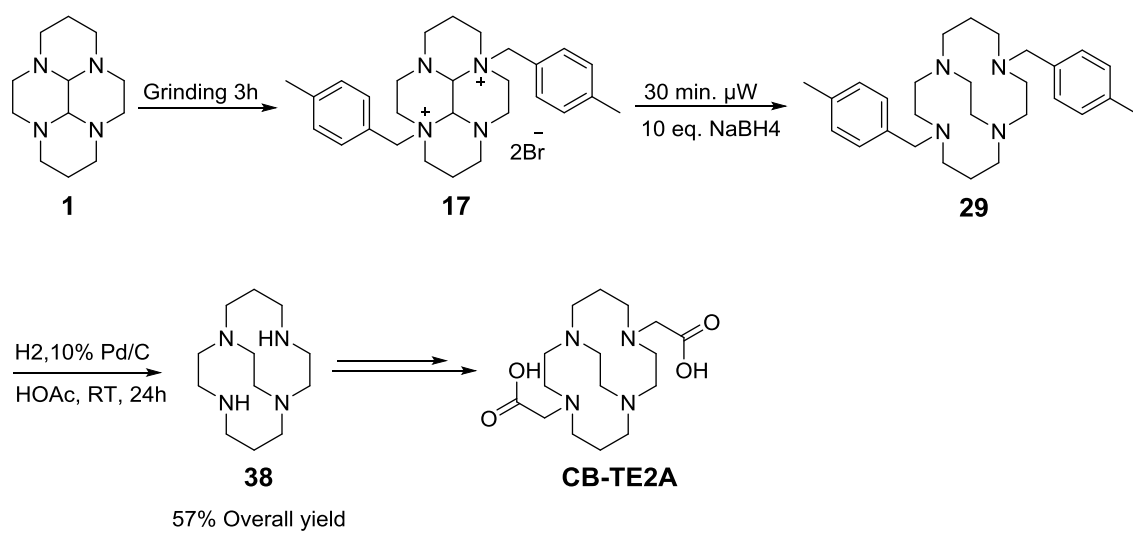
The second strategy relies on preparation of an unsubstituted cross bridged cyclam first (following the first approach using a highly reactive side arm which is removed after the cross bridged formation by catalytical hydrogenation) which then is functionalised with a desired pendent arm. Thus, the second approach is much more versatile and is generally preferred, see **Scheme 27**.¹³⁹

CB-TE2A (**Scheme 27**) is a widely used copper(II) chelator in radiopharmaceuticals consisting of a cross bridged cyclam N-substituted by methylcarboxylic acid pendent arms.^{139,160} It has been previously prepared by Weisman and co-workers following the second approach.¹³⁹ First, unsubstituted cross bridged cyclam was prepared via a bis-benzyl aminal intermediate followed by reduction and hydrolysis and then it was reacted with ethyl bromoacetate yielding the bis-substituted cross bridged species. Finally, the ethyl ester protecting groups were subjected to acid hydrolysis, revealing CB-TE2A's carboxymethyl arms which are responsible for improvement of metal ion coordination characteristics as compared with unsubstituted cross bridged cyclam.

The synthesis of CB-TE2A by conventional methods is a time consuming six step process taking 35 days and presenting an average 45% yield (calculated from cyclam).¹³⁹ The most time consuming steps are glyoxal bridged cyclam alkylation (16 days for original benzyl bromide) and reductive ring opening in presence of the large excess of NaBH_4 (14 days).¹³⁹ These two steps have been shortened to half a day by successfully replacing the conventional in solution alkylation reaction by liquid assisted grinding (LAG)

and speeding up the reductive ring cleavage by applying microwave catalysis. As the bis-*N*-benzyl substitution is only required to direct the opening of the bridged system towards cross-bridged cyclam, in our synthesis we replaced non-activated benzyl bromide by more reactive tolyl bromide. Thus, mechanochemical alkylation required only four-fold excess of tolyl bromide and was completed in 3 hours as described in Section **2.3.2.2**. In a similar way, while applying microwave heating and using only 10 eq. of NaBH₄ for reductive ring opening, in as short time as 30 minutes, bis-*N*-tolyl cross-bridged cyclam **29** was obtained in 83% yield. The debenzylation of **29** can be managed according to the method described by Weisman and co-workers.¹³⁹ Our modification of this synthesis proceeded using tolyl as arms, whereas the literature method usually use benzyl. The debenzylation of **29** complete after 24 hours hydrogenolysis in acidic solution with yield 80% of **38**, this cross bridged cyclam chelator now has two secondary amine available for further functionalization. Dialkylation of the available secondary amine in acetonitrile with *tert*-butylbromoacetate and converted to CB-TE2A is a well published.^{139,149,161}

However, the optimisation of the first two steps by employing non-conventional synthesis methods would potentially allow us to prepare CB-TE2A in one week, which would represent a five-fold improvement compared to conventional five weeks' synthesis, see **Scheme 27**.



Scheme 27-Synthesis of CB-TE2A via efficient synthesis.

2.5 Conclusion

The rapid synthesis of various glyoxal-bridged cyclen and cyclam derivatives has been achieved using mechanochemical activation under Liquid Assisted Grinding (LAG) conditions. To the best of our knowledge, this is the first report of preparation of mono- and/or di-N-substituted glyoxal-bridged tetraazamacrocyclic derivatives which, after a further transformation, could lead to interesting bifunctional chelators. Using a stoichiometric ratio of reagents, mono-N-alkylated products were obtained in short times and in moderate to high yields. The content of bis-alkylated products in the final reaction mixtures can be increased by selecting electronically activated alkyl bromides, increasing their vs macrocycle ratio and by prolonging grinding time. The syntheses were easy to execute and often approached quantitative yields. Furthermore, the ability to stop the reaction at the mono alkylation stage is very important and permits application of this technique to the design of more sophisticated molecules. In the field of functionalised azamacrocycle preparation, these findings present grinding methodology as an attractive alternative to traditional conventional methods. As a proof of principle, mechanochemical activation together with a novel microwave methodology has been used for preparation of cross-bridged cyclam (**38**) with overall yield 57%, a key intermediate in the synthesis of CB-TE2A. The novel synthetic route showed significant increased reaction time efficiency, reducing the expected synthesis time five-fold.

Chapter 3

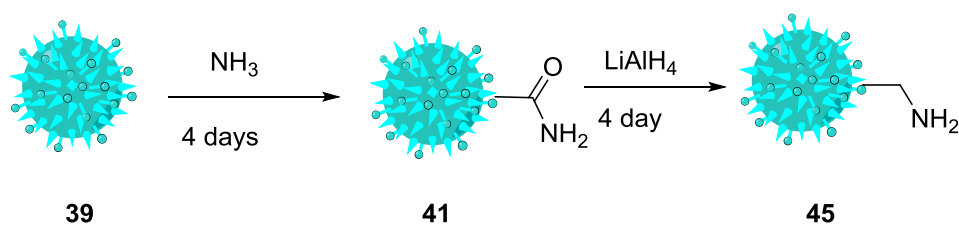
Surface activation of date spore exines

3. Surface activation of date spore exines

3.1 Aims

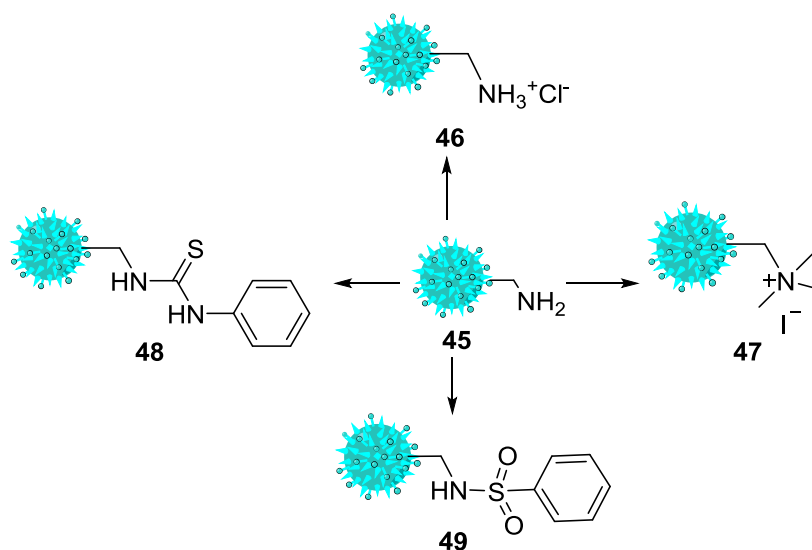
This chapter reports an investigation into the structure of a sporopollenin derived from the spores of the date palm (*Phoenix dactylifera* L.). The study is presented as follows:

- (i) Extraction of date spores to remove the genetic, protein and other components from the exine, see section **3.3.1**.
- (ii) Attempts at a direct amidation reaction with ammonia followed by reduction of the resulting amide to a primary amine (**Scheme 28**), see Section **3.3.2**.



Scheme 28-A proposed synthetic pathway to amine functionalised date palm spores via amide formation.

- (iii) Investigation of the reactivity of the generated primary amine in different amino group specific reactions, see **Scheme 29**.



Scheme 29-Synthetic strategies to modify the primary amino group on the surface of compound **45**

3.2 Sporopollenin biopolymer characteristics

Spores are produced by ferns, gymnosperms and flowering plants (angiosperms). Different types of spores and pollen grains are found throughout nature. Their size varies between a few micrometres (*e.g.* pollen grain of forget-me-not, *Myosotis spec.* L. is *ca.* 5 μm in diameter) to a few hundred micrometres (*e.g.* pollen grain of pumpkin, *Cucurbita maxima* Duchesne, is *ca.* 250 μm in diameter).¹⁶² The size and characteristics are fixed and unique to a given plant or a sub-species of a plant.^{163,164,165} Using high magnification microscopy, spores can be categorized by: (i) their global shape (a ratio between polar and equatorial diameters); (ii) the presence of scars (*laesurae*) on the proximal face or *sacci* on the sides; (iii) the presence, position and shape of apertures; (iv) the external ornamentations (tectal elements), and (v) the sculpturing of the layers (sexine).

Flowering plants are commonly known as heterosporous because they bear two different types of spores: megaspores (large spores) and microspores (small spores). The megaspores develop into the female reproductive parts, whereas the microspores metamorphose into male reproductive parts. The female gametophytes are well protected inside the spore and are never released. On the other hand, male gametophytes (microspores or pollen grains) are released from the plant by the phenomenon of dispersal of the spores. They are tiny structures, similar to dust particles, and can disperse by various means, such as the wind, water, pollinating insects, *etc.*¹⁶⁶ Usually each microspore contain one cell protected by two coats or layers. The outer layer is called the exine, and the inner layer is known as intine, see **Figure 25**. The exine is a hard and cutinized layer with spines on the outer surface. The intine is smooth and mainly composed of cellulose and other polysaccharides.^{167,168} G. Shaw *et al.* discovered that the intine is stained by iodine in H_2SO_4 and could be removed by 80% phosphoric acid confirming its polysaccharide nature.¹⁶⁹

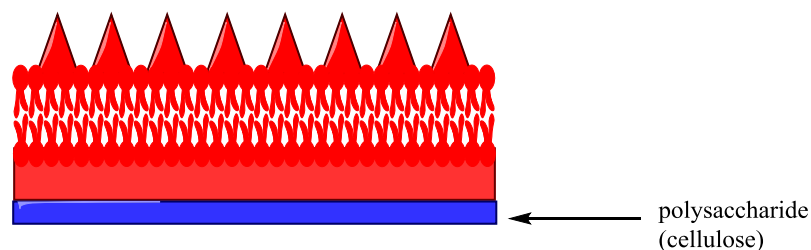


Figure 25-Simplified structure of the exine (red) and intine (blue).¹⁷⁰

3.2.1 Exine

The first scientists to offer an extensive examination of the exine and its chemistry, and to use the term “pollenin” to characterise inert exines were John and Braconnot in the early eighteenth century.^{168,171} At the beginning of the 20th century, Zetsche and Kalin introduced the term “sporonin” to describe the exine of *Lycopodium clavatum* spores.¹⁷² Later Zetzche *et al.* coined the term “sporopollenin” to describe the exines and this term is still in use.¹⁷³ Undamaged spore exines have been found in 500 million year old sedimentary rocks,¹⁷⁴ hence, the sporopollenin exine is considered to be “one of the most unusual and resistant materials in the organic world”.¹⁷⁵ Sporopollenin is not soluble in water and does not swell in organic solvents, and it is highly resistant to strong alkaline or acidic substances.¹⁷⁶⁻¹⁷⁸ The exact structure of sporopollenin remains unknown. However, it is agreed that it is a polymer composed of carbon, hydrogen and oxygen deriving from oxidised carotenoids or polyunsaturated fatty acids containing various functional groups such as alcohols, carboxylic acids, unsaturated bonds and aromatic rings.¹⁷⁹⁻¹⁸² Zetzsche^{183,184} represented all sporopollenins by a general arbitrary formula based on a C₉₀ unit, a summary of which is shown in **Table 11**.

Table 11- Arbitrary formulae of different sporopollenins.

Material	Arbitrary formula	Ref
<i>Lycopodium clavatum</i>	$C_{90}H_{144}O_{27}$	184
<i>Equisetum arvense</i>	$C_{90}H_{144}O_{31}$	184
<i>Ceratozamia Mexicana</i>	$C_{90}H_{148}O_{31}$	184
<i>Picea exelsa</i>	$C_{90}H_{144}O_{26}$	184
<i>Picea orientalis</i>	$C_{90}H_{144}O_{25}$	184
<i>Taxus baccata</i>	$C_{90}H_{138}O_{26}$	184

The exine is composed of two layers, known as nexine and sexine, as shown in **Figure 26**. The nexine is the smooth inner part of exine located under the sexine, which constitutes the rough sculptured outside layer of exine.¹⁷⁰

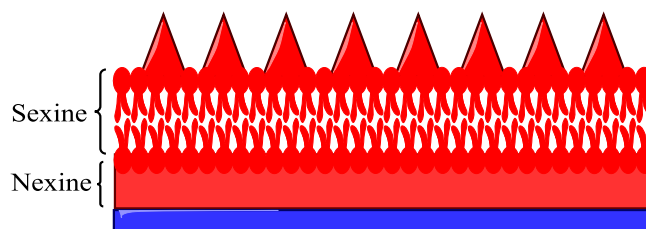


Figure 26- The schematic diagram showing the nexine and the sexine within the exine.¹⁷⁰

The substructures (nexine and sexine) of *Fagus pollen grains* and *Lycopodium clavatum* spores exines were investigated in detail using scanning tunnelling microscopy and were found to be entirely different.¹⁸⁵ The *Lycopodium clavatum* spores contain a trilete scar with no visible germination pores. The *Fagus* pollen grains have a trilete scar with germination pores, which are multi-helical structures with a total diameter of 100 – 200 nm and a micro-channel width of 40 – 120 nm.¹⁸⁵ A study of *Pinus Sylvestre* spores suggests that the nexine is composed of an ultrafiltering membrane that restricts protein access but allows the sugar intake necessary for nutrition. The sexine is reported to contain a membrane that allows the passage of large polymer molecules and latex particles up to 200 nm.¹⁸⁶ The presence of the nano-channels or pores allows for intine removal in a chemical extraction process and also enables the use of sporopollenin for encapsulation applications.¹⁸⁷

3.2.2 Method of extraction

The analysis of the sporopollenin exine is challenging using the intact spores. Therefore, historically, different extraction methods were developed to remove polysaccharides of the intine, genetic material, lipids and proteins, leaving empty spheres, which then could be used in a variety of applications.

The first method of extraction was described by Zetzsche *et al.* in 1930.^{164,173,188,189} It was based on a rationally devised sequential treatment with (1) organic solvent to remove lipids, followed by (2) aqueous strong alkali and (3) acid treatments, capable of dissolving and removing intine polysaccharides and other biological materials. Later, modifications of this procedure by using different acids and alkalis followed.^{181,190,191} Other authors reported a one-step extraction process, using only strong acid, such as 9 M hydrochloric acid or treatment with a mixture of acetic anhydride and sulphuric acid.¹⁹²⁻¹⁹⁴ Alternative procedures included treatment with (i) melted potash, (ii) a mixture of sulphuric acid and hydrogen peroxide, (iii) nitrobenzene or *N*-methyl morpholine *N*-oxide.¹⁹⁵⁻¹⁹⁷ All of these treatments modified the composition of the extracted sporopollenin. Therefore, there was a need to develop milder procedures that would not affect its chemical composition.^{195,198-200} In 1998, Domínguez developed a method using anhydrous hydrofluoric acid in pyridine at 40°C, which allowed isolation of unaltered sporopollenin.²⁰⁰ The obtained exines were analysed by IR spectrometry. The total removal of polysaccharide material was confirmed by the absence of fluorescence on calcofluor staining. Still milder protocols using gastric digestion enzymes such as cellulases, proteases, lipases, amylases and pectinases followed by washing with hot methanol have also been described.^{195,198,201}

3.2.3 Uses of Sporopollenin

The useful properties of these microcapsule shells include size homogeneity, stability to both acids and bases, and the ability to resist temperatures up to 250°C. The hollow microcapsules have the potential to encapsulate and release active molecules in a controlled way. Their mucoadhesion to intestinal tissues may contribute to the extended contact of the sporopollenin with the intestinal mucosa leading to an increased efficiency of delivery of nutraceuticals and drugs. The sporopollenin can be filled with a solution of the active in a liquid form via simply mixing both together, and in some cases applying a vacuum, which can then be dried. The active payload can be expelled in the human body dependent on compression of the microcapsule, solubility properties of the encapsulated materials and/or pH. Active release can be further controlled by co-encapsulation of other compounds to influence these factors.¹⁸¹

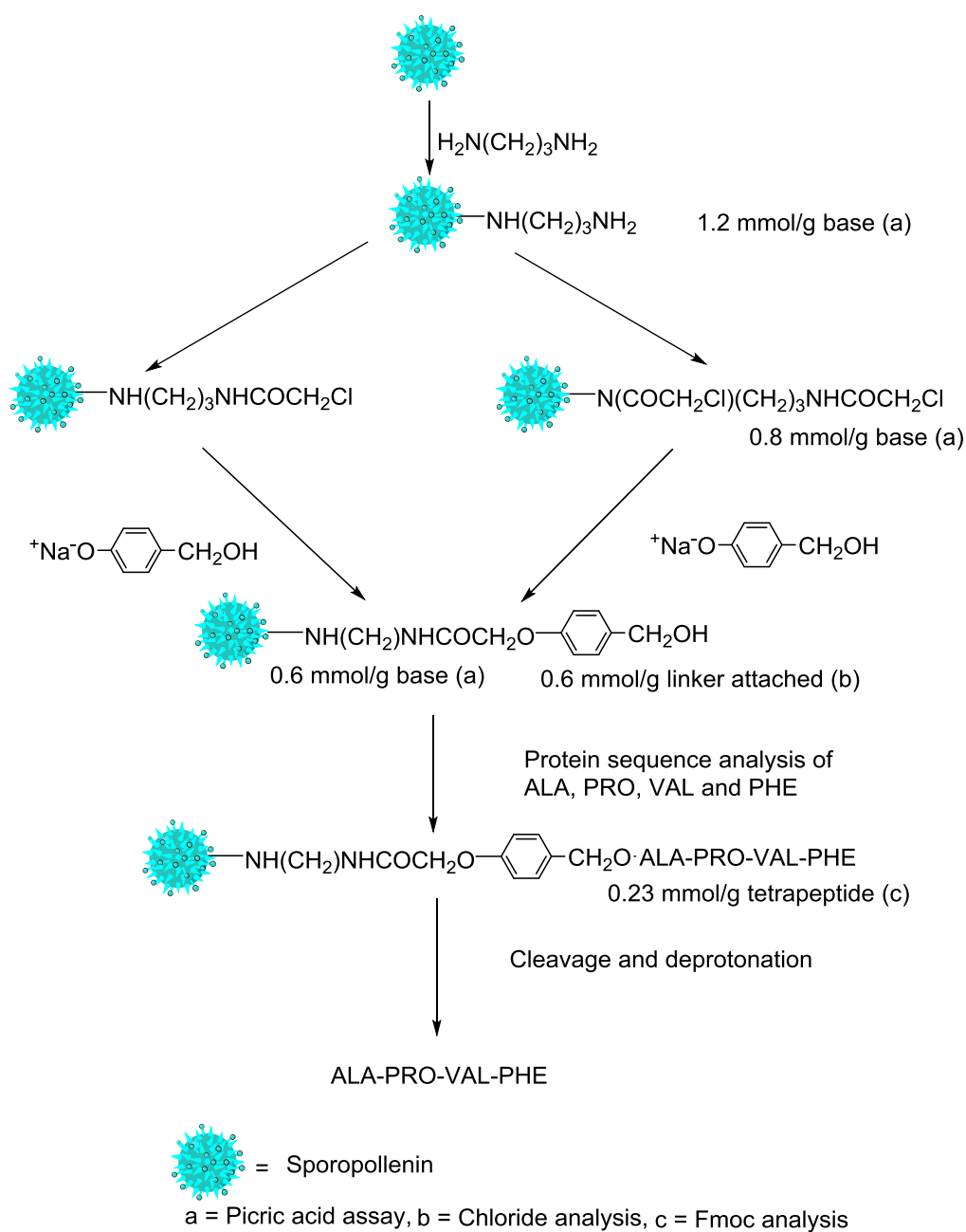
3.2.4 Application of sporopollenin exine

There are several applications of sporopollenin based on its inertness to harsh chemicals, high surface area to volume ratio, facile modification and functionalisation amongst others properties. They include use as a solid phase support for peptide synthesis, action as ion exchange materials or drug delivery as already discussed.

3.2.4.1 Solid phase peptide synthesis

Sporopollenin has been used as a support or platform for peptide synthesis after it has been functionalised.^{202,203} Previous work has shown that sporopollenin (*Lycopodium clavatum*) can be chloromethylated using stannic chloride and chlorodimethyl ether.²⁰² One mmol/g of chloride loading was achieved, as determined by pyridine abstraction. Amino acids were attached to the chloromethylated sporopollenin and subsequently removed by HBr in TFA (trifluoroacetic acid) when synthesis was complete. Pure tripeptides could be prepared, isolated and purified. The morphology of the sporopollenin was not affected by these reagents. A tetrapeptide has

also been synthesised, see **Scheme 30**, again utilising functionalised sporopollenin from *Lycopodium clavatum*.²⁰⁴ Sporopollenin was initially aminated with 1,3-diaminopropane (loading of 1.2 mmol/g based on the picric acid assay) when heated at reflux for 16 hours and a maximum loading of 1.6 mmol/g could be achieved with a longer reaction time of 24 hours.



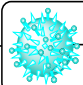
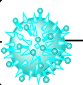
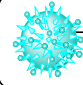
Scheme 30-Sporopollenin in peptide synthesis³⁵

The tetrapeptide was prepared using sporopollenin with a 4-hydroxybenzyl alcohol linker attached. It was made by sequential addition of individual Fmoc-amino acid anhydrides with each addition followed by reaction with acetic anhydride as a capping agent for any unreacted hydroxyl groups. The tetrapeptide was produced in a 19% yield (based on initial loading of the linker at, 0.23 mmol/g).

3.2.4.2 Use as an ion exchange medium

Ion exchange is the ability to exchange ions of the same charge polarity between a stationary phase and an electrolyte solution or between two electrolytes. Functionalised sporopollenin obtained from *Lycopodium clavatum* was used as an ion exchange medium for the separation of nucleosides, nucleotides, α -amino acids and transition metals.^{203,205} To give an example, ribonucleotides, α -amino acids and ribonucleosides have been successfully separated by functionalising the sporopollenin with 1,2-diaminoethane, followed by either chlorosulphonic acid or bromoacetate, and finally CuCl_2 , with respective loading capacities of 1.59, 1.60 and 1.40 mmol/g, see

Scheme 31.

Reagents	Sporopollenin Derivative	Compounds separated (Loading)	Loading determination method
1,2-Diaminoethane	 $\text{NH}(\text{CH}_2)_2\text{NH}_2$	Ribonucleotides (1.59 mm/g)	Picric acid assay
Chlorosulphonic acid	 $\text{NH}(\text{CH}_2)_2\text{NH}\text{SO}_3\text{H}$	α -amino acids (1.60 mm/g)	Titrimetric analysis
Bromoacetate and CuCl_2	 $\text{NH}(\text{CH}_2)_2\text{N}(\text{CH}_2\text{CO}_2)_3\text{Cu}$	Ribonucleosides (1.40 mm/g)	Unstated

Scheme 31-Functionalised sporopollenin used as an ion exchange medium.²⁰³

The aminated sporopollenin could also be functionalised with chelators for metal ions and subsequently used in the extraction of heavy metal ions from solutions.²⁰⁶ This principle could be applied to the treatment of water contaminated with such heavy metal ions.

3.2.4.3 Encapsulation

In this case, the term encapsulation refers to the entrapment of a selected entity such as a dye, protein, vitamin, flavouring or living cells into another material. The encapsulated material can also be termed the active, internal phase or payload, it is most often encapsulated in the liquid state but could also be a solid or gas.²⁰⁷ There is no particular classification for the size of microcapsules, some researchers considered capsules which have diameter 1-100 μm as microcapsules and those with diameter of less than 1 μm as nanocapsules.²⁰¹

The primary purpose of encapsulation is protection of the contents from the surrounding environment whilst allowing small molecules to pass through a membrane. This can improve the retention time of a nutrient in food to allow controlled release over a specific time period. Some microcapsules are designed to control the release of the contents in response to changes in temperature, pH, enzymatic reactions, ultrasound, grinding or photo-activated processes.²⁰⁷

Sporopollenin has been used to encapsulate organic and inorganic compounds.²⁰⁸ The exine capsules can be used as an enhanced delivery vehicle for oils as dietary supplements and other medical grade products. The encapsulation of living cells has also been demonstrated.²⁰² Sporopollenin is hydrophobic, but with some amphiphilicity and this enables lipids to be encapsulated preferentially and retained within it.²⁰⁹ Lipids, enzymes, and drugs have all been successfully encapsulated and released. For example, it was demonstrated that encapsulated enzymes can be released into a stirred buffer solution and still retain their catalytic activity.¹⁸¹ It has also been

demonstrated that oil filled exine can gradually release the oil when rubbed between two surfaces due to the elastic nature of the exines.²¹⁰

3.2.4.4 Drug delivery

One of the major applications of sporopollenin is in controlled drug delivery.²⁰⁹ Drugs are routinely administered to the body in the form of tablet or injection but there is a need for drugs to be released at a predetermined rate into the system. Sporopollenin serves as an excellent support for the drug delivery since it is physically and mechanically stable and can offer oral bioavailability to drugs that are otherwise too unstable for administration via this route.^{211,212}

Diego-Taboada *et al.* loaded ibuprofen into sporopollenin exine capsules (SEC) of *L. clavatum*.²¹³ A model system was developed to test the stability of the encapsulated material in transit through the stomach by use of simulated gastric fluid and phosphate buffer (pH 7.4) showing an overall reduction of extractable drug by only $12 \pm 1\%$ from the microcapsules. The *in vitro* properties for controlled delivery of ibuprofen were also investigated with sporopollenin microcapsules extracted from date palm (*Phoenix dactylifera* L.) spores which were coated using a natural polymer composite (chitosan with glutaraldehyde). Loading at pH 6.0 gave 97.2% encapsulation (with 50 mg/ml) and the maximum releasing was observed when the pH was raised from 1.4 to 7.4.^{213,214}

3.2.3 Availability of different types of sporopollenin

The bulk of commercially available sporopollenin comes from *Lycopodium clavatum* (LC) which belongs to *Lycopodiaceae* family and is can be called by different common names including club moss, clubfoot moss, foxtail, ground pine, sulfur, wolf's claw, *etc.* It is a flowerless green plant from *Pteridophyte* division, related to ferns, found in tropical, subtropical and moderate climate zones. The colour of *Lycopodiaceae* family plants' spores varies from green to yellow.^{215,181} The *Lycopodium clavatum* spores have been studied by microscopy under various magnification (light microscopy (LM)),

scanning electron microscopy (SEM) and laser confocal scanning microscope (LSCM)) and, depending on their size, are divided into “S” for small and “L” for large populations.²¹⁶ The majority of published work is based on studies of the S-type.²¹⁷ L-type spores are still not well identified and are sold under the trade name “Lycopodium”, it is not yet clear if they are generated by the same *Lycopodium clavatum* (LC) plants or come from the different type of club mosses that are mixed in.²¹⁸ The LC spores have been used in various traditional medicines for the treatment of stomach pain, rheumatic disease, muscle pain, Alzheimer’s disease etc.²¹⁹ *Lycopodium clavatum* (LC) plants are small which limits the amount of spores available for harvest and more abundant sources of sporopollenin would be of interest.

3.2.1 Date palm (*Phoenix dactylifera* L.)

In the Arabic countries the date palm (*Phoenix dactylifera* L.) is considered as an important traditional crop. In many parts of the world, dates are very commonly consumed and are a vital component of the diet in most of the Arabic world. The dates grown in this region are around 70% of the total world production and evidence of date palm cultivation goes as far back as 400 B.C.²²⁰ The most likely birthplace of the date palm is in southern Iraq (Mesopotamia), however, date farming spread to many different countries starting in ancient times.²²¹ The date palm is considered to be a renewable natural resource because of its ability to be replanted in a comparatively short period of time. There are more than 2000 species of date palm known over the world with variation in their genetic properties with a few key species assessed for their agronomic performance and fruit quality.^{222,223} The morphological diagram of a typical date palm tree and fresh fruits, as shown in **Figure 27**.

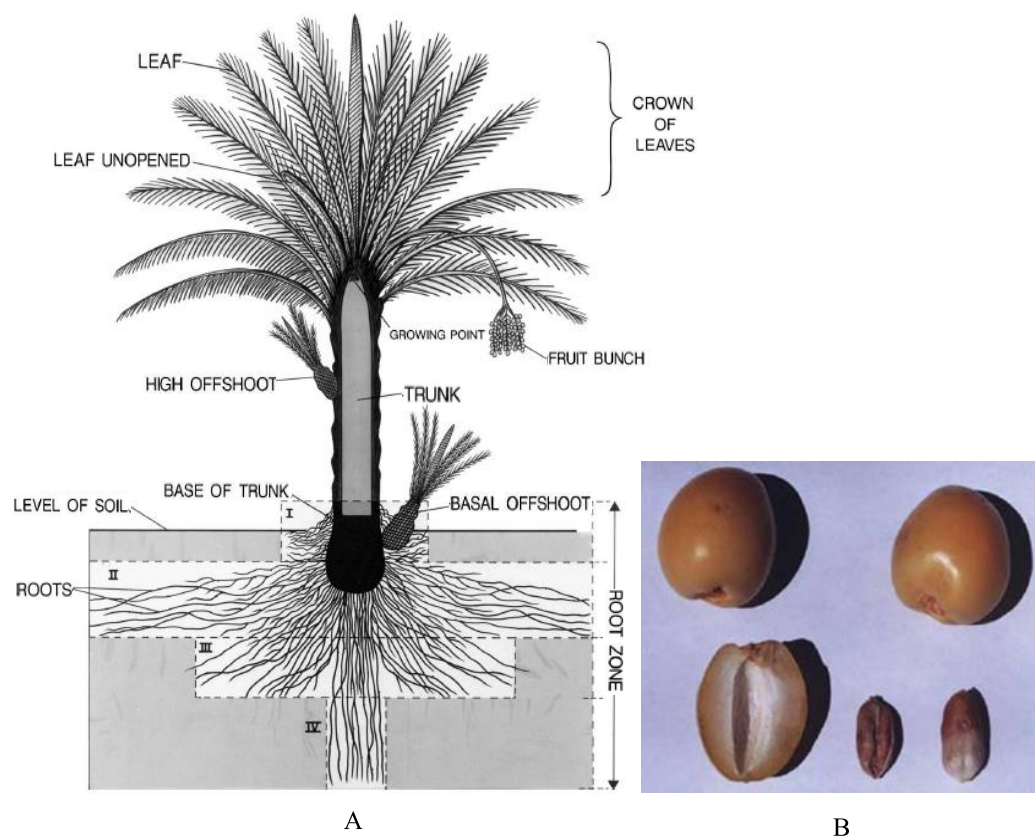
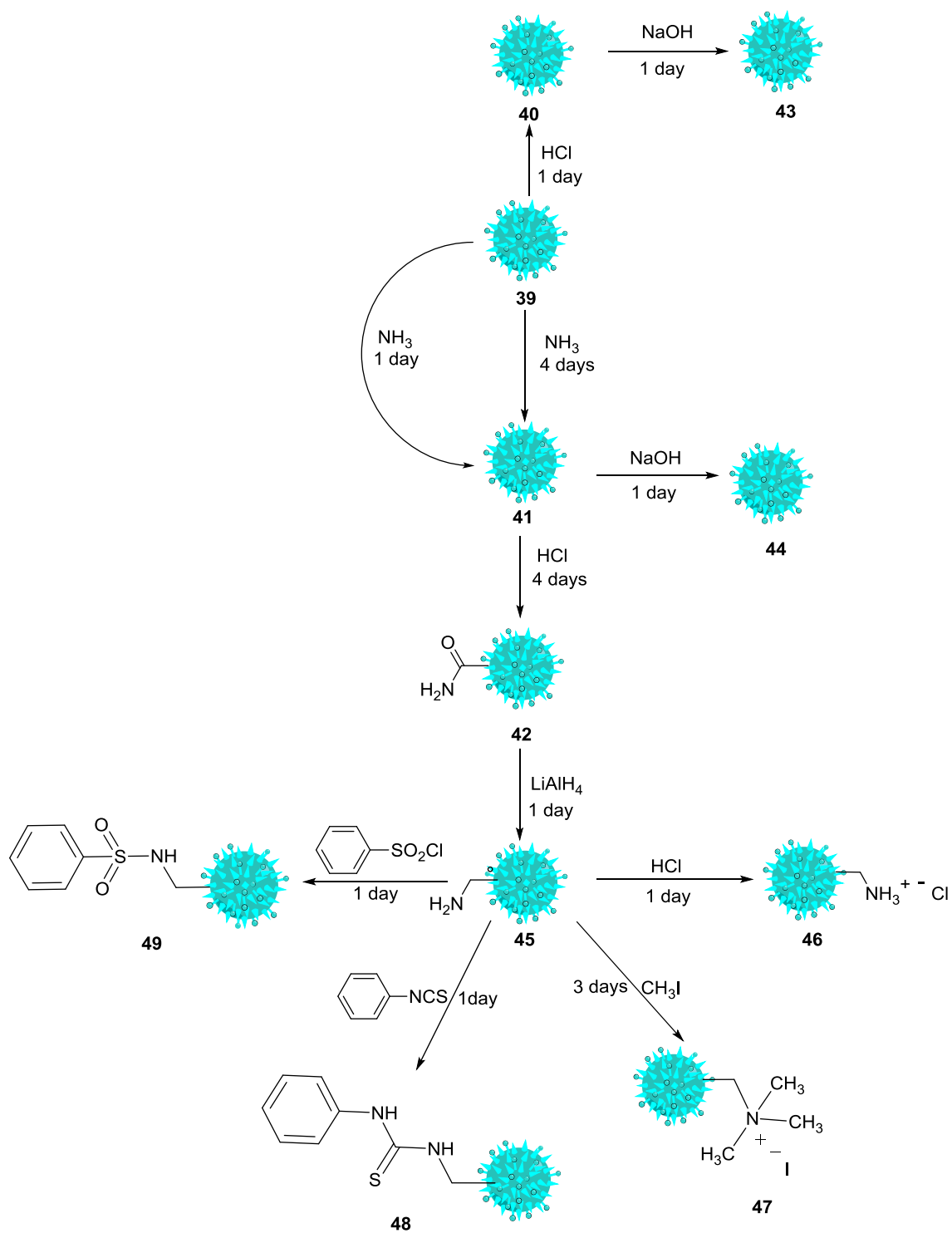


Figure 27-A Morphological diagram of a date tree and B Date palm. ^{17,224}

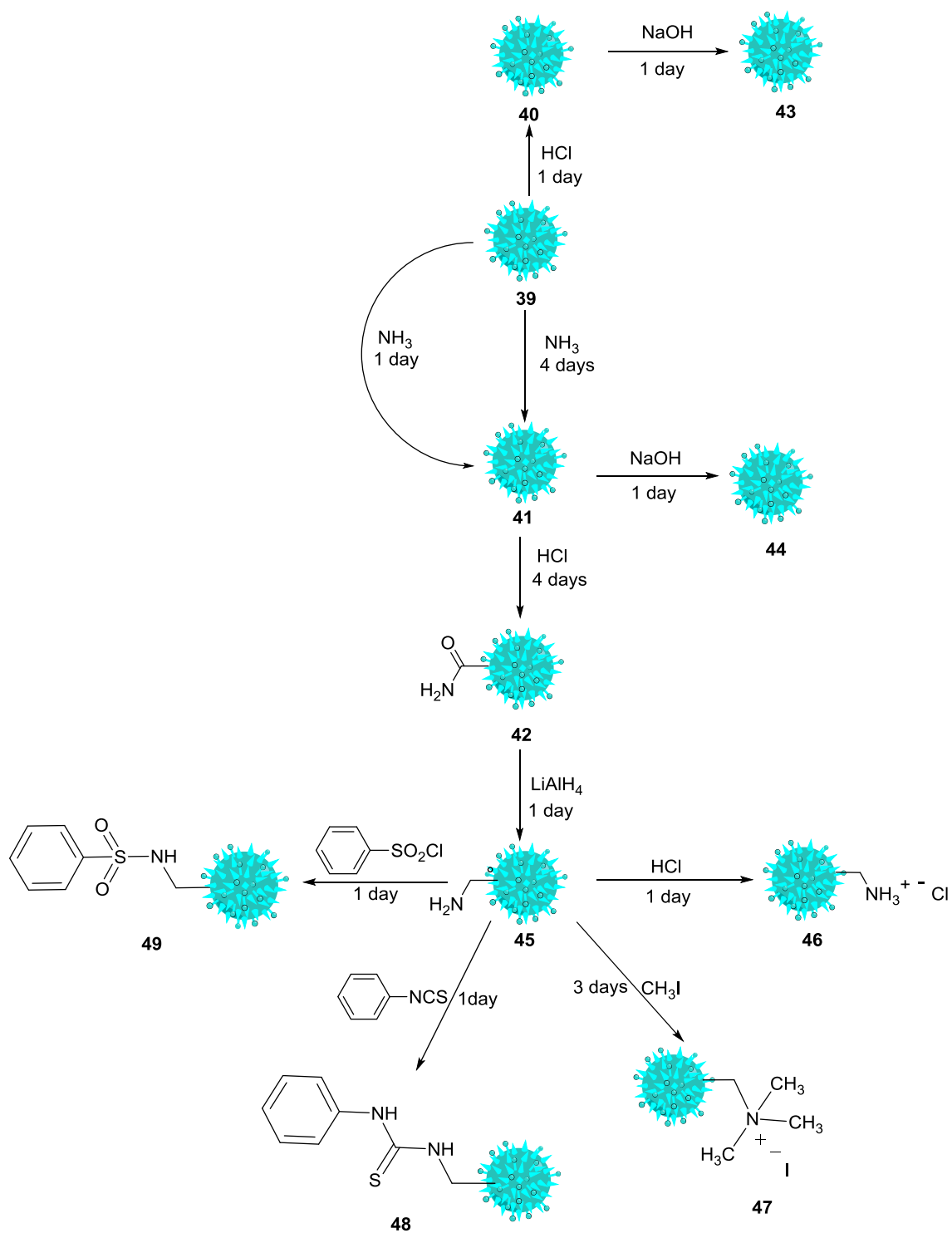
The pollen grains of date males (*Phoenix dactylifera* L.) for a number of species of date have been examined and photographed using scanning electron microscopy (SEM) to find differences in the morphological properties. The analysis of the pollen grains showed some specific variations in some morphological properties. In general they are monad, elliptical, and fusiform with the exine pattern reticulate and irregular. Differences in shape, size, pollen weight, germination percentage, length, width and number of pores were observed.

3.3 Characterisation and functionalisation of date spore exines

Although, many studies have been performed on exines, the chemical structure is still poorly characterised due to its relative inertness.²²⁵ Some of the common elements of composition are carbon, hydrogen and oxygen, with an aliphatic framework and aromatic moieties. Some of the functional groups observed include aliphatic carbons including methyl groups, oxygenated functionalities, olefinic and aromatic unsaturated groups, carboxylic acids and esters. Sporopollenin could be considered as a lipidic copolymer of para-hydroxycinnamic acids (ferulic acid and p-coumaric acid) and fatty acids, whose linear hydrocarbon chains, mainly composed of 16 or 18 carbons, are highly cross-linked by ether and ester functions.²²⁵ To better understand the structure and the availability of functional groups on the surface, derivatisation of sporopollenin with simple reagents is required.^{199,226-229} Date spores are an attractive source of sporopollenin. However, the researchers using date spores (*Phoenix dactylifera* L.) are limited and its chemical composition/structure has never been extensively studied. Here we report the following investigation: (i) Extraction of date spores to remove the genetic and other components for the exine see Section 3.3.1. (ii) Followed by direct amidation and subsequent reductive amination of date spores by simple reaction of ammonia, and then reduction of generated primary amide group to primary amine *via* using lithium aluminium hydride (LiAlH₄), see Section 3.3.2. (iii) Examine the reactivity of generated amines (product 45) in different primary amino group specific reactions, see



Scheme 32

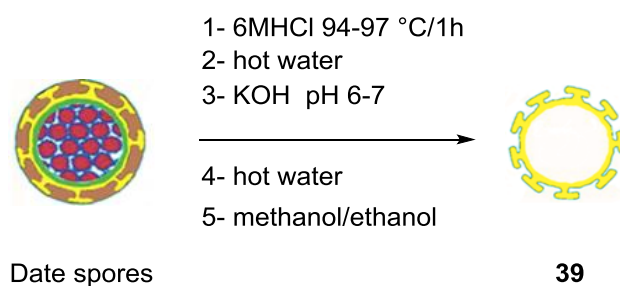


Scheme 32-Extraction and functionalisation of date palm sporopollenin.

3.3.1 Extraction of date spore exines

The extraction of sporopollenin exines from raw spores is an essential step before investigation of the materials properties. A number of different methods have been described in the literature for the preparation of sporopollenin exine capsules see section 3.2.2. An appropriate extraction process aims to: (i) minimise damage to the sporopollenin exine to yield intact microcapsules. (ii) remove the allergenic nitrogenous materials, e.g. proteins and nucleic acids, to give a material with 0.00% nitrogen. (iii) maximise cytoplasm and cellulose extraction to produce a large internal cavity which can be exploited for microencapsulation. (iv) remove the chaff and any other plant remnants that may be present.

In this work, raw spores (loose powder, 25 g) were first suspended in an aqueous solution of HCl (9 M, 112.5 ml) and heated at 95°C for 1 hour to remove the polysaccharides and cellulose. The suspension was washed with hot water and then neutralised with a 50% aqueous solution of KOH to hydrolyse the proteins, nucleic acids or other nitrogenous products. The spores were filtered and washed several times with hot water, methanol and ethanol, then dried. The procedure is depicted in **Scheme 33**.



Scheme 33 Preparation of date sporopollenin exines.¹⁸¹

The combustion elemental analysis results were 44.89% carbon, 6.10% hydrogen and 0.00% N. The material can now be considered as allergen free and empty of any proteins due to the absence of nitrogen. The yield of recovered material based on

starting mass was 42%. The SEM images in **Figure 28** show that before extraction, the spore shape was elliptical-oblate pollen with one deep germinal furrow across the polar surface (deflated or collapsed). Whereas, after extraction, the sporopollenin exines obtained are intact, but open from the one side. That could be attributed to one or both of the following factors: (i) removal of the cellulose intine which provides structural stability to maintain the shape of the spores and/or (ii) the application of vacuum during the SEM analysis which could cause opening of the sporopollenin exines.

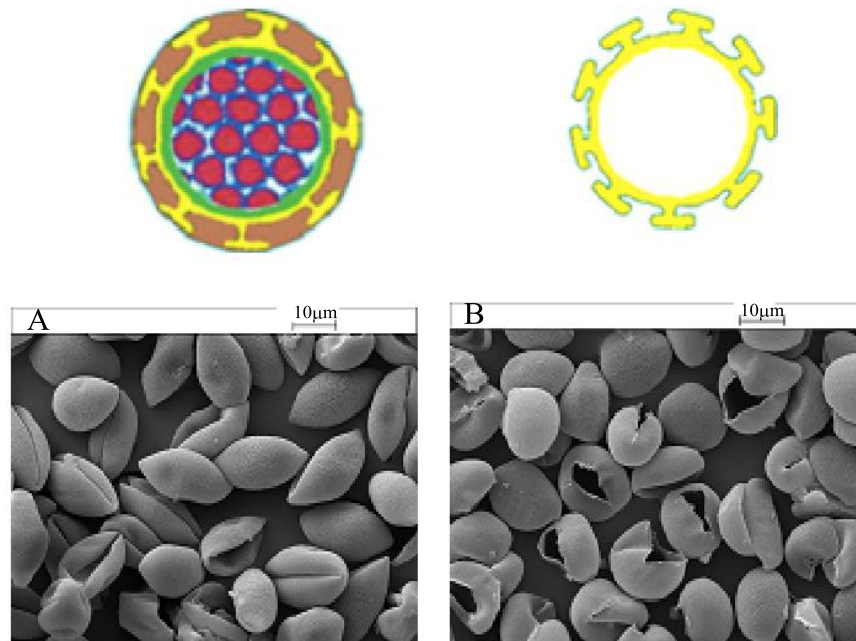
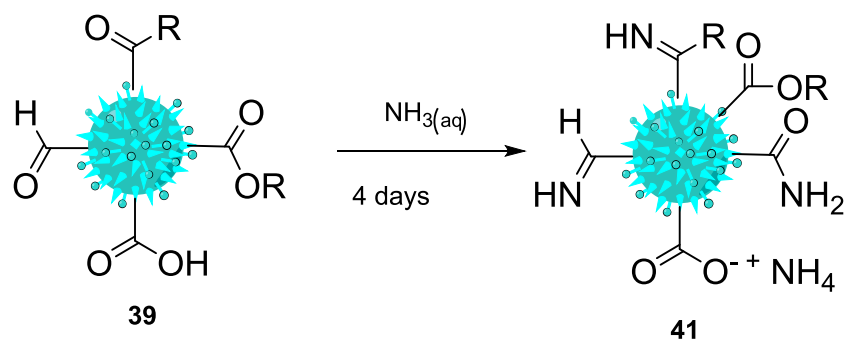


Figure 28-SEM images of date spores (a) before extraction (b) after extraction.

3.3.2 Reaction with ammonia

It is possible to modify sporopollenin by amination reaction.²³⁰ This involves subjecting it to the treatment with concentrated aqueous ammonia followed by a thorough wash with water and drying, see **Scheme 34**.

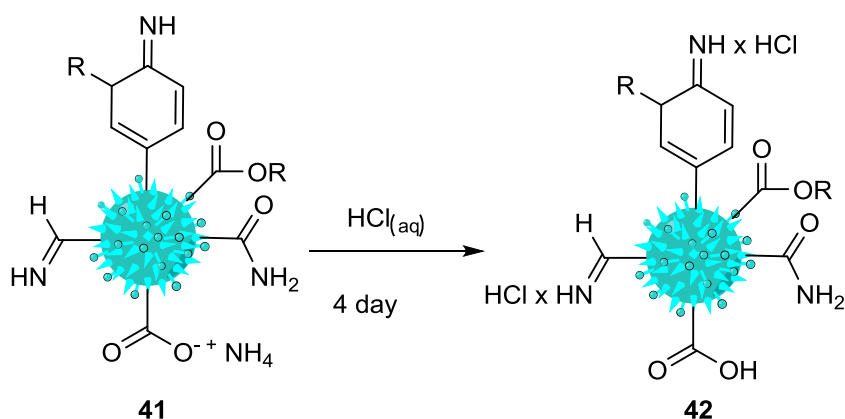


Scheme 34-Treatment of date sporopollenin with ammonium hydroxide

Thus, the date spore exines were treated with concentrated aqueous ammonia at room temperature for 24 hours, washed and dried to form **41**. The elemental analysis shows that product **41** contains 44.55% carbon, 5.92% hydrogen and 0.90% (0.64 ± 0.04 mmol. g⁻¹) nitrogen. Increasing the reaction time to 4 days, led to an increase in the nitrogen content up to 1.4% (1.00 ± 0.05 mmol. g⁻¹). Before treatment with ammonia, sporopollenin does not contain any nitrogen. The FTIR spectra of sporopollenin **39** shows signals in 1720-1600 cm⁻¹ range attributed to C=O and C-O vibrations, see **Figure 29**. The FTIR spectra of aminated sporopollenin **41** presents a similar pattern with 1720 cm⁻¹ band disappearing and 1680 cm⁻¹ signal increasing, which is consistent with expected amidification of esters and/or amination of aldehydes/ketones.²³¹⁻²³³

3.3.3 Treatment of aminated sporopollenin with 2M HCl_(aq)

In order to further investigate the nature of the reaction of ammonia with the date spore exines, **41** was treated with dilute hydrochloric acid (2M) at room temperature for 4 days to give **42**, see **Scheme 35**. This treatment should distinguish between a covalently bound nitrogen and nitrogen retained in form of ammonium salts in terms of reactivity and retention of the nitrogen containing species.

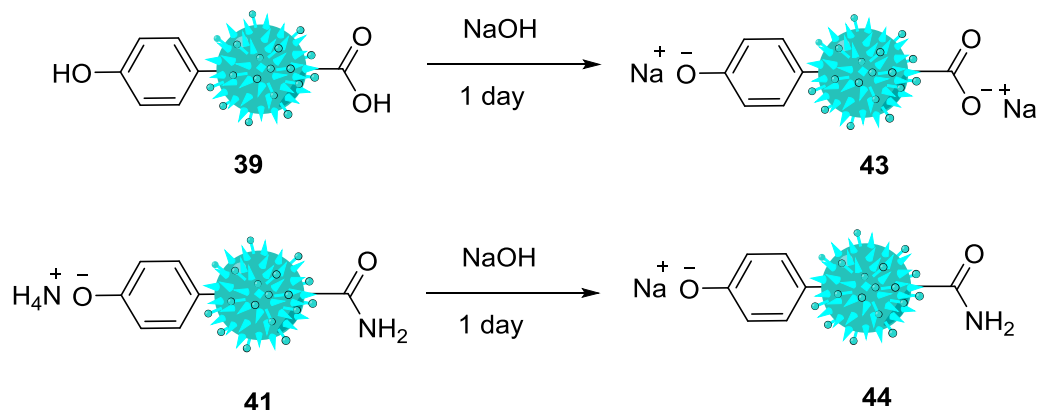


Scheme 35-Treatment of aminated date sporopollenin with hydrochloric acid

The elemental analysis of **42** revealed a 20% relative reduction of nitrogen content as compared with **41** (0.80 ± 0.04 mmol. g⁻¹ vs 1.00 ± 0.05 mmol. g⁻¹ nitrogen). This loss can be explained by the displacement of non-covalently bound ammonium ions or acid hydrolysis of metastable imines. Chlorine analysis of **42** indicates 1.451 mmol. g⁻¹ of chlorine, with similarly treated **39** showing no retention of chlorine. Amides are very weak bases and could not be protonated by 2M HCl, thus the detection of chlorine in **42** indicates the formation of aromatic imines.²³⁰ It is concluded that the nitrogen retained by exines **42** was covalently bound in acid stable groups, such as amides or imines stabilised by conjugation.⁷⁸

3.3.4 Ion exchange properties of ammonia - treated date sporopollenin

It was found that when date spore exines **39** (directly from extraction) and **41** (treated with ammonia) were treated with aqueous sodium hydroxide, forming the derivatives **43** and **44** respectively, they retain sodium ions indicating the presence of acidic functional groups., see **Scheme 36**. This ability to exchange cations opens the potential application of sporopollenin as cation exchange resin.



Scheme 36-Reaction of date sporopollenin and aminated sporopollenin with sodium hydroxide

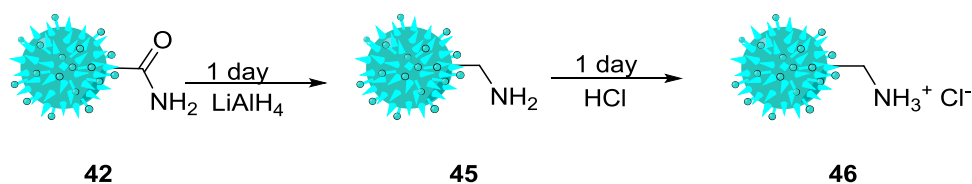
The elemental analysis of **43** and **44** did not show an expected variation of CHN content due to retention of sodium, as measured by ICP analysis, at 8.17% (3.55 mmol. g⁻¹) and 3.20% (1.391 mmol. g⁻¹) for **43** and **44**, respectively, see **Table 12**. Unfortunately, the products **39** and **41** were not analysed by ICP and we can only hypothesise that some content other than carbon, nitrogen and hydrogen was removed by sodium hydroxide treatment and replaced by sodium leaving CHN content unchanged. The almost three-fold higher sodium retention in **43** vs **44**, thus, could be explained by partial transformation of ester groups into amides during the ammonia treatment generating **41**, leaving fewer ester groups to be hydrolysed by sodium hydroxide treatment revealing sodium trapping carboxylates.

Table 12-Sodium and nitrogen content of compound **4** and **5**

Compound No.	N%	Na%
43	0	8.17
44	1.07	3.20

3.3.5 Reduction of date spore exine

Reduction of **42** by lithium aluminium hydride was investigated, see **Scheme 37**. The resulting material **45** has elemental composition of 44.23% carbon, 6.11% hydrogen and 0.84% (0.6 mmol. g⁻¹) nitrogen. When **45** was reacted with hydrochloric acid at room temperature, a chloride salt **46** was formed, indicating that the starting material is basic in nature. The elemental composition of **46** was found to be 44.72% carbon, 6.01 % hydrogen, 0.83% (0.592 mmol. g⁻¹) nitrogen and 2.06% (0.580 mmol. g⁻¹) chlorine. The molar amount of the chloride ion is close to the molar amount of nitrogen in **45**. This reinforces the belief that, all of the nitrogenous functional groups were reduced to give basic functional groups. These results are in line with a primary amide being converted to a primary amine.

**Scheme 37**-Reduction of aminated date sporopollenin.

The FTIR analysis of **45** (formed on lithium aluminium hydride reduction of **41**) reveals the absence of the characteristic carbonyl peak at 1720 cm⁻¹, previously observed for **41**. The FTIR spectra of both **41** and **45** retain a broad peak at 3500-3400 cm⁻¹ corresponding to O-H and asymmetric and symmetric N-H stretchings. The signal corresponding to the C-N stretching vibration shifts from 1093 cm⁻¹ to 1030 cm⁻¹, which is in agreement with the expected change in C-N bond stretches for amine vs amide functional group.²³¹⁻²³³ Overall, the FTIR data supports the initial hypothesis that ammonia treatment of sporopollenin produces amide functional groups, which can then

be converted into amine functional groups by lithium aluminium hydride reduction, see **Figure 29**.

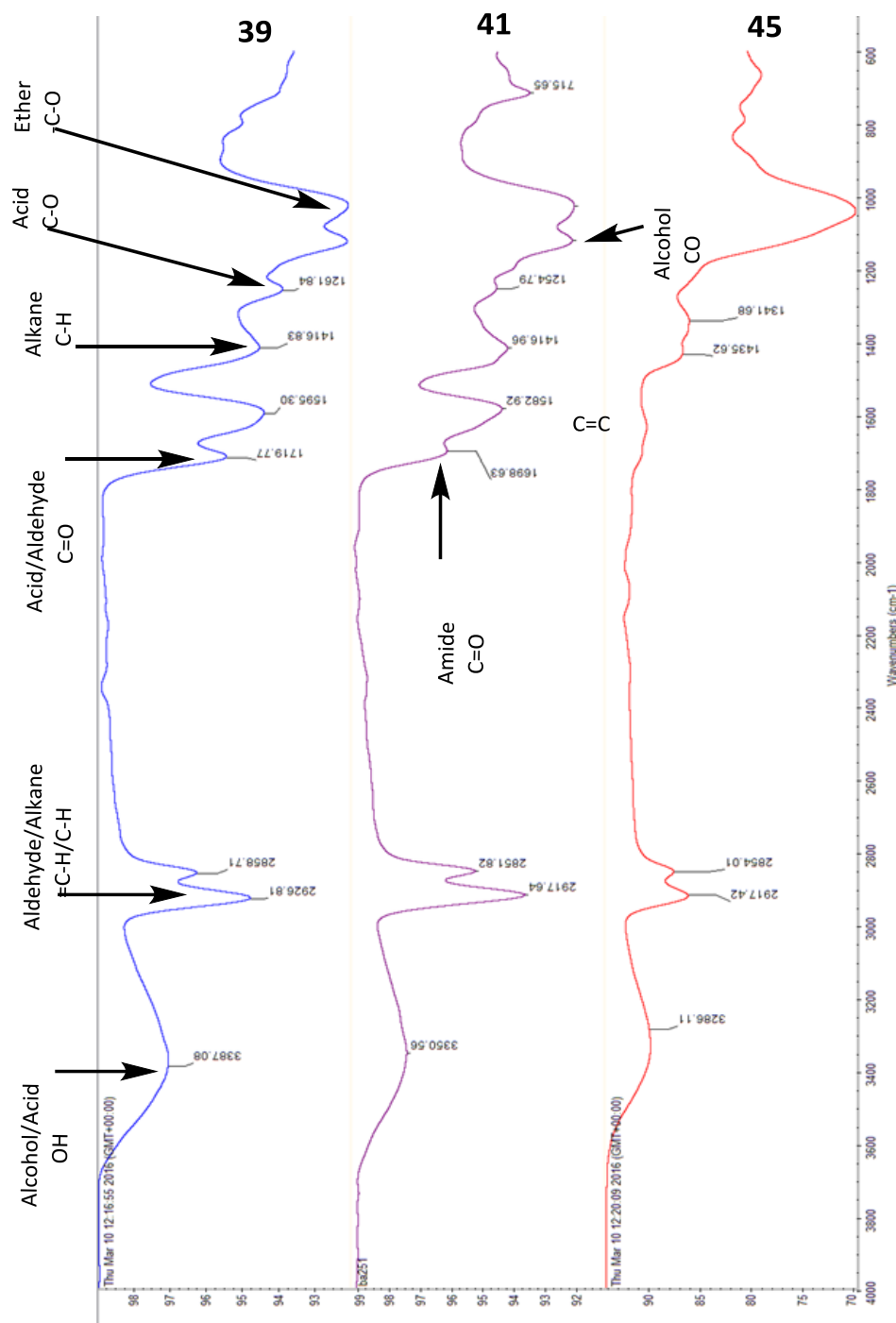
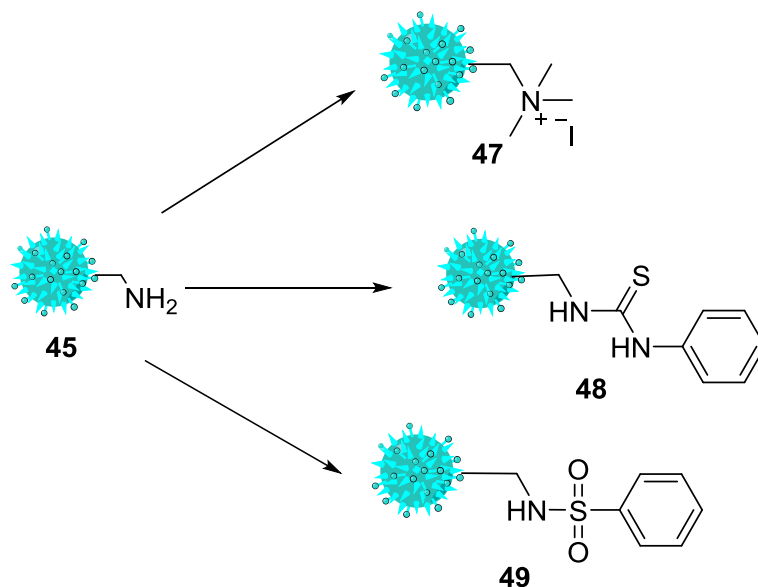


Figure 29-FTIR spectra for date sporopollenin before/after treatment with ammonia and after reduction by lithium aluminium hydride

3.3.6 Further derivatisation of sporopollenin

In order to confirm the presence of amine functional groups on the date sporopollenin material **45**, it was subjected to three different types of reactions which are typical of primary amino groups, see **Scheme 38**.



Scheme 38-Three different reactions suitable for primary amine product **45**

The first reaction involved methylation of **45** by methyl iodide to give material **47** using Hofmann's reaction conditions. The elemental composition of **47** shows that it is 42.41% carbon, 6.41% hydrogen, 0.86% (0.614 mmol. g^{-1}) nitrogen and 5.31% (0.306 mmol. g^{-1}) iodide ion. This demonstrated that 50% of the nitrogenous groups of **45**, considered as primary amines, successfully formed quaternary ammonium iodides in **47**.

The second reaction attempted was the nucleophilic addition reaction between **45** and phenyl isothiocyanate to give material **48** with elemental composition of 44.25% carbon, 6.04% hydrogen, 0.78% (0.557 mmol/g) nitrogen. Using ICP for analysis, the sulphur content was found to be 0.91% (0.284 mmol/g). This reaction confirms that the nitrogenous functions in **45** are primary amino groups.

In the third reaction (nucleophilic substitution), **45** was reacted with benzene sulfonyl chloride to give product **49**. The elemental composition of **49** is 45.02% carbon, 6.20% hydrogen, 0.82% (0.585 mmol/g) nitrogen, with the sulphur content found to be 1.43% (0.446 mmol/g). This reaction also indicated that the nitrogenous functions in **45** are likely to be primary amino groups, see **Table 13**.

Table 13-Elemental result for derivatisation of sporopollenin

Comp. No.	%						Mmol g ⁻¹			
	C	H	N	Cl	I	S	N	Cl	I	S
45	44.23	7.11	0.84				0.60			
46	44.72	7.01	0.83	2.06			0.59	0.58		
47	42.41	6.41	0.84		0.31		0.60		0.18	
48	40.25	6.04	0.86			0.91	0.61			0.28
49	45.02	6.92	0.82			0.43	0.58			0.44

3.3.8 Solid state NMR characterisation

Solid-state ¹³C NMR spectra of **39**, **41** and **45** were compared, following normalisation of the spectra at 128 ppm, interpreted as the carbonyl resonance, see **Figure 30**. It was anticipated that the carbonyl could serve as a useful handle for the transformations and would appear in an area with no other peak overlap. Treatment with ammonia did not significantly alter the signals observed. This was expected since, if amide bonds were to form, the peak position would have approximately the same chemical shift (173 ppm) as that of the carboxylic acid groups.²³⁴ In contrast, when **41** was reduced to **45**, the band assigned to the C=O of the carboxyl groups (173 ppm) is no longer present. In conclusion, interpretation of the solid-state ¹³C NMR spectra of the series of compounds was in agreement with the functional group transformations assigned to **39**, **41** and **45**.

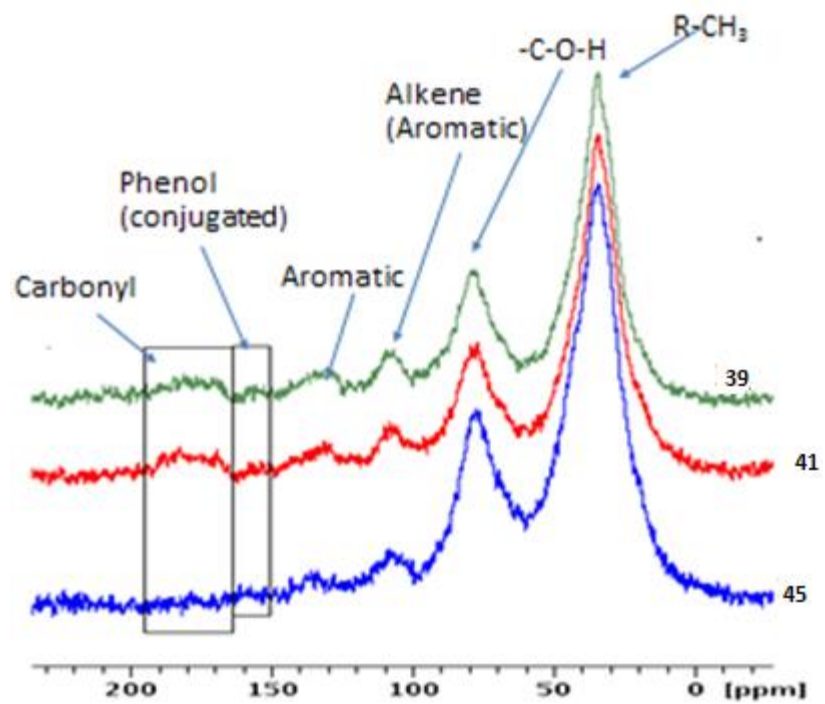


Figure 30- ^{13}C solid state NMR for sporopollenins **39**, **41** and **45**.

3.4 Conclusion

Based on the analytical data collected, when the date spores are reacted with ammonia, primary amide functional groups form by reaction of carboxylic acid groups present on the sporopollenin structure. This knowledge offers an advance in understanding of this relatively unexplored natural polymer and surface functional groups available for reaction. A search of the literature did not locate any reports of characterisation of functional groups on date spore exines. The reduction of nitrogenous groups by lithium aluminium hydride gave basic functions ($N = 0.64 \pm 0.04 \text{ mmol. g}^{-1}$). This showed that, using a simple direct treatment, ammonia can react with date spores, with a nitrogen loading in the same range as that of commercial aminoresins ($0.5\text{-}1 \text{ mmol.g}^{-1}$).²³⁰ These results are supported by FTIR and solid state ^{13}C NMR studies. This work also shows that it is comparatively easily to prepare a solid-supported primary amine on the sporopollenin with a loading comparable to commercial synthetic polymers. The uniformity, reproducibility and widespread availability of such particles could put them in competition with commercial polymeric particles for ion exchange, chromatographic stationary phases and solid supports for catalysts.

Chapter 4

Radiolabelling of sporopollenin

4. Chapter 4: Radiolabeling of sporopollenin

4.1 Aims

The chemical structure of the exines extracted from *Lycopodium clavatum* has been widely reviewed and its physical and biological properties have been investigated. The aim of this study is to attempt to radiolabel various modified sporopollenin materials using the gallium-68 isotopes which will offer the potential for future *in vivo* imaging studies, see section 4.2.2. The initial step was to use mechanochemistry to activate the sporopollenin with different chain lengths of alkyl diamines (to provide a free amine which can be conjugated with other reactive groups for surface functionalisation). This allows the attachment of a macrocyclic chelator (DOTA) which has high affinity for gallium(III) to form stable complexes, see Section 4.3.1 and 4.4.2. This functionalisation was followed by radiolabelling of the sporopollenin and sporopollenin derivatives with gallium-68, see Section 4.3.3 and **Figure 31**. The stability of the radiolabelled material was then studied *in vitro* using phosphate-buffered saline (PBS), transferrin (TF) and simulated gastric fluid (SGF).

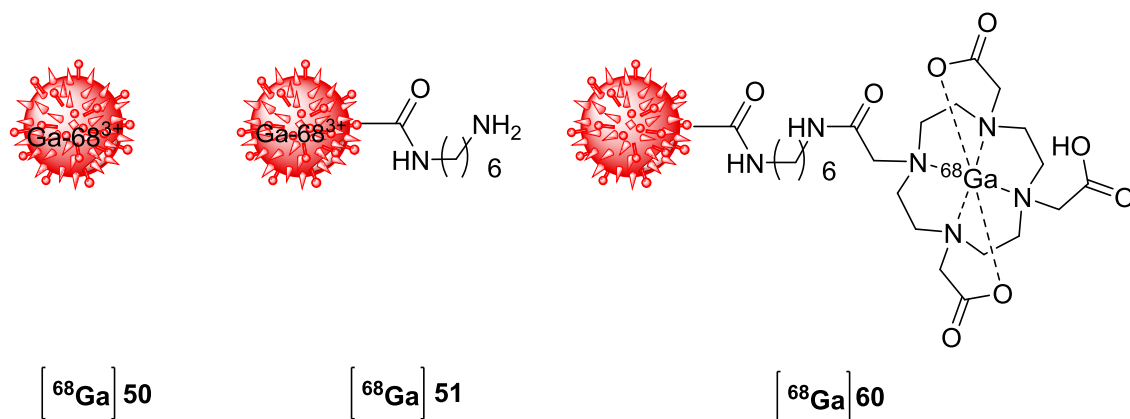


Figure 31-Radiolabelling of sporopollenin and functionalised sporopollenin

4.2 Introduction

The interest has increased in the use of plant origin products in pharmaceuticals due to their effectiveness against various diseases.²³⁵⁻²³⁸ Extraction of effective agents from plants has been crucial for both traditional and modern medicine.^{239,240} At present there is a keen interest in the production of compounds from natural plants, their purification, and radiolabelling with different convenient radioisotopes like ^{99m}Tc or $^{131/125}\text{I}$ to examine their potential use in treatment and diagnosis of diseases.

Historically medicinal plants have been used extensively, however, the side effects of the biological and chemical contents are not well characterised. Due to high consumption without the knowledge of the side effects of plant extract contents, researchers are now focused on the investigation of interactions between plant extracts and biological systems. Radiolabelling and *in vivo* nuclear medicine techniques have been used to advance this understanding. Sensitive molecular imaging techniques such as SPECT and PET are ideal for determining molecular interactions and biodistribution in animals and patients.

This chapter is focused on the sporopollenin exine which extracts from *Lycopodium clavatum* (LC), usually called club moss, which has been used in various traditional medicinal products for the treatment of stomach pain, rheumatic disease, muscle pain and Alzheimer's disease amongst others.²¹⁹ This sporopollenin was activated with diamines and DOTA was attached, it was then radiolabelled with gallium-68 and a study of the stability carried out for these derivatives under biological conditions.

4.2.1 Radiolabelling for monitoring of medical plant extracts' behaviour *in vivo*

Recently, there was a strong renewal of interest in the potential use of plant origin products for the treatment and diagnosis of different diseases. Hence, many researchers have been focusing their efforts on radiolabelling of plant isolated bioactive compounds with radioisotopes such as ^{131}I , ^{125}I and $^{99\text{m}}\text{Tc}$ in order to investigate their biological activities (*in vivo/in vitro*).²⁴¹⁻²⁴⁷ For example, Bapat *et al.* have studied *Psoralea corylifolia* plant which is commonly used in traditional Asian medicine and isolated the active ingredient named bakuchiol. It has been radiolabelled with ^{125}I which, along with its therapeutic potential, provides the opportunity for *in vitro* studies.²⁴¹ *In vitro* cell uptake results showed elevated cell uptake in both lymphosarcoma (LS-A) and radiation induced solid thymic lymphoma indicating the potential for a novel cytotoxic agent development.²⁴¹ Prompted by a growing use of red clover isoflavones in dietary supplements, Engelmann *et al.* used radiolabelled derivatives to study their metabolism deficiency in animal models.²⁴² In a similar way, Tekin *et al.* have studied Lawsonia leaves (henna), which is one of most effective medicinal plant used for treatment of wounds and burns. Biodistribution study of ^{131}I -radiolabelled extracts in Balb/c mice revealed accumulation of active principals in nuterus, breast and ovaries of female and prostate of male animals.²⁴⁶

Olive tree (*Olea europea L.*) products such as olives, olive oil and olive leaves have been studied by multiple groups. The hydroxytyrosol (HT) has been identified as the main phenolic compound; it has been radiolabelled with ^{131}I by Ozkan *et al.*, and its effects studied on various cell lines *in vitro* and in healthy male and female rats *in vivo*.²⁴⁴

Amorim *et al.* studied the effect of the medicinal plant *Punica granatum* on the bioavailability of the radiopharmaceutical ^{99m}Tc -sodium pertechnetate ($\text{Na}^{99m}\text{TcO}_4$) in rats. Their results indicated that there was a substantial increment of the activity of ^{99m}Tc in spleen, heart, abdomen, liver, stout bowel, pancreas, lungs and testis at 5 minutes. 40 minutes after the governing body of the ^{99m}Tc , there was a decisive increase in the spleen, head, heart, abdomen, liver, stout bowel, muscle, femur, lungs, pancreas, kidneys, and testis. The authors indicated that these effects could be justified by therapeutic effect of this extract and/or by the generation of active metabolites capable of interfering with the biodistribution of ^{99m}Tc .^{248,249} Also, Holanda *et al.* looked into the effect of aqueous extract of Aloe Vera, tropical plant popularly known in Brazil as Balboa, on the biodistribution of ^{99m}Tc . There was a substantial increase of radioactivity in blood, femur, kidneys, liver, stomach, testis and thyroid and also in levels of biochemical parameters while there was a significant reduction in levels of glucose, cholesterol, triglycerides, creatinine and urea.²⁴⁹

4.2.2 Molecular Imaging

Molecular imaging provides a method to detect and monitor mechanistic processes in cells, tissues, or living organisms by use of instruments and contrast mechanisms that act without disturbing their living system.²⁵⁰ The term molecular imaging covers many nuclear medicine techniques such as single photon emission computed tomography (SPECT), positron emission tomography (PET), magnetic resonance imaging (MRI), X-ray, computed tomography CT, ultrasound, optical bioluminescence imaging and optical fluorescence imaging.²⁵¹

The imaging is sometimes used to describe the modalities which receive a signal from the specific molecule, tag possibly (in case: PET or SPECT) with a radioisotope. These techniques can provide functional information under physiological conditions, such as receptor occupancy or enzyme flux. On the other hand, imaging modalities (ultrasound or MRI) can provide predominantly anatomic information such as organ size and shape. However, this is not a substantial difference between them due to in reality

all modalities give a mixture of anatomic and functional information.²⁵² Hence, The images can provide valuable information (structural/functional) under physiological conditions, simulation the situation observed in the clinic. In addition, non-invasive and ability to repeat the study on same sample different time lead to reduce the number of animals required and decreases statistical variance thus cost.^{253,254}

In the past decades, interest has grown steadily in using PET as a molecular imaging modality in the clinical inquiry. Due to the ability to diagnostic of the disease in the early stages and monitor therapeutic responses, now gained much importance in the routine hospitals practice.²⁵⁵ Typically an appropriate compound for PET imaging is radiolabelled with positron-emitting radionuclides such as ^{18}F , ^{64}Cu , ^{68}Ga , or ^{89}Zr and administered to a living subject.²⁵⁶

Radiolabelling complexes with targeting vectors play an imperative role for selective imaging of particular tumors/tissue types. Radio-labelled complexes enable the diagnostic imaging of a particular tissue or organ type. To successfully evaluate of such compounds, many disciplines should come altogether such as physics (chose and production isotopes), chemistry (fix the isotope to the vector molecule), biochemistry (which vector molecule is needed and how it binds to the receptors) and medicine (effectivity of the system *in vivo*). Isotopes must meet certain requirements to use in nuclear medicine, (i) for diagnostic applications the isotopes must be γ emitters, whereas for therapy must be β emitters, (ii) half-life times, not too short nor too long, (iii) energy, can be detected outside the body or significant penetration in the tumour tissue.²⁵⁷ The development of targeted delivery techniques and slow release of drugs *in vivo* met keen interest.

Generally, inorganic drug carriers such as silica nanoparticles, superparamagnetic iron oxide nanoparticle, gold nanoparticles, quantum dots etc. which have short half live (few hours), the short-lived or intermediate-lived radioisotopes (^{68}Ga ($t_{1/2}$ = 68 minutes), ^{18}F ($t_{1/2}$ = 109.8 minutes), ^{44}Sc ($t_{1/2}$ = 3.9 hours),

^{66}Ga ($t_{1/2} = 9.7$ hours), ^{64}Cu ($t_{1/2} = 12.7$ hours), etc) would be suitable. However, organic drug carriers such as carbon nanotubes, polymeric nanoparticles, micelles, and liposomes, which can circulate *in vivo* for 24 hours, the ideal choices is intermediate-lived or long-lived radioisotopes such as ^{66}Ga ($t_{1/2} = 9.7$ hours), ^{64}Cu ($t_{1/2} = 12.7$ hours), ^{89}Zr ($t_{1/2} = 78.4$ hours), or ^{124}I ($t_{1/2} = 4.17$ day).²⁵⁸⁻²⁶¹

4.2.3 Why image sporopollenin exines

The development of targeted delivery techniques and slow release of drugs *in vivo* met great interest. *Lycopodium clavatum* (LC) (**Figure 32**) are one of the species which most widely studied as sporopollenin exine capsule (ESCs), and have been used for a long time as a natural powder lubricant, a base for cosmetics, and in herbal medicine.^{215,262-265} The LC exine has higher resistance to alkali and acid treatment than other species.¹⁷⁵ Recent research of *L. clavatum* (SECs) as encapsulation has demonstrated high efficiencies with drugs, vaccines, proteins, cells, oils and food supplements in comparison to conventional encapsulation materials.^{181,202,209,213,230,266,267}

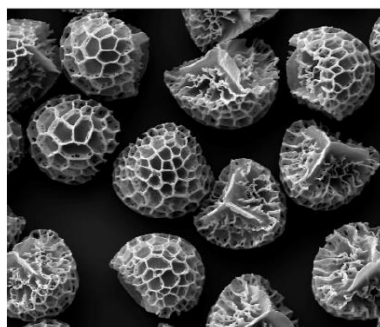


Figure 32-*Lycopodium clavatum* SEM

There is a report of *L. clavatum* formulation for gadolinium (III) encapsulation used as MRI contrast agent in the clinic. Empty sporopollenin is loaded by the desired compound, and depended on partially enzymatic digestion of sporopollenin contents will be released.²⁶⁸ The hypothesis for this mechanism is based on sporopollenin protecting the contrast agent from the stomach acid till the microcapsules reach the gut

and attach to the gut wall. The behaviour of the sporopollenin adsorbed to the gut is not clear. It has been proposed that microcapsules may cross into the blood stream either intact or partially digested by specific non identified enzymes. Therefore, this chapter tries to fill this gap in understanding of sporopollenin's behaviour *in vivo* or/and investigate the process responsible for the therapeutic effect, via gallium-68 radiolabelling of sporopollenin and monitoring the radiolabelled sporopollenin *in vivo*. The work has been done as following: aminated sporopollenin with different length diamine by using mechanochemistry, followed by reacted with DOTA and then radiolabelling them with Gallium-68, finally, study the stability of radiolabelling sporopollenin *in vitro*.

4.2.4 Chemistry of gallium

Gallium is found in the crust of the earth in trace quantities, and there is no natural biochemical function known for it. However, there are some low-valence gallium compounds known. Almost all applications of gallium in radiopharmaceuticals synthesis occurs in +3 oxidation state. The gallium with this oxidation state classified as a strong Lewis acid and binding strongly to non-polarizable Lewis bases.²⁶⁹ Thus, commonly it is coordinated with ligands containing oxygen or/and nitrogen as donor atoms. In general coordination chemistry of gallium is similar to that of a high spin ferric ion with coordination number six.

The gallium isotopes Gallium-67 and Gallium-68 are attractive for use in nuclear medicine due to nuclear properties. The Ga-67 is produced by cyclotron and the two formulas available in the commercial are gallium chloride and gallium citrate. Due to the relatively long half-life (3.3 days), this isotope (Gallium-67) is used in researchs which required time over the period of several days. Whereas gallium-68 is one of the few short-life positron emitting radionuclides from generator system. The long half-life of germanium-68 (271 days) is enough to avoid problems in generator delivery, the short half-life for Gallium-68 (68 minutes) is suitable for radiopharmaceutical synthesis and reduced the radiation dose received by patient. Thus, this kind of generator ideal as a

source of positron emitting radiopharmaceuticals for imaging with positron emission tomography (PET), in institutions that do not have access to a cyclotron.

Cationic Gallium-68 eluted from the $^{68}\text{Ge}/^{68}\text{Ga}$ generator using 0.1M hydrochloric acid, providing an extensive radiopharmaceutical synthesis. Most isotope synthesis procedures use weakly coordination ligands such as citrate, acetate or oxalate to prevent the formation of insoluble gallium tri-hydroxide $\text{Ga}(\text{OH})_3$ and soluble $\text{Ga}(\text{OH})_4^-$, which significantly reduce the kinetics of complex formation. Bifunctional chelators (BFCs) are used to attach Gallium-68 into a targeting vector. BFC is required the mild condition to form useful radiolabelled complexes, which help to avoid degradation of the linked biomolecule. Due to the short half-life of the gallium-68 ($t_{1/2} = 68$) enables improved dosimetry and repeat imaging and fast carry out the procedure, making these agents ideal for clinical use. Whereas gallium-68 has been used largely with DOTA-TOC, DOTA-TATE and DOTA-NOC,²⁷⁰⁻²⁷² DOTA-peptide derivatives which are neuroendocrine tumour targeting agents. There are many more Gallium-68 peptides conjugates at different stages of clinical trials.^{273,274}

Clinically, there are too much more Gallium-68 peptides conjugated at different phases of clinical trials.^{273,274} The area was first searched by make and co-workers, then recently expanded into further clinical trials by Baum and co-workers.²⁷⁵⁻²⁷⁷

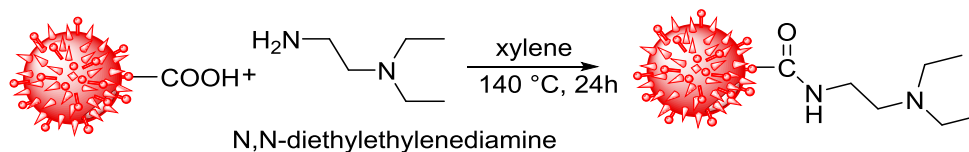
4.3 Functionalisation of sporopollenin exines

4.3.1 Isolation of exines

The amount of intine varies, and it depends on the type of pollen, spore source, the intact contents and extraction methods. *Lycopodium clavatum* has been chosen for this study due to the availability of different suppliers, and many previous studies have used these spores, hence the chemical composition has less ambiguity and functionalisation is better understood. *Lycopodium clavatum* is also considered a renewable and sustainable raw material.²⁷⁸ The extraction methods used in this study have been already described in chapter 3.

4.3.2 Amination of sporopollenin by mechanochemistry

Multiple research groups have investigated the amination of the sporopollenin exine due to its potential applications in drug delivery, encapsulation and solid phase synthesis, as previously discussed.²⁷⁸⁻²⁸⁰ Adamson *et al.* described a method for the amination of the sporopollenin exine with 1,3-diaminopropane and also develop a technique that can be used to estimate the amount of free amine on the surface (based on amine reaction with picric acid) however, the results they obtained were variable.^{204,280} Youkui *et al.* reported a sporopollenin exine amination method that consisted of heating sporopollenin with *N,N*-diethylethylenediamine, *N,N*-diethyl-1,3-propanediamine or diethylenetriamine at reflux in xylene for 24 hours, to achieve loadings of 2.11 mmolg⁻¹, 2.58 mmolg⁻¹ and 4.2 mmolg⁻¹ respectively. Protonating the free amine groups with 2M hydrochloric acid solution and determining the amount of amine present by ICP chloride analysis was the preferred method to determine the free amine available for reaction, see **Scheme 39**.²⁸¹



Scheme 39-Amination of sporopollenin with *N,N*-diethylethylenediamine.²⁸¹

The possibility for amination of the sporopollenin exine via mechanochemistry was studied using hexane-1,6-diamine. Mechanochemical parameters, such as speed of milling, the presence of a solvent, and time required to either (i) optimise the yields or (ii) optimise the time for functionalisation, were investigated. Crude mixtures were washed multiple times and successively with distilled water, methanol and ethanol. They were then dried at room temperature under vacuum followed by further drying at 40°C in the oven for 24 hours. The nitrogen content was taken as the key indicator for amination efficacy. The highest nitrogen content was found when the sporopollenin was ground together with hexane-1,6-diamine at 400 RPM in the absence of solvent for 1 hour, see **Table 14**.

Table 14- Grinding sporopollenin with hexane-1,6-diamine

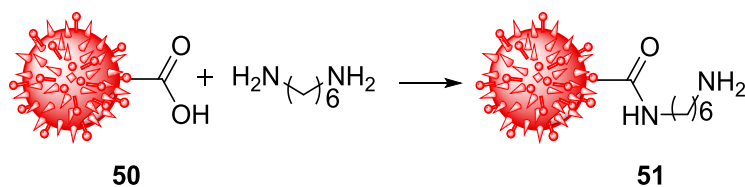
Entry	conditions	C%	H%	N%	N mmol.g ⁻¹
		62.12	9.03	0.00	0.00
50.1	30 min, 400 RPM, No solvent	60.76	9.06	1.63	1.16
50.2	1h, 400 RPM, No solvent	60.55	8.92	2.47	1.70 ± 0.04
50.3	2h, 300 RPM, 90 µl CH ₃ CN	66.06	10.60	1.66	1.18
50.4	3h, 200 RPM, No solvent	60.40	8.77	2.36	1.68 ± 0.03

The comparison of nitrogen content measured by elemental analysis and chlorine content determined by chloride analysis was a useful indicator of the free amino groups present relative to the amount of diamine reacted, see **Table 14** and **Table 15**.

Table 15-Result for chloride analysis to compound **50.1** and **50.2**

Compound No.	Cl%	Cl mmol.g ⁻¹
51.1	1.62	0.456
51.2	1.48	0.416

This result shows that only one-third of amine groups can be protonated, indicating that around 50% of the hexane-1, 6-diamine is bound to the sporopollenin with a single amide bond presenting free amino groups on the surface that are available for further conjugation, see **Scheme 40**.



Scheme 40-Amination of sporopollenin with hexane diamine

The diamines can couple to the sporopollenin either (i) via a single amide bond, leaving a free amino group available for further reaction or (ii) via formation of two amide bonds, crosslinking to adjacent carboxylic acid groups and losing the potential for further reaction, see **Figure 33**.

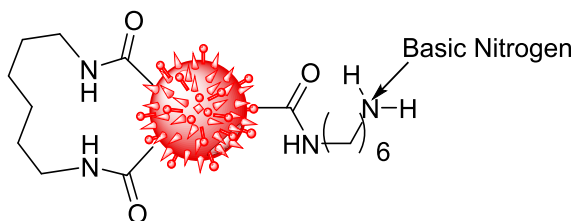
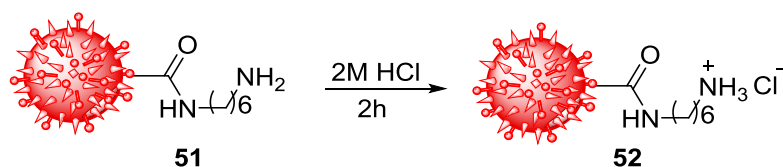


Figure 33-Primary amine nitrogen and schematic showing crosslinking via formation of two amide bonds for the diamine with sporopollenin.

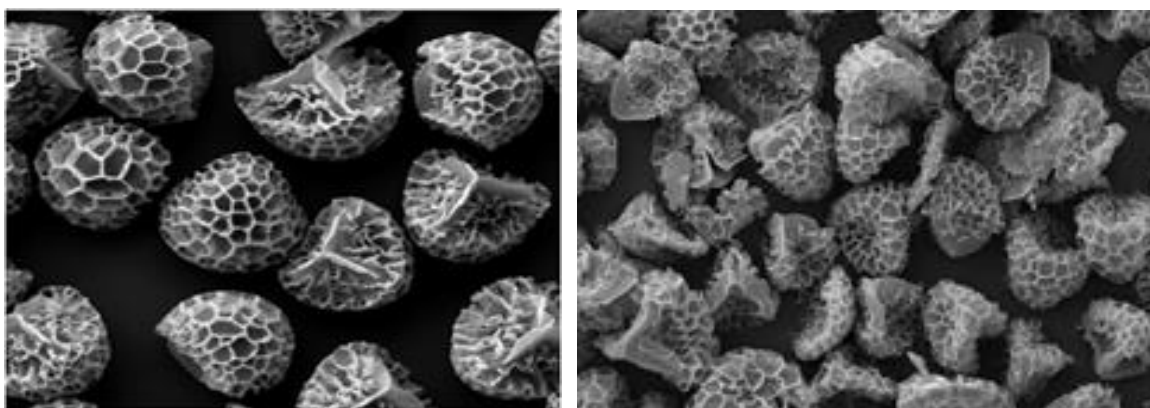
Only unreacted amino groups retain their basicity and, consequently, can be transformed into the hydrochloride salt by treatment with HCl, see **Scheme 41**. Thus, the aminated product was suspended in aqueous hydrochloric acid (2 M), stirred for 2 hours at room temperature, recovered by filtration and then washed several times with water, followed by methanol and ethanol before drying under *vacuum*.



Scheme 41-Protonated aminated sporopollenin with 2M hydrochloric acid at RT

Grinding could potentially destroy or significantly damage the three dimensional structure of the sporopollenin exine potentially compromising its use as a carrier. Scanning electron microscope (SEM) analysis was carried out, revealing that the applied mechanochemical stress did not significantly change the morphology of the sporopollenin, see

Figure 34.

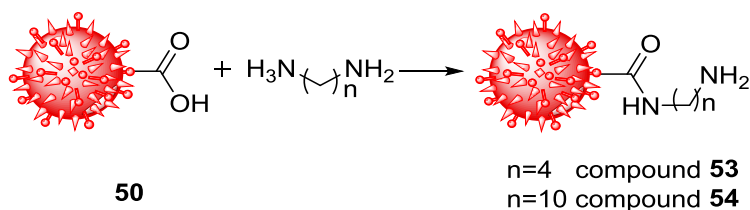


Before grinding

After grinding

Figure 34-SEM image for sporopollenin before and after grinding for 1h.

In order to validate the optimised conditions, the amination has also been carried out using shorter chain (butane-1,4-diamine) and longer chain (decane-1,10-diamine) diamines, see **Scheme 42**.



Scheme 42-Grinding sporopollenin with different chain lengths of diamine

The attachment of diamine was confirmed by the presence of nitrogen see **Table 16** which was absent in the starting material and could not be removed by washing repeatedly with large volumes of solvents (methanol, ethanol, and water). The data shows that for butane-1,4-diamine (**53**), 1.964 mmol g⁻¹ loading was achieved, whereas for decane-1,10-diamine (**54**) the loading was 1.671 mmol g⁻¹. As previously, the amount of unreacted amino groups was determined by treatment with 2M HCl for 2 hours at room temperature to produce **55** and **56**.

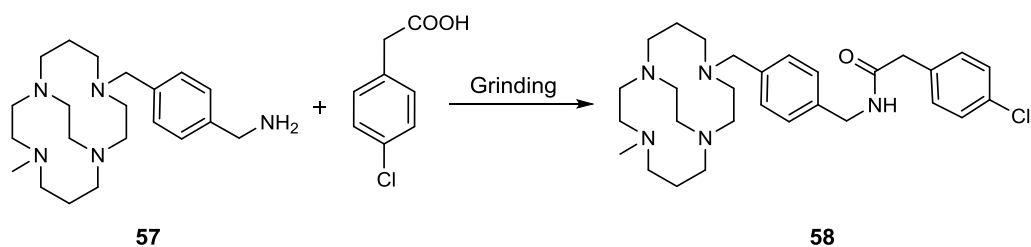
Table 16-Grinding sporopollenin with different chain length diamine

Compound No.	C%	H%	N%	N mmolg ⁻¹	Cl%	Cl mmol g ⁻¹
53	60.20	5.22	2.75	1.96		
54	60.25	5.77	2.34	1.67		
55					0.73	0.20
56					0.90	0.25

4.3.2 Functionalisation of sporopollenin with the azamacrocycle DOTA

DOTA (1,4,7,10-tetraazacyclododecane-1,4,7,10-tetraacetic acid) is a widely used transition metal chelator based on cyclen, and discussed extensively in chapter 2. Dependent on the chelated metal ion, DOTA complexes have been employed in various medical applications from targeted MRI contrast agent design to radioimmunotherapy. To the best of the author's knowledge, there are no reports of conjugation of DOTA to sporopollenin and moreover, effecting the conjugation by mechanochemical methods.

A model reaction for amide formation was attempted based on precursors available in the laboratory. This was carried out by grinding 4-chlorophenyl acetic acid with (4-((11-methyl-1,4,8,11-tetraazabicyclo[6.6.2]hexadecan-4-yl)methyl)phenyl) methan amine **57**, see **Scheme 43**. Suitable conditions for amide formation were obtained after multiple attempts.



Scheme 43-Grinding of **57** with carboxylic compound.

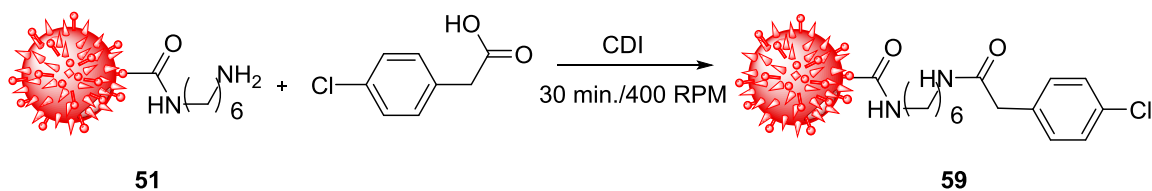
Initially, the starting materials were ground together (400 RPM) for 30 minutes in the presence of acetonitrile, the reaction was monitored by mass spectrometry, and there was no indication that the desired product had been formed. This result led to modification of the process to use an amide bond formation coupling reagent, either *N,N'*-diisopropyl carbodiimide (NDP) or carbonyldiimidazole (CDI) were utilised in different ratios; suitable conditions were found to be grinding the carboxylic acid with CDI, with each as four equivalents to the amine to be added, for 5 minutes. This was followed by further grinding with one equivalent of the amine for 10 minutes. The crude product was then ground with water for 10 minutes. The resultant crude material was extracted with dichloromethane and the solvent evaporated under vacuum to obtain the desired product in a 75% isolated yield see **Table 17**.

Table 17- Multiple attempts to optimise grinding for the peptide coupling reaction

Catalyst	Time	solvent	ratio	product
None	30 minutes	CH ₃ CN	1:1	SM
NDP	30 minutes	CH ₃ CN	1:1:1	mix.
NDP	3 hours	CH ₃ CN	1:1:1	mix.
CDI	5:10:5 minutes	none	1:1:0.9	mix.
CDI	5:30:5 minutes	none	1:1:0.9	mix.
CDI	5:90:5 minutes	none	1:1:0.9	mix.
CDI	5:10:5 minutes	none	2:2:1	mix.
CDI	5:10:10 minutes	none	4:4:1	75%

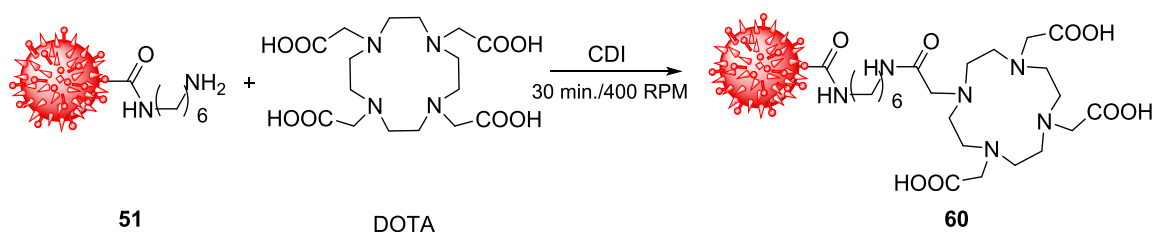
Ratio = carboxylic acid: Catalyst: Amine

The conditions determined in this set of experiments were then used for grinding of sporopollenin with hexane-1,6-diamine with a four fold excess of 4-chlorophenyl acetic acid (per amino group) and a four fold excess of coupling reagent (carbonyldiimidazole, CDI), at 400 RPM for 30 minutes, see **Scheme 44**. As previously, the crude mixture was washed multiple times with distilled water, methanol and ethanol, and dried at room temperature under vacuum followed by 24 hours at 40°C. The chloride analysis showed that the amount of chloride is 0.52 mmol g⁻¹ clearly showing that the carboxylic acid had reacted with the free amino groups available on the surface of the sporopollenin.



Scheme 44-Grinding of aminated sporopollenin with carboxylic acid

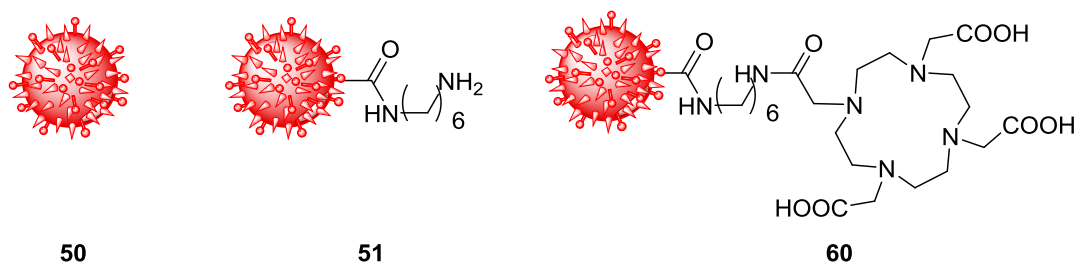
Finally, the developed conditions were used for conjugation of a tetraazamacrocyclic (DOTA) with aminated sporopollenin, see **Scheme 45**. The elemental analysis showed that the amount of nitrogen increase from 1.7 mmol g^{-1} to $2.228 \text{ mmol g}^{-1}$, indicating that the reaction of DOTA with the free amino groups on the surface of sporopollenin had occurred.



Scheme 45-Grinding aminated sporopollenin with DOTA

4.3.3 Radiolabelling of sporopollenin with gallium-68

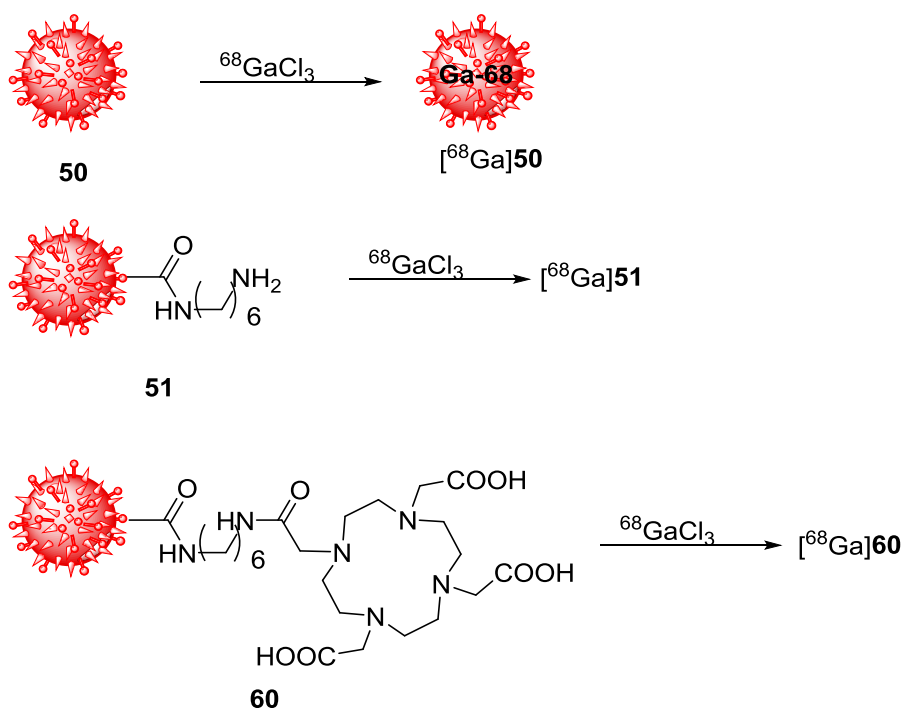
This section reports the gallium-68 radiolabelling of the functionalised sporopollenin derivatives **50**, **51** and **60**, for potential use in positron emission tomography (PET) imaging, see **Scheme 46**.



Scheme 46-The compounds which used in radiolabelling experiments

Compounds **50** and **51** will have surface donor atoms capable of binding to gallium-68 but they do not have the added chelating ligand for gallium-68 complex formation, whereas derivative **60** has been functionalised with the well characterised chelating ligand DOTA.²⁸²

The reactions were carried out using 0.2 mg of **50**, **51** or **60** in 0.2 mL buffer solution with formulated gallium-68 (ca. 40-80 MBq). Sodium acetate buffer (0.2M) at pH 5, was used to prevent the formation of unreactive and insoluble gallium hydroxide species that can be produced at higher pH. The sporopollenin derivatives were reacted with gallium-68 at either room temperature or 90 °C for 30 minutes, see **Scheme 47**. All Gallium-68 reactions were carried out in triplicate and the results are presented as an average along with representative radio-TLC chromatograms.



Scheme 47-Gallium-68 radiolabelling of native and functionalised sporopollenin

Radiochemical complex formation reactions were analysed by radio-TLC chromatograms (eluting with 0.2 M citric acid) with the complex staying on the baseline of the TLC, and the 'free' gallium-68 moving with the solvent front, see **Figure 35**.

Increasing the reaction temperature to 90°C, dramatically increased gallium-68 incorporation by compound **51** (up to 96% (n=3)), whereas there was no change in chelation yields with **50**. Compound **60** presented an unexpected radiolabelling behaviour indicating that our assumption that DOTA was covalently conjugated to sporopollenin was not correct. The observed significant increase in the amount of nitrogen may be explained by some non-covalent trapping of DOTA by sporopollenin that was not removed by washing. This hypothesis is strengthened by detection of free DOTA-⁶⁸Ga complex in radiolabelling mixture of **60** by radio-TLC, see **Figure 37**.

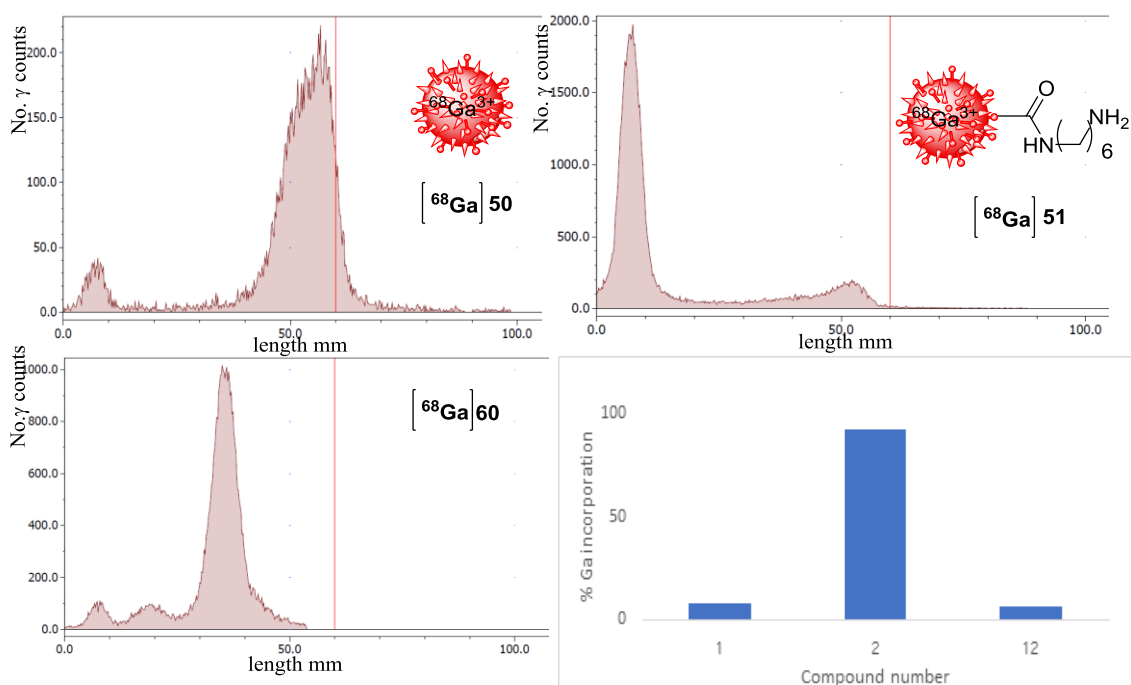


Figure 37- Radio-TLC for gallium-68 reactions with **50**, **51** and **60** at 90°C

Given the ineffective radiolabelling results of **50** and **60**, only **51** was studied further for *in vitro* stability.

4.3.3.1 Phosphate-buffered saline and transferrin stability measurements

The purpose of the *in vitro* stability study is to gain an initial insight into how a drug or a formulation might behave *in vivo*.²⁸³ Thus, the *in vitro* assays conditions should as closely as possible mimic the expected *in vivo* situation. The first requirement for a metal ion bound in the form of chelate to be administrable to human is the chelate stability at physiological pH and when challenged by other metal ion binding competitors that are naturally present in blood plasma. The high similarity between iron(III) and gallium(III) means that gallium(III) ions will typically complex with the protein transferrin to form high stability complexes.

The physiological pH can be reproduced in phosphate-buffered saline (PBS) (0.1 M, pH 7.4, 37°C). There was only very limited release of free gallium from [⁶⁸Ga]**51** within 3 hours' incubation window as shown by the radio-TLC traces, see **Figure 38**.

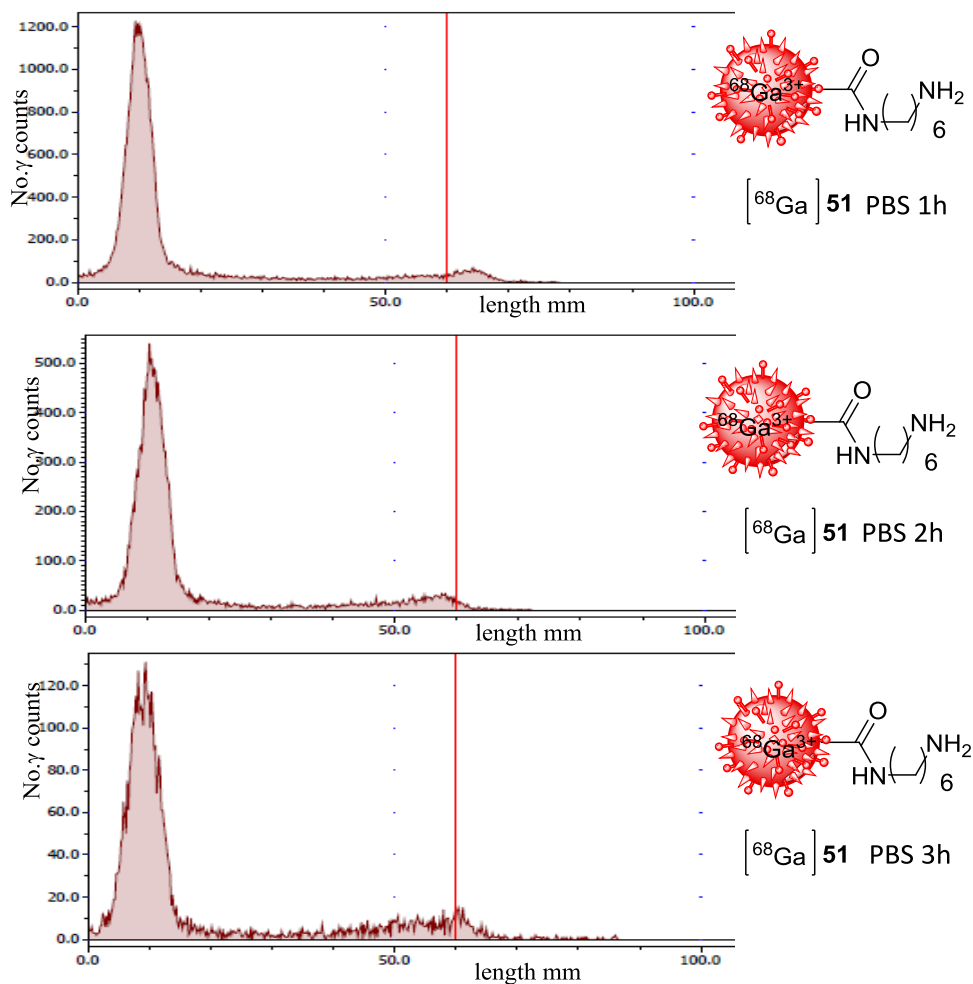


Figure 38- Radio-TLC stability of $[^{68}\text{Ga}]\mathbf{51}$ in PBS at 37 °C for 1h, 2h and 3h

The expected challenge to $[^{68}\text{Ga}]\mathbf{51}$ by other chelators present in blood was mimicked by its incubation in presence of a 2.5-fold excess of apo-transferrin (apo-TF). The iron binding protein, which plays an important role in the control of and trafficking of iron in biological systems.²⁸⁴ Ga(III) possesses the same charge and a similar ionic radius to Fe(III), thus it is reasonable to assume that it will be handled *in vivo* by the same proteins as Fe(III). Radio-TLC analysis at 1 hour, 2 hours, and 3 hours time points did not show any apo-TF-Ga complex formation and showed only a negligible release of free Ga(III).

The TF-Ga-68 is expected to move to the middle of the plate ($R_f = 0.5$) whereas 'free' gallium is eluted at solvent front ($R_f = 1$)), see **Figure 40**. The apparent stable retention of gallium by the functionalised sporopollenin can be explained by suitably positioned amines and carboxylic acid groups on the biopolymer that are coordinating to the metal centre, see **Figure 39**.

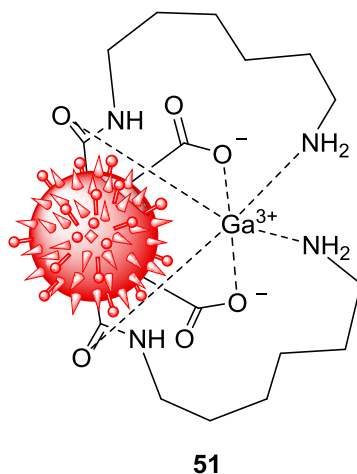


Figure 39-Potential method for attachment of gallium-68 with aminated sporopollenin

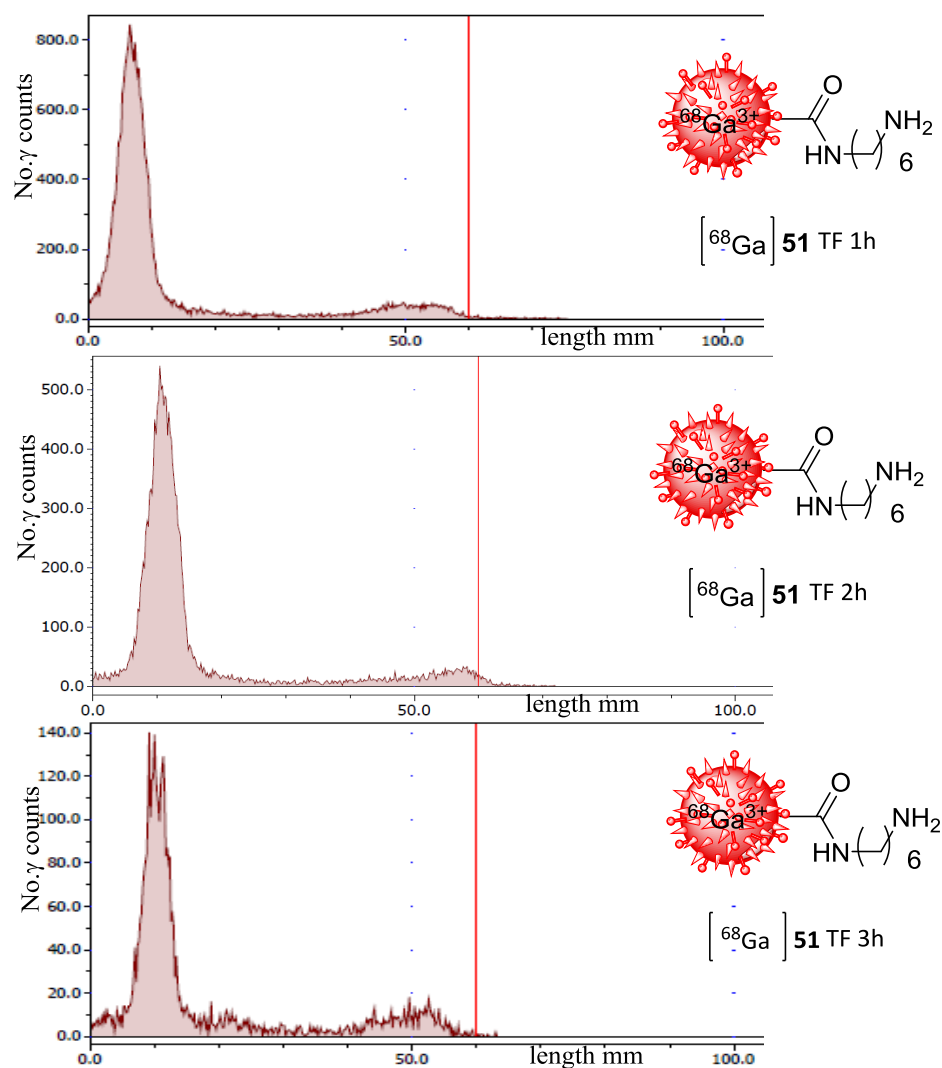


Figure 40-Radio-TLC stability of $[^{68}\text{Ga}]51$ against transferrin at 37°C for 1h, 2h and 3h

The ability to attach metal ions in a stable manner directly to the surface of the nanoparticles without need for chelating ligands such as DOTA has recently developed as a validated method in radiolabelling. Labelling directly onto silica surfaces or metal oxides surfaces can be achieved with sufficient in vivo stability for medical imaging to be carried out. Recently, Chakravarty *et al.* reported a method for producing PET/MRI agents using intrinsically labelled ^{68}Ge on chelate-free nanoparticles,²⁸⁵ inspired by ^{68}Ga generators whereby the parent ^{68}Ge ($t_{1/2} = 279$ days) is bound to metal oxide supports, such as TiO_2 , ZrO_2 , CeO_2 , SnO_2 , Fe_2O_3 , Fe_3O_4 or Al_2O_3 . In our group, the development of silica coated iron oxide nanorods radiolabelled with ^{68}Ga for PET/MR multimodal

imaging in the absence of a chelate has been carried out.²⁸⁶ Wong *et al.* reported the synthesis of dextran-coated ⁶⁴Cu-doped iron oxide nanoparticles that were also validated *in vivo*.²⁸⁷ Finally, in two recent reports, Sun *et al.* provided an elegant demonstration of chelate-free ⁶⁴Cu-radiolabeling of Au nanorods, and ⁶⁴Cu doped CdSe/ZnS quantum dots.^{288,289} Overall the previous work in this area suggests that stable chelator-free attachment of gallium-68 to the surface of aminated sporopollenin **51** could be possible as suitable functional group are available for coordination to gallium(III) on the material surface.²⁸⁶

4.3.3.2 Simulated gastric fluid (SGF)

One of the main areas of interest for sporopollenin in drug delivery is the protection of less stable drugs for oral administration and to improve uptake for compounds with low oral bioavailability. Therefore, the stability of a [⁶⁸Ga]**51** was assessed in presence of simulated gastric fluid (SGF), which mimics the highly acidic conditions encountered in stomach.²⁰⁸ Once again, the radio-TLC analyses at 1 hour, 2 hour and 3-hour time points did not show any detectable gallium release from the sporopollenin, see **Figure 41**.

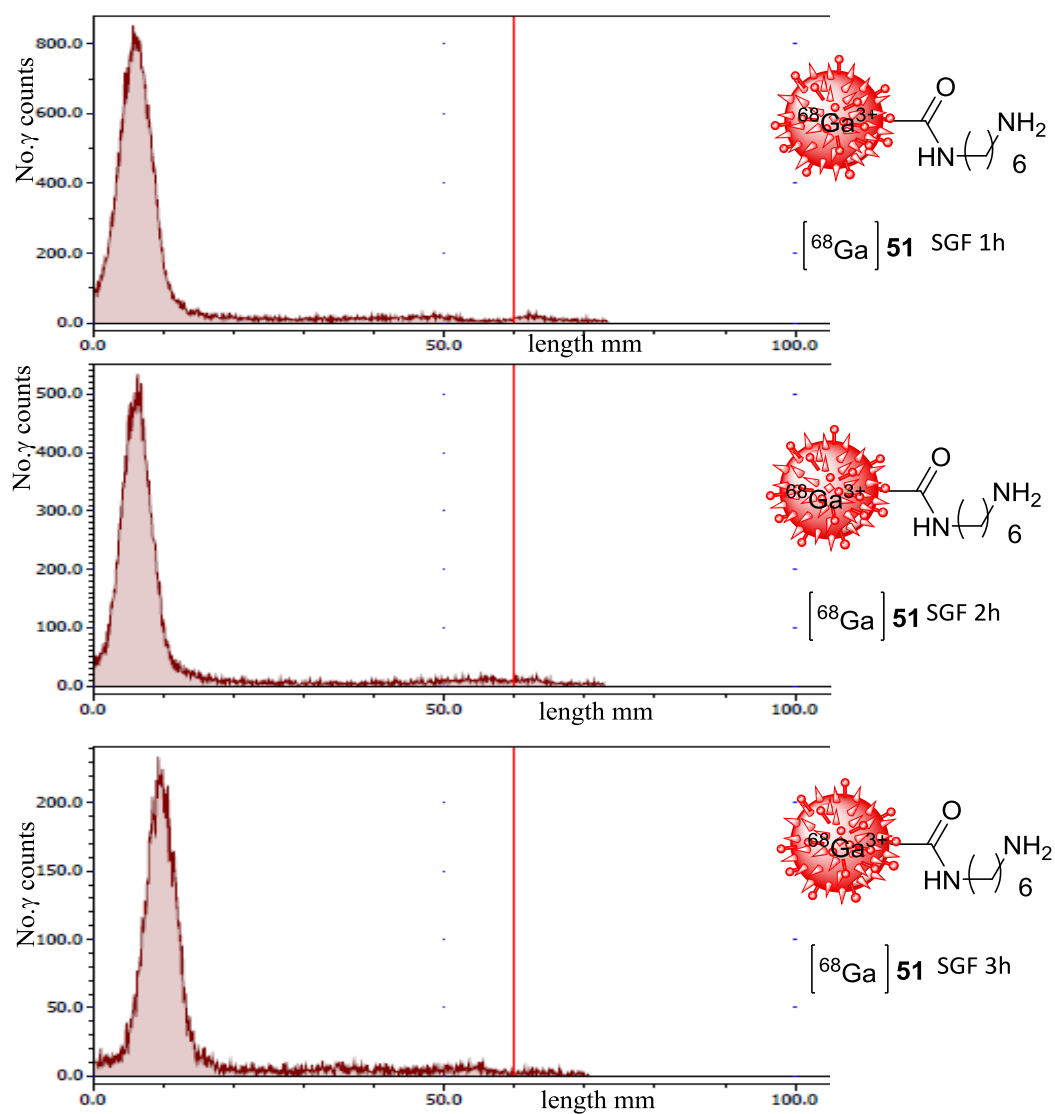


Figure 41-Radio-TLC stability of $[^{68}\text{Ga}]$ **51** complex in SGF at 37°C

4.4 Conclusion

This chapter includes details of surface modification and gallium-68 radiolabelling of sporopollenin (extract from *Lycopodium clavatum* L.C) to potentially use as a tool to understand the behaviour of sporopollenin *in vivo*. Initially, mechanochemistry was used to attach a diamine (1,6-hexane diamine) with a loading of ($1.70 \pm 0.04 \text{ mmol.g}^{-1}$) onto the sporopollenin to give a reactive group (free amine), which could be used for conjugation of DOTA on the surface. This was followed by gallium-68 radiolabelling of sporopollenin derivatives at room temperature and 90°C. Aminated sporopollenin was found to have superior gallium-68 complexation characteristics at 90°C, whereas the sporopollenin and DOTA conjugated derivative did not show significant incorporation of the gallium-68. The radiolabelling clearly demonstrated that there was an issue with the attachment process for covalent bonding of DOTA onto the spore surface. However, this highlighted the stability of labelling for **51** and the potential for a ‘chelator free’ method of stable labelling. The DOTA chelator does compete effectively with the sporopollenin surface for binding when both are present on gallium-68 addition. This is evidenced by the observation that all of the gallium-68 is coordinated to DOTA when the reaction is carried out at 90°C. Further investigation is required to develop improved methodology for the covalent attachment of DOTA to the sporopollenin surface. However, the stability of [⁶⁸Ga]**51** may be sufficient for further studies of the radiolabelled biomaterial.

[⁶⁸Ga]**51** was shown to be stable in competition with transferrin and PBS for up to 3 hours. It was also tested in simulated gastric fluid to determine if the radiolabelled sporopollenin could be used on oral delivery studies *in vivo*. The results of this study indicate that [⁶⁸Ga]**51** can be efficiently radiolabelled and has sufficient stability to progress to *in vivo* studies. The first studies would be to administer the radiolabelled sporopollenin to wild type mice by oral gavage and to collect dynamic PET scans that would show the location of the spores and the time taken for transfer out of the gut.

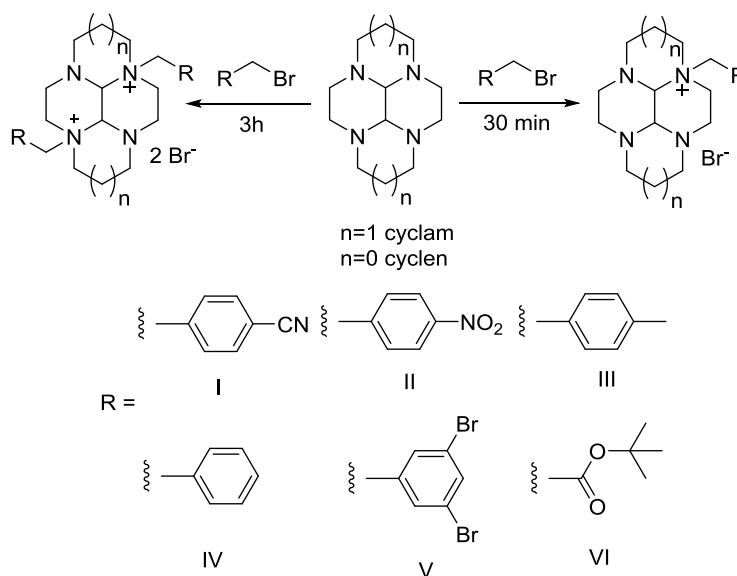
Chapter 5

Concluding Remarks and Future Directions

5. Concluding Remarks and Future Directions

There is a major drive for organic chemists to improve the efficiency of chemical process to reduce waste, save energy and generate more environmentally benign synthetic processes.^{50,290}

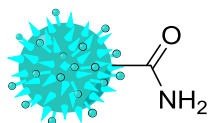
Mechanochemistry is a process wherein the efficiency of chemical reactions can be improved (higher yields) and the requirement for solvents can be reduced. In chapter two, mechanochemistry has been used for the production of various glyoxal-bridged cyclen and cyclam derivatives under liquid assisted grinding (LAG) conditions, see **Scheme 48**. This is the first reported mechanochemical syntheses of mono/or di-N-substituted glyoxal/bridged tetraazamacrocyclic derivatives which, after a further transformation, could lead to bifunctional chelators for use as pharmaceuticals. Mono-substitution was achieved by using a stoichiometric ratio of reagents with a short reaction time to give moderate to high yields. Increasing the reaction time to 3 hours and using four-fold excess of the alkyl bromide reagent allowed access to bis-alkylated products, see **Scheme 48**. The syntheses were easy to work up and often approached quantitative yields.



Scheme 48- General schematic for mono- and bis-N-alkylation of cyclam/cyclen

Ring opening of the bisaminal species to form bridged cyclam/cyclen compounds was carried out *via* microwave irradiation. Using sodium borohydride as a reducing agent, side bridged and cross bridged cyclam/cyclen products were obtained in short reaction times and, again, in moderate to high yields. Microwave heating offers a facile methodology to generate new routes for syntheses and is becoming widely used by academic research and industrial chemists to optimise synthetic procedures. Microwave irradiation causes efficient heating of the reagents, and can give improved yields as well as reduced reaction times.

The extraction of date sporopollenin exines was conducted in chapter three. Date sporopollenin has the potential to be used in pharmaceutical applications for drug delivery due to their uniform size and remarkable resistance of the material to a wide pH range. To better understand the chemical nature of the date sporopollenin exines, a variety of reactions were carried out. The sporopollenin was treated with ammonium hydroxide to form an aminated derivative, see **Figure 42**. Elemental analysis confirmed the presence of nitrogen on the date sporopollenin, which was absent in untreated sporopollenin, hence indicating that reaction had occurred. This was confirmed by FTIR and solid-state NMR studies.

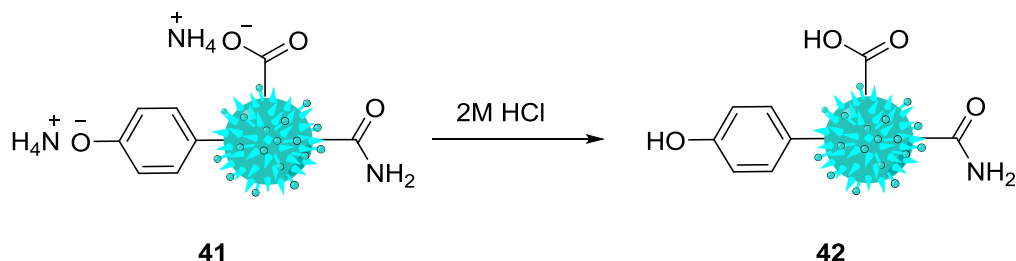


41

Figure 42-Aminated date sporopollenin

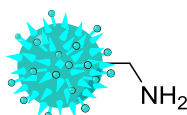
The nature of the attachment of amine/ammonium species to the date spore exine surface was investigated, by reaction of **41** with 2 M hydrochloric acid to investigate if the nitrogen species could be released (i.e. was present as an ammonium salt). Elemental analysis showed a reduction in the amount of nitrogen from $1.00 \text{ mmol. gm}^{-1} \pm 0.05$ to $0.8 \text{ mmol. gm}^{-1} \pm 0.04$. The nitrogen removed from **41** was most likely

associated as ammonium salts with some of the acidic groups on the date spore exine surface, see **Scheme 49**.



Scheme 49-Reaction of hydrochloric acid with aminated date sporopollenin

Compound **41** was reduced by lithium aluminum hydride (LiAlH_4) to obtain compound **45**, which should have basic function groups (primary amines) on the surface. The formation of primary amine was demonstrated using solid-state ^{13}C NMR, which showed the disappearance of the peak due to the amide group (173 ppm). This result was also confirmed using FTIR, where the strong carbonyl peak in **45** was significantly weaker indicating that the amide was successfully reduced, see **Figure 43**.



45

Figure 43-Primary amine date sporopollenin

Compound **45** was subjected to three different reactions to transform primary amines. It was reacted with methyl iodide, phenyl isothiocyanate, and benzene sulfonyl chloride to yield **47**, **48** and **49**. In compound **47**, the presence of iodide ($0.306 \text{ mmol. gm}^{-1}$) indicates the reaction of methyl iodide to alylate the primary amine on the surface of date sporopollenin. Using ICP, the sulphur content was found to be (0.284 mmol/gm) and (0.446 mmol/gm) for **48** and **49** respectively. These reactions provided further evidence that the nitrogenous functional groups in **45** are primary amino groups. Overall, this study indicates a convenient approach to the synthesis of a solid-supported

primary amine material with a loading comparable to the commercial synthetic polymeric materials.

There is significant interest in sporopollenin materials for drug delivery, hence it is relevant to determine if they can be easily radiolabelled for *in vivo* tracking by nuclear medicine imaging techniques such as positron emission tomography. In chapter four, sporopollenin was radiolabelled with gallium-68 to determine the potential for *in vivo* tracking. Sporopollenin was extracted from fresh pollen and spores of *Lycopodium clavatum* (L C). This sporopollenin was selected as it is the most commonly used and has been extensively tested in drug delivery applications. Initially, the sporopollenin was modified with 1,6-diamine hexane by using mechanochemistry, see **Figure 44**. The attachment of the diamine was confirmed by the presence of nitrogen, using elemental analysis, which was absent in the starting material and which could not be removed by washing with an large amounts of solvent (methanol, ethanol, and water).

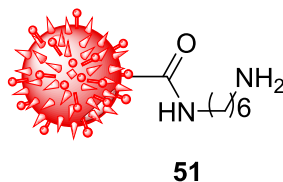
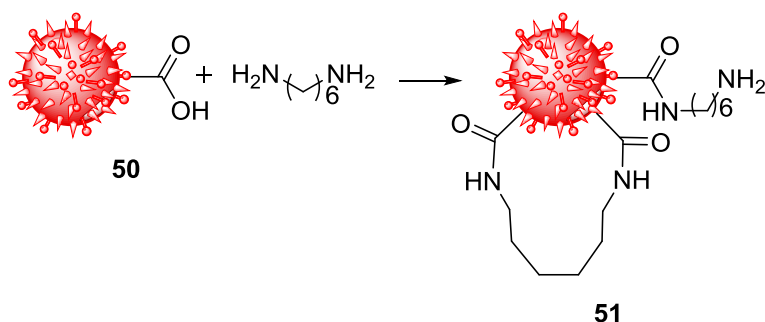


Figure 44-Aminated sporopollenin with 1,6-diaminohexane

In order to understand how the diamine is attached to the sporopollenin, compound **51** was suspended in hydrochloric acid (2 M) for 2 hours at room temperature to obtain the ammonium chloride salt. The chloride analysis result illustrates that only one-third of amine groups can be protonated, indicating that around 50% of hexane-1,6-diamine is bound to sporopollenin in mono-linked fashion with a free amine group available for further reaction, see **Scheme 50**.



Scheme 50-Amination of sporopollenin exine

An attempt was made to conjugate DOTA with the aminated sporopollenin **51** by grinding with DOTA in the presence of carbonyldiimidazole (CDI) as a coupling reagent. Elemental analysis showed nitrogen increase from 1.70 mmol.g⁻¹ to 2.228 mmol.g⁻¹, which indicates that the DOTA is associated with the free amine on the surface of sporopollenin, see **Figure 45**.

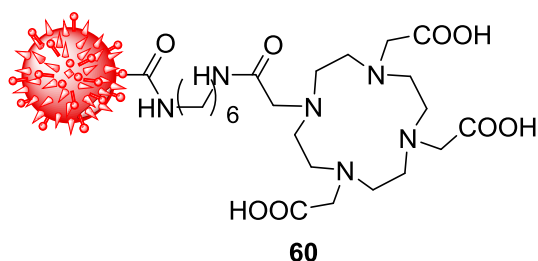


Figure 45-Aminated sporopollenin with DOTA

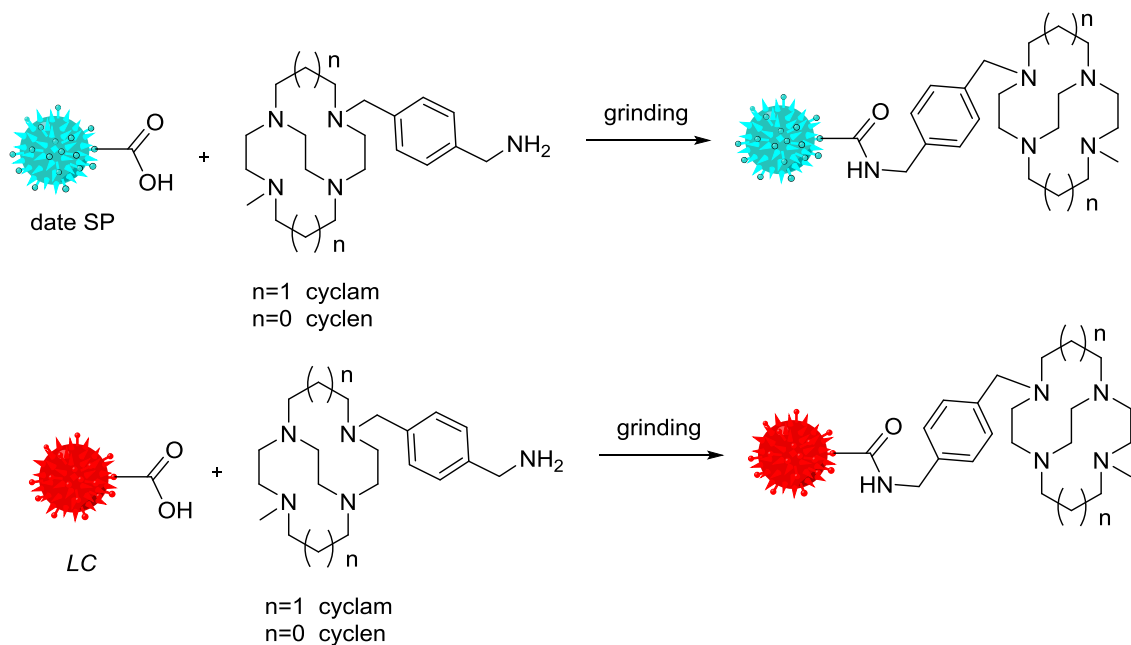
This was followed by gallium-68 radiolabelling experiments with sporopollenin **50** and the aminated derivatives (aminated sporopollenin **51** and DOTA conjugated **60**) at both room temperature and at 90°C. The aminated sporopollenin **51** was found to give a stable complex when labelled at 90°C, while the compounds **50** and **60** did not show significant incorporation of the gallium-68. Therefore, compound **51** was selected for further stability tests in phosphate-buffered saline (PBS) and in the presence apo-transferrin (apo-TF). The results show that radiolabelled compound **51** is stable in competition with apo-transferrin and PBS. Subsequently, the stability of labelled **51** was

tested in simulated gastric fluid (SGF). The radio-TLC analyses at 1 hour, 2 hour and 3 hour time points did not show any detectable free gallium-68 ion release. This radiolabelled sporopollenin derivative appears to be suitable for *in vivo* assessment.

5.2. Future directions

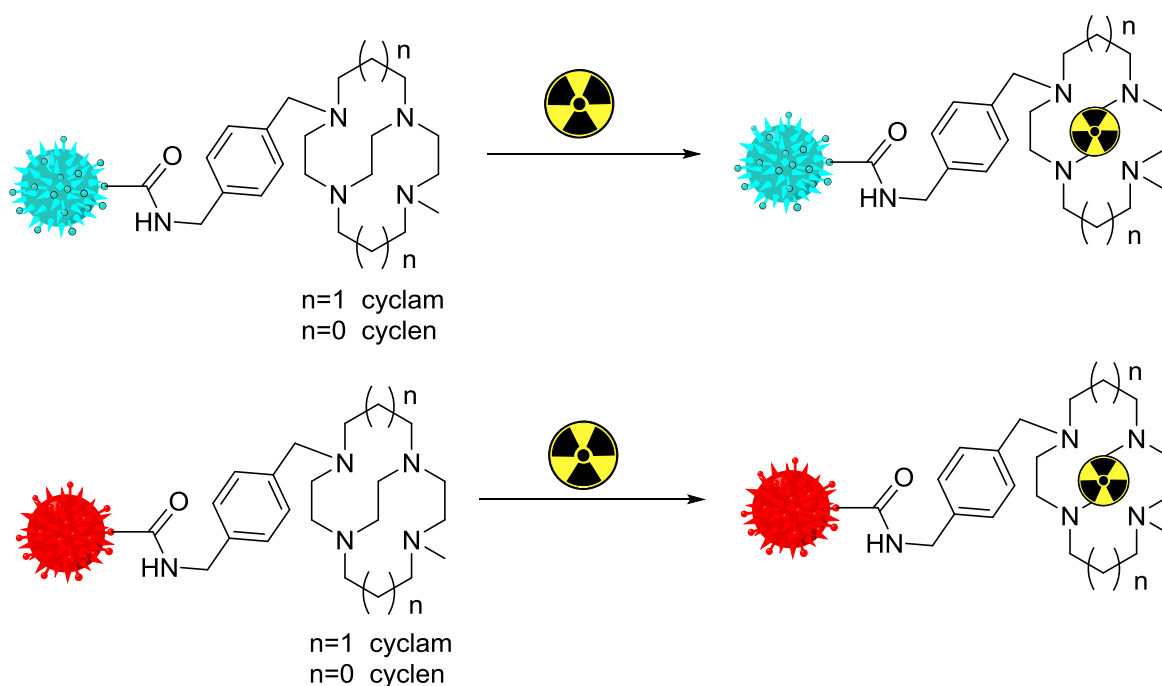
This research has scope for further development. Several of the key areas highlighted within this thesis provide avenues for future studies.

Once mechanochemistry conditions have been optimised and a purification method established for alkylation of bridged cyclam/cyclen these derivatives can be effectively applied to peptide coupling and the formation of suitable derivatives for targeted imaging. This would also be supported by the use of microwave technique for synthesising the side and cross bridged cyclam/cyclen derivatives. Further efforts could also be focused on the attachment of macrocyclic compounds to sporopollenin with these new derivatives combined with mechanochemistry techniques, see **Scheme 51**.



Scheme 51- Proposed reaction of *Lycopodium clavatum* and date spore with cyclam/cyclen derivatives.

In addition, there is motivation to develop this system for *in vivo* use. In order to do this a range of studies must be completed. Firstly, the complex must be shown to be stable and non-toxic *in vitro* for the duration of an emulated *in vivo* study (ca. 3 hours) to determine if demetallation could occur *in vivo*, causing the background signal increase and providing inaccurate data. This can be followed by a specific activity study, carried out in order to determine how much of the chelator can be radiolabelled at the lowest concentration of material. This is important for *in vivo* use when the targeted moiety has a relatively low target concentration, therefore causing receptor saturation.



Scheme 52- Proposed scheme for radiolabeling of *Lycopodium clavatum* and date spore derivatives.

Chapter 6

Experimental

6. Experimental

6.1 General notes

Novel compounds in this work are **7**, **9**, **13**, **23** and **26** (with many of the other compounds synthesised by new pathways). For all novel compounds full characterisation has been provided, for compounds which have been synthesised previously and alternative synthetic methodology is presented sufficient characterization to establish identity (by analogy with published data) and the purity of the compound is included. In all reactions, the bulk solvent was removed by evaporation under reduced pressure (rotary evaporator), and trace solvent was removed using a Schlenk line and/or heating at 40 °C. Reactions were carried out at room temperature (RT) unless otherwise stated. Inductively Coupled Plasma-Optical Emission Spectrometry (ICP-OES) was carried out by Dr. Bob Knight, Department of Chemistry. Scanning electron microscope images (SEM) were collected by Tony Sinclair, Microscopy Suite, University of Hull. Elemental analyses (CHN) were conducted at the University of Hull by Carol Kennedy. Single crystal X-ray diffraction was carried out at the University of Hull by Dr. Timothy J Prior. Solid state NMR was run at the University of Hull by Dr. Rahul Saurabh. All ^{68}Ga radiochemistry experiments were carried out at the Positron Emission Tomography Research Centre, University of Hull.

6.2 Method used for ^{68}Ga preparation

^{68}Ga must be formulated to be in a manner suitable for the radiochemical reaction. $^{68}\text{GaCl}_3$ is eluted from a 20 mCi Eckert & Ziegler IGG100 $^{68}\text{Ge}/^{68}\text{Ga}$ generator in 5mL of 0.1 M HCl. This is then loaded on a phenomenex strata X-C solid-phase extraction cartridge. The sample is then eluted using an acetone:0.1 M HCl solution (98:2) to give the desired amount of activity for the reaction. The solution is then dried using a heating block at 90°C with a flow of argon.

6.3 Materials

For chemical reactions, all chemicals were purchased from Aldrich Chemical co., CheMatech, Acros, Sigma or Fisher. Chemicals and solvents were used as received without further purification, except when dry solvents were required. Solvents were dried over activated (oven dried at 350°C for 14 hours) 4 Å molecular sieves following a literature method.²⁹¹ Date palms (*Phoenix dactylifera* L.) were collected from the male date palm plants grown in the south of Iraq (Basrah).

6.4 Instrumentation

6.4.1 Grinding equipment

Grinding experiments were carried out using a Retsch PM100 (Retsch (U.K.) Limited) planetary ball mill with a 12 mL stainless steel grinding jar and a single 10 mm diameter stainless steel ball at 400 RPM. Dry acetonitrile was used as a liquid phase throughout all LAG experiments.

6.4.2 Microwave apparatus

Microwave-assisted reduction was carried out in a 35 mL reactor using a CEM Discovery (CEM Microwave Technology Ltd.) apparatus with the temperature measured via an external infrared sensor.

6.4.3 NMR spectroscopy

¹H NMR and ¹³C NMR were obtained at 400 MHz for ¹H spectra and 100 MHz for ¹³C spectra and were referenced against standard internal TMS or residual non deuterated solvent signal. Splitting patterns are designated as s (singlet), d (doublet), t (triplet), m (multiplet), and dt (double triplet). When a mixture of products was present, a ratio of characteristic protons unique to each molecule in the ¹H NMR spectrum was used to determine ratios and calculate yields. Double-quantum filtered correlation spectroscopy (¹H DQF-COSY) was carried out on **17**. Solid-state NMR experiments were carried out (at 293 K) on a Bruker Avance II 500 MHz spectrometer using a 4 mm MAS probe operating at frequencies of 50.6747 MHz (¹⁵N) and 125.7546 MHz (¹³C). Spectra

were externally referenced to tetramethylsilane at 0 ppm. Experiments were carried out at 8 kHz MAS speeds and spectra were acquired using cross polarization and TPPM decoupling during the acquisition period. All NMR data was processed using 'Topspin' Version 1.3 (Bruker Instruments, Karlsruhe, Germany).

6.4.4 MS

High- and low-resolution mass spectra were recorded using an electrospray ion-trap LC-MS in positive mode at the University of Hull using a Finnegan MAT 900 XLT system.

6.4.5 Single crystal X-ray diffraction

Single crystal X-ray diffraction data were collected using an imaging plate diffractometer (Stoe IPDS II) operating with Mo radiation.

6.4.6 CHN

Elemental analyses were performed on a Fisons instrument Carlo Erba EA 100 CHN analyser.

6.4.7 ICP-OES

Inductively Coupled Optical Emission Spectroscopy (ICP-OES) analysis was carried out using a Perkin Elmer Optima 5300 DV to determine ion concentrations.

6.4.8 Scanning electron microscope (SEM)

Scanning electron microscope images were obtained using a Leica Cambridge Stereo scan 360 Scanning Electron Microscope (SEM).

6.4.9 Fourier transform infrared (FTIR)

IR spectra were recorded using a Perkin-Elmer Paragon 1000 Fourier Transform Infra-Red Spectrometer. Samples were ground with anhydrous potassium bromide (spectrosol grade) to produce disks to a ratio of 1/9 (w/w). FTIR spectra were a result of 4 scans against a background.

6.4.10 Radio-Thin layer chromatography (Radio-TLC)

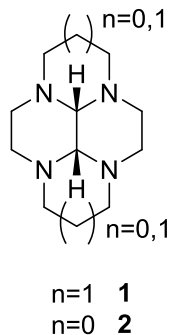
Radio-TLCs analyses were carried out using silica gel 60 on aluminium sheets' (Merck USA), eluting with 0.2M citric acid. Radio-TLC traces were recorded using a Lablogic Scan-Ram, equipped with a NaI detector at a speed of 10mm/min. Data was recorded using Lablogic Laura (version 4.1.7.70).

6.4.11 Method for calculation of nitration in mmol/g

- 1- $(N\%/100) = X$
- 2- $X/\text{atomic mass} = Y$
- 3- $Y \times 1000 = \text{mmol.gm}^{-1}$

6.5 Experimental procedures

6.5.1 Synthesis of dodecahydro-3a,5a,8a,10a-tetraazapyrene (1) and decahydro-2a,4a,6a,8a-tetraazacyclopenta [fg] acenaphthylene (2) ²⁹²



General procedure

Glyoxal bridged derivatives of cyclen and cyclam have been synthesised previously. ²⁹²

The macrocycle was dissolved in MeOH and cooled to -10°C . A cold (0°C) aqueous solution of glyoxal was added dropwise over 90 min. The clear solution was stirred at -10°C for 30 min, then at RT for 3 hours. The solvent was removed in vacuo and the crude solid was redissolved in diethyl ether. The filtrate was dried (MgSO_4), filtered and solvent removed *in vacuo*.

Synthesis of cis-3a,5a,8a,10a-tetraazaperhydropyrene (1)

This compound has been previously synthesised using standard synthetic techniques. ²⁹² Cyclam (12 g, 47.5 mmol), methanol (300 mL), glyoxal (40% w/w, 8.7 g, 149.8 mmol), diethyl ether (250 mL). To yield a white solid (9.65 g, 91%). ^1H NMR (CDCl_3): δ 1.23-1.43 (m, 2H, N- β - CH_2), 2.09-2.34 (m, 8H, N- α - CH_2), 2.72 (d, $J=11$ Hz, 2H, N- β - CH_2), 2.90-2.97 (m, 6H, N- α - CH_2), 3.08 (s, 2H, Haminal), 3.53 (t, $J=10$ Hz, 2H, N- α - CH_2). ^{13}C NMR (CDCl_3): δ 19.29 (N- β - CH_2), 44.47 (N- α - CH_2), 52.20 (N- α - CH_2), 54.07 (N- α - CH_2), 55.76 (Caminal). MS: (ESI) m/z 223 ($100[\text{M}]^+$).

Synthesis of cis-13-1,4,7,10- tetraazatetracyclo[5.5.1.0^{4,14}.0^{10,13}]tetradecane (2)

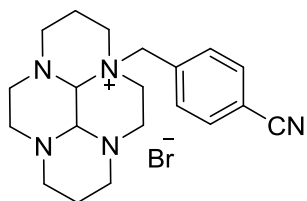
This compound has been previously synthesised using standard synthetic techniques.²⁹² Cyclen (8.36 g, 48.6 mmol), MeOH (300 mL), glyoxal (40% w/w, 7.04 g, 121.4 mmol), diethyl ether (250 mL). To yield a cream solid (8.80 g, 93%). ¹H NMR (400 MHz, CDCl₃) δ: 2.49-2.59 (m, N-CH₂, 4H), 2.63 (br s, N-CH₂, 4H), 2.88-2.96 (m, N-CH₂, 8H), 3.07 (s, CH, 2H). ¹³C NMR (100 MHz, CDCl₃) δ: 50.27 (N-CH₂), 51.05 (N-CH₂), 77.44 (CH).

6.5.2 Synthesis of Mono- and Bis-N-Alkylation of Glyoxal-Bridged Cyclam via Grinding.

General Procedure

A mixture of alkyl bromide and glyoxal-bridged cyclam in 1:1 molar ratio was ground in the presence of dry acetonitrile (90 µL) for 30 min (for one arm) and in 1:4 molar ratio for 3 h (for two arms). The crude products were scraped off the walls of the grinding jar and washed multiple times with diethyl ether and tetrahydrofuran (THF) to remove unreacted starting materials and give expected mono- or bis-substituted products (pure or in mixtures) in powdery form.

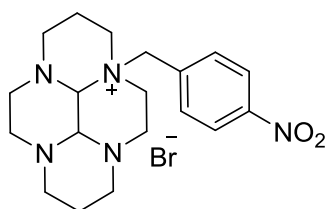
6.5.2.1 Synthesis of 10 a-(4-Cyanobenzyl)dodecahydro-1H-3a,5a,8a,10a-tetraazapyren-10a-ium Bromide (3)



3

This compound has been previously synthesised using standard synthetic techniques.¹⁴⁶ From cis-3a,5a,8a,10a-tetraazaperhydropyrene (100 mg, 0.45 mmol, 1equiv) and 4- equiv), white solid (184 mg, 98%). From cis-3a,5a,8a,10a-tetraazaperhydropyrene (100 mg, 0.45 mmol, 1 equiv) and 4-(bromomethyl)-benzonitrile (352.8 mg, 1.8 mmol, 4 equiv), white solid (184 mg, 98%). ¹H NMR (400 MHz, D₂O, δ): 1.40 (d, J = 13.5 Hz, 1H), 1.73 (d, J = 13.5 Hz, 1H), 2.05–2.32 (m, 3H), 2.38–2.49 (m, 2H), 2.57 (td, J = 3.1 Hz, J = 12.4 Hz, 1H), 2.90–4.13 (m, 7H), 3.15–3.34 (m, 2H), 3.39–3.63 (m, 2H), 3.92 (s, 1H), 4.19 (td, J = 3.6 Hz, J = 13.1 Hz, 1H), 4.29 (d, J = 1.6 Hz, 1H), 4.75 (d, J = 13.1 Hz, 1H), 5.18 (d, J = 13.1 Hz, 1H), 7.66 (d, J = 8.4 Hz, 2H), 7.87 (d, J = 8.4 Hz, 2H).

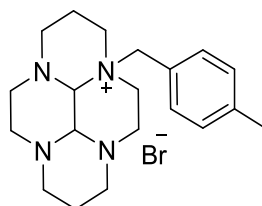
6.5.2.2 Synthesis of 10a-(4-Nitrobenzyl)dodecahydro-1H-3a,5a,8a,10a-tetraazapyren-10a-ium Bromide (4)



4

This compound has been previously synthesised using standard synthetic techniques.¹⁴⁶ From *cis*-3a,5a,8a,10a-tetraazaperhydropyrene (100 mg, 0.45 mmol, 1 equiv) and 4-(bromomethyl)nitrobenzene (389 mg, 1.8 mmol, 4 equiv), white solid (212 mg, 98%). ¹H NMR (400 MHz, D₂O, δ): 1.45 (d, J = 14.9 Hz, 1H), 1.77 (d, J = 14.9 Hz, 1H), 2.08–2.36 (m, 3H), 2.43–2.52 (m, 2H), 2.63 (td, J = 3.5 Hz, J = 13.0 Hz, 1H), 2.95–3.18 (m, 7H), 3.19–3.38 (m, 2H), 3.44–3.64 (m, 2H), 3.71 (d, J = 2.0 Hz, 1H), 4.15–4.27 (m, 1H), 4.34 (d, J = 2.0 Hz, 1H), 4.83 (d, J = 13.3 Hz, 1H), 5.26 (d, J = 13.3 Hz, 1H), 7.76 (d, J = 8.8 Hz, 2H), 8.35 (d, J = 8.8 Hz, 2H).

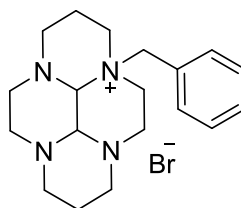
6.5.2.3 Synthesis of 10a-(4-Methylbenzyl)dodecahydro-1H-3a,5a,8a,10a-tetraazapyren-10a-ium Bromide (5).



5

This compound has been previously synthesised using standard synthetic techniques.¹⁴⁶ Decahydro-1H,6H-3a,5a,8a,10a-tetraazapyrene **1** (100 mg, 0.45 mmol, 1 equiv) and 1-(bromomethyl) 4-methylbenzene (83 mg, 0.45 mmol, 1 equiv). The crude solid was purified by washing with chloroform to yield a soluble product which was dried in vacuo to yield a white solid (166 mg, 90%). ¹H NMR (400 MHz, D₂O, δ): 1.43 (d, J = 14.1 Hz, N- β -CH₂, 1H), 1.75 (d, J = 14.1 Hz, N- β -CH₂, 1H), 2.02–2.29 (m, N- α -CH₂, 3H), 2.36 (s, Ar CH₃, 3H), 2.38–2.48 (m, N- β -CH₂, 2H), 2.60 (td, J = 3.7 Hz, J = 12.7 Hz, N- α -CH₂, 1H), 2.92–3.13 (m, N- α -CH₂, 7H), 3.14–3.36 (m, N- α -CH₂, 2H), 3.40–3.56 (m, N- α -CH₂, 2H), 3.62 (d, J = 1.8 Hz, CH, 1H), 4.14 (td, J = 4.1 Hz, J = 13.4 Hz, N- α -CH₂, 1H), 4.33 (d, J = 1.8 Hz, CH, 1H), 4.73 (d, J = 13.5 Hz, Ar CH₂, 1H), 4.96 (d, J = 13.5 Hz, Ar CH₂, 1H), 7.35 (d, J = 8.4 Hz, Ar H, 2H), 7.39 (d, J = 8.4 Hz, Ar H, 2H). ¹³C NMR (100 MHz, D₂O, δ): 18.0 (CH₂), 18.4 (CH₂), 20.4 (CH₃), 42.0 (CH₂), 46.6 (CH₂), 48.6 (CH₂), 51.3 (CH₂), 52.0 (CH₂), 53.3 (CH₂), 54.0 (CH₂), 59.7 (CH₂), 62.5 (CH₂), 69.6 (CH), 81.7 (CH), 122.5 (C), 129.9 (CH), 133.2 (CH), 141.9 (CH). HRMS: calcd for C₂₀H₃₁N₄: 327.2543, found: 327.2548. Elemental analysis calcd for C₂₀H₃₁BrN₄·2H₂O: C, 54.17; H, 7.96; N, 12.64%; found: C, 54.16; H, 8.22; N, 12.82. Mp 144–145 °C.

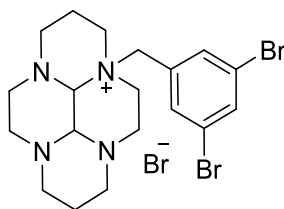
6.5.2.4 Synthesis of 10a-Benzyldecahydro-1H-3a,5a,8a,10a-tetraazapyren-10aium bromide (6)



6

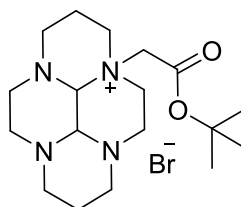
This compound has been previously synthesised using standard synthetic techniques.¹⁴⁶ From cis-3a,5a,8a,10a-tetraazaperhydropyrene (100 mg, 0.45 mmol, 1 equiv) and benzyl bromide (77 mg, 0.45 mmol, 1 equiv), white solid (143 mg, 81%). ¹H NMR (400 MHz, D₂O, δ): 1.39 (d, J = 14.5 Hz, 1H), 1.70 (d, J = 14.5 Hz, 1H) 2.02–2.26 (m, 3H), 2.33–2.48 (m, 2H), 2.56 (td, J = 4.0 Hz, J = 13.5 Hz, 1H), 2.86–3.11 (m, 7H), 3.13–3.33 (m, 2H), 3.37–3.56 (m, 2H), 3.59 (d, J = 1.5 Hz, 1H), 4.06–4.18 (m, 1H), 4.30 (d, J = 1.5 Hz, 1H), 4.72 (d, J = 13.5 Hz, 1H), 4.99 (d, J = 13.5 Hz, 1H), 7.43–7.58 (m, 5H).

6.5.2.5 Synthesis of 10a-(3,5-Dibromobenzyl)dodecahydro-1H-3a,5a,8a,10a-tetraazapyren-10a-ium Bromide (7)



This compound has been previously synthesised using standard synthetic techniques.¹⁴⁶ From cis-3a,5a,8a,10a-tetraazaperhydropyrene (100 mg, 0.45 mmol, 1 equiv) and 1,3-dibromo-5-(bromomethyl) benzene (127 mg, 0.45 mmol, 1 equiv), white solid (159 mg, 64%). From cis-3a,5a,8a,10a-tetraazaperhydropyrene (100 mg, 0.45 mmol, 1 equiv) and 1,3-dibromo-5-(bromomethyl)benzene (508 mg, 1.8 mmol, 4 equiv), white solid (229 mg, 92%). ¹H NMR (400 MHz, D₂O, δ): 1.39 (d, J = 14.4 Hz, 1H), 1.73 (d, J = 14.4 Hz, 1H), 2.02–2.32 (m, 3H), 2.36–2.49 (m, 2H), 2.55 (td, J = 3.0 Hz, J = 13.0 Hz, 1H), 2.85–3.21 (m, 8H), 3.31 (d, J = 11.5 Hz, 1H), 3.36–3.55 (m, 2H), 3.63 (d, J = 1.1 Hz, 1H), 4.08–4.22 (m, 1H), 4.24 (d, J = 1.1 Hz, 1H), 4.64 (d, J = 13.4 Hz, 1H), 5.03 (d, J = 13.4 Hz, 1H), 7.64 (d, J = 1.0 Hz, 2H), 7.91–7.99 (m, 1H). ¹³C NMR (100 MHz, D₂O, δ): 18.0, 18.4, 41.9, 46.5, 48.6, 51.3, 51.9, 53.3, 53.9, 60.2, 69.6, 82.5, 123.2, 129.3, 134.7, 136.6. HRMS: calcd for C₁₉H₂₇N₄Br₂: 471.0581, found 471.0577. Elemental analysis calcd for C₁₉H₂₇Br₂N₄: C, 41.40; H, 4.94; N, 10.17%; found: C, 41.79; H, 5.12; N, 10.01. Mp 178–179 °C.

6.5.2.6 Synthesis of 10a-(2-(tert-Butoxy)-2-oxoethyl)dodecahydro-1H-3a,5a,8a, 10a-tetraazapyren-10a-ium Bromide (**8**)



8

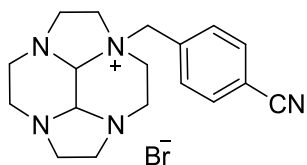
This compound has been previously synthesised using standard synthetic techniques.¹⁴⁶ From cis-3a,5a,8a,10a-tetraazaperhydropyrene (100 mg, 0.45 mmol, 1 equiv) and t-butyl bromoacetate (88 mg, 0.45 mmol, 1 equiv), white solid (60 mg, 32%). From cis-3a,5a,8a,10a-tetraazaperhydropyrene (100 mg, 0.515 mmol, 1 equiv) and t-butyl bromoacetate (351 mg, 1.8 mmol, 4 equiv), white solid (94 mg, 50%). ¹H NMR (400 MHz, D₂O, δ): 1.42 (d, J = 13.0 Hz, 1H), 1.56 (s, 9H), 1.90 (d, J = 13.0 Hz, 1H), 2.12–2.29 (m, 1H), 2.30–2.62 (m, 5H), 2.83–3.21 (m, 7H), 3.49 (t, J = 11.2 Hz, 1H), 3.64 (d, J = 12.7 Hz, 1H), 3.81 (t, J = 11.2 Hz, 1H), 3.91–4.10 (m, 3H), 4.30–4.49 (m, 2H), 4.67 (d, J = 15.6 Hz, 1H).

6.5.2.7 Synthesis of mono and Bis-N-Alkylation substituted bridged cyclen *via* grinding

General Procedure

A mixture of alkyl bromide and glyoxal-bridged cyclen in 1:1 molar ratio was ground in the presence of dry acetonitrile (90 μ L) for 30 min (for one arm) and in 1:4 molar ratio for 3 h (for two arms). The crude products were scraped off the walls of the grinding jar and washed multiple times with diethyl ether and tetrahydrofuran (THF) to remove unreacted starting materials and give expected mono- or bis-substituted products (pure or in mixtures) in powdery form.

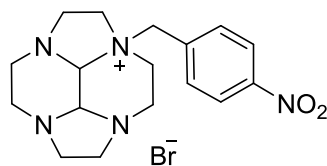
6.5.2.8 Synthesis of 8a-(4-Cyanobenzyl)decahydro-1H-2a,4a,6a,8a-tetraazacyclopenta[fg] acenaphthylene 8a ium bromide (9).



9

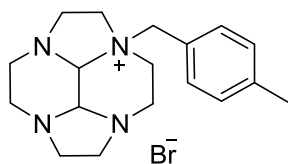
From decahydro-2a,4a,6a,8a-tetraazacyclopenta[fg]acenaphthylene (100 mg, 0.515 mmol, 1equiv) and 4-cyanobenzyl bromide (101 mg, 0.515 mmol, 1 equiv), white solid (178 mg, 89%). ^1H NMP(400 MHz, D_2O , δ): 2.45–2.62 (m, 2H), 2.73–2.98 (br m, 4H), 3.05–3.35 (br m, 5H), 3.43–3.65 (m, 4H), 3.77 (d, $J = 1.8$ Hz, 1H), 4.06 (d, $J = 1.8$ Hz, 1H), 4.13–4.29 (m, 1H), 4.74 (d, $J = 13.5$ Hz, 1H), 4.99 (d, $J = 13.5$ Hz, 1H), 7.76 (d, $J = 8.2$ Hz, 2H), 7.91 (d, $J = 8.2$ Hz, 2H). ^{13}C NMP (100 MHz, D_2O , δ): 43.7, 47.5, 47.6, 48.2, 48.2, 51.3, 57.1, 60.6, 61.5, 71.6, 83.1, 113.8, 118.6, 132.0, 133.1, 133.5. HRMS: calcd for $\text{C}_{18}\text{H}_{24}\text{N}_5^+$: 310.2026; found: 310.2022. Elemental analysis calcd for $\text{C}_{18}\text{H}_{24}\text{BrN}_5$: C%, 55.39; H%, 6.20; N%, 17.94; found: C%, 55.18; H%, 6.04; N%, 17.73. Mp 200–202°C.

6.5.2.9 Synthesis of 8a-(4-Nitrobenzyl)decahydro-1H-2a,4a,6a,8a-tetraaza cyclopenta[fg] acenaphthylen-8a-ium Bromide (**10**)

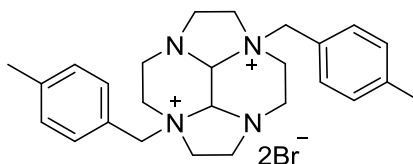


This compound has been previously synthesised using standard synthetic techniques.²⁹³ From decahydro-2a,4a,6a,8a-tetraazacyclopenta[fg]acenaphthylene (100 mg, 0.515 mmol, 1 equiv) and 4-nitrobenzyl bromide (111 mg, 0.515 mmol, 1 equiv), white solid obtained in 10:1 mixture with **22** (138 mg, 65%). From decahydro-2a,4a,6a,8a-tetraazacyclopenta[fg]acenaphthylene (100 mg, 0.515 mmol, 1 equiv) and 4-nitrobenzyl bromide (445 mg, 2.06 mmol, 4 equiv), white solid (175 mg, 89%). ¹H NMR(400 MHz, D₂O, δ): 2.33–2.46 (m, 2H), 2.59–2.73 (br m, 3H), 2.74–2.84 (m, 1H), 2.94–4.03 (m, 1H), 3.10–3.22 (m, 3H), 3.28–3.39 (m, 1H), 3.40–3.59 (m, 4H), 3.65 (d, J = 2.3 Hz, 1H), 3.94 (d, J = 2.3 Hz, 2H), 4.03–4.13 (m, 1H), 4.88 (d, J = 13.5 Hz, 1H), 7.67 (d, J = 8.5 Hz, 2H), 8.2 (d, J = 8.5 Hz, 2H).

6.5.2.10 Attempted preparation of 4,11-8a-(4-Methylbenzyl)decahydro-1H-2a,4a,6a,8a-tetraazacyclopenta[fg] acenaphthylen-8a-ium Bromide (11). Actual preparation of a mixture of (11) and (23).



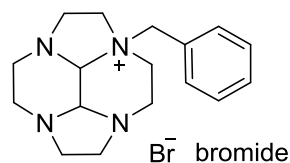
11



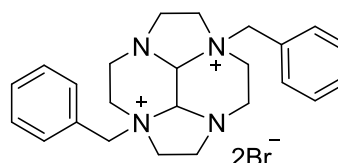
23

From decahydro-2a,4a,6a,8a-tetraazacyclopenta[fg]acenaphthylene (100 mg, 0.515 mmol, 1 equiv) and 4-methylbenzyl bromide (95 mg, 0.515 mmol, 1 equiv), white solid obtained in 5:1 mixture with **23** (153 mg, 78%). From decahydro-2a,4a,6a,8a-tetraazacyclopenta[fg]acenaphthylene (100 mg, 0.515 mmol, 1 equiv) and 4-methylbenzyl bromide (380 mg, 2.06 mmol, 4 equiv), white solid obtained in 6:1 mixture with **23** (152 mg, 77%). The yield ratio was determined according to the ratio of the integrals of the peaks in the ^1H NMR with chemical shift 4.5 ppm ($-\text{CH}_2\text{-Ph}$ for mono-substituted) and 4.7 ppm ($-\text{CH}_2\text{-Ph}$ for bis-substituted), see **A1** in Appendices.

6.5.2.11 Attempted preparation of 8a-Benzyldecahydro-1H-2a,4a,6a,8a-tetraazacyclopenta[fg]acenaphthylene 8a ium Bromide (12). Actual preparation of a mixture of (12) and (24).



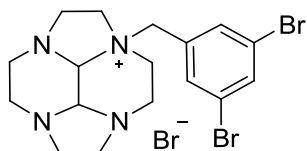
12



24

From decahydro-2a,4a,6a,8a-tetraazacyclopenta[fg]acenaphthylene (100 mg, 0.515 mmol, 1 equiv) and benzyl bromide (88 mg, 0.515 mmol, 1 equiv), white solid obtained in 17:1 mixture with **24** (149 mg, 79%). From decahydro-2a,4a,6a,8a-tetraazacyclopenta[fg]acenaphthylene (100 mg, 0.515 mmol, 1equiv) and benzyl bromide (352 mg, 2.06 mmol, 4 equiv), white solid obtained in 8:1 mixture with **24** (128 mg, 72%). The yield ratio was determined according to the ratio of the integrals of the peaks in the ¹H NMR with chemical shift 4.7 ppm (-CH₂-Ph for mono-substituted) and 4.8 ppm (-CH₂-Ph for bis-substituted), see **A2** in Appendices.

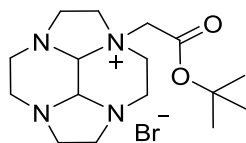
6.5.2.12 Synthesis of 8a-(3,5-Dibromobenzyl)decahydro-1H-2a,4a,6a,8a-tetraazacyclopenta[fg] acenaphthylen 8a ium Bromide (13).



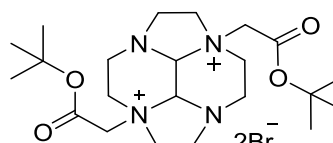
13

From decahydro-2a,4a,6a,8a-tetraazacyclopenta[fg]acenaphthylene (100 mg, 0.515 mmol, 1 equiv) and 1,3-dibromo-5-(bromomethyl)benzene (145 mg, 0.515 mmol, 1 equiv), white solid (162 mg, 60%). From decahydro-2a,4a,6a,8a-tetraazacyclopenta[fg]acenaphthylene (100 mg, 0.515 mmol, 1 equiv) and 1,3-dibromo-5-(bromomethyl)benzene (580 mg, 2.06 mmol, 4 equiv), white solid (210 mg, 85%). ^1H NMR (400 MHz, D_2O , δ): 2.42–2.56 (br m, 2H), 2.70–2.86 (m, 3H), 2.84–2.98 (br m, 1H), 3.00–3.18 (m, 2H), 3.20–3.34 (m, 3H), 3.40–3.51 (m, 1H), 3.51–3.64 (m, 3H), 3.71 (d, J = 2.5 Hz, 1H), 4.00 (d, J = 2.5 Hz, 1H), 4.08–4.20 (m, 1H), 4.63 (d, J = 13.4 Hz, 1H), 4.82 (d, J = 13.4 Hz, 1H), 7.71 (d, J = 1.6 Hz, 2H), 7.96 (t, J = 1.6 Hz, 1H); ^{13}C NMR (100 MHz, D_2O , δ): 43.7, 47.4, 47.6, 48.2, 48.2, 51.2, 57.1, 59.9, 61.4, 71.6, 83.0, 123.4, 130.4, 134.0, 136.6. HRMS: calcd. for $\text{C}_{17}\text{H}_{23}\text{Br}_2\text{N}_4^+$: 441.0284, found: 441.0277. Elemental analysis calcd for $\text{C}_{17}\text{H}_{23}\text{Br}_3\text{N}_4$: C, 39.03; H, 4.43; N, 10.71; found: C, 39.01; H, 4.35; N, 10.66. Mp dec at 187 °C.

6.5.2.13 Attempted preparation of 8a-(2-(tert-Butoxy)-2-oxoethyl) dodecahydro-2a, 4a,6a,8a-tetraazacyclopenta [fg]acenaphthylene-8a-ium Bromide (14). Actual preparation of a mixture of (14) and (26).



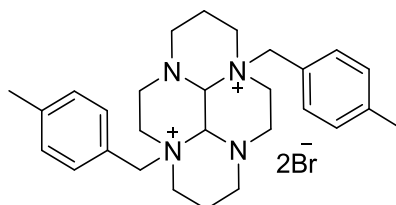
14



26

From decahydro-2a,4a,6a,8a-tetraazacyclopenta[fg]acenaphthylene (100 mg, 0.515 mmol, 1 equiv) and t-butyl bromoacetate (101 mg, 0.515 mmol, 1 equiv), white solid obtained in 2:1 mixture with **26** (127 mg, 68%). From decahydro-2a,4a,6a,8a-tetraazacyclopenta[fg]acenaphthylene (100 mg, 0.515 mmol, 1 equiv) and 4-methylbenzyl bromide (380 mg, 2.06 mmol, 4 equiv), white solid obtained in 4:1 mixture with **26** (113 mg, 60%). The yield ratio was determined according to the ratio of the integrals of the peaks in the ^1H NMR with chemical shift 4.3 ppm ($-\text{CH}_2\text{-COO}^t\text{Bu}$ for mono-substituted) and 4.4 ppm ($\text{CH}_2\text{-COO}^t\text{Bu}$ for bis-substituted), see **A3** in Appendices.

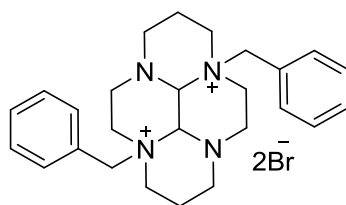
6.5.2.14 Synthesis of 5a,10a-Bis(4-methylbenzyl)tetradecahydro-3a,5a,8a,10a-tetraazapyrene 5a,10a-diiium Bromide (17)



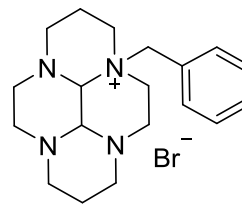
17

This compound has been previously synthesised using standard synthetic techniques.¹⁴⁶ From *cis*-3a,5a,8a,10a-tetraazaperhydropyrene (100 mg, 0.45 mmol, 1 equiv) and 4-methylbenzyl bromide (333 mg, 1.8 mmol, 4 equiv). The crude solid was purified by washing with chloroform to yield a white insoluble solid (253 mg, 95%). ¹H NMR (400 MHz, D₂O, δ): 1.87 (d, J = 15.4 Hz, N- β -CH₂, 2H), 2.14–2.32 (m, N- α -CH₂, 2H), 2.37(s, Ar CH₃, 6H), 2.81 (td, J = 3.5 Hz, J = 12.5 Hz, N- β -CH₂, 2H), 3.18 (d, J = 13.0 Hz, N- α -CH₂, 4H), 3.34–3.59 (m, N- α -CH₂, 2H), 3.63–3.77 (m, N- α -CH₂, 4H), 3.72 (td, J = 4.0 Hz, J = 12.6 Hz, N- α -CH₂, 2H), 4.34 (td, J = 5.5 Hz, J = 13.0 Hz, N- α -CH₂, 2H), 4.70 (d, J = 13.0 Hz, Ar CH₂, 1H), 5.08 (s, CH, 2H), 5.22 (d, J = 13.0 Hz, Ar CH₂, 2H), 7.37 (d, J = 7.8 Hz, Ar H, 4H), 7.46 (d, J = 7.8 Hz, Ar H, 4H).

6.5.2.15 Attempted preparation of 3a,8a-Dibenzyltetradecahydro-3a,5a,8a,10a-tetraazapyrene 3a,8a diium Bromide (18). Actual preparation of a mixture of (18) and (6).



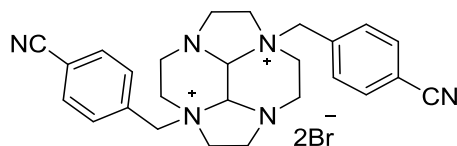
18



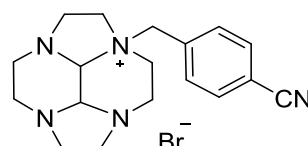
6

From cis-3a,5a,8a,10a-tetraazaperhydropyrene (100 mg, 0.45 mmol, 1equiv) and benzyl bromide (308 mg, 1.8 mmol, 4 equiv), white solid obtained in a 1:2 mixture with **6** (127 mg, 50%). The yield ratio was determined according to the ratio of the integrals of the peaks in the ^1H NMR with chemical shift 4.8 ppm ($-\text{CH}_2\text{-Ph}$ for mono-substituted) and 5.07 ppm ($-\text{CH}_2\text{-Ph}$ for bis-substituted), see **A4** in Appendices.

6.5.3.16 Attempted preparation of 4a,8a-Bis(4-cyanobenzyl)dodecahydro-2a,4a,6a,8a-tetraazacyclopenta [fg]acenaphthylene-4a,8a-diium Bromide (21) . Actual preparation of a mixture of (21) and (9).



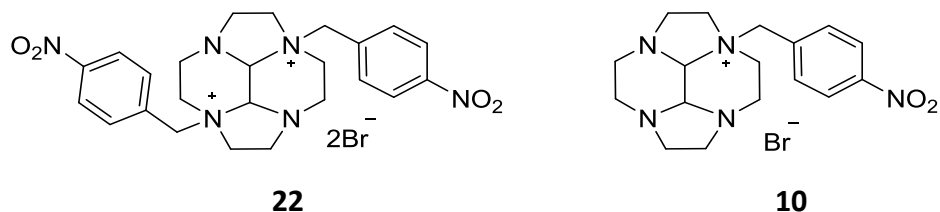
21



9

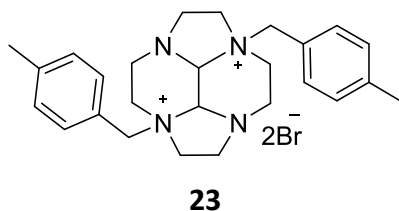
From decahydro-2a,4a,6a,8a-tetraazacyclopenta[fg]acenaphthylene (100 mg, 0.515 mmol, 1 equiv) and 4-cyanobenzyl bromide (404 mg, 2.06 mmol, 4 equiv), white solid obtained in 1:8 mixture with **9** (262 mg, 87%). The yield ratio was determined according to the ratio of the integrals of the peaks in the ^1H NMR with chemical shift 4.6 ppm ($-\text{CH}_2\text{-ph}$ for mono-substituted) and 4.9 ppm ($-\text{CH}_2\text{-ph}$ for bis-substituted), see **A5** in Appendices.

6.5.2.17 Attempted preparation of 4a,8a-Bis(4-nitrobenzyl)dodecahydro-2a,4a,6a,8a-tetraazacyclopenta[fg] acenaphthylene-4a,8a-dium bromide (22). Actual preparation of a mixture of (22) and (10).



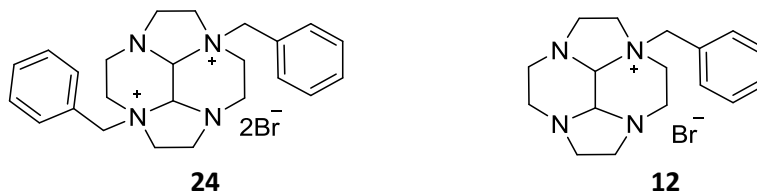
From decahydro-2a,4a,6a,8a-tetraazacyclopenta[fg]acenaphthylene (100 mg, 0.515 mmol, 1 equiv) and 4-nitrobenzyl bromide (445 mg, 2.06 mmol, 4 equiv), white solid obtained in 3:1 mixture with **10** (310 mg, 96%). The yield ratio was determined according to the ratio of the integrals of the peaks in the ^1H NMR with chemical shift 7.95 ppm (-*Ph*- for mono-substituted) and 8.02 ppm (-*Ph*- for bis-substituted), see **A6** in Appendices.

6.5.2.18 Synthesis of 4a,8a-Bis(4-methylbenzyl)dodecahydro-2a,4a,6a, 8a tetraaza- cyclopenta[fg] acenaphthylene-4a,8a-dium bromide (23).



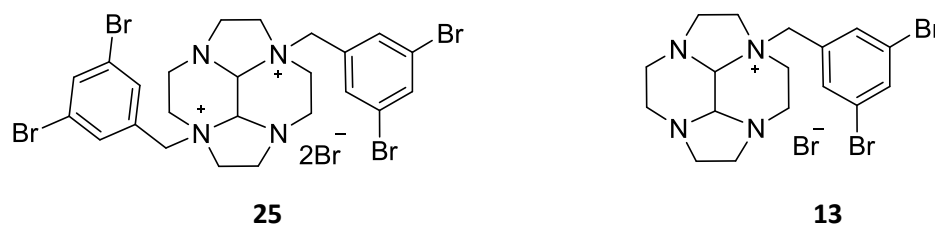
From decahydro-2a,4a,6a,8a-tetraazacyclopenta[fg]acenaphthylene (100 mg, 0.515 mmol, 1 equiv) and 4-methylbenzyl bromide (381 mg, 2.06 mmol, 4 equiv), white solid (253 mg, 94%). ^1H NMR (400 MHz, D_2O , δ): 2.36 (s, 6H), 3.03–3.12 (br m, 2H), 3.37 (d, $J = 7.0$ Hz, 4H), 3.50–3.66 (br m, 6H), 3.76–3.88 (m, 2H), 4.19–4.30 (m, 2H), 4.71 (d, $J = 13.3$ Hz, 2H), 4.88 (d, $J = 13.3$ Hz, 2H), 7.36 (d, $J = 7.7$ Hz, 4H), 7.45 (d, $J = 7.7$ Hz, 4H); ^{13}C NMR (100 MHz, D_2O , δ): 20.4, 42.8, 46.1, 54.8, 60.8, 60.9, 77.4, 123.1, 130.3, 132.2, 142.2. HRMS: calcd for $\text{C}_{26}\text{H}_{36}\text{N}_4^{2+}$: 202.1465, found: 202.1473. Elemental analysis calcd for $\text{C}_{26}\text{H}_{36}\text{Br}_2\text{N}_4 \cdot 2\text{H}_2\text{O}$: C, 52.01; H, 6.71; N, 9.33; found: C, 51.98; H, 6.65; N, 9.09. Mp 182–185°C.

6.5.2.19 Attempted preparation of 4a,8a-Bis-benzyldecahydro-2a,4a,6a,8a-tetraazacyclopenta[fg] acenaphthylene-4a,8a-dium bromide (24). Actual preparation of a mixture of (24) and (12).



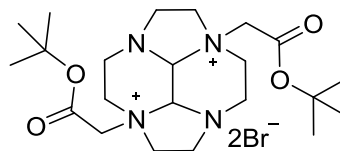
From decahydro-2a,4a,6a,8a-tetraazacyclopenta[fg]acenaphthylene (100 mg, 0.515 mmol, 1 equiv) and benzyl bromide (352 mg, 2.06 mmol, 4 equiv), white solid obtained in 1:1 mixture with **12** (270 mg, 98%). The yield ratio was determined according to the ratio of the integrals of the peaks in the ^1H NMR with chemical shift 4.7 ppm ($-\text{CH}_2\text{-Ph}$ for mono-substituted) and 4.8 ppm ($-\text{CH}_2\text{-Ph}$ for bis-substituted), see **A7** in Appendices.

6.5.2.20 Attempted preparation of 4a,8a-Bis(3,5-dibromobenzyl) dodecahydro 2a,4a,6a,8a-tetraazacyclopenta [fg]acenaphthylene-4a,8a-dium bromide (25). Actual preparation of a mixture of (25) and (13).



From decahydro-2a,4a,6a,8a-tetraazacyclopenta[fg]acenaphthylene (100 mg, 0.515 mmol, 1 equiv) and 1,3-dibromo-5-(bromomethyl) benzene (677 mg, 2.06 mmol, 4 equiv), white solid obtained in 1:4 mixture with **13** (404 mg, 92%). The yield ratio was determined according to the ratio of the integrals of the peaks in the ^1H NMR with chemical shift 4.95 ppm ($-\text{CH}_2\text{-Ph}$ for mono-substituted) and 5.18 ppm ($-\text{CH}_2\text{-Ph}$ for bis-substituted), see **A8** in Appendices.

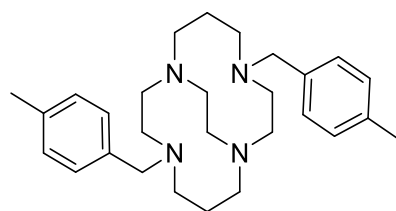
6.5.2.21 Synthesis of 4a,8a-Bis(2-(tert-butoxy)-2-oxoethyl)dodecahydro-2a,4a,6a,8a-tetraaza- cyclopenta[fg]acenaphthylene-4a,8a-dium bromide (26)



26

From decahydro-2a,4a,6a,8a-tetraazacyclopenta[fg]acenaphthylene (100 mg, 0.515 mmol, 1 equiv) and t-butyl bromoacetate (402 mg, 2.06 mmol, 4 equiv), white solid (260 mg, 86%). ^1H NMR (400 MHz, D_2O , δ): 1.47 (s, 18H), 2.92–3.03 (m, 2H), 3.03–3.16 (m, 2H), 3.36 (d, $J = 13.9$ Hz, 2H), 3.53–3.64 (m, 2H), 4.00–4.13 (m, 6H), 4.17–4.27 (m, 2H), 4.41 (d, $J = 16.7$ Hz, 2H), 4.51 (s, 2H), 4.64 (d, $J = 16.7$ Hz, 2H). ^{13}C NMR (100 MHz, D_2O , δ): 27.1, 42.9, 47.0, 56.9, 57.2, 64.0, 79.1, 87.4, 163.3. HRMS: calcd for $\text{C}_{22}\text{H}_{40}\text{N}_4\text{O}_4 \text{ Br}^+$: 503.2227, found: 503.2228. Elemental analysis calcd for $\text{C}_{22}\text{H}_{40}\text{Br}_2\text{N}_4\text{O}_4 \cdot 4\text{H}_2\text{O}$: C, 40.25; H, 7.37; N, 8.53; found: C, 40.77; H, 7.29; N, 8.75. Mp 125–127 °C.

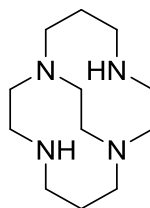
6.5.3 Synthesis of 4,11-Bis(4-methylbenzyl)-1,4,8,11-tetraaza bicycle[6.6.2]hexa decane(29)



29

This compound has been previously synthesised using standard synthetic techniques.¹⁴⁶ To a stirred solution of 5a,10a-bis(4-methylbenzyl)tetradecahydro-3a,5a,8a,10a-tetraazapyrene 5a,10a-diium bromide **17** (100 mg, 0.168 mmol) in ethanol (10 mL) was added slowly sodium borohydride (317 mg, 8.3 mmol) and the mixture was stirred for 30 min at rt before heated using microwave irradiation at 100 °C for 30 min. After cooling to rt, water (10 mL) was added to decompose excess NaBH₄ and solvents were removed under vacuum. Water (30 mL) was added to the residue, the solution was made basic by addition of excess of solid KOH (pH 14), and extracted with dichloromethane (4 × 30 mL). Combined organic extracts were dried and solvent was removed to yield a white solid (139 mg, 83%). ¹H NMR (400 MHz, CDCl₃, δ): 1.33–1.43 (m, 2H), 1.52–1.63 (m, 2H), 2.30 (s, 6H), 2.35–2.37 (m, 8H), 2.46–2.51 (m, 3H) 2.8–2.9 (m, 2H), 3.15 (d, *J* = 13.5 Hz, 2H), 3.21 (d, *J* = 8.6 Hz, 2H), 3.74 (d, *J* = 13.5 Hz, 2H), 3.89–4.00 (m, 2H), 7.12 (d, *J* = 8.0 Hz, 4H), 7.23 (d, *J* = 8.0 Hz, 4H).

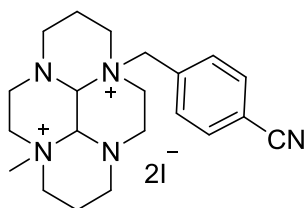
6.5.4 Synthesis of 1,4,8,11-Tetra-azabicyclo [6.6.2]hexadecane (**38**)



38

This compound has been previously synthesised using standard synthetic techniques.¹⁴⁶ A solution of **29** (200 mg, 0.46 mmol) in glacial acetic acid (20 mL) was added to a stirred suspension of 10% palladium on carbon (25 mg) in glacial acetic acid (2 mL), and the reactor was flushed with nitrogen and hydrogen before filling with hydrogen. The mixture was stirred at rt under 1 bar of hydrogen for 24 h. Then, the reactor was flushed with nitrogen, and the reaction mixture was filtered through a pad of Hyflo filtration aid and washed with glacial acetic acid (3 × 15 mL). Solvents were removed under vacuum, and the residue dried to yield a yellow oil (83 mg, 80%). ¹H NMR (400 MHz, C₆D₆, δ): 1.11–1.23 (m, 2H), 1.40–1.54 (m, 2H), 2.00–2.08 (m, 2H), 2.09–2.19 (m, 12H), 2.22–2.30 (m, 2H), 2.40–2.56 (m, 6H), 2.72–2.86 (m, 4H), 2.13–2.26 (m, 2H), 3.55 (br s, 2H).

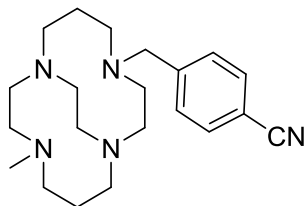
6.5.5 Synthesis of 3a-[4-cyanobenzyl]-8a[methyl]-decahydro-3a,5a,8a,10a,tetra aza-pyrenium diiodide (13).



13

This compound has been previously synthesised using standard synthetic techniques.²⁹² 3a-[4-Cyanobenzyl]-decahydro-3a,5a,8a,10a-tetraaza-pyrenium bromide **3** (5.00 g, 11.9 mmol), was suspended in dry MeCN (220 mL) under nitrogen. Iodomethane (62.5 mL, 1037.0 mmol) was added dropwise. The white suspension was left to stir for 10 days. A second portion of iodomethane (32.5 mL, 520.0 mmol) was added after 5 days. Excess iodomethane was removed by flowing nitrogen through the suspension for 30 minutes. The solid was collected by filtration, washed with ether (3 x 50 mL) and dried in vacuo to yield a white powder (7.0 g, 96%). ¹H NMR (DMSO): δ 1.75 (d, 1H, N- β -CH₂), 1.89(d, 1H, N- β -CH₂), 2.08-2.19 (m, 3H, CH₃), 2.27 (m, 1H, N- β -CH₂), 2.51 (m, 1H, N- β -CH₂), 2.65 (m, 1H, N- α -CH₂), 2.91 (m, 2H, N- α -CH₂), 3.10 (m, 2H, N- α -CH₂), 3.17 (d, 2H, N- α -CH₂), 3.20 (m, 2H, N- α -CH₂), 3.39 (m, 2H, N- α -CH₂), 3.53-3.63 (m, 2H, N- α -CH₂), 3.81 (d, 1H, N- α -CH₂), 4.32 (m, 2H, N- α -CH₂), 4.98 (m, 2H, Haminal), 5.16 (m, 2H, CH₂-Ar), 7.83 (d, 2H, H-Ar), 8.06 (d, 2H, H-Ar). ¹³C NMR (DMSO): δ 1.15 (-CH₃), 17.97 (N- β -CH₂), 18.21 (N- β -CH₂), 45.69 (N- α -CH₂), 45.89 (N- α -CH₂), 47.34(N- α -CH₂), 48.68 (N- α -CH₂), 50.15 (N- α -CH₂), 50.34 (N- α -CH₂), 59.54 (N- α -CH₂), 59.83 (N- α -CH₂), 63.92 (CH₂-Ar), 75.05 (C_{aminal}), 75.17 (C_{aminal}), 113.41 (C-Ar), 118.05 (CN), 131.10 (CH-Ar), 132.87 (CH-Ar), 134.36 (C-Ar). HRMS (*m/z*): [M - 2I]²⁺ calcd for C₂₁H₃₁N₅, 176.6280; found, 176.6284. Anal. calcd for C₂₁H₃₁I₂N₅·3H₂O: C, 38.14; H, 5.64; N, 10.59. Found: C, 38.45; H, 4.82; N, 10.46.

6.5.6 Synthesis of 1-[4-cyanobenzyl]-8-[methyl]- 1,4,8,11-tetraazabicyclo [6.6.2] hexadecane (14).



14

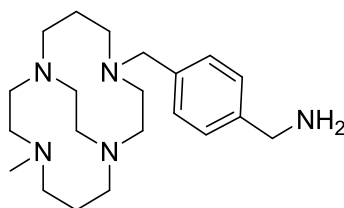
Method A

This compound has been previously synthesised using standard synthetic techniques.²⁹² To a stirred solution of 3a-[4-Cyanobenzyl]-8a-[methyl]-decahydro-3a,5a,8a,10a,tetraaza-pyreniumdiiiodide **13** (100 mg, 0.194 mmol) in ethanol (10 mL) was added slowly sodium borohydride (380 mg, 1.94 mmol) and the mixture was stirred for 30 min at rt before heated using microwave irradiation at 100 °C for 30 min. After cooling to rt, water (10 mL) was added to decompose excess NaBH₄ and solvents were removed under vacuum. Water (30 mL) was added to the residue, the solution was made basic by addition of excess of solid KOH (pH 14), and extracted with dichloromethane (4 × 30 mL). Combined organic extracts were dried and solvent was removed to yield a white solid (57 mg, 83%).

Method B

3a-[4-Cyanobenzyl]-8a-[methyl]-decahydro-3a,5a,8a,10a,tetraaza-pyreniumdiiodide **13** (5.0 g, 8.2 mmol) was dissolved in ethanol (250 mL) and sodium borohydride (12.58 g, 324.0 mmol) was added in small portions over a period of 1 hour. The clear solution was stirred for 14 days. Water (150 mL) was added to quench the reaction and solvents were removed in vacuo. The residue was taken up in water (200 mL) and made strongly basic (pH 14, KOH). The basic solution was extracted with DCM (5 x 100 mL), the combined organic extracts were dried (Na₂SO₄) and evaporated in vacuo to yield a colourless/yellow oil (2.1g, 72%). ¹H NMR (CDCl₃): δ 1.38-1.49 (m, 4H, N-β-CH₂), 2.18-2.49 (br m, 16H, N-α-CH₂), 2.55-2.67 (m, 3H, -CH₃), 2.80-2.90 (m, 1H, N-α-CH₂), 3.07 (d, 1H, N-α-CH₂), 3.26 (d, 1H, N-α-CH₂), 3.71-3.82 (m, 2H, CH₂-Ar), 4.09 (dt, 1H, N-α-CH₂), 7.46 (d, 2H, H-Ar), 7.60 (d, 2H, HAr). ¹³C NMR (CDCl₃): δ 26.94 (N-β-CH₂), 27.95 (N-β-CH₂), 42.72 (-CH₃), 51.88 (N-α-CH₂), 52.12(N-α-CH₂), 54.09 (N-α-CH₂), 55.04 (N-α-CH₂), 55.94 (N-α-CH₂), 56.16 (N-α-CH₂), 56.74 (N-α-CH₂), 56.98 (N-α-CH₂), 57.84 (N-α-CH₂), 59.52 (N-α-CH₂), 59.93 (CH₂-Ar), 110.30 (C-Ar), 119.09 (CN), 129.36 (CH-Ar), 131.89 (CH-Ar), 146.98 (C-Ar). HRMS (*m/z*): [M + H]⁺ calcd for C₂₁H₄₃N₅, 356.2811; found, 356.2809.

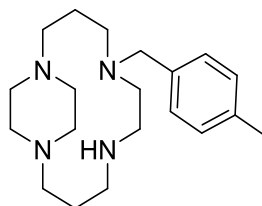
6.5.7 Synthesis of 1-[4-aminomethylbenzyl]-8-[methyl]-1,4,8,11-tetraazabicyclo[6.6.2]hexadecane (15). ²⁹²



15

Lithium aluminium hydride (0.19 g, 5.0 mmol) was dissolved in dry THF (20 mL). To this, 1-[4- cyanobenzyl]-8-[methyl]-1,4,8,11-tetraaza-bicyclo[6.6.2]hexadecane **14** (1.45 g, 4.1 mmol) in dry THF (20 mL) was added dropwise under ice-cooling. After complete addition the mixture was stirred for 30 minutes then heated to reflux for 3 hours. The reaction was cooled in an ice-bath, water (0.21 mL) was added dropwise followed by 15% sodium hydroxide (0.21 mL) followed by a second portion of water (0.62 mL). The resulting white precipitate was filtered and washed with THF (2 x 10 mL) then water (2 x 5 mL). The aqueous layer was made strongly basic (pH > 12, KOH) and extracted with THF (5 x 25 mL). The organic phases were dried (Na₂SO₄), filtered and concentrated *in vacuo* to yield yellow oil (1.40 g, 95%). ¹H NMR (CDCl₃): δ 1.38-1.50 (m, 8H), 2.16-2.33 (m, 6H), 2.36-2.51 (m, 6H), 2.50-2.57 (m, 1H), 2.60-2.73 (m, 3H), 2.83-3.20 (m, 3H), 3.64-3.66 (d, 1H) 3.73 (d, 2H), 3.86 (d, 3H), 7.22-7.24 (d, 2H, CH₂-Ar), 7.29-7.33 (d, 2H, CH₂-Ar). ¹³C NMR (CDCl₃): δ 26.68 (N-β-CH₂), 27.64 (N-β-CH₂), 43.02 (-CH₃), 52.13 (N-α-CH₂), 52.38 (N-α-CH₂), 53.85 (N-α-CH₂), 54.71 (N-α-CH₂), 55.83 (N-α-CH₂), 56.25(N-α-CH₂), 56.47 (N-α-CH₂), 57.96 (N-α-CH₂), 58.89 (N-α-CH₂), 59.65 (N-α-CH₂), 62.19 (CH₂-NH₂), 67.97 (CH₂-Ar), 127.16 (CH-Ar), 129.83 (CH-Ar), 135.66 (C-Ar), 139.56 (C-Ar). MS: (ESI) m/z 359.4 (100 [M + H]⁺)

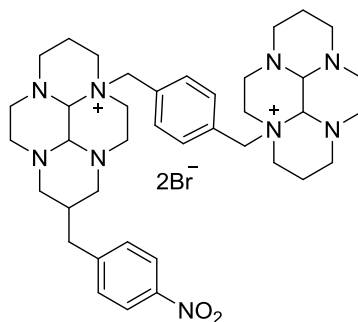
6.5.8 Synthesis of 5-(4-methylbenzyl)-1,5,8,12tetraazabicyclo[10.2.2] hexa decane (30).



30

This compound has been previously synthesised using standard synthetic techniques.¹⁴⁶ To a stirred solution of **5** (150 mg, 0.359 mmol) in ethanol (10 mL) was added slowly sodium borohydride (0.33 mg, 8.8 mmol), and the mixture was stirred for 30 min at r.t., then heated in microwave for 10 min. After cooling to r.t., water (10 mL) was added to decompose excess NaBH₄, and solvents were removed. Water (30 mL) was added to the residue, the solution was made basic (KOH, pH 14), and extracted with dichloromethane (4 x 30 mL). Combined organic extracts were dried, and solvent was removed to yield a colourless oil (80 mg, 98%). ¹H NMR (CDCl₃): δ 7.13-7.09 (m, 4H, H(Ar)), 3.62 (s, 2H, CH₂-Ar), 3.29-3.25 (m, 2H, CH₂-N), 3.12-2.99 (m, 2H, CH₂-N), 2.93 (t, 2H, *J* = 6.0 Hz, CH₂-N), 2.74-2.35 (m, 11H, CH₂-N), 2.34 (s, 3H, CH₃), 2.26 (td, 2H, *J* = 11.0, 4.5 Hz, CH₂-N), 2.06 (td, 1H, *J* = 11.0, 4.5 Hz, CH₂-N), 1.83-1.71 (m, 4H, CH₂-β-N). MS, *m/z*: 331 [M⁺], 100 %.

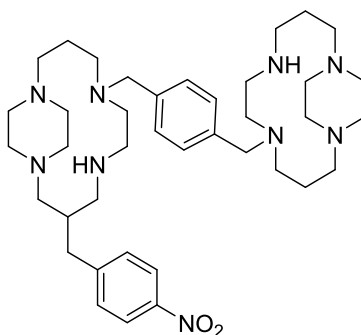
6.5.9 Synthesis of 10a-(4-((decahydro-1H-3a,5a,8a,10a-tetraazapyren-5a-ium-5a(6H)-yl)methyl) benzyl)-7-(4-nitrobenzyl)dodecahydro-6H-3a,5a,8a,10a-tetraazapyren-10a-ium (31).



31

This compound **31** was supplied by Ali Al-Zirgani.²⁹³

6.5.10 Synthesis of 8-(4-(1,5,8,12-tetraazabicyclo[10.2.2]hexadecan-5-ylmethyl) benzyl)-3-(4-nitrobenzyl)-1,5,8,12-tetraazabicyclo[10.2.2]hexadecane (32).

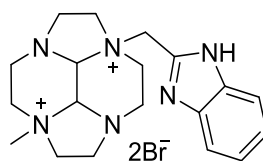


32

This compound has been previously synthesised using standard synthetic techniques.²⁹⁴ To a stirred solution of **31** (100 mg, 0.118 mmol) in (10 mL) ethanol and water 9:1 was added slowly sodium borohydride (22 mg, 0.59 mmol), and the mixture was stirred for 30 min at r.t., then heated in microwave for 10 min. After cooling to r.t., water (10 mL) was added to decompose excess NaBH₄, and solvents were removed. Water (30 mL) was added to the residue, the solution was made basic (KOH, pH 14), and extracted with dichloromethane (4 x 30 mL). The organic extracts were combined, dried over anhydrous magnesium sulphate, filtered and concentrated *in vacuo* to yield a light

yellow solid (63.5m g, 78%). ^1H NMR (CDCl_3): δ 1.67 (m, 4H, NCH_2), 1.75 (s, 4H, NCH_2), 2.20 (m, 4H, NCH_2), 2.55 (m, 12H, NCH_2), 2.65 (m, 8H, NCH_2), 2.81 (m, 4H, NCH_2), 3.01 (m, 4H, NCH_2), 3.20 (m, 4H, NCH_2), 3.35 (m, 4H, NCH_2), 3.57 (m, 4H, NCH_2Ar), 7.22 (m, 6H, $\text{CH}_{\text{aromatic}}$), 8.09 (m, 2H, $\text{CH}_{\text{aromatic}}$). HRMS calcd. for $\text{C}_{39}\text{H}_{63}\text{N}_9\text{O}_2$. 690.5177 $[\text{M}+\text{H}]^+$. found 690.5173 $[\text{M}+\text{H}]^+$.

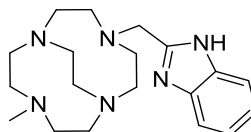
6.5.10 Synthesis of 8a-((1H-benzo[d]imidazol-2-yl)methyl)-4a-methyldodecahydro-2a,4a, 6a, 8a-tetraaza cyclopenta[fg] acenaphthylene-4a,8a-diiium(34)



34

This compound **34** was provided by Ali Al-Zirgani.²⁹³

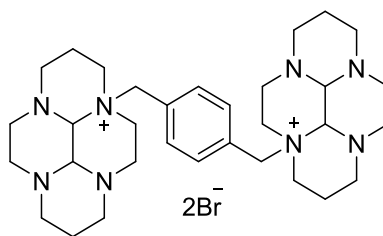
6.5.11 Synthesis of 4-((1H-benzo[d]imidazol-2-yl)methyl)-10-methyl-1,4,7,10-tetraazabicyclo[5.5.2]tetradecane (35).



35

This compound has been previously synthesised using standard synthetic techniques.²⁹⁴ To a stirred solution of **34** (100 mg, 0.199 mmol) in ethanol (10 mL) was added slowly sodium borohydride (361 mg, 9.5 mmol), and the mixture was stirred for 30 min at r.t., and then heated in microwave for 30 min. After cooling to r.t., water (10 mL) was added to decompose excess NaBH₄, and solvents were removed. Water (30 mL) was added to the residue, the solution was made basic (KOH, pH 14), and extracted with dichloromethane (4 x 30 mL). Combined organic extracts were dried, and solvent was removed and evaporated in *vacuo* to yield a dark orange solid (51 mg, 75 %). ¹ H NMR (CD₃OD) δ 2.2 (quin. 6H), 2.3 (t, 8H), 2.5 (m, CH₃) 2.52 (t, 2H), 2.71 (q, 2H), 2.87-3.34 (m, 2H), 4.01 (s, 2H), 5.27 (t, 2H), 7.15 (m, 2H, Ar H), 7.59 (m, 2H, ArH) ; MS: (ESI) m/z 343.26(100[M]⁺).

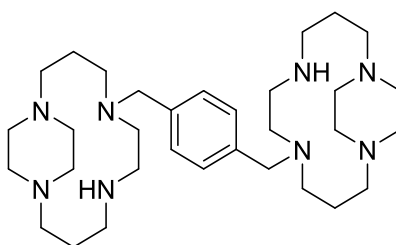
6.5.12 5a,5a''-(1,4-phenylenebis(methylene))bis(dodecahydro-1H-3a,5a,8a,10a-tetraazapyren-5a-ium) (27)



27

This compound **27** was provided by Ali Al-Zirgani.²⁹³

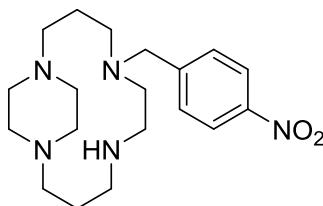
6.5.13 Synthesis of 1,4-bis((1,5,8,12-tetraazabicyclo[10.2.2]hexadecan-5-yl) methyl) benzene (28)



28

This compound has been previously synthesised using standard synthetic techniques.²⁹⁵ To a stirred solution of **27** (100 mg, 0.141 mmol) in ethanol (10 mL) was added slowly sodium borohydride (53.7 mg, 1.414 mmol), and the mixture was stirred for 30 min at r.t., and then heated in microwave for 30 min. After cooling to r.t., water (10 mL) was added to decompose excess NaBH₄, and solvents were removed. Water (30 mL) was added to the residue, the solution was made basic (KOH, pH 14), and extracted with dichloromethane (4 x 30 mL). Combined organic extracts were dried, and solvent was removed and evaporated in *vacuo* to yield a dark orange solid (75 mg, 96 %). ¹H NMR (400 MHz, CDCl₃) δ = 1.72 (m, 4H), 1.81 (s, 4H, CH₂), 2.26 (m, 4H, CH₂), 2.56 (m, 12H, CH₂), 2.63 (m, 8H, CH₂), 2.70 (m, 4H, CH₂), 2.93 (m, 4H, CH₂), 3.02 (m, 4H, CH₂), 3.27 (m, 4H, CH₂), 3.65 (s, 4H, CH₂Ar), 7.20 (s, 4H, ArH). ES-MS: *m/z*: 556 (MH⁺).

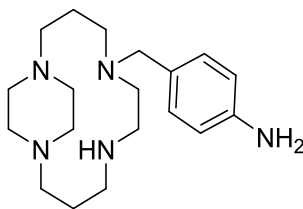
6.5.14 Synthesis of 5-(4-nitrobenzyl)-1,5,8,12-tetraazabicyclo[10.2.2]hexadecane (36).



36

This compound has been previously synthesised using standard synthetic techniques.¹⁴⁶ To a stirred solution of **4** (150 mg, 0.359 mmol) in ethanol (10 mL) was added slowly sodium borohydride (68 mg, 1.795 mmol), and the mixture was stirred for 30 min at r.t., then heated in microwave for 10 min. After cooling to r.t., water (10 mL) was added to decompose excess NaBH₄, and solvents were removed. Water (30 mL) was added to the residue, the solution was made basic (KOH, pH 14), and extracted with dichloromethane (4 x 30 mL). Combined organic extracts were dried, and solvent was removed to yield a colourless oil (80 mg, 98%). ¹H NMR (CDCl₃): δ 7.13-7.09 (m, 4H, H(Ar)), 3.62 (s, 2H, CH₂-Ar), 3.29-3.25 (m, 2H, CH₂-N), 3.12-2.99 (m, 2H, CH₂-N), 2.93 (t, 2H, *J* = 6.0 Hz, CH₂-N), 2.74-2.35 (m, 11H, CH₂-N), 2.34 (s, 3H, CH₃), 2.26 (td, 2H, *J* = 11.0, 4.5 Hz, CH₂-N), 2.06 (td, 1H, *J* = 11.0, 4.5 Hz, CH₂-N), 1.83-1.71 (m, 4H, CH₂-β-N). MS, *m/z*: 331 [M⁺], 100 %

6.5.15 Synthesis of 4-((1,5,8,12-tetraazabicyclo[10.2.2]hexadecan-5-yl)methyl)aniline (37)



37

Method A:

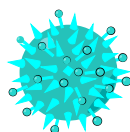
This compound has been previously synthesised using standard synthetic techniques.⁹³ To a stirred solution of sulfur (0.531 g, 16.6 mmol) and sodium borohydride (0.314 g, 8.30 mmol) in dry THF (50 mL), and the mixture was stirred for 1h at r.t. under nitrogen, then **36** (150 mg, 0.415 mmol) was add as a solution in dry THF and reaction mixture heated by microwave for 30 minutes. The result solution was then cooled to room temperature, water (10 mL) was added to decompose excess NaBH₄, and solvents were removed. Water (30 mL) was added to the residue, the solution was made basic (KOH, pH 14), and extracted with dichloromethane (4 x 30 mL). Combined organic extracts were dried, and solvent was removed to yield a yellow oil, (100mg, 80%).

Method B:

To a stirred solution of sulfur (293 mg, 9.153 mmol) and sodium borohydride (172 mg, 4.56 mmol) in dry THF (50 mL), and the mixture was stirred for 1h at r.t. under nitrogen, then **4** (100 mg, 0.228 mmol) was add as a solution in dry THF and reaction mixture heated by microwave for 30 minutes. The result solution was then cooled to room temperature, water (10 mL) was added to decompose excess NaBH₄, and solvents were removed. Water (30 mL) was added to the residue, the solution was made basic (KOH, pH 14), and extracted with dichloromethane (4 x 30 mL). Combined organic extracts were dried, and solvent was removed to yield a yellow oil, (97 mg, 78.4%). ¹H NMR (CDCl₃): δ 8.12 and 7.47 (4H, *J* = 9.0 Hz, H(Ar)), 3.65 (s, 2H, CH₂-Ar), 3.18-3.11 (m, 2H, CH₂-N), 3.08-3.02 (m, 2H, CH₂-N), 2.86-2.63 (m, 6H, CH₂-N), 2.60-2.54 (m, 4H, CH₂-

N), 2.51 (t, 2H, $J = 5.0$ Hz, CH₂-N), 2.44-2.22 (m, 4H, CH₂-N), 1.89-1.82 (m, 2H, CH₂-β-N), 1.69-1.61 (m, 2H, CH₂-β-N). ¹³C NMR (CDCl₃): δ 147.2 (C(Ar)-CH₂), [129.8, 129.6] (C(Ar)), 123.5 (C(Ar)-NO₂), 57.7 (CH₂-Ar), [56.5, 55.0, 54.7, 51.2, 50.1, 48.7, 48.0] (CH₂-N), [26.1, 23.5] (CH₂-β-N) MS, m/z : 332 [M+H]⁺. HRMS: calcd. For C₁₉H₃₄N₅: 332.2809; found 332.2810.

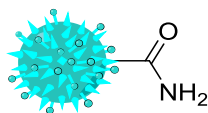
6.6 Extraction of date spore exine microcapsules (*Phoenix dactylifera*) with HCl (39)



39

In the preparation of date spore exines, Raw *Phoenix dactylifera* L. spores (loose powder, 100 gm) were suspended in 9M HCl aqueous solution (1 L) and heated at ca. 95°C for 1 h. After this the suspension was neutralised with an aqueous solution of KOH (50%) to pH 6-7. After filtration, the sporopollenin were washed with hot water (10-15 x 250 mL), ethanol (4 x 250 mL) and DCM (4 x 250 mL) and dried in an oven at 40°C. The SEC (30 g) obtained by this protocol were nitrogen-free. Solid state ¹³C NMR: δ 179 (C_{carbonyl}), 160 (C-C_{phenol}), 135 (C_{aromatic}), 110, 83, 40. FTIR: 3387 cm⁻¹, 2926 cm⁻¹, 2858 cm⁻¹, 1720 cm⁻¹, 1595 cm⁻¹, 1416 cm⁻¹, 1261 cm⁻¹, 1050 cm⁻¹. The combustion elemental analysis results were %C 44.89; %H 6.10; %N 0.0. SEM images were recorded, see **A9** and **A10** in the Appendix.

6.6.1 Synthesis of **41** by reaction with ammonia (**39**)



41

Date sporopollenin exines **39** (0.5 g) were suspended in aqueous (0.88) ammonia (25 mL) and stirred at room temperature for 4 days. The exines were recovered by filtration, washed with water (5 x 20 mL), ethanol (2 x 20 mL) and methanol (2 x 20 mL), dried under vacuum and then at 40°C temperature in the oven for 24 h to a constant weight to yield product **41** (mass recovery: 0.5 g). Solid state ^{13}C NMR: δ 179 ($\text{C}_{\text{carbonyl}}$), 160 ($\text{C-C}_{\text{phenol}}$), 135 ($\text{C}_{\text{aromatic}}$), 110, 83, 40. FTIR: 3387 cm^{-1} , 2926 cm^{-1} , 2858 cm^{-1} , 1720 cm^{-1} , 1595 cm^{-1} , 1416 cm^{-1} , 1261 cm^{-1} , 1050 cm^{-1} . The combustion elemental analysis of product **41** was: %C 44.85, %H 6.22, %N 1.4.

6.6.2 Synthesis of **40** by treatment of **39** with hydrochloric acid

Compound **40** (0.5 g) was suspended in aqueous hydrochloric acid (2M, 25 mL) and stirred overnight at room temperature. The solid was recovered by filtration, washed with water (5 x 20 mL), ethanol (2 x 20 mL) and methanol (20 mL) and dried under vacuum and at 40°C temperature in the oven for 24 h to a constant weight to yield **41** (mass recovery: 0.5 g). The combustion elemental analysis of product **40** was: %C 44.06, %H 5.52, %N 1.12.

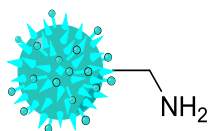
6.6.3 Synthesis of **43** by treatment of **39** with sodium hydroxide

Date sporopollenin exines **39** (0.5 g) were suspended in aqueous sodium hydroxide (2 M, 25 mL) and stirred overnight at room temperature. The solid was recovered by filtration, washed with water (5 x 20 mL), ethanol (2 x 20 mL) and methanol (20 mL) and dried under vacuum and at 40°C temperature in the oven for 24 h to a constant weight to yield **43** (mass recovery: 0.5 g). The combustion elemental analysis of product **43** was: %C 44.89, %H 6.10, %N 0.0.

6.6.4 Synthesis of **44** by treatment of **41** with sodium hydroxide

Date sporopollenin exines **41** (0.5 g) were suspended in aqueous sodium hydroxide (2 M, 25 mL) and stirred overnight at room temperature. The solid was recovered by filtration, washed with water (5 x 20 mL), ethanol (2 x 20 mL) and methanol (20 mL) and dried under vacuum and at 40 °C temperature in the oven for 24h to a constant weight to yield **44** (mass recovery: 0.5 g). The combustion elemental analysis of product **44** was: %C 44.33, %H 5.64, %N 1.07.

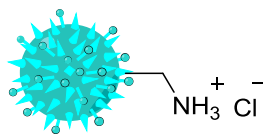
6.6.5 Synthesis of **45** by reduction of **42** with lithium aluminium hydride



45

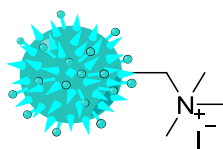
Compound **42** (0.5 g) was suspended in dried 1,4-dioxane (20 mL) and lithium aluminium hydride (1.0 g) was added. The mixture was stirred for 4 days under reflux in nitrogen. Excess reducing agent was quenched at 0 °C by successive addition of ethyl acetate (100 mL), ethanol (50 mL), water (100 mL) and 2 M sulfuric acid (200 mL). Particles were recovered by filtration, washed with water (3 x 50 mL), ethanol (3 x 30 mL) and methanol (2 x 30 mL) and dried under vacuum and at 40 °C temperature in the oven for 24 h to a constant weight to yield **45** (mass recovery: 0.4 g). Solid state ¹³C NMR: δ 160 (C-C_{phenol}), 135 (C_{aromatic}), 110, 83, 40. FTIR: 3387 cm⁻¹, 2917 cm⁻¹, 2858 cm⁻¹, 1435 cm⁻¹, 1341 cm⁻¹, 1040 cm⁻¹. The typical combustion elemental analysis of product **45** was: %C 44.23, %H 6.3, %N 0.84.

6.6.6 Synthesis of **46** by treatment of **45** with hydrochloric acid



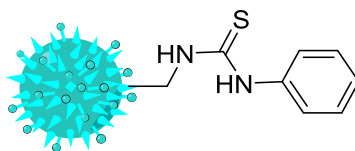
Sporopollenin **45** (0.5 g) was suspended in aqueous hydrochloric acid (2 M, 25 mL) and stirred overnight at room temperature. The solid was recovered by filtration, washed with water (5 x 20 mL), ethanol (2 x 20 mL) and methanol (20 mL) and dried under vacuum and at 40 °C temperature in the oven for 24 h to a constant weight to yield **46** (mass recovery: 0.5 g). The typical combustion elemental analysis of product **46** was: %C 44.72, %H 6.01, %N 0.83.

3.6.7 Synthesis of **47** by Hoffman quaternisation of **45**



Compound **45** (0.5 g) was suspended in acetonitrile (10 mL) and methyl iodide (2 mL) was added. The mixture stirred under reflux for 3 days. The solid was recovered by filtration, washed with acetonitrile (2 x 20 mL), ethanol (2 x 20 mL) and methanol (20 mL) and dried under vacuum and at 40°C temperature in the oven for 24 h to a constant weight to yield product **47** (mass recovery: 2.6 g). The combustion elemental analysis of product **47** was: %C 42.41, %H 6.14, %N 0.86.

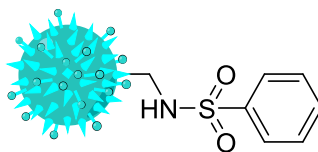
6.6.8 Synthesis of 48



48

Product **45** (0.2 g) was suspended in dichloromethane (10 mL). Phenyl isothiocyanate (2 mL) was added and the mixture was stirred overnight at room temperature. The solid was recovered by filtration, washed with dichloromethane (3 x 10 mL) and methanol (2 x 20mL) dried under vacuum and at 40 °C temperature in the oven for 24 h to a constant weight to yield product **48** (mass recovery: 0.8 g). The combustion elemental analysis of product **48** was: %C 44.25, %H 6.04, %N 0.78 The level of sulfur determined by ICP-OES was 0.91%.

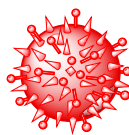
6.6.9 Synthesis of 49



49

Product **45** (0.2 g) was suspended in chloroform (10 mL). Benzene sulfonyl chloride (2 mL) was added and the mixture was stirred overnight at room temperature. The solid was recovered by filtration, washed with dichloromethane (3 x 10 mL) and methanol (2 x 20 mL) and dried under vacuum and at 40°C temperature in the oven for 24 h to a constant weight to yield product **49** (mass recovery: 0.8 g). The typical combustion elemental analysis of product **49** was: %C 45.02, %H 6.20, %N 0.82. The level of sulfur determined by ICP-OES was 1.43%.

6.7 Amination of sporopollenin (**50**) by mechanochemistry

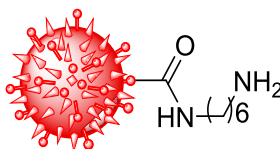


50

General procedure

A mixture of sporopollenin (*Lycopodium clavatum*) (**50** was supplied by Alberto Diego-Taboada) and the diamine in 1:10 molar ratio was ground for one hour at a speed 400 rpm. The crude products were scraped off the walls of the grinding jar and crude mixtures were washed multiple times with, successively, distilled water, methanol and ethanol, dried at room temperature under vacuum and at 40°C temperature in the oven for 24h. SEM images were recorded, see **A11**.

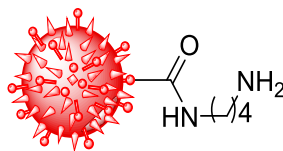
6.7.1 Synthesis of **51**



51

From sporopollenin **50** (100 mg, 0.2 mmol) and hexane-1,6-diamine (232 mg, 2 mmol), to yield product **51** (mass recovery: 100 mg). The combustion elemental analysis (CHN) of product **51** gave: %C 60.55, %H 8.92, %N 2.47.

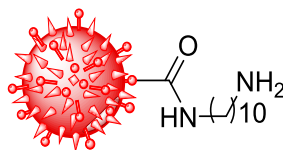
6.7.2 Synthesis of **53**



53

From sporopollenin **50** (100 mg, 0.2 mmol) and butane-1,4-diamine (176 mg, 2 mmol), to yield product **53** (mass recovery: 100 mg). The combustion elemental analysis (CHN) of product **53** gave: %C 60.20, %H 5.22, %N 2.75.

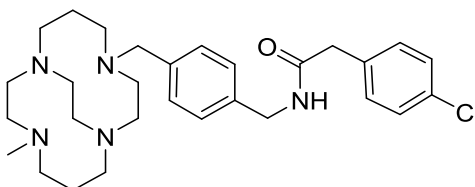
6.7.3 Synthesis of **54**



54

From sporopollenin **50** (100 mg, 0.2 mmol) and decane-1,10-diamine (344 mg, 2 mmol), to yield product **54** (mass recovery: 100 mg). The combustion elemental analysis (CHN) of product **54** gave: %C 60.25, H % 5.77, N% 2.34.

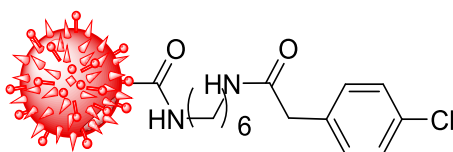
6.7.4 Synthesis of 2-(4-chlorophenyl)-N-(4-((11-methyl-1,4,8,11-tetraazabicyclo[6.6.2] hexa decan-4-yl)methyl)benzyl)acetamide (58)



58

A mixture of (4-((11-methyl-1,4,8,11-tetraazabicyclo[6.6.2]hexadecan-4-yl)methyl)phenyl)methanamine (100 mg, 0.278 mmol), 4-chlorophenyl acetic acid (190 mg, 1.114 mmol) and carbonyldiimidazole (CDI) (180.65 mg, 1.114 mmol) was ground for half hour at a speed of 400 rpm. The crude products were scraped off the walls of the grinding jar and crude mixtures were dissolved in water (30 mL). The solution was made basic (KOH, pH 14), and extracted with dichloromethane (4 x 30 mL). Combined organic extracts were dried, and solvent was removed and dried at room temperature under vacuum to yield a colourless oil (106 mg, 75%). ¹ H NMR (CDCl₃): δ 7.13-7.09 (m, 4H, H(Ar)), 3.62 (s, 2H, CH₂-Ar), 3.29-3.25 (m, 2H, CH₂-N), 3.12-2.99 (m, 2H, CH₂-N), 2.93 (t, 2H, J 6.0 Hz, CH₂-N), 2.74-2.35 (m, 11H, CH₂-N), 2.34 (s, 3H, CH₃), 2.26 (td, 2H, J 11.0, 4.5 Hz, CH₂-N), 2.06 (td, 1H, J 11.0, 4.5 Hz, CH₂-N), 1.83-1.71 (m, 4H, CH₂-β-N). MS, m/z: 511 [M⁺].

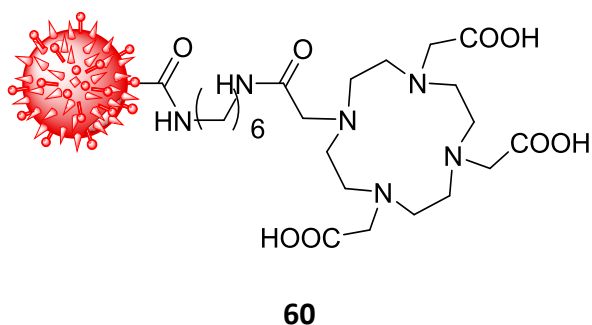
6.7.5 Synthesis of *N*-(6-acetamidohexyl)-2-(4-chlorophenyl)acetamide carboxylate of sporopollenin **59**



59

A mixture of aminated sporopollenin (*Lycopodium clavatum*) **51** (100 mg, 0.2 mmol), 4-chlorophenyl acetic acid (135 mg, 0.8 mmol) and carbonyldiimidazole (CDI) (129.72 mg, 0.8 mmol) was ground for half hour at a speed of 400 rpm. The crude products were scraped off the walls of the grinding jar and crude mixtures were washed multiple times with, successively, distilled water, methanol and ethanol, dried at room temperature under vacuum and at 40°C temperature in oven for 24h. The combustion elemental analysis (CHN) of product **59** gave: %C 60.02, %H 8.37, (%N 2.12, 1.51 mmol/g). ICP Cl analysis: found: (2.28%, 0.65 mmol/g).

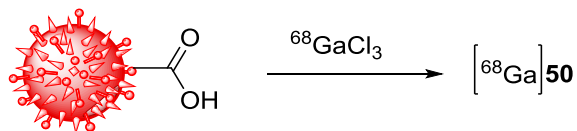
6.7.6 Synthesis of 2,2',2''-(10-(2-((6-acetamidohexyl)amino)-2-oxoethyl)-1,4,7,10-tetraazacyclododecane-1,4,7-triyl)triacetic acid sporopollenin **60**



A mixture of aminated sporopollenin (*Lycopodium clavatum*) **51** (100 mg, 0.2 mmol), 1,4,7,10-tetraazacyclododecane-1,4,7,10-tetraacetic acid (DOTA) (323.53 mg, 0.8 mmol) and carbonyldiimidazole (CDI) (259.2 mg, 1.6 mmol) was ground for half hour at a speed of 400 rpm. The crude products were scraped off the walls of the grinding jar and crude mixtures were washed multiple times with, successively, distilled water, methanol and ethanol, dried at room temperature under vacuum and at 40°C temperature in oven for 24h. The combustion elemental analysis (CHN) of product **60** gave: %C 55.00, %H 7.81, (%N 2.93, 2.09 mmol/g).

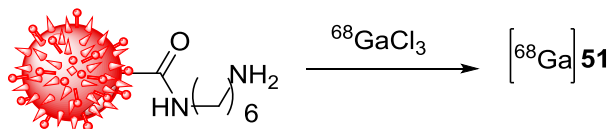
6.8 Radiolabeling of sporopollenin

6.8.1 Synthesis of Ga-68 complex of sporopollenin (*Lycopodium clavatum*) ([⁶⁸Ga]**49**)



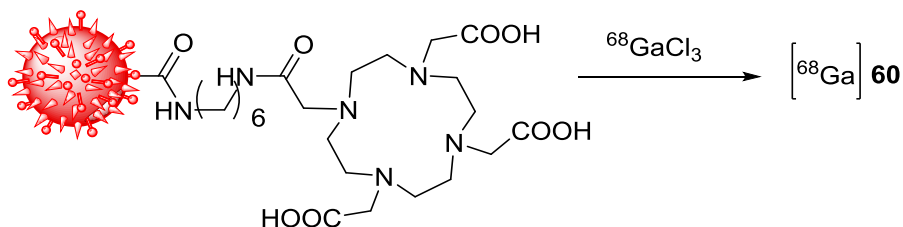
Sporopollenin (**50**) (1mg, 0.002mmol) in sodium acetate buffer (0.2 M, pH 5) was added to formulated ⁶⁸GaCl₃ (45-70 MBq) and the reaction was mixed either at room temperature (RT) or 90°C using a vortex stirrer over 30 minutes.

6.8.2 Synthesis of ^{68}Ga complex of N-(6-aminohexyl)acetamide sporopollenin ($[^{68}\text{Ga}]51$)



Sporopollenin **51** (1mg, 0.002mmol) in sodium acetate buffer (0.2 M, pH 5) was added to formulated $^{68}\text{GaCl}_3$ (50-77 MBq) and the reaction was mixed either at room temperature (RT) or 90°C using a vortex stirrer over 30 minutes.

6.8.3 Synthesis of ^{68}Ga complex for 2,2',2''-(10-(2-((6-acetamidohexyl)amino)-2-oxoethyl)-1,4,7,10-tetraazacyclododecane-1,4,7-triyl)triacetic acid ($[^{68}\text{Ga}]60$)

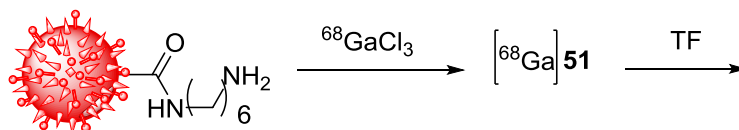


Sporopollenin **60** (1mg, 0.002mmol) in sodium acetate buffer (0.2 M, pH 5) was added to formulated $^{68}\text{GaCl}_3$ (50-70 MBq) and the reaction was mixed either at room temperature (RT) or 90°C using a vortex stirrer over 30 minutes.

6.8.4 Radiochemical stability

The radiochemical stability of aminated sporopollenin was analysed in both phosphate-buffered saline (PBS) and human serum apo-transferrin (apo-TF).

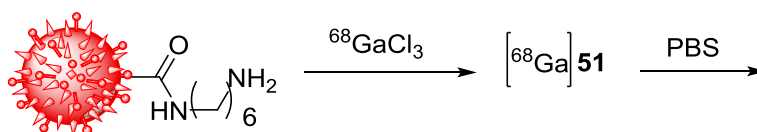
6.8.4.1 Apo-transferrin (apo-TF) stability of Ga-68 complex of aminated sporopollenin



2.5 mg of apo-transferrin in PBS at pH 7 was added to 100 μL of complex $[\text{}^{68}\text{Ga}]51$ and mixed at 37°C using a vortex stirrer. The complex stability was determined using radio-TLC at 1h, 2h and 3h.

Radio-TLC	
Time (h)	% RCY
1	94
2	90
3	88

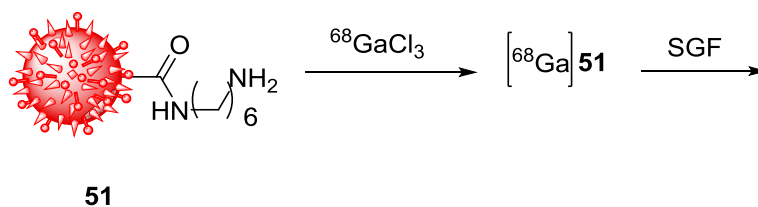
6.8.4.2 Phosphate buffer solution stability of ${}^{68}\text{Ga}$ complex of aminated sporopollenin



500 μL of PBS (pH = 7) was added to 100 μL of complex $[\text{}^{68}\text{Ga}]51$ and mixed at 37°C using a vortex stirrer. The complex stability was determined using radio-TLC at 1h, 2h and 3h.

Radio-TLC	
Time (h)	% RCY
1	95
2	93
3	89

6.8.4.3 Simulated gastric fluid (SGF)



100 μ L of SGF (pH = 1.5) was added to complex [^{68}Ga]**51** and mixed at 37°C using a vortex stirrer. The complex stability was determined using radio-TLC at 1h, 2h and 3h.

Radio-TLC	
Time (h)	% RCY
1	94
2	93
3	93

References

- (1) Kaneda, K.; Mizugaki, T. *Energy & Environmental Science* **2009**, *2*, 655.
- (2) Zhang, W. *Green Chemistry* **2009**, *11*, 911.
- (3) Candeias, N. R.; Branco, L. C.; P. Gois, P. M.; Afonso, C. A.; Trindade, A. F. *Chemical reviews* **2009**, *109*, 2703.
- (4) Chowdhury, S. A.; Scott, J. L.; MacFarlane, D. R. *Pure and Applied Chemistry* **2008**, *80*, 1325.
- (5) Newman, S. G.; Jensen, K. F. *Green Chemistry* **2013**, *15*, 1456.
- (6) Simon, M.-O.; Li, C.-J. *Chemical Society Reviews* **2012**, *41*, 1415.
- (7) Gawande, M. B.; Bonifácio, V. D.; Luque, R.; Branco, P. S.; Varma, R. S. *ChemSusChem* **2014**, *7*, 24.
- (8) Guo, W.; Shi, Y.; Wang, H.; Yang, H.; Zhang, G. *Ultrasonics Sonochemistry* **2010**, *17*, 680.
- (9) Xia, H.; Wang, Q. *Chemistry of materials* **2002**, *14*, 2158.
- (10) Kashkoush, I.; Busnaina, A.; Kern, F.; Kunesh, R. *Particles on Surfaces* **1992**, *3*, 217e237.
- (11) Yang, J.-M.; Ji, S.-J.; Gu, D.-G.; Shen, Z.-L.; Wang, S.-Y. *Journal of organometallic chemistry* **2005**, *690*, 2989.
- (12) Strauss, C. R.; Rooney, D. W. *Green Chemistry* **2010**, *12*, 1340.
- (13) Caddick, S.; Fitzmaurice, R. *Tetrahedron* **2009**, *65*, 3325.
- (14) Giguere, R. J.; Bray, T. L.; Duncan, S. M.; Majetich, G. *Tetrahedron Letters* **1986**, *27*, 4945.
- (15) Polshettiwar, V.; Varma, R. S. *Chemical Society Reviews* **2008**, *37*, 1546.
- (16) Pedersen, S. L.; Tofteng, A. P.; Malik, L.; Jensen, K. J. *Chemical Society Reviews* **2012**, *41*, 1826.
- (17) Kempe, K.; Becer, C. R.; Schubert, U. S. *Macromolecules* **2011**, *44*, 5825.
- (18) Tompsett, G. A.; Conner, W. C.; Yngvesson, K. S. *Chemphyschem* **2006**, *7*, 296.
- (19) Baghbanzadeh, M.; Carbone, L.; Cozzoli, P. D.; Kappe, C. O. *Angewandte Chemie-International Edition* **2011**, *50*, 11312.
- (20) Collins, J. M.; Leadbeater, N. E. *Organic & Biomolecular Chemistry* **2007**, *5*, 1141.
- (21) L, B. *Microwave synthesis chemistry at speed of light*; CEM Publishing: USA, 2002.
- (22) Caddick, S. *Tetrahedron* **1995**, *51*, 10403.
- (23) Lidstrom, P.; Tierney, J.; Wathey, B.; Westman, J. *Tetrahedron* **2001**, *57*, 9225.
- (24) Neochoritis, C. G.; Zarganes-Tzitzikas, T.; Tsoleridis, C. A.; Stephanidou-Stephanatou, J.; Kontogiorgis, C. A.; Hadjipavlou-Litina, D. J.; Choli-Papadopoulou, T. *European Journal of Medicinal Chemistry* **2011**, *46*, 297.
- (25) Wang, S.-L.; Cheng, C.; Wu, F.-Y.; Jiang, B.; Shi, F.; Tu, S.-J.; Rajale, T.; Li, G. *Tetrahedron* **2011**, *67*, 4485.
- (26) Jacob, J. *Int. J. Chem. (Toronto, ON, Can.)* **2012**, *4*, 29.
- (27) Kappe, C. O. *Angewandte Chemie-International Edition* **2004**, *43*, 6250.
- (28) Hayes, B. L. *Aldrichimica Acta* **2004**, *37*, 66.
- (29) Heravi, M. M.; Farhangi, N.; Beheshtiha, Y. S.; Ghassenizadeh, M.; Tabar-Hydar, K. *Indian Journal of Chemistry Section B-Organic Chemistry Including Medicinal Chemistry* **2004**, *43*, 430.
- (30) Bogdal, D.; Pielichowski, J.; Boron, A. *Synlett* **1996**, 873.
- (31) Seijas, J. A.; Vazquez-Tato, M. P.; Martinez, M. M.; Nunez-Corredoira, G. *Journal of Chemical Research-S* **1999**, 420.
- (32) Stiasni, N.; Kappe, C. O. *Arkivoc* **2002**, *8*, 71.

- (33) Alexandre, F.-R.; Berecibar, A.; Wigglesworth, R.; Besson, T. *Tetrahedron letters* **2003**, 44, 4455.
- (34) Spencer, J.; Anjum, N.; Patel, H.; Rathnam, R. P.; Verma, J. *Synlett* **2007**, 2007, 2557.
- (35) Quinn, J. F.; Bryant, C. E.; Golden, K. C.; Gregg, B. T. *Tetrahedron Letters* **2010**, 51, 786.
- (36) Piras, L.; Genesio, E.; Ghiron, C.; Taddei, M. *Synlett* **2008**, 1125.
- (37) Dal Zotto, C.; Virieux, D.; Campagne, J.-M. *Synlett* **2009**, 0276.
- (38) James, S. L.; Adams, C. J.; Bolm, C.; Braga, D.; Collier, P.; Friscic, T.; Grepioni, F.; Harris, K. D. M.; Hyett, G.; Jones, W.; Krebs, A.; Mack, J.; Maini, L.; Orpen, A. G.; Parkin, I. P.; Shearouse, W. C.; Steed, J. W.; Waddell, D. C. *Chemical Society Reviews* **2012**, 41, 413.
- (39) Friscic, T.; Reid, D. G.; Halasz, I.; Stein, R. S.; Dinnebier, R. E.; Duer, M. J. *Angew. Chem., Int. Ed.* **2010**, 49, 712.
- (40) Sepelak, V.; Duevel, A.; Wilkening, M.; Becker, K.-D.; Heitjans, P. *Chem. Soc. Rev.* **2013**, 42, 7507.
- (41) Balaz, P.; Achimovicova, M.; Balaz, M.; Billik, P.; Cherkezova-Zheleva, Z.; Criado, J. M.; Delogu, F.; Dutkova, E.; Gaffet, E.; Gotor, F. J.; Kumar, R.; Mitov, I.; Rojac, T.; Senna, M.; Streletsii, A.; Wieczorek-Ciurawa, K. *Chem. Soc. Rev.* **2013**, 42, 7571.
- (42) Declerck, V.; Nun, P.; Martinez, J.; Lamaty, F. *Angew. Chem., Int. Ed.* **2009**, 48, 9318.
- (43) Strukil, V.; Igrec, M. D.; Eckert-Maksic, M.; Friscic, T. *Chemistry-a European Journal* **2012**, 18, 8464.
- (44) Stolle, A.; Szuppa, T.; Leonhardt, S. E. S.; Ondruschka, B. *Chem. Soc. Rev.* **2011**, 40, 2317.
- (45) Schneider, F.; Szuppa, T.; Stolle, A.; Ondruschka, B.; Hopf, H. *Green Chem.* **2009**, 11, 1894.
- (46) Suryanarayana, C. *Progress in Materials Science* **2001**, 46, 1.
- (47) Bruckmann, A.; Krebs, A.; Bolm, C. *Green Chem.* **2008**, 10, 1131.
- (48) Burmeister, C. F.; Kwade, A. *Chem. Soc. Rev.* **2013**, 42, 7660.
- (49) Friscic, T.; Childs, S. L.; Rizvi, S. A. A.; Jones, W. *CrystEngComm* **2009**, 11, 418.
- (50) Baig, R. B. N.; Varma, R. S. *Chem. Soc. Rev.* **2012**, 41, 1559.
- (51) Braga, D.; Curzi, M.; Johansson, A.; Polito, M.; Rubini, K.; Grepioni, F. *Angew. Chem., Int. Ed.* **2006**, 45, 142.
- (52) Takacs, L. *Journal of Thermal Analysis and Calorimetry* **2007**, 90, 81.
- (53) Solsona, P.; Doppiu, S.; Spassov, T.; Surinach, S.; Baro, M. D. *Journal of Alloys and Compounds* **2004**, 381, 66.
- (54) Escobedo, C. A. C.; Jesus, F. S. d.; Miro, A. M. B.; Munoz-Saldana, J. In *Physica Status Solidi C - Current Topics in Solid State Physics, Vol 4, No 11*; Ulloa, S. E., Prieto, P. P., Eds. 2007; Vol. 4, p 4054.
- (55) Nachbaur, V.; Tauvel, G.; Verdier, T.; Jean, M.; Juraszek, J.; Houvet, D. *Journal of Alloys and Compounds* **2009**, 473, 303.
- (56) Kaupp, G.; Naimi-Jamal, M. R.; Schmeyers, J. *Tetrahedron* **2003**, 59, 3753.
- (57) Nun, P.; Martin, C.; Martinez, J.; Lamaty, F. *Tetrahedron* **2011**, 67, 8187.
- (58) Gawande, M. B.; Bonifacio, V. D. B.; Luque, R.; Branco, P. S.; Varma, R. S. *ChemSusChem* **2014**, 7, 24.
- (59) Hernandez, J. G.; Juaristi, E. *J. Org. Chem.* **2010**, 75, 7107.
- (60) Delgado, R.; Felix, V.; Lima, L. M. P.; Price, D. W. *Dalton Trans.* **2007**, 2734.
- (61) Liang, X.; Sadler, P. J. *Chem. Soc. Rev.* **2004**, 33, 246.
- (62) Caravan, P.; Ellison, J. J.; McMurry, T. J.; Lauffer, R. B. *Chem. Rev. (Washington, D. C.)* **1999**, 99, 2293.
- (63) Ozay, H.; Ulgen, A.; Baran, Y. *Wuji Huaxue Xuebao* **2012**, 28, 1680.
- (64) Mewis, R. E.; Archibald, S. J. *Coordination Chemistry Reviews* **2010**, 254, 1686.

- (65) Cabbiness, D. K.; Margerum, D. W. *J. Amer. Chem. Soc.* **1969**, *91*, 6540.
- (66) Price, E. W.; Orvig, C. *Chem. Soc. Rev.* **2014**, *43*, 260.
- (67) Bianchi, A.; Calabi, L.; Corana, F.; Fontana, S.; Losi, P.; Maiocchi, A.; Paleari, L.; Valtancoli, B. *Coord. Chem. Rev.* **2000**, *204*, 309.
- (68) Reany, O.; Gunnlaugsson, T.; Parker, D. *Chem. Commun. (Cambridge)* **2000**, 473.
- (69) Froidevaux, S.; Eberle, A. N.; Christe, M.; Sumanovski, L.; Heppeler, A.; Schmiti, J. S.; Eisenwiener, K.; Beglinger, C.; Macke, H. R. *Int. J. Cancer* **2002**, *98*, 930.
- (70) Ali, M.; Zilbermann, I.; Cohen, H.; Shames, A. I.; Meyerstein, D. *Inorg. Chem.* **1996**, *35*, 5127.
- (71) Wiener, E. C.; Abadjian, M.-C.; Sengar, R.; Vander Elst, L.; Van Niekerk, C.; Grotjahn, D. B.; Leung, P. Y.; Schulte, C.; Moore, C. E.; Rheingold, A. L. *Inorg. Chem.* **2014**, Ahead of Print.
- (72) Fisher, C. M.; Fuller, E.; Burke, B. P.; Mogilireddy, V.; Pope, S. J. A.; Sparke, A. E.; Dechamps-Olivier, I.; Cadiou, C.; Chuburu, F.; Faulkner, S.; Archibald, S. J. *Dalton Trans.* **2014**, *43*, 9567.
- (73) Schwarzenbach, G. *Helv. Chim. Acta* **1952**, *35*, 2344.
- (74) Hubin, T. J. *Coord. Chem. Rev.* **2003**, *241*, 27.
- (75) Hancock, R. D.; Dobson, S. M.; Evers, A.; Wade, P. W.; Ngwenya, M. P.; Boeyens, J. C. A.; Wainwright, K. P. *J. Am. Chem. Soc.* **1988**, *110*, 2788.
- (76) Wainwright, K. P. *Inorg. Chem.* **1980**, *19*, 1396.
- (77) Weisman, G. R.; Rogers, M. E.; Wong, E. H.; Jasinski, J. P.; Paight, E. S. *J. Am. Chem. Soc.* **1990**, *112*, 8604.
- (78) Ramasubbu, A.; Wainwright, K. P. *J. Chem. Soc., Chem. Commun.* **1982**, 277.
- (79) Ronconi, L.; Sadler, P. J. *Coord. Chem. Rev.* **2007**, *251*, 1633.
- (80) Thompson, K. H.; Orvig, C. *Dalton Trans.* **2006**, 761.
- (81) Storr, T.; Thompson, K. H.; Orvig, C. *Chem. Soc. Rev.* **2006**, *35*, 534.
- (82) Caravan, P. *Acc. Chem. Res.* **2009**, *42*, 851.
- (83) Fisher, C. M.; Fuller, E.; Burke, B. P.; Mogilireddy, V.; Pope, S. J. A.; Sparke, A. E.; Dechamps-Olivier, I.; Cadiou, C.; Chuburu, F.; Faulkner, S.; Archibald, S. J. *Dalton Trans.* **2014**, *43*, 9567.
- (84) Tropiano, M.; Record, C. J.; Morris, E.; Rai, H. S.; Allain, C.; Faulkner, S. *Organometallics* **2012**, *31*, 5673.
- (85) New, E. J.; Parker, D.; Smith, D. G.; Walton, J. W. *Current Opinion in Chemical Biology* **2010**, *14*, 238.
- (86) Breeman, W. A. P.; de Blois, E.; Chan, H. S.; Konijnenberg, M.; Kwekkeboom, D. J.; Krenning, E. P. *Seminars in Nuclear Medicine* **2011**, *41*, 314.
- (87) Ambrosini, V.; Nanni, C.; Zompatori, M.; Campana, D.; Tomassetti, P.; Castellucci, P.; Allegri, V.; Rubello, D.; Montini, G.; Franchi, R.; Fanti, S. *European Journal of Nuclear Medicine and Molecular Imaging* **2010**, *37*, 722.
- (88) Franz, J.; Volkert, W. A.; Barefield, E. K.; Holmes, R. A. *Nuclear Medicine and Biology* **1987**, *14*, 569.
- (89) Troutner, D. E.; Simon, J.; Ketring, A. R.; Volkert, W.; Holmes, R. A. *Journal of Nuclear Medicine* **1980**, *21*, 443.
- (90) Jensen, A. I.; Binderup, T.; Kumar, P. E. K.; Kjaer, A.; Rasmussen, P. H.; Andresen, T. L. *Biomacromolecules* **2014**, *15*, 1625.
- (91) Yapp, D. T. T.; Ferreira, C. L.; Gill, R. K.; Boros, E.; Wong, M. Q.; Mandel, D.; Jurek, P.; Kiefer, G. E. *Molecular Imaging* **2013**, *12*, 263.

- (92) Smith, R.; Huskens, D.; Daelemans, D.; Mewis, R. E.; Garcia, C. D.; Cain, A. N.; Freeman, T. N. C.; Pannecouque, C.; De Clercq, E.; Schols, D.; Hubin, T. J.; Archibald, S. J. *Dalton Trans.* **2012**, 41, 11369.
- (93) Khan, A.; Silversides, J. D.; Madden, L.; Greenman, J.; Archibald, S. J. *Chem. Commun. (Cambridge, U. K.)* **2007**, 416.
- (94) Amoyaw, P. N. A.; Pham, K.; Cain, A. N.; McClain, J. M.; Hubin, T. J.; Khan, M. O. F. *Current Organic Synthesis* **2014**, 11, 916.
- (95) Hubin, T. J.; Amoyaw, P. N. A.; Roewe, K. D.; Simpson, N. C.; Maples, R. D.; Carder Freeman, T. N.; Cain, A. N.; Le, J. G.; Archibald, S. J.; Khan, S. I.; Tekwani, B. L.; Khan, M. O. F. *Bioorg. Med. Chem.* **2014**, 22, 3239.
- (96) Hubin, T. J.; McCormick, J. M.; Collinson, S. R.; Buchalova, M.; Perkins, C. M.; Alcock, N. W.; Kahol, P. K.; Raghunathan, A.; Busch, D. H. *J. Am. Chem. Soc.* **2000**, 122, 2512.
- (97) He, H. T.; Yin, G.; Hiler, G.; Kitko, D.; Carter, J. D.; Scheper, W. M.; Day, V.; Busch, D. H. *J. Coord. Chem.* **2008**, 61, 45.
- (98) Busch, D. H. *Chem. Rev.* **1993**, 93, 847.
- (99) Garcia-Sanchez, M. A.; Rojas-Gonzalez, F.; Menchaca-Campos, E. C.; Tello-Solis, S. R.; Quiroz-Segoviano, R. I. Y.; Diaz-Alejo, L. A.; Salas-Banales, E.; Campero, A. *Molecules* **2013**, 18, 588.
- (100) Garrison, J. M.; Bruce, T. C. *J. Am. Chem. Soc.* **1989**, 111, 191.
- (101) Bencini, A.; Bianchi, A.; Borselli, A.; Chimichi, S.; Ciampolini, M.; Dapporto, P.; Micheloni, M.; Nardi, N.; Paoli, P.; Valtancoli, B. *Inorg. Chem.* **1990**, 29, 3282.
- (102) Ciampolini, M.; Micheloni, M.; Vizza, F.; Zanobini, F.; Chimichi, S.; Dapporto, P. *J. Chem. Soc., Dalton Trans.* **1986**, 505.
- (103) Sun, X.; Wuest, M.; Weisman, G. R.; Wong, E. H.; Reed, D. P.; Boswell, C. A.; Motekaitis, R.; Martell, A. E.; Welch, M. J.; Anderson, C. J. *J. Med. Chem.* **2002**, 45, 469.
- (104) Collinson, S.; Alcock, N. W.; Raghunathan, A.; Kahol, P. K.; Busch, D. H. *Inorg. Chem.* **2000**, 39, 757.
- (105) Mewis, R. E.; Archibald, S. J. *Coord. Chem. Rev.* **2010**, 254, 1686.
- (106) Delgado, R.; Felix, V.; Lima, L. M. P.; Price, D. W. *Dalton Transactions* **2007**, 2734.
- (107) Archibald, S. J. *Annu. Rep. Prog. Chem., Sect. A: Inorg. Chem.* **2011**, 107, 274.
- (108) Anderson, C. J.; Welch, M. J. *Chem. Rev. (Washington, D. C.)* **1999**, 99, 2219.
- (109) Jones-Wilson, T. M.; Deal, K. A.; Anderson, C. J.; McCarthy, D. W.; Kovacs, Z.; Motekaitis, R. J.; Sherry, A. D.; Martell, A. E.; Welch, M. J. *Nucl. Med. Biol.* **1998**, 25, 523.
- (110) Kukis, D. L.; Diril, H.; Greiner, D. P.; DeNardo, S. J.; DeNardo, G. L.; Salako, Q. A.; Meares, C. F. *Cancer (Philadelphia)* **1994**, 73, 779.
- (111) Meggers, E. *Chem. Commun. (Cambridge, U. K.)* **2009**, 1001.
- (112) De, C. E.; Yamamoto, N.; Pauwels, R.; Balzarini, J.; Witvrouw, M.; De, V. K.; Debyser, Z.; Rosenwirth, B.; Peichl, P.; Datema, R. *Antimicrob Agents Chemother* **1994**, 38, 668.
- (113) Khan, A.; Nicholson, G.; Greenman, J.; Madden, L.; McRobbie, G.; Pannecouque, C.; De Clercq, E.; Ullom, R.; Maples, D. L.; Maples, R. D. *Journal of the American Chemical Society* **2009**, 131, 3416.
- (114) Parker, D. *Chem. Soc. Rev.* **1990**, 19, 271.
- (115) Liu, S.; Edwards, D. S. *Bioconjugate Chem.* **2001**, 12, 7.
- (116) Fichna, J.; Janecka, A. *Bioconjugate Chem.* **2003**, 14, 3.
- (117) Li, Z.; Conti, P. S. *Adv. Drug Delivery Rev.* **2010**, 62, 1031.
- (118) Valko, M.; Morris, H.; Cronin, M. T. D. *Curr. Med. Chem.* **2005**, 12, 1161.
- (119) Zalutsky, M. R.; Vaidyanathan, G. *Curr. Pharm. Des.* **2000**, 6, 1433.

- (120) Philpott, G. W.; Schwarz, S. W.; Anderson, C. J.; Dehdashti, F.; Connett, J. M.; Zinn, K. R.; Meares, C. F.; Cutler, P. D.; Welch, M. J.; Siegel, B. A. *J Nucl Med* **1995**, *36*, 1818.
- (121) Hughes, O. D. M.; Bishop, M. C.; Perkins, A. C.; Frier, M.; Price, M. R.; Denton, G.; Smith, A.; Rutherford, R.; Schubiger, P. A. *Eur. J. Nucl. Med.* **1997**, *24*, 439.
- (122) Bhattacharyya, S.; Dixit, M. *Dalton Trans.* **2011**, *40*, 6112.
- (123) He, P.; Haswell, S. J.; Pamme, N.; Archibald, S. J. *Appl. Radiat. Isot.* **2014**, *91*, 64.
- (124) Burke, B. P.; Clemente, G. S.; Archibald, S. J. *Contrast Media Mol. Imaging* **2015**, *10*, 96.
- (125) Burke, B. P.; Clemente, G. S.; Archibald, S. J. *J. Labelled Compd. Radiopharm.* **2014**, *57*, 239.
- (126) Khan, A.; Greenman, J.; Archibald, S. J. *Curr Med Chem* **2007**, *14*, 2257.
- (127) Takano, A. *Curr. Pharm. Des.* **2010**, *16*, 371.
- (128) Murphy, P. S.; McCarthy, T. J.; Dzik-Jurasz, A. S. K. *Br. J. Radiol.* **2008**, *81*, 685.
- (129) Serdons, K.; Verbruggen, A.; Bormans, G. M. *Methods (Amsterdam, Neth.)* **2009**, *48*, 104.
- (130) Shokeen, M.; Fettig, N. M.; Rossin, R. *Q J Nucl Med Mol Imaging* **2008**, *52*, 267.
- (131) Knight, J. C.; Wuest, M.; Saad, F. A.; Wang, M.; Chapman, D. W.; Jans, H.-S.; Lapi, S. E.; Kariuki, B. M.; Amoroso, A. J.; Wuest, F. *Dalton Trans.* **2013**, *42*, 12005.
- (132) Liu, S.; Kim, Y.-S.; Wang, L.; Shi, J.; Yang, C.-T.; American Chemical Society: 2008, p INOR.
- (133) Cole, W. C.; DeNardo, S. J.; Meares, C. F.; McCall, M. J.; DeNardo, G. L.; Epstein, A. L.; O'Brien, H. A.; Moi, M. K. *Int J Rad Appl Instrum B* **1986**, *13*, 363.
- (134) Cole, W. C.; DeNardo, S. J.; Meares, C. F.; McCall, M. J.; DeNardo, G. L.; Epstein, A. L.; O'Brien, H. A.; Moi, M. K. *J. Nucl. Med.* **1987**, *28*, 83.
- (135) Wadas, T. J.; Wong, E. H.; Weisman, G. R.; Anderson, C. J. *Curr. Pharm. Des.* **2007**, *13*, 3.
- (136) Pandya, D. N.; Dale, A. V.; Kim, J. Y.; Lee, H.; Ha, Y. S.; An, G. I.; Yoo, J. *Bioconjugate Chem.* **2012**, *23*, 330.
- (137) Silversides, J. D.; Allan, C. C.; Archibald, S. J. *Dalton Trans.* **2007**, 971.
- (138) Bencini, A.; Bianchi, A.; Bazzicalupi, C.; Ciampolini, M.; Fusi, V.; Micheloni, M.; Nardi, N.; Paoli, P.; Valtancoli, B. *Supramol. Chem.* **1994**, *3*, 141.
- (139) Wong, E. H.; Weisman, G. R.; Hill, D. C.; Reed, D. P.; Rogers, M. E.; Condon, J. S.; Fagan, M. A.; Calabrese, J. C.; Lam, K.-C.; Guzei, I. A.; Rheingold, A. L. *J. Am. Chem. Soc.* **2000**, *122*, 10561.
- (140) Boswell, C. A.; Sun, X.; Niu, W.; Weisman, G. R.; Wong, E. H.; Rheingold, A. L.; Anderson, C. J. *J. Med. Chem.* **2004**, *47*, 1465.
- (141) Hubin, T. J.; Alcock, N. W.; Seib, L. L.; Busch, D. H. *Inorg. Chem.* **2002**, *41*, 7006.
- (142) Kimura, E. *Pure Appl. Chem.* **1993**, *65*, 355.
- (143) Silversides, J. D.; Burke, B. P.; Archibald, S. J. *Comptes Rendus Chimie* **2013**, *16*, 524.
- (144) Silversides, J. D. *thesis* **2006**.
- (145) Weisman, G. R.; Wong, E. H.; Hill, D. C.; Rogers, M. E.; Reed, D. P.; Calabrese, J. C. *Chem. Commun. (Cambridge)* **1996**, 947.
- (146) Silversides, J. D. *thesis*, HULL, 2006.
- (147) Rohovec, J.; Gyepes, R.; Cisarova, I.; Rudovsky, J.; Lukes, I. *Tetrahedron Lett.* **2000**, *41*, 1249.
- (148) Smith, R.; Huskens, D.; Daelemans, D.; Mewis, R. E.; Garcia, C. D.; Cain, A. N.; Freeman, T. N. C.; Pannecouque, C.; De Clercq, E.; Schols, D.; Hubin, T. J.; Archibald, S. J. *Dalton Transactions* **2012**, *41*, 11369.
- (149) Lewis, E. A.; Boyle, R. W.; Archibald, S. J. *Chem. Commun. (Cambridge, U. K.)* **2004**, 2212.
- (150) Pandya, D. N.; Bhatt, N.; An, G. I.; Ha, Y. S.; Soni, N.; Lee, H.; Lee, Y. J.; Kim, J. Y.; Lee, W.; Ahn, H.; Yoo, J. *J. Med. Chem.* **2014**, *57*, 7234.

- (151) Aue, W.; Bartholdi, E.; Ernst, R. R. *The Journal of Chemical Physics* **1976**, 64, 2229.
- (152) Abdulwahaab, B. H.; Burke, B. P.; Domarkas, J.; Silversides, J. D.; Prior, T. J.; Archibald, S. J. *The Journal of organic chemistry* **2015**.
- (153) Denat, F.; Lacour, S.; Brandes, S.; Guillard, R. *Tetrahedron Lett.* **1997**, 38, 4417.
- (154) Bernier, N.; Allali, M.; Tripier, R.; Conan, F.; Patinec, V.; Develay, S.; Le Baccon, M.; Handel, H. *New J. Chem.* **2006**, 30, 435.
- (155) Kolinski, R. A. *Pol. J. Chem.* **1995**, 69, 1039.
- (156) Setamdideh, D.; Khezri, B.; Mollapour, M. *Orient. J. Chem.* **2011**, 27, 991.
- (157) Hanaya, K.; Muramatsu, T.; Kudo, H.; Chow, Y. L. *J. Chem. Soc., Perkin Trans. 1* **1979**, 2409.
- (158) Lalancette, J. M.; Freche, A.; Brindel, J. R.; Laliberte, M. *Synthesis* **1972**, 526.
- (159) Hubin, T. J.; McCormick, J. M.; Collinson, S. R.; Busch, D. H.; Alcock, N. W. *Chem. Commun. (Cambridge)* **1998**, 1675.
- (160) Boiocchi, M.; Bonizzoni, M.; Fabbrizzi, L.; Foti, F.; Licchelli, M.; Poggi, A.; Taglietti, A.; Zema, M. *Chem. - Eur. J.* **2004**, 10, 3209.
- (161) Camus, N.; Halime, Z.; Le Bris, N.; Bernard, H.; Platas-Iglesias, C.; Tripier, R. *J. Org. Chem.* **2014**, 79, 1885.
- (162) P. D. Moore, J. A. W. a. M. E. C. *Oxford: Blackwell Scientific Publications* **1991**, pp 216
- (163) Harley, R. K. a. M. *London: Papadakis* **2004**, pp 264.
- (164) Zetzsche, F.; Huggler, K. *Justus Liebigs Ann. Chem.* **1928**, 461, 89.
- (165) Webb, P. D. M. a. J. A. *Hodder & Stoughton, London* **1978**, pp 133.
- (166) Wiermann, R.; Gubatz, S. *Int. Rev. Cytol.* **1992**, 140, 35.
- (167) MAEDA, Y. *Microbiology* **1985**, 131, 201.
- (168) de Souza, S. P.; Bassut, J.; Marquez, H. V.; Junior, I. I.; Miranda, L. S.; Huang, Y.; Mackenzie, G.; Boa, A. N.; de Souza, R. O. *Catalysis Science & Technology* **2015**, 5, 3130.
- (169) Shaw, G.; Yeadon, A. *Grana* **1964**, 5, 247.
- (170) Punt, W.; Hoen, P.; Blackmore, S.; Nilsson, S.; Le Thomas, A. *Review of Palaeobotany and Palynology* **2007**, 143, 1.
- (171) John, J. J. *Chem. Phys* **1814**, 12, 244.
- (172) Zetzsche, F.; Kälin, O. *Helvetica Chimica Acta* **1931**, 14, 517.
- (173) Zetzsche, F.; Kalt, P.; Liechti, J.; Ziegler, E. *Journal für Praktische Chemie* **1937**, 148, 267.
- (174) Brooks, J.; Shaw, G. **1968**.
- (175) Barrier, S., University of Hull, 2008.
- (176) Brooks, J.; Shaw, G. *Grana* **1978**, 17, 91.
- (177) Dominguez, E.; Mercado, J. A.; Quesada, M. A.; Heredia, A. *Sex. Plant Reprod.* **1999**, 12, 171.
- (178) Hesse, M.; Waha, M. *Plant Systematics and Evolution* **1989**, 163, 147.
- (179) Shaw, G.; Yeadon, A. *J. Chem. Soc. C* **1966**, 16.
- (180) Brooks, J.; Shaw, G. *Chemical Geology* **1972**, 10, 69.
- (181) Diego-Taboada, A.; Beckett, S. T.; Atkin, S. L.; MacKenzie, G. *Pharmaceutics* **2014**, 6, 80.
- (182) Domínguez, E.; Mercado, J. A.; Quesada, M. A.; Heredia, A. *Sexual Plant Reproduction* **1999**, 12, 171.
- (183) Zetzsche, F.; Kalt, P.; Liechti, J.; Ziegler, E. *J. Prakt. Chem. (Leipzig)* **1937**, 148, 267.
- (184) J. Brooks and G. Shaw *Origin and development of living systems* Academic Press London and New York., 1973.
- (185) WITTBORN, J.; Rao, K.; El-Ghazaly, G.; Rowley, J. *Annals of Botany* **1998**, 82, 141.
- (186) Böhne, G.; Richter, E.; Woehlecke, H.; Ehwald, R. *Annals of botany* **2003**, 92, 289.
- (187) Rowley, J. R.; Skvarla, J. J.; El-Ghazaly, G. *Canadian journal of botany* **2003**, 81, 1070.

- (188) Zetzsche, F.; Kalin, O. *Helv. Chim. Acta* **1931**, 14, 517.
- (189) Zetzsche, F.; Vicari, H. *Helvetica Chimica Acta* **1931**, 14, 62.
- (190) Guilford, W. J.; Schneider, D. M.; Labovitz, J.; Opella, S. J. *Plant Physiol.* **1988**, 86, 134.
- (191) Apperley, G. S. D. C. *Grana* **1996**, 35, 125.
- (192) Amer, M. S.; Tawashi, R.; Google Patents: 1991.
- (193) Amer, M. S.; Tawashi, R.; Google Patents: 1994.
- (194) Tawashi, R.; Google Patents: 1997.
- (195) Schulze Osthoff, K.; Wiermann, R. *Journal of Plant Physiology* **1987**, 131, 5.
- (196) Loewus, F. A.; Baldi, B. G.; Franceschi, V. R.; Meinert, L. D.; McCollum, J. J. *Plant Physiology* **1985**, 78, 652.
- (197) Tarlyn, N. M.; Franceschi, V. R.; Everard, J. D.; Loewus, F. A. *Plant Science* **1993**, 90, 219.
- (198) Atkin, S. L. *APPLICATION FOR THE APPROVAL OF SPOROPOLLENIN EXINE CAPSULES FROM LYCOPODIUM CLAVATUM SPORES*; Sporomex Ltd: 11 Newland Avenue, Drifffield, East Yorkshire, YO25 6TX, 2013
- (199) Shaw, G.; Apperley, D. C. *Grana* **1996**, 35, 125.
- (200) Domínguez, E.; Mercado, J. A.; Quesada, M. A.; Heredia, A. *Grana* **1998**, 37, 93.
- (201) Hamad, S. A. *NOVEL TECHNIQUES FOR MICROENCAPSULATION OF PROBIOTIC BACTERIA*; University of Hull: Hull, UK, 2012.
- (202) Hamad, S. A.; Dyab, A. F. K.; Stoyanov, S. D.; Paunov, V. N. *Journal of Materials Chemistry* **2011**, 21, 18018.
- (203) Shaw, G.; Sykes, M.; Humble, R. W.; Mackenzie, G.; Marsden, D.; Pehlivan, E. *Reactive Polymers, Ion Exchangers, Sorbents* **1988**, 9, 211.
- (204) Adamson, R.; Gregson, S.; Shaw, G. *International Journal of Peptide and Protein Research* **1983**, 22, 560.
- (205) Pehlivan, E.; Ersoz, M.; Yildiz, S.; Duncan, H. J. *Separation Science and Technology* **1994**, 29, 1757.
- (206) Havinga, A. J. *Pollen et Spores* **1984**, 26, 541.
- (207) Wilson, N.; Shah, N. *ASEAN Food Journal* **2007**, 14, 1.
- (208) Paunov, V. N.; Mackenzie, G.; Stoyanov, S. D. *Journal of Materials Chemistry* **2007**, 17, 609.
- (209) Wakil, A.; Mackenzie, G.; Diego-Taboada, A.; Bell, J. G.; Atkin, S. L. *Lipids* **2010**, 45, 645.
- (210) Diego-Taboada, A.; Cousson, P.; Raynaud, E.; Huang, Y.; Lorch, M.; Binks, B. P.; Queneau, Y.; Boa, A. N.; Atkin, S. L.; Beckett, S. T.; MacKenzie, G. J. *Mater. Chem.* **2012**, 22, 9767.
- (211) Brannon-Peppas, L. *Medical Plastic and Biomaterials* **1997**, 4, 34.
- (212) Ranade, V. V. *The Journal of Clinical Pharmacology* **1990**, 30, 107.
- (213) Diego-Taboada, A.; Maillet, L.; Banoub, J. H.; Lorch, M.; Rigby, A. S.; Boa, A. N.; Atkin, S. L.; Mackenzie, G. J. *Mater. Chem. B* **2013**, 1, 707.
- (214) Alshehri, S. M.; Al-Lohedan, H. A.; Chaudhary, A. A.; Al-Farraj, E.; Alhokbany, N.; Issa, Z.; Alhousine, S.; Ahamad, T. *European Journal of Pharmaceutical Sciences* **2016**.
- (215) Banerjee, J.; Biswas, S.; Madhu, N. R.; Karmakar, S. R.; Biswas, S. J. *J. Pharmacogn. Phytochem.* **2014**, 3, 207.
- (216) Kremp, G. O. W. *Lycopodium clavatum." in The spores of the Pteridophytes.* ; Hirokawa: Tokyo, 1972.
- (217) Paunov, V. N.; Mackenzie, G.; Stoyanov, S. D. *J. Mater. Chem.* **2007**, 17, 609.
- (218) Barrier, S., University of Hull, 2008.
- (219) Baytop, T. *Therapy with medicinal plants in Turkey (past and present)*; edition second ed.; Nobel Tip Kitabevleri: Istanbul, 1999.

- (220) El-Juhany, L. I. *Australian Journal of Basic and Applied Sciences* **2010**, 4, 3998.
- (221) El Hadrami, A.; El Idrissi-Tourane, A.; El Hassni, M.; Daayf, F.; El Hadrami, I. C. R. *Biol.* **2005**, 328, 732.
- (222) Askari, E.; Al-Khalifa, N. S.; Ohmura, T.; Al-Hafedh, Y. S.; Khan, F. A.; Al-Hindi, A.; Okawara, R. *Pak. J. Bot.* **2003**, 35, 323.
- (223) Al-Hooti, S.; Sidhu, J. S.; Qabazard, H. *Plant Foods Hum. Nutr. (Dordrecht, Neth.)* **1997**, 50, 101.
- (224) Chao, C. T.; Krueger, R. R. *HortScience* **2007**, 42, 1077.
- (225) van Bergen, P. F.; Blokker, P.; Collinson, M. E.; Sinninghe Damsté, J.; de Leeuw, J. W. *Evolution of plant physiology. Elsevier, Amsterdam* **2004**, 133.
- (226) Guilford, W. J.; Schneider, D. M.; Labovitz, J.; Opella, S. J. *Plant Physiology* **1988**, 86, 134.
- (227) Hemsley, A. *Cour. Forschungsinst. Senckenberg* **1992**, 147, 93.
- (228) Hemsley, A. R.; Barrie, P. J.; Chaloner, W. G.; Scott, A. C. *Grana* **1993**, 32, 2.
- (229) HEMSLEY, A. R.; JENKINS, P. D.; COLLINSON, M. E.; VINCENT, B. *Botanical Journal of the Linnean Society* **1996**, 121, 177.
- (230) Barrier, S.; Löbbert, A.; Boasman, A. J.; Boa, A. N.; Lorch, M.; Atkin, S. L.; Mackenzie, G. *Green Chemistry* **2010**, 12, 234.
- (231) Lambert, J. B.; Shurvell, H. F.; Lightner, D. A.; Cooks, R. G. *Introduction to Organic Spectroscopy. New York: Macmillan Publishing Company* **1987**, 169.
- (232) Williams, D.; Fleming, I.; Pretsch, E. *Organic Chemistry* **1989**.
- (233) Booth, H.; Wiley Online Library: 1992.
- (234) Joseph, B. L.; Shurvell, H.; Lightner, D.; Cooks, R.; Macmillan Publishing Company, New York: 1987.
- (235) Lin, J.; Kamat, A.; Gu, J.; Chen, M.; Dinney, C. P.; Forman, M. R.; Wu, X. *Cancer Epidemiology Biomarkers & Prevention* **2009**, 18, 2090.
- (236) Mengesha, A. E.; Youan, B.-B. C. *Journal of nutritional science and vitaminology* **2010**, 56, 311.
- (237) Bouallagui, Z.; Han, J.; Isoda, H.; Sayadi, S. *Food and chemical toxicology* **2011**, 49, 179.
- (238) Johnson, R.; Bryant, S.; Huntley, A. L. *Maturitas* **2012**, 73, 280.
- (239) Laszczyk, M. N. *Planta medica* **2009**, 75, 1549.
- (240) Efferth, T.; Li, P. C.; Konkimalla, V. S. B.; Kaina, B. *Trends in molecular medicine* **2007**, 13, 353.
- (241) Bapat, K.; Chintalwar, G.; Pandey, U.; Thakur, V.; Sarma, H.; Samuel, G.; Pillai, M.; Chattopadhyay, S.; Venkatesh, M. *Applied Radiation and Isotopes* **2005**, 62, 389.
- (242) Engelmann, N. J.; Reppert, A.; Yousef, G.; Rogers, R. B.; Lila, M. A. *Plant Cell, Tissue and Organ Culture (PCTOC)* **2009**, 98, 147.
- (243) Cekic, B.; Kilcar, A. Y.; Muftuler, F. Z. B.; Unak, P.; Medine, E. I. *Acta Cirúrgica Brasileira* **2012**, 27, 294.
- (244) Ozkan, M.; Muftuler, F.; Kilcar, A. Y.; Medine, E.; Unak, P. *Radiochimica Acta* **2013**, 101, 585.
- (245) Kilcar, A. Y.; Cekic, B.; Muftuler, F. Z. B.; Unak, P.; Medine, E. I. *Journal of Radioanalytical and Nuclear Chemistry* **2013**, 295, 593.
- (246) Tekin, V.; Muftuler, F. Z. B.; Kilcar, A. Y.; Unak, P. *Journal of Radioanalytical and Nuclear Chemistry* **2014**, 302, 225.
- (247) Tekin, V.; Muftuler, F. Z. B.; Guldu, O. K.; Kilcar, A. Y.; Medine, E. I.; Yavuz, M.; Unak, P.; Timur, S. *Journal of Radioanalytical and Nuclear Chemistry* **2015**, 303, 701.

- (248) Muftuler, F. Z. B.; Kilcar, A. Y.; Unak, P. *Journal of Radioanalytical and Nuclear Chemistry* **2015**, 306, 1.
- (249) Holanda, C. M. d. C. X.; Costa, M. B. d.; Silva, N. C. Z. d.; Júnior, S.; Barbosa, V. S. d. A.; Silva, R. P. d.; Medeiros, A. d. C. *Acta Cirurgica Brasileira* **2009**, 24, 383.
- (250) Sletten, E. M.; Bertozzi, C. R. *Angew. Chem., Int. Ed.* **2009**, 48, 6974.
- (251) Massoud, T. F.; Gambhir, S. S. *Genes & development* **2003**, 17, 545.
- (252) Waterton, J. C. *RSC Drug Discovery Ser.* **2012**, 15, 1.
- (253) Niu, G.; Chen, X. *Drug delivery (London, England. 2007)* **2009**, 3, 109.
- (254) Willmann, J. K.; van Bruggen, N.; Dinkelborg, L. M.; Gambhir, S. S. *Nature Reviews Drug Discovery* **2008**, 7, 591.
- (255) Chakravarty, R.; Hong, H.; Cai, W. *Molecular pharmaceuticals* **2014**, 11, 3777.
- (256) Ametamey, S. M.; Honer, M.; Schubiger, P. A. *Chemical reviews* **2008**, 108, 1501.
- (257) Kaden, T. A. *Dalton Trans.* **2006**, 3617.
- (258) Lankveld, D. P.; Rayavarapu, R. G.; Krystek, P.; Oomen, A. G.; Verharen, H. W.; Van Leeuwen, T. G.; De Jong, W. H.; Manohar, S. *Nanomedicine* **2011**, 6, 339.
- (259) Ohno, K.; Akashi, T.; Tsujii, Y.; Yamamoto, M.; Tabata, Y. *Biomacromolecules* **2012**, 13, 927.
- (260) Zhao, X.; Zhao, H.; Chen, Z.; Lan, M. *Journal of nanoscience and nanotechnology* **2014**, 14, 210.
- (261) Liu, X.; Tao, H.; Yang, K.; Zhang, S.; Lee, S.-T.; Liu, Z. *Biomaterials* **2011**, 32, 144.
- (262) Orhan, I.; Kupeli, E.; Sener, B.; Yesilada, E. *J Ethnopharmacol* **2007**, 109, 146.
- (263) Pathak, S.; Banerjee, A.; Paul, S.; Khuda-Bukhsh, A. R. *Indian journal of experimental biology* **2009**, 47, 602.
- (264) Ma, X.; Gang, D. R. *Natural product reports* **2004**, 21, 752.
- (265) Durdun, C.; Papuc, C.; Crivineanu, M.; Nicorescu, V. *Scientific Works-University of Agronomical Sciences and Veterinary Medicine, Bucharest Series C, Veterinary Medicine* **2011**, 57, 61.
- (266) Barrier, S.; Diego-Taboada, A.; Thomasson, M. J.; Madden, L.; Pointon, J. C.; Wadhawan, J. D.; Beckett, S. T.; Atkin, S. L.; MacKenzie, G. J. *Mater. Chem.* **2011**, 21, 975.
- (267) Ma, H.; Zhang, P.; Wang, J.; Xu, X.; Zhang, H.; Zhang, Z.; Zhang, Y.; Ning, Y. *Journal of microencapsulation* **2014**, 31, 667.
- (268) Lorch, M.; Thomasson, M. J.; Diego-Taboada, A.; Barrier, S.; Atkin, S. L.; MacKenzie, G.; Archibald, S. J. *Chem. Commun. (Cambridge, U. K.)* **2009**, 6442.
- (269) Prakash, G. S.; Mathew, T.; Olah, G. A. *Accounts of chemical research* **2011**, 45, 565.
- (270) Oh, S.; Prasad, V.; Lee, D. S.; Baum, R. *International journal of molecular imaging* **2011**, 2011.
- (271) Baum, R. P.; Kulkarni, H. R. *Theranostics* **2012**, 2, 437.
- (272) Buchmann, I.; Henze, M.; Engelbrecht, S.; Eisenhut, M.; Runz, A.; Schäfer, M.; Schilling, T.; Haufe, S.; Herrmann, T.; Haberkorn, U. *European journal of nuclear medicine and molecular imaging* **2007**, 34, 1617.
- (273) Smith, D. L.; Breeman, W. A.; Sims-Mourtada, J. *Applied Radiation and Isotopes* **2013**, 76, 14.
- (274) Fani, M.; Andre, J. P.; Maecke, H. R. *Contrast media & molecular imaging* **2008**, 3, 53.
- (275) Sainz-Esteban, A.; Prasad, V.; Schuchardt, C.; Zachert, C.; Carril, J. M.; Baum, R. P. *European journal of nuclear medicine and molecular imaging* **2012**, 39, 501.
- (276) Prasad, V.; Ambrosini, V.; Hommann, M.; Hoersch, D.; Fanti, S.; Baum, R. P. *European journal of nuclear medicine and molecular imaging* **2010**, 37, 67.

- (277) Antunes, P.; Ginj, M.; Zhang, H.; Waser, B.; Baum, R.; Reubi, J.-C.; Maecke, H. *European journal of nuclear medicine and molecular imaging* **2007**, *34*, 982.
- (278) de Souza, S. P.; Bassut, J.; Alvarez, H. M.; Junior, I. I.; Miranda, L. S. M.; Huang, Y.; MacKenzie, G.; Boa, A. N.; de Souza, R. O. M. A. *Catal. Sci. Technol.* **2015**, *5*, 3130.
- (279) Mackenzie, G.; Shaw, G. *International Journal of Peptide and Protein Research* **1980**, *15*, 298.
- (280) Adamson, R.; Gregson, S.; Shaw, G. *Int. J. Pept. Protein Res.* **1983**, *22*, 560.
- (281) Huang, Y., University of Hull, 2013.
- (282) Stasiuk, G. J.; Long, N. J. *Chemical Communications* **2013**, *49*, 2732.
- (283) Lorian, V. *J Clin Microbiol* **1989**, *27*, 2403.
- (284) Zhang, X.-f.; Lan, L.; Chen, L.; Chen, H.-b.; Yang, Q.-f.; Li, Q.; Li, Q.-l.; Sun, X.-r.; Tang, Y.-l. *J. Phys. Org. Chem.* **2016**, *29*, 127.
- (285) Boros, E.; Bowen, A. M.; Josephson, L.; Vasdev, N.; Holland, J. P. *Chemical Science* **2015**, *6*, 225.
- (286) Burke, B. P.; Baghdadi, N.; Kownacka, A. E.; Nigam, S.; Clemente, G. S.; Al-Yassiry, M. M.; Domarkas, J.; Lorch, M.; Pickles, M.; Gibbs, P. *Nanoscale* **2015**, *7*, 14889.
- (287) Wong, R. M.; Gilbert, D. A.; Liu, K.; Louie, A. Y. *ACS nano* **2012**, *6*, 3461.
- (288) Sun, X.; Huang, X.; Yan, X.; Wang, Y.; Guo, J.; Jacobson, O.; Liu, D.; Szajek, L. P.; Zhu, W.; Niu, G. *ACS nano* **2014**, *8*, 8438.
- (289) Sun, X.; Huang, X.; Guo, J.; Zhu, W.; Ding, Y.; Niu, G.; Wang, A.; Kiesewetter, D. O.; Wang, Z. L.; Sun, S. *Journal of the American Chemical Society* **2014**, *136*, 1706.
- (290) Gawande, M. B.; Bonifacio, V. D. B.; Luque, R.; Branco, P. S.; Varma, R. S. *Chem. Soc. Rev.* **2013**, *42*, 5522.
- (291) Williams, D. B. G.; Lawton, M. *The Journal of organic chemistry* **2010**, *75*, 8351.
- (292) Smith, R. thesis, Hull, **2012**.
- (293) Oukhatar, F.; Beyler, M.; Tripier, R.; Centre National de la Recherche Scientifique CNRS , Fr.; Universite de Bretagne Occidentale . 2016, p 64pp.
- (294) Al-Zirgani, A. S. Z. thesis, Hull, **2015**.
- (295) Valks, G. C.; McRobbie, G.; Lewis, E. A.; Hubin, T. J.; Hunter, T. M.; Sadler, P. J.; Pannecouque, C.; De Clercq, E.; Archibald, S. J. *J. Med. Chem.* **2006**, *49*, 6162.

Appendices

Table A. Crystal data and structure refinement for compound 17.

Identification code	compound 17	
Empirical formula	C ₂₈ H ₄₂ Br ₂ N ₄ O	
Formula weight	610.47	
Temperature	150(2) K	
Wavelength	0.71073 Å	
Crystal system	Orthorhombic	
Space group	C 2 2 21	
Unit cell dimensions	a = 10.7048(7) Å	$\alpha = 90^\circ$.
	b = 13.9924(8) Å	$\beta = 90^\circ$.
	c = 18.8717(13) Å	$\gamma = 90^\circ$.
Volume	2826.7(3) Å ³	
Z	4	
Density (calculated)	1.434 Mg/m ³	
Absorption coefficient	2.895 mm ⁻¹	
F(000)	1264	
Crystal size	0.400 × 0.400 × 0.100 mm ³	
Theta range for data collection	2.396 to 29.282°.	
Index ranges	-14 ≤ h ≤ 14, -19 ≤ k ≤ 19, -25 ≤ l ≤ 25	
Reflections collected	10839	
Independent reflections	3821 [R(int) = 0.1380]	
Completeness to theta = 25.242°	99.9 %	
Refinement method	Full-matrix least-squares on F ²	
Data / restraints / parameters	3821 / 2 / 164	
Goodness-of-fit on F ²	0.914	
Final R indices [I > 2sigma(I)]	R1 = 0.0626, wR2 = 0.1441	
R indices (all data)	R1 = 0.0842, wR2 = 0.1532	
Absolute structure parameter	0.20(2)	
Largest diff. peak and hole	1.827 and -0.914 e.Å ⁻³	

Table B. Atomic coordinates ($\times 10^4$) and equivalent isotropic displacement parameters ($\text{\AA}^2 \times 10^3$) for **17**. U(eq) is defined as one third of the trace of the orthogonalized U^{ij} tensor.

	x	y	z	U(eq)
N(2)	1055(5)	-444(4)	6682(3)	35(1)
N(1)	907(5)	-1279(4)	8095(3)	39(1)
C(5)	1829(6)	-1294(5)	6887(4)	41(2)
C(4)	2060(6)	-1319(6)	7669(4)	45(2)
C(3)	1267(7)	-1251(6)	8845(3)	47(2)
C(2)	107(7)	-1287(6)	9299(4)	45(2)
C(1)	-746(7)	-477(5)	9108(4)	39(2)
C(6)	-169(5)	-446(5)	7104(3)	34(1)
C(7)	1727(6)	513(5)	6827(3)	35(1)
C(8)	2824(5)	718(4)	6346(4)	35(1)
C(9)	4028(6)	442(6)	6526(4)	45(2)
C(10)	5036(7)	662(6)	6081(5)	51(2)
C(11)	4862(6)	1149(5)	5453(4)	43(2)
C(12)	3644(7)	1439(5)	5278(4)	42(1)
C(13)	2654(6)	1227(6)	5721(4)	41(1)
C(14)	5941(7)	1381(6)	4968(5)	54(2)
Br(1)	6263(1)	6767(1)	8693(1)	52(1)
O(1W)	5000	8324(8)	7500	72(3)

Table D. Anisotropic displacement parameters ($\text{\AA}^2 \times 10^3$) for **17**. The anisotropic displacement factor exponent takes the form: $-2\pi^2 [h^2 a^{*2} U^{11} + 2 h k a^* b^* U^{12}]$

	U ¹¹	U ²²	U ³³	U ²³	U ¹³	U ¹²
N(2)	33(3)	36(3)	36(3)	0(2)	4(2)	2(2)
N(1)	39(3)	32(3)	45(3)	6(2)	4(2)	8(2)
C(5)	37(3)	30(3)	56(4)	-5(3)	10(3)	6(3)
C(4)	34(3)	43(4)	58(4)	10(3)	7(3)	12(3)
C(3)	41(3)	51(4)	49(4)	9(3)	2(3)	9(3)
C(2)	52(4)	42(4)	42(4)	8(3)	0(3)	8(3)
C(1)	42(3)	35(4)	40(3)	5(3)	6(3)	2(3)
C(6)	30(3)	28(3)	42(3)	-2(3)	4(2)	0(2)
C(7)	34(3)	30(3)	40(3)	0(3)	3(2)	-1(2)
C(8)	33(3)	35(3)	38(3)	0(3)	4(3)	-2(2)
C(9)	35(3)	49(4)	52(4)	8(3)	0(2)	-2(3)
C(10)	33(3)	56(5)	64(5)	5(4)	3(3)	1(3)
C(11)	43(3)	34(4)	50(4)	-1(3)	11(3)	-6(3)
C(12)	46(3)	37(3)	44(3)	5(3)	1(3)	-3(3)
C(13)	36(3)	40(4)	45(3)	0(3)	1(3)	0(3)
C(14)	47(4)	52(5)	62(4)	-3(4)	22(3)	-6(3)
Br(1)	60(1)	46(1)	51(1)	-6(1)	4(1)	-20(1)
O(1W)	41(4)	56(6)	118(8)	0	-4(4)	0

Table C. Bond lengths [Å] and angles [°] for **17**

N(2)-C(5)	1.501(9)
N(2)-C(1)#1	1.528(9)
N(2)-C(6)	1.533(8)
N(2)-C(7)	1.545(9)
N(1)-C(6)#1	1.457(8)
N(1)-C(3)	1.467(9)
N(1)-C(4)	1.474(8)
C(5)-C(4)	1.498(11)
C(5)-H(5A)	0.9900
C(5)-H(5B)	0.9900
C(4)-H(4A)	0.9900
C(4)-H(4B)	0.9900
C(3)-C(2)	1.510(10)
C(3)-H(3A)	0.9900
C(3)-H(3B)	0.9900
C(2)-C(1)	1.499(10)
C(2)-H(2A)	0.9900
C(2)-H(2B)	0.9900
C(1)-N(2)#1	1.528(9)
C(1)-H(1A)	0.9900
C(1)-H(1B)	0.9900
C(6)-N(1)#1	1.457(8)
C(6)-C(6)#1	1.539(13)
C(6)-H(6)	1.0000
C(7)-C(8)	1.511(9)
C(7)-H(7B)	0.9900
C(7)-H(7A)	0.9900
C(8)-C(9)	1.387(9)
C(8)-C(13)	1.391(10)
C(9)-C(10)	1.402(10)
C(9)-H(9)	0.9500
C(10)-C(11)	1.380(11)
C(10)-H(10)	0.9500
C(11)-C(12)	1.404(10)
C(11)-C(14)	1.507(9)

C(12)-C(13)	1.382(10)
C(12)-H(12)	0.9500
C(13)-H(13)	0.9500
C(14)-H(14A)	0.9800
C(14)-H(14B)	0.9800
C(14)-H(14C)	0.9800
O(1W)-H(1C)	0.92(2)
C(5)-N(2)-C(1)#1	110.3(6)
C(5)-N(2)-C(6)	109.7(5)
C(1)#1-N(2)-C(6)	108.8(5)
C(5)-N(2)-C(7)	112.6(5)
C(1)#1-N(2)-C(7)	107.5(5)
C(6)-N(2)-C(7)	107.9(5)
C(6)#1-N(1)-C(3)	111.7(6)
C(6)#1-N(1)-C(4)	110.1(5)
C(3)-N(1)-C(4)	107.9(5)
C(4)-C(5)-N(2)	111.3(6)
C(4)-C(5)-H(5A)	109.4
N(2)-C(5)-H(5A)	109.4
C(4)-C(5)-H(5B)	109.4
N(2)-C(5)-H(5B)	109.4
H(5A)-C(5)-H(5B)	108.0
N(1)-C(4)-C(5)	113.5(5)
N(1)-C(4)-H(4A)	108.9
C(5)-C(4)-H(4A)	108.9
N(1)-C(4)-H(4B)	108.9
C(5)-C(4)-H(4B)	108.9
H(4A)-C(4)-H(4B)	107.7
N(1)-C(3)-C(2)	109.3(6)
N(1)-C(3)-H(3A)	109.8
C(2)-C(3)-H(3A)	109.8
N(1)-C(3)-H(3B)	109.8
C(2)-C(3)-H(3B)	109.8
H(3A)-C(3)-H(3B)	108.3
C(1)-C(2)-C(3)	109.8(6)
C(1)-C(2)-H(2A)	109.7

C(3)-C(2)-H(2A)	109.7
C(1)-C(2)-H(2B)	109.7
C(3)-C(2)-H(2B)	109.7
H(2A)-C(2)-H(2B)	108.2
C(2)-C(1)-N(2)#1	112.9(6)
C(2)-C(1)-H(1A)	109.0
N(2)#1-C(1)-H(1A)	109.0
C(2)-C(1)-H(1B)	109.0
N(2)#1-C(1)-H(1B)	109.0
H(1A)-C(1)-H(1B)	107.8
N(1)#1-C(6)-N(2)	109.3(5)
N(1)#1-C(6)-C(6)#1	112.2(4)
N(2)-C(6)-C(6)#1	107.7(6)
N(1)#1-C(6)-H(6)	109.2
N(2)-C(6)-H(6)	109.2
C(6)#1-C(6)-H(6)	109.2
C(8)-C(7)-N(2)	114.9(5)
C(8)-C(7)-H(7B)	108.6
N(2)-C(7)-H(7B)	108.6
C(8)-C(7)-H(7A)	108.6
N(2)-C(7)-H(7A)	108.6
H(7B)-C(7)-H(7A)	107.5
C(9)-C(8)-C(13)	118.1(6)
C(9)-C(8)-C(7)	121.5(6)
C(13)-C(8)-C(7)	120.3(6)
C(8)-C(9)-C(10)	120.5(7)
C(8)-C(9)-H(9)	119.7
C(10)-C(9)-H(9)	119.7
C(11)-C(10)-C(9)	121.3(7)
C(11)-C(10)-H(10)	119.4
C(9)-C(10)-H(10)	119.4
C(10)-C(11)-C(12)	117.9(6)
C(10)-C(11)-C(14)	121.6(7)
C(12)-C(11)-C(14)	120.5(7)
C(13)-C(12)-C(11)	120.6(6)
C(13)-C(12)-H(12)	119.7

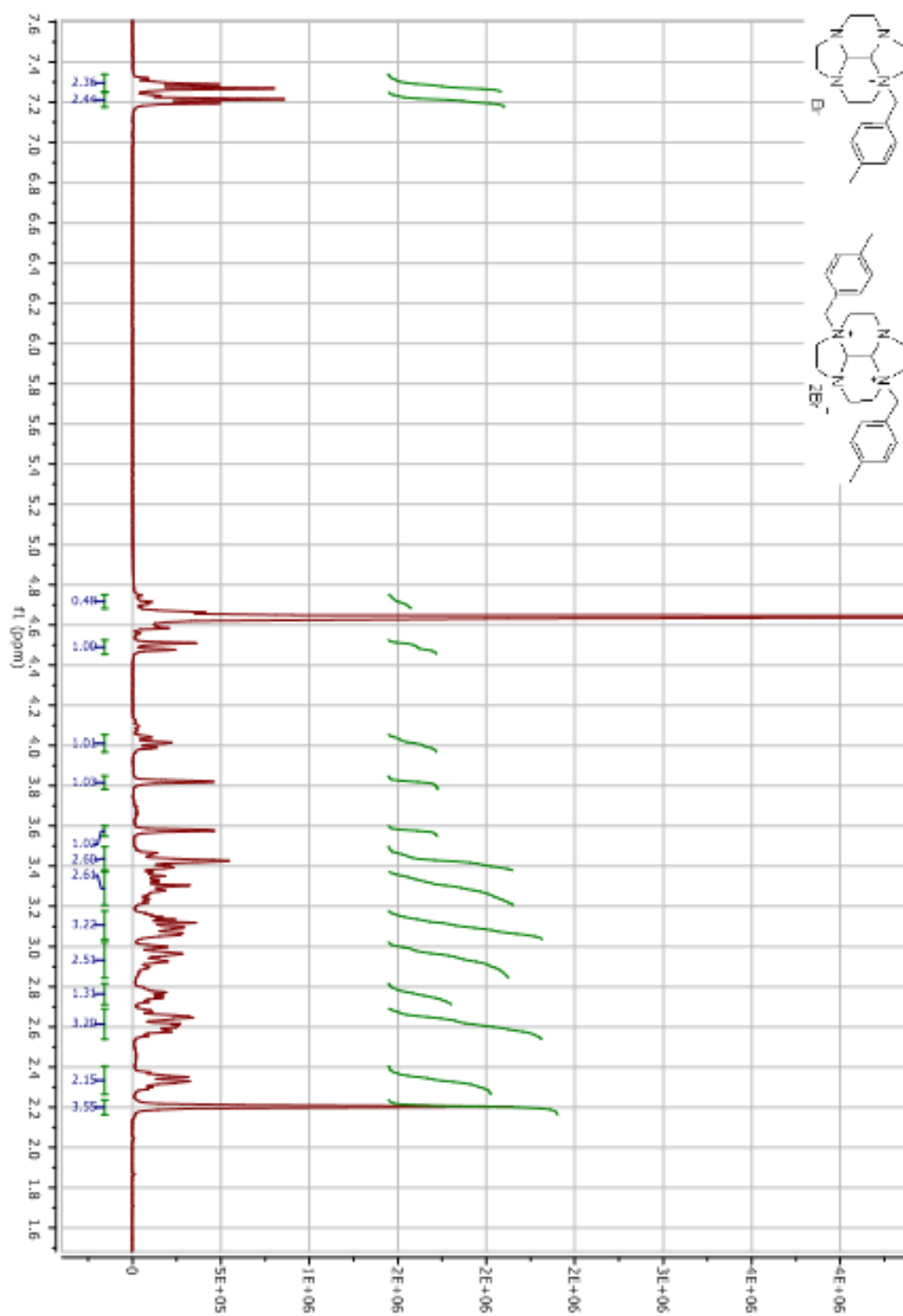
C(11)-C(12)-H(12)	119.7
C(12)-C(13)-C(8)	121.5(6)
C(12)-C(13)-H(13)	119.3
C(8)-C(13)-H(13)	119.3
C(11)-C(14)-H(14A)	109.5
C(11)-C(14)-H(14B)	109.5
H(14A)-C(14)-H(14B)	109.5
C(11)-C(14)-H(14C)	109.5
H(14A)-C(14)-H(14C)	109.5
H(14B)-C(14)-H(14C)	109.5

Symmetry transformations used to generate equivalent atoms:

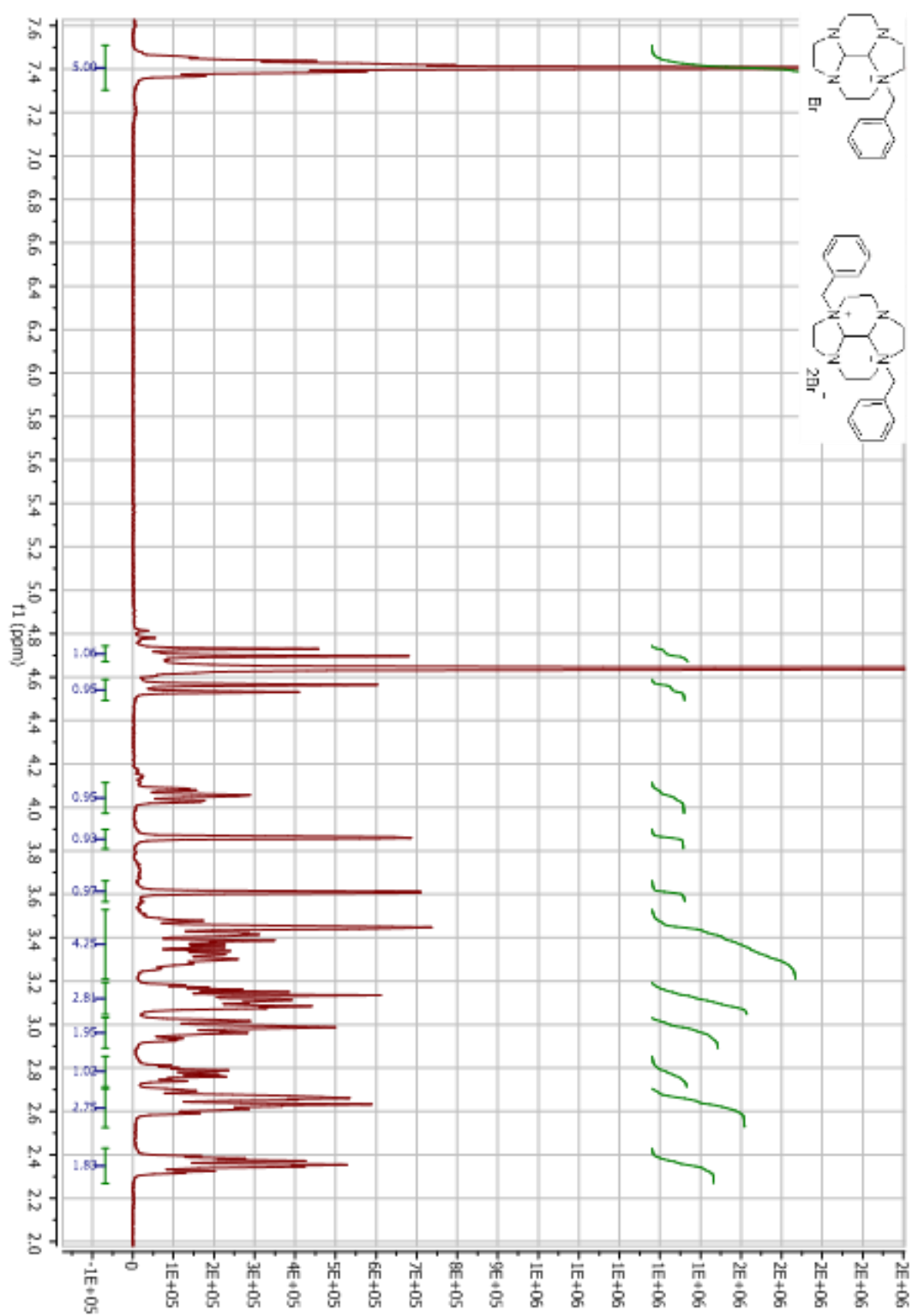
#1 -x,y,-z+3/2

Table E. Hydrogen coordinates ($\times 10^4$) and isotropic displacement parameters ($\text{\AA}^2 \times 10^3$) for **17**.

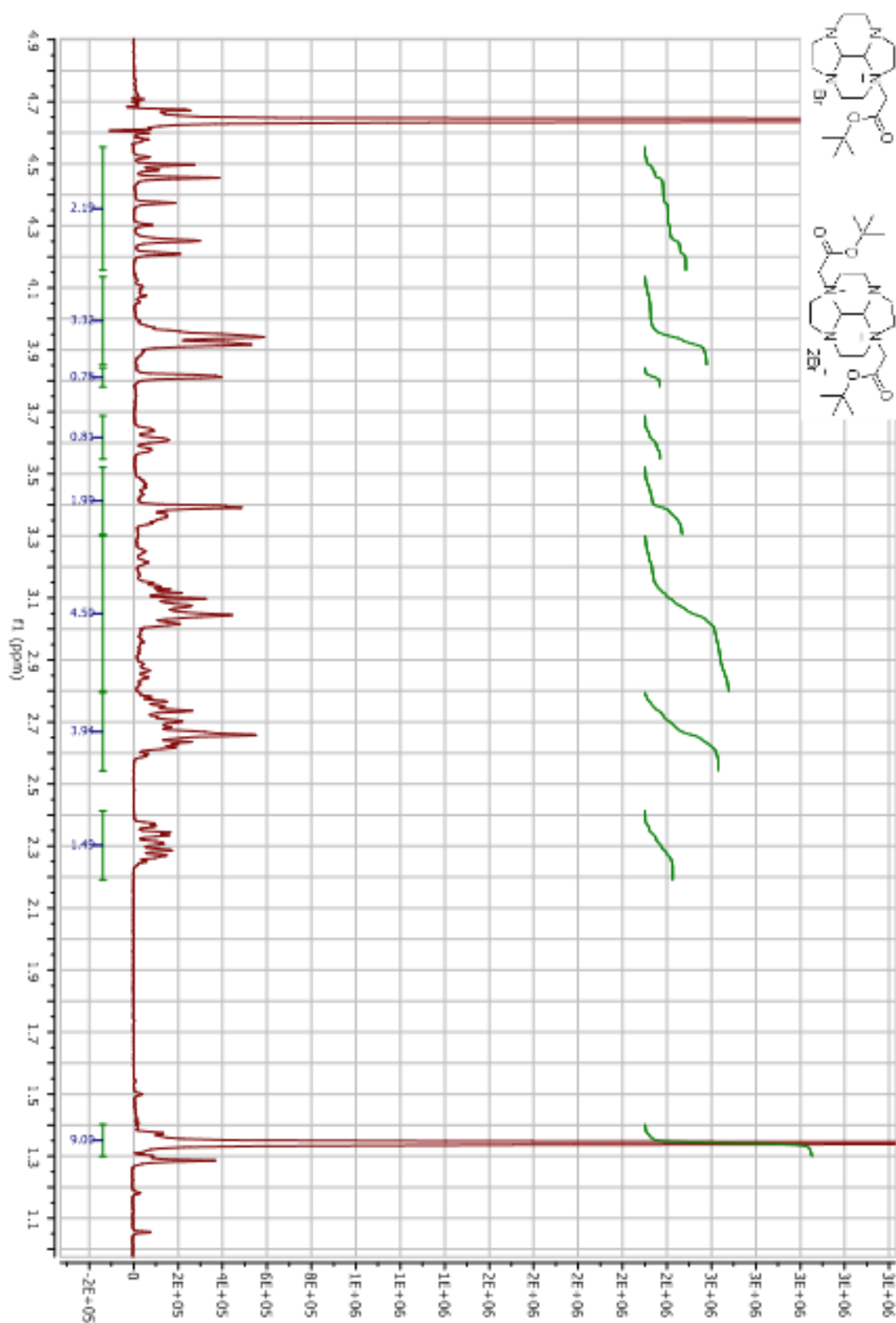
	x	y	z	U(eq)
H(5A)	1394	-1886	6741	49
H(5B)	2639	-1269	6634	49
H(4A)	2517	-1913	7787	54
H(4B)	2600	-772	7800	54
H(3A)	1738	-657	8944	57
H(3B)	1814	-1802	8956	57
H(2A)	-329	-1903	9226	54
H(2B)	342	-1241	9806	54
H(1A)	-347	133	9248	47
H(1B)	-1532	-540	9381	47
H(6)	-651	147	6991	40
H(7B)	1113	1039	6777	42
H(7A)	2024	514	7324	42
H(9)	4170	101	6954	54
H(10)	5855	473	6214	61
H(12)	3500	1784	4853	51
H(13)	1838	1432	5594	49
H(14A)	5711	1915	4658	80
H(14B)	6142	820	4679	80
H(14C)	6671	1559	5253	80
H(1C)	5210(110)	7980(80)	7900(40)	107



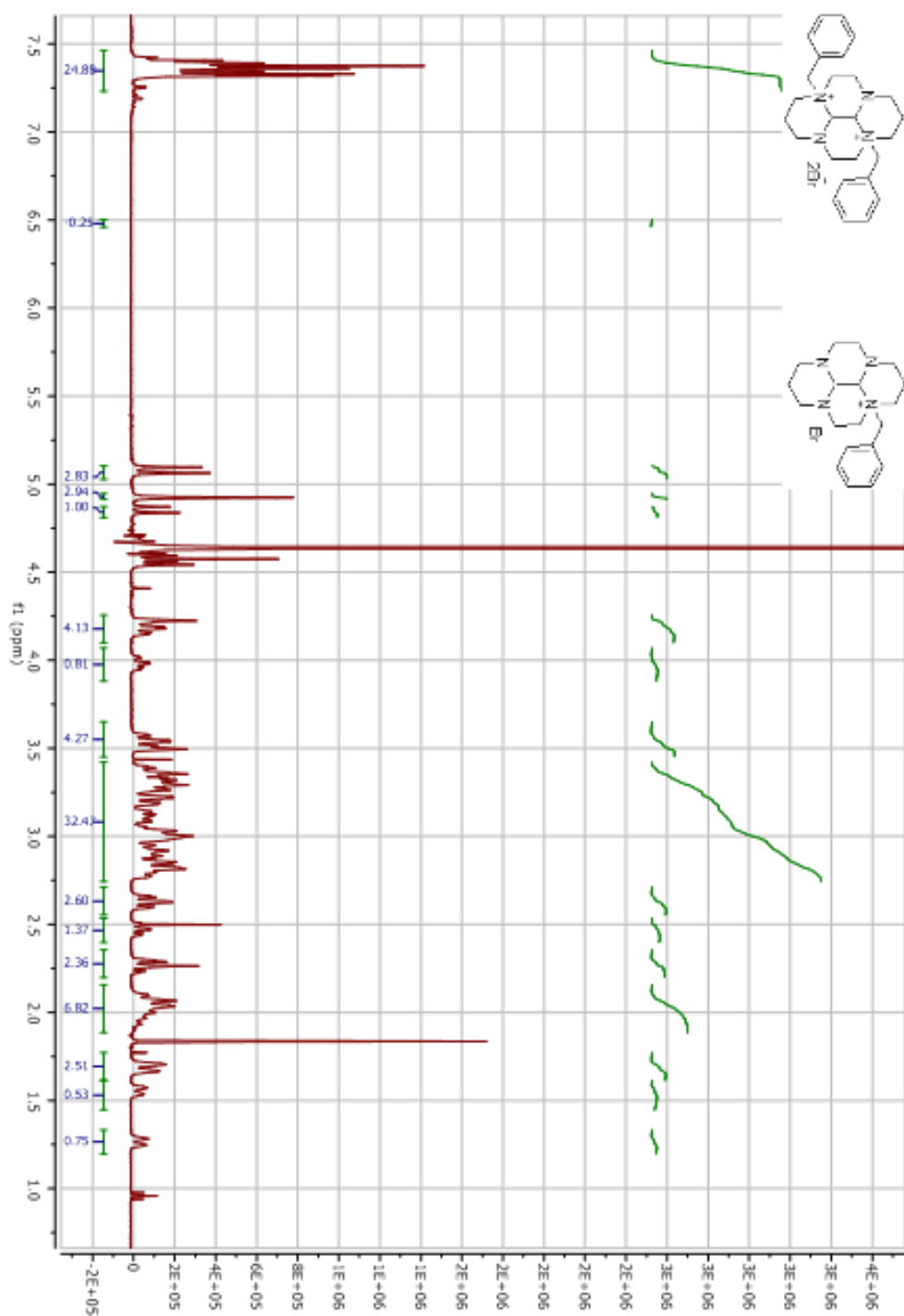
A1- ^1H NMR spectrum of **11**



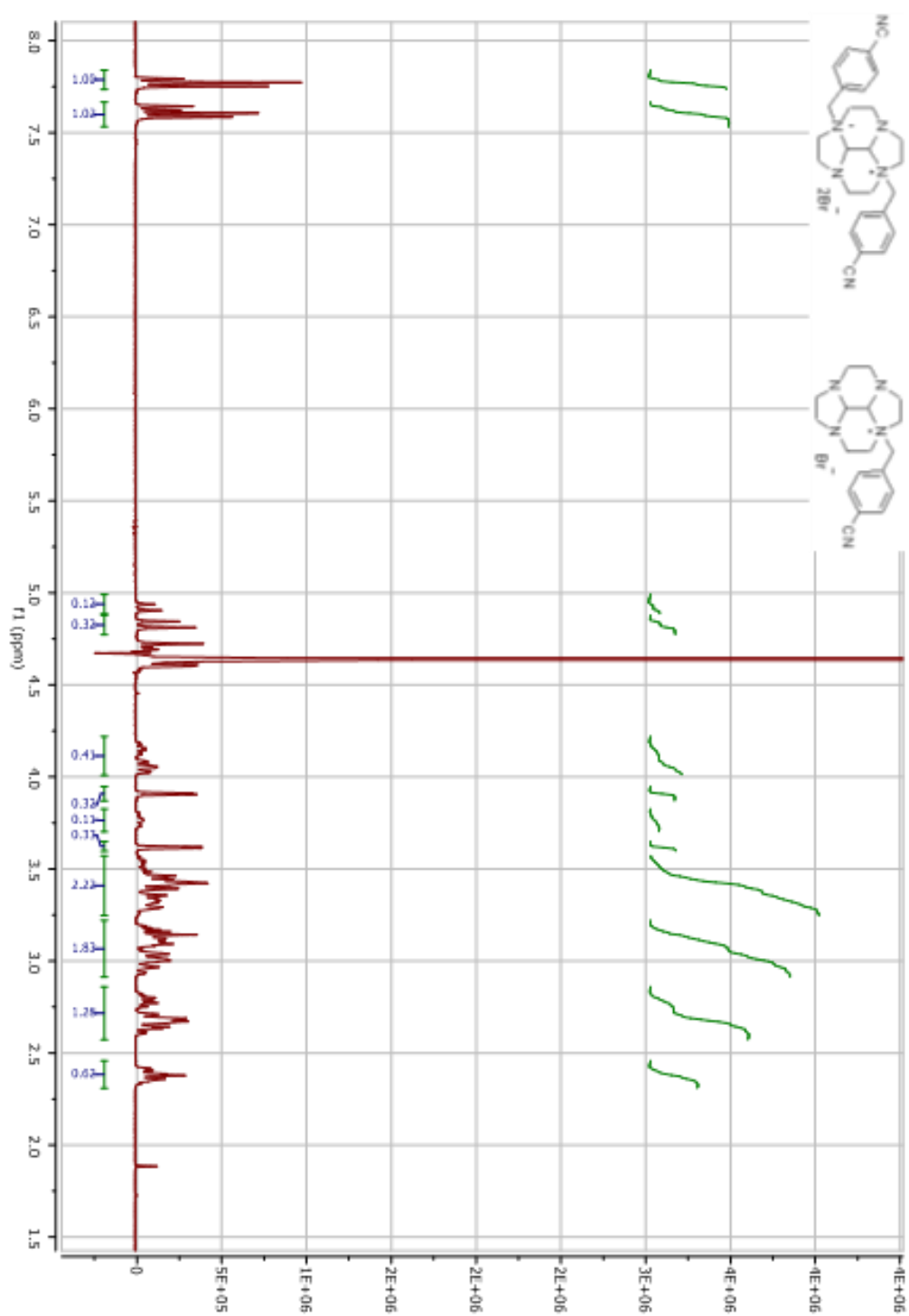
A2-¹H NMR spectrum of **12**



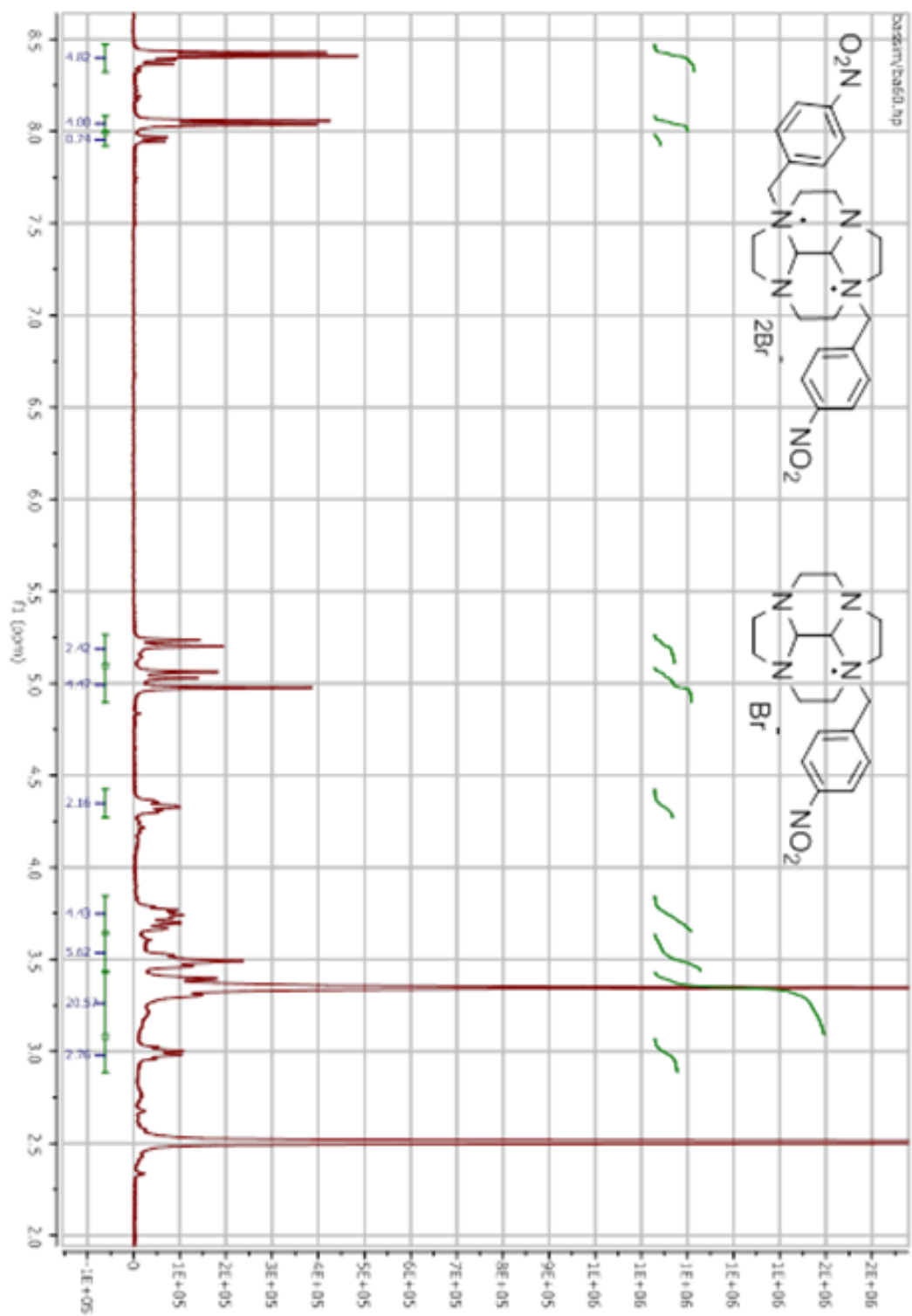
A3- ^1H NMR spectrum of **14**



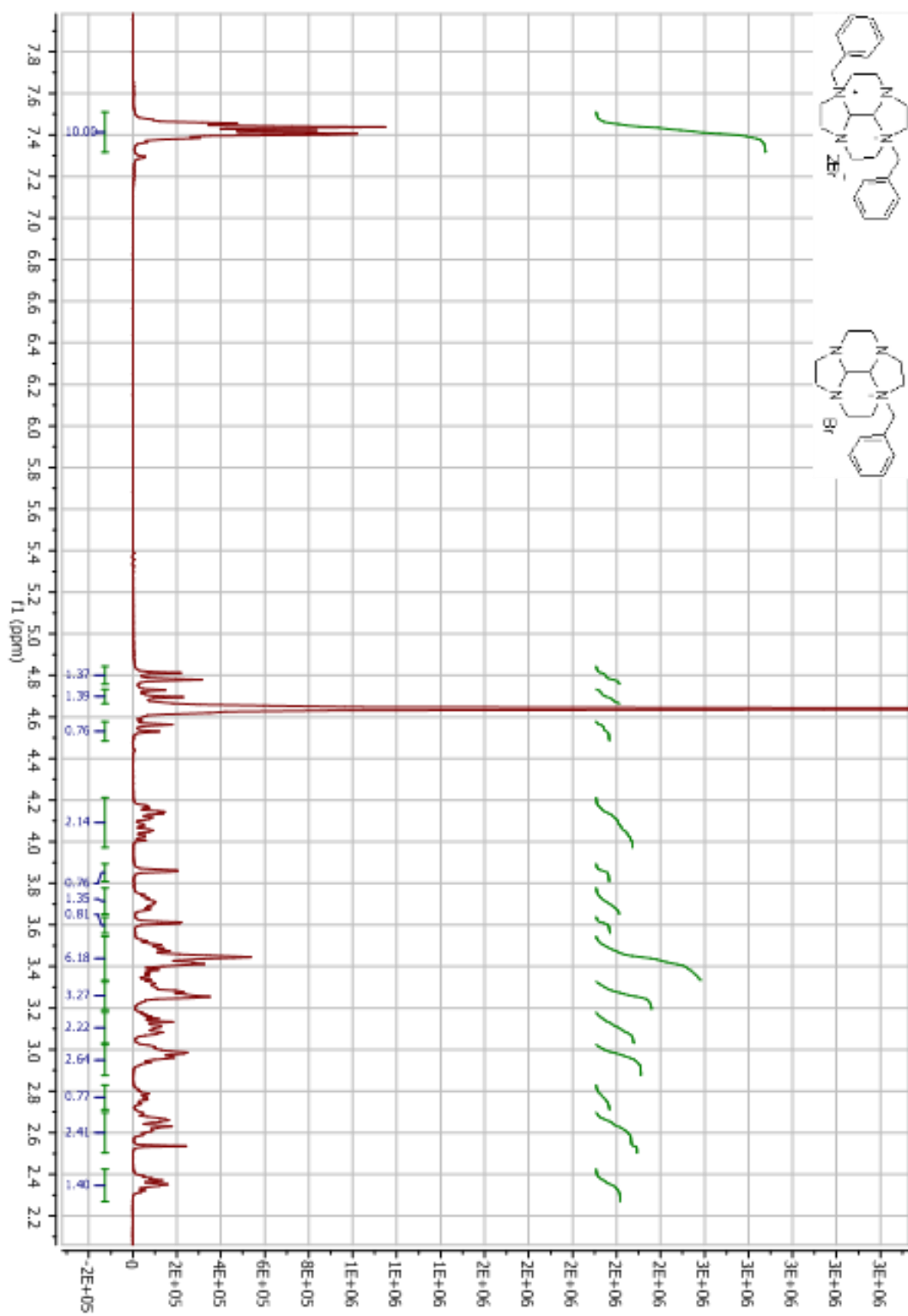
A4- ^1H NMR spectrum of **18**



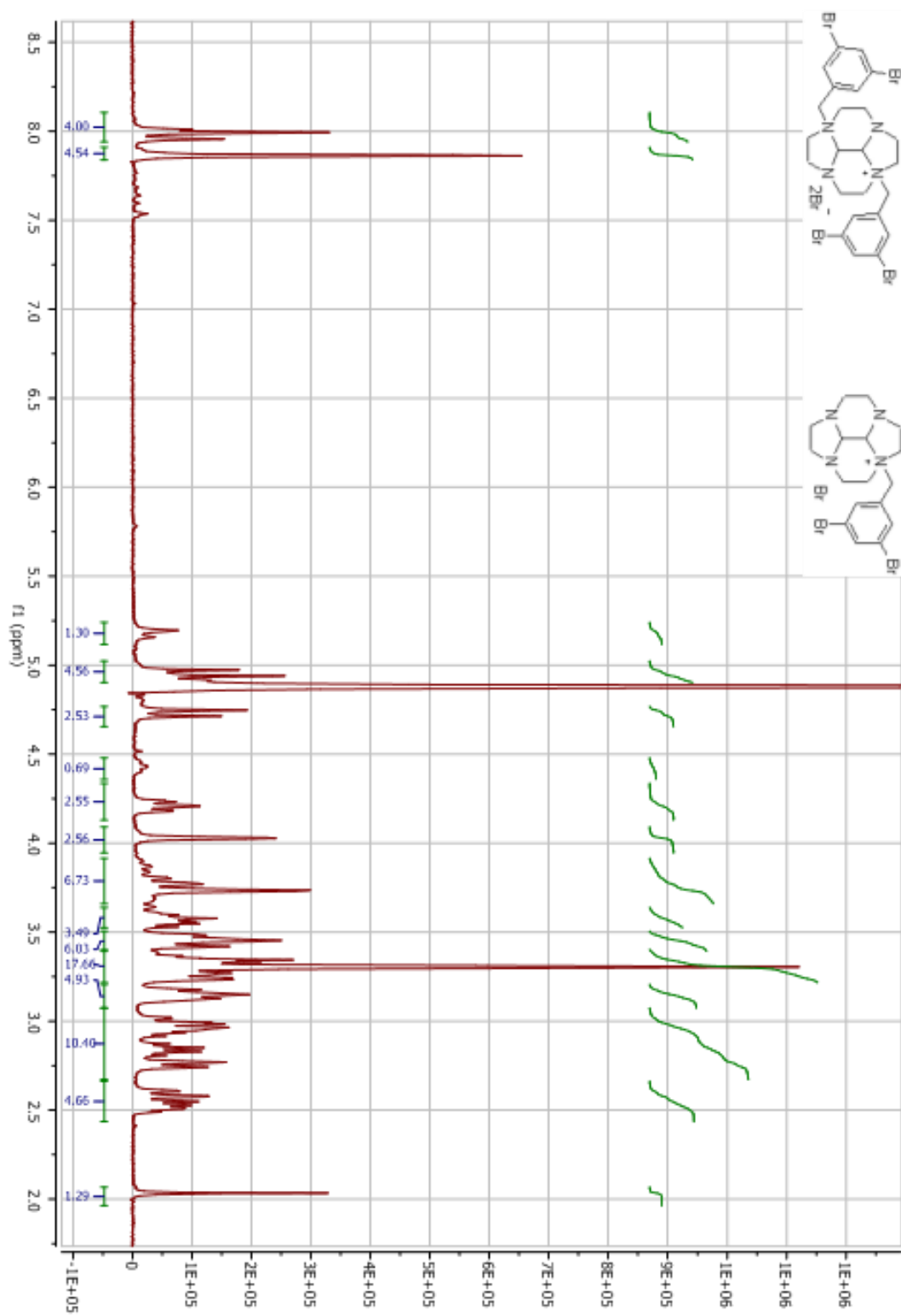
A5- ¹H NMR spectrum of **21**



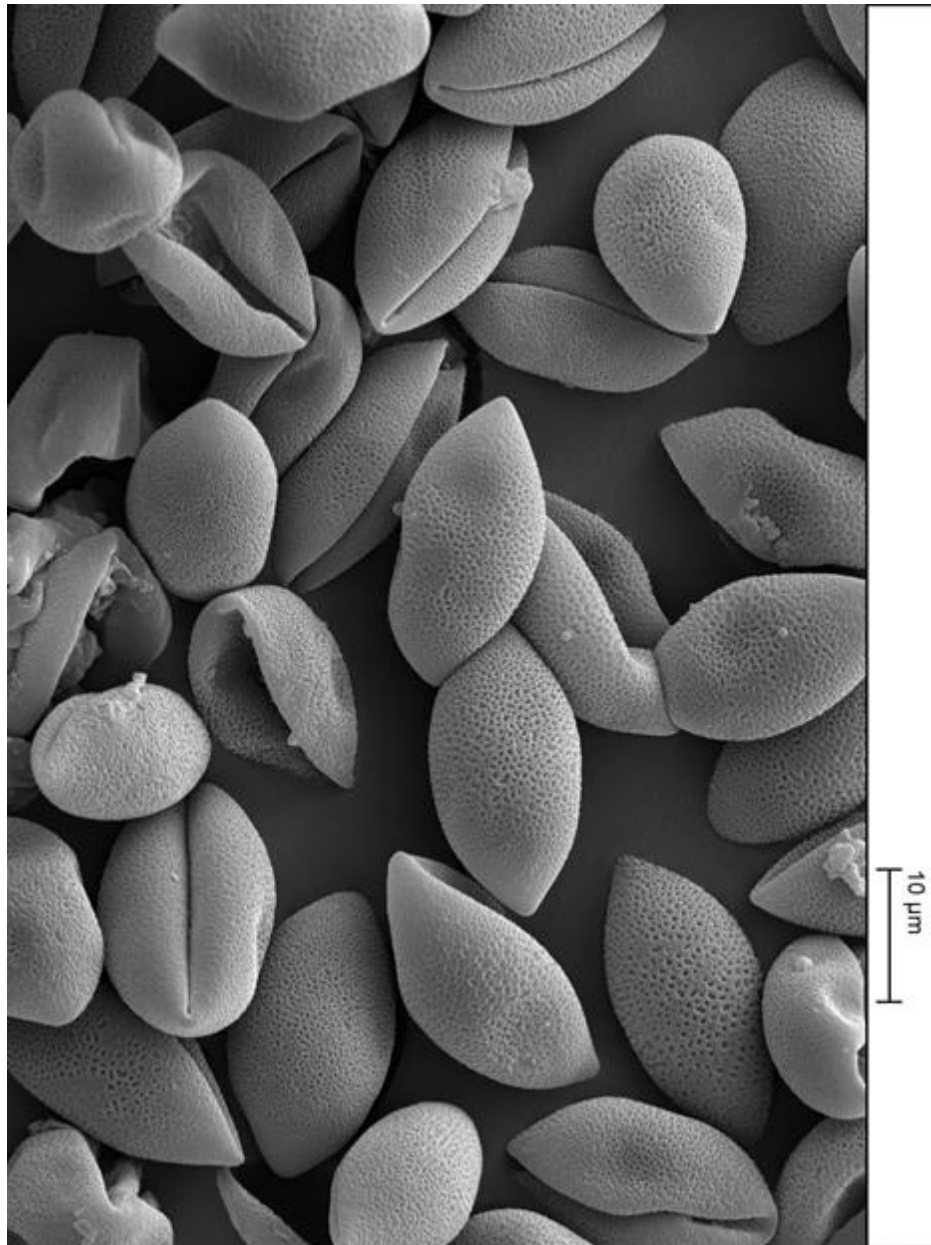
A6- ¹H NMR spectrum of **22**



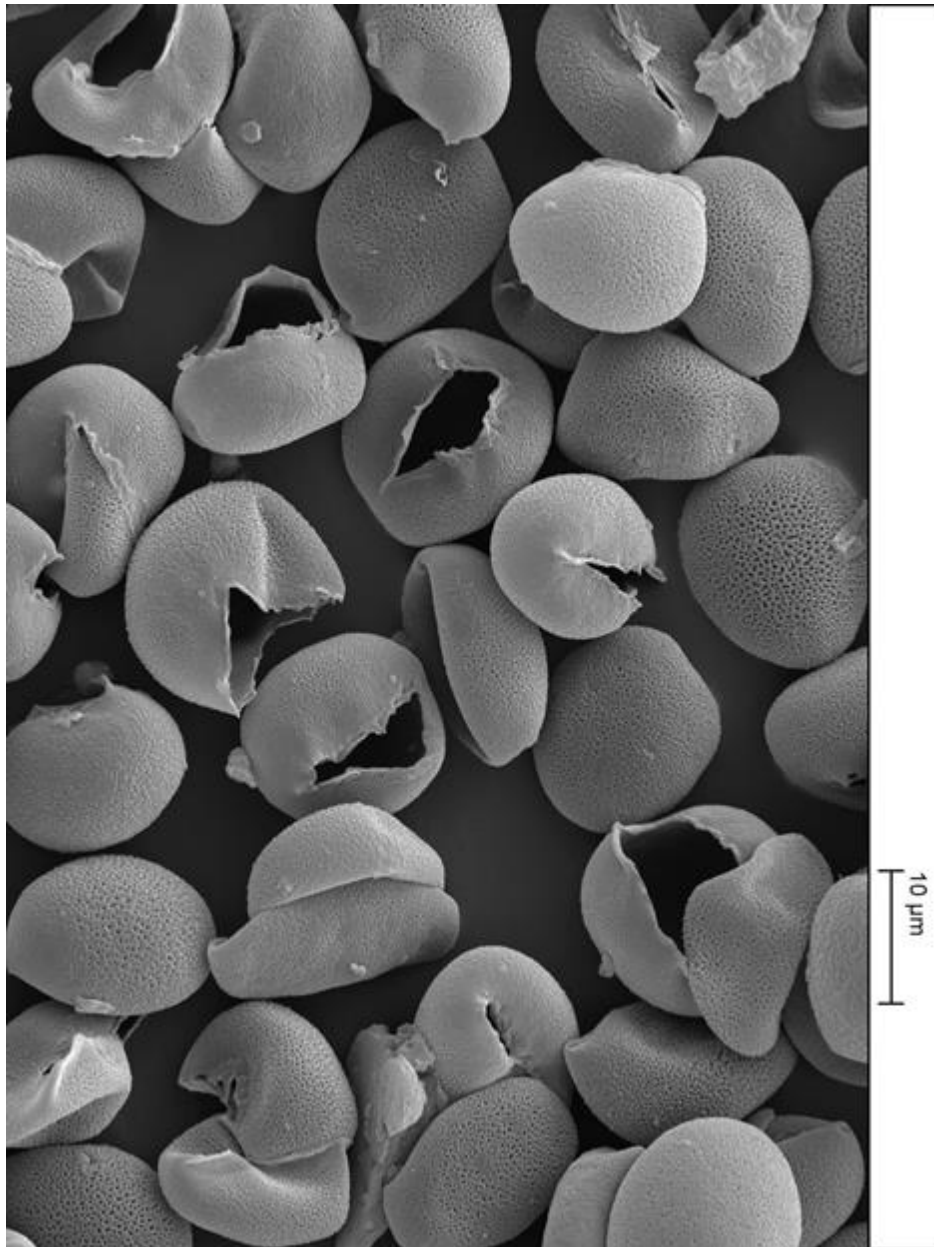
A7- 1H NMR spectrum of **24**



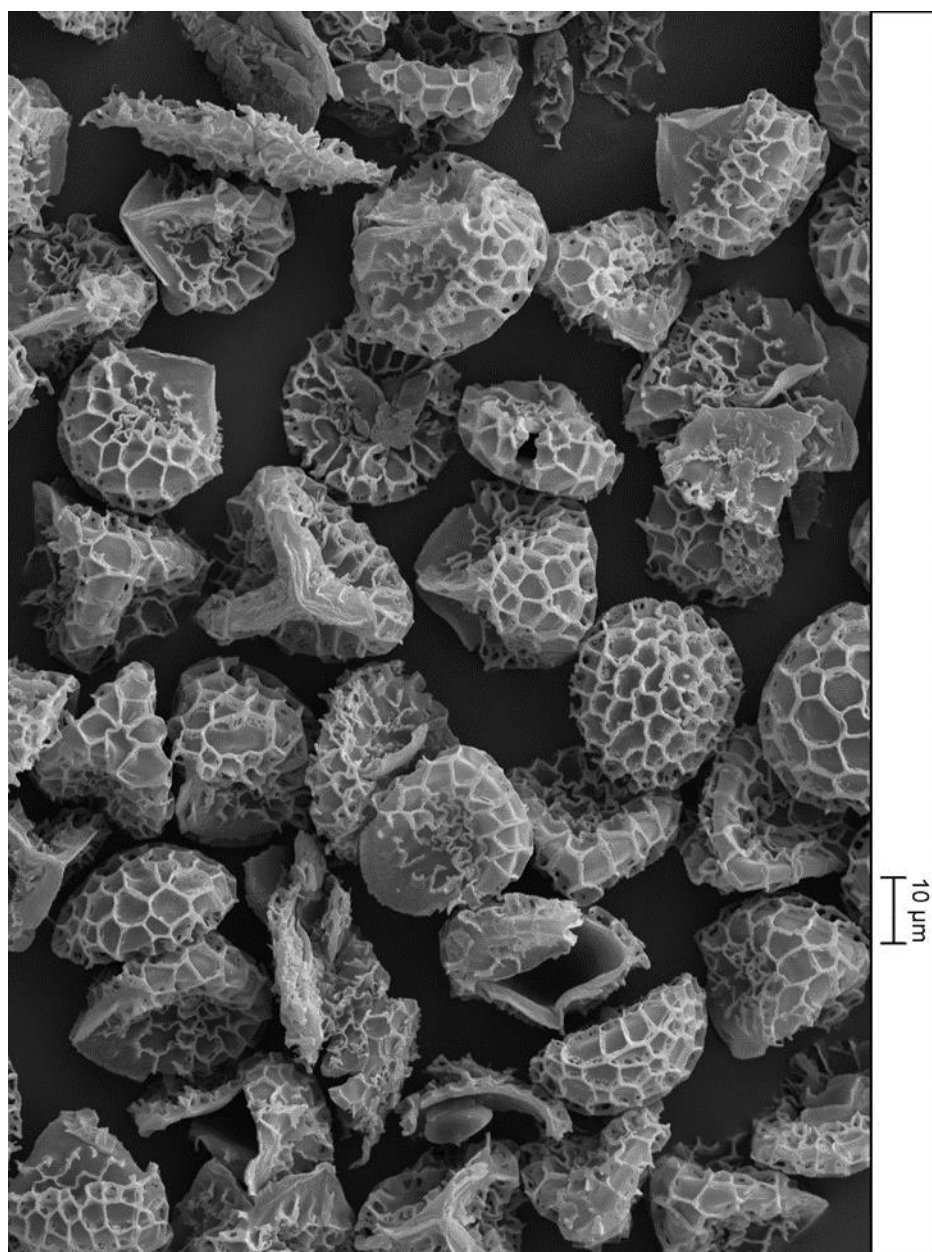
A8- ^1H NMR spectrum of **25**



A9- SEM image for date spore 39 before extraction



A10- A9 SEM image for date spore **39** after extraction



A11 A9- SEM image for sporopollenin **50** after grinding for 30 min.